Mechanistic Studies of the Enzymatic Synthesis of Polyesters

A thesis submitted in partial fulfilment for the Degree of Doctor of Philosophy

By

Alan Taylor

August 2001

Centre for Material Science
Department of Physics, Astronomy and Mathematics
University of Central Lancashire

For Janet

"It is a capital mistake to theorise before one has data. Insensibly one begins to twist the facts to suit the theory instead of the theory to suit the" facts.

"Sherlock Holmes"

Sir Arthur Conan-Doyle 1859-1930

Acknowledgements

Particular thanks are due to Prof. Kalle Hult of the Royal Institute, Stockholm. Dr. Sham Paktar of Novo A/S, Kobenhavn. Dr. Alison Rodger of the University of Warwick and my wife Janet without whose support the project could not have taken place.

Thanks are also due to:- Dr. Falmai Binns, Baxenden Chemicals Ltd. Dr. Gary Bond, UCLAN. Dr. John Burgoyne, UCLAN. Dr. David Clarke, SRS Daresbury. Mr. John Davidson, Baxenden Chemicals Ltd. Dr. Paul Harffey, University of Liverpool. Dr. Janine Maguire, UCLAN. Ms. Victoria May, UCLAN. Dr. Marie-Claire Parker, University of Glasgow. Mr. Steve Stone, Heath Scientific Ltd. Dr.Allan Svendsen, Novo A/S Kobenhavn. The Board of Baxenden Chemicals Ltd for sponsoring this research. Heath Scientific Ltd for the use of the ITC instrument. Novo A/S for the gifts of *Candida antarctica* lipase B and *Novozyme* 435™. Roche Diagnostics GmbH for the gift of *Chirazyme* L-2 lyo™.

Last but not least my supervisor Richard McCabe for three years guidance and friendship.

Abstract

A thermogravimetric technique for following lipase reaction kinetics has been developed. The relationships between the reaction rate and substrate have been determined for *Candida antarctica* lipase B. At higher concentrations, evidence of substrate inhibition was found, due to the pH of the system decreasing as the concentration of acid increased. This has a dramatic adverse effect on the enzyme activity as it moves away from the optimum pH 7.0. Buffering the system closer to optimum pH increased the reaction rate. Also, it was found that as the hydrophobicity of the medium, expressed as C logP, increased the reaction rate became slower.

The effect of substitution on the acid substrates was studied; it was found that the enzyme accepted substrates with substitution in the 3-position but not in the 2-position. As a result of modelling, this effect was explained by the disruption of hydrogen bonding, which stabilised the acyl enzyme tetrahedral intermediate.

The thermodynamic reaction parameters were determined using Isothermal Titration Calorimetry. The difference in reactivity of ester and acid carbonyls was determined together with the entropy and enthalpy of formation of the acyl intermediates. In the solvent free reaction low dispersity and high molecular weight polyesters are formed due to the limited solubility of the polyester in the diol, only limited transesterification occurring at the ends of the chain.

Molecular modelling was used to map the surface hydrophobicity around the enzyme active site in an attempt to explain the observed hydrophobic effects. Modelling around and within the active site was carried out in order to explain the activity of different substrates. The information gained from these studies led to the synthesis of several novel polyesters and polyurethanes, which may have commercial utility in coatings and adhesives.

We have investigated the secondary structure of the *Candida antarctica* lipase B enzyme using conventional CD and synchrotron radiation CD in aqueous buffers and solvents. The secondary structure was determined under different conditions, using the CDSSTR and Selcon programs. Little difference was found between the structure in aqueous buffers and solvents such as hexane, however, really polar solvents like dioxane and THF unfolded the protein.

Novel Near Infrared (NIR) spectroscopic methods were developed for the determination of the acid number and the hydroxyl number of polyesters. The effect of changes in the backbone structure of the polyester on the NIR spectrum of the polyester was determined and calibration curves developed for all the common types of linear aliphatic polyesters. The importance of the intra-molecular hydrogen bonding between the acid carbonyl and the hydroxyl groups has been established and the effect of temperature on the degree of association determined. It was found that even at a temperature of 120°C there was still substantial association between the two groups. Partial least squares analysis was developed for the simultaneous determination of both acid number and hydroxyl number. It has been shown that the principal difference between the conventionally synthesised polyesters and those synthesised using enzymatic catalysis is that the latter have little or no carboxyl termination at the ends of the polymer chain. This effect has been explained by the mechanism of the enzymatic polymerisation.

Table of Contents

1 Introduction.

1.1 Background.

Linear polyesters are a commercially important class of polymers that find their way into many different applications. The most common polyesters are those derived from ethylene glycol and terephthalic acid by intermolecular condensation of the diacid and diol or by transesterification of the dimethyl ester with the diol.[1]

These polyesters form high molecular weight polymers, which are used extensively as fibres in clothing and tire cord, as film in the manufacture of magnetic tapes and as a thermoplastic polymer in the manufacture of bottles.[2] There are other types of polyesters made by the condensation of adipic acid and diols, for example 1,4-butanediol and 1,6-hexanediol (see Scheme 1).

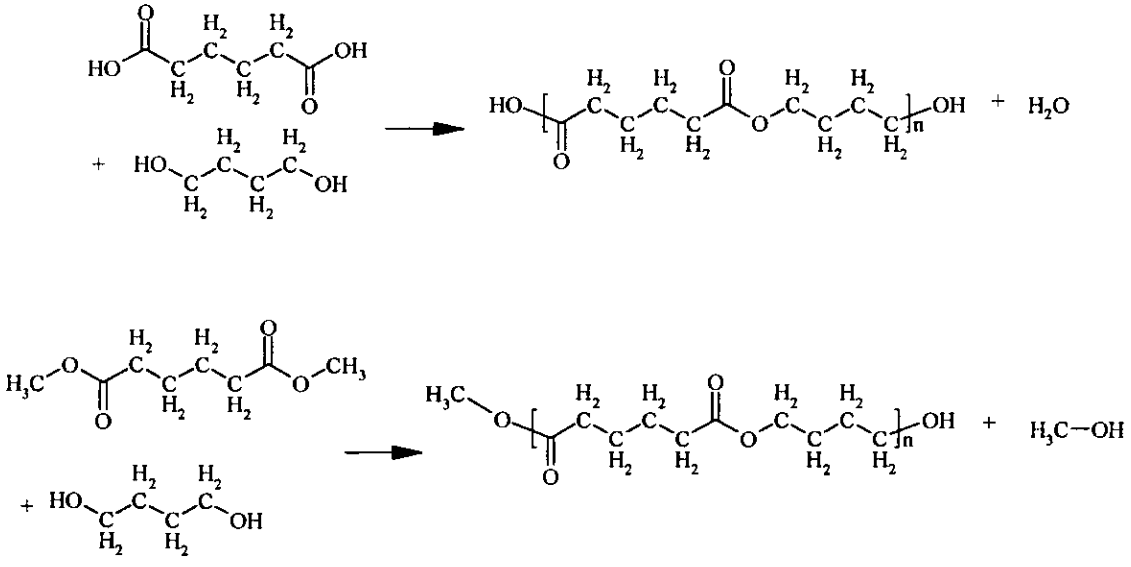

Scheme 1 Reaction of adipic acid and 1,4-butanediol.

These adipate polyesters are used as intermediates in the manufacture of polyurethane polymers by reaction of the hydroxyls of the polyester with isocyanates such as

2,4-/2,6-di-isocyanatotoluene and 4,4'-di-isocyanatodiphenylmethane (MDI),[3] see Scheme 2.

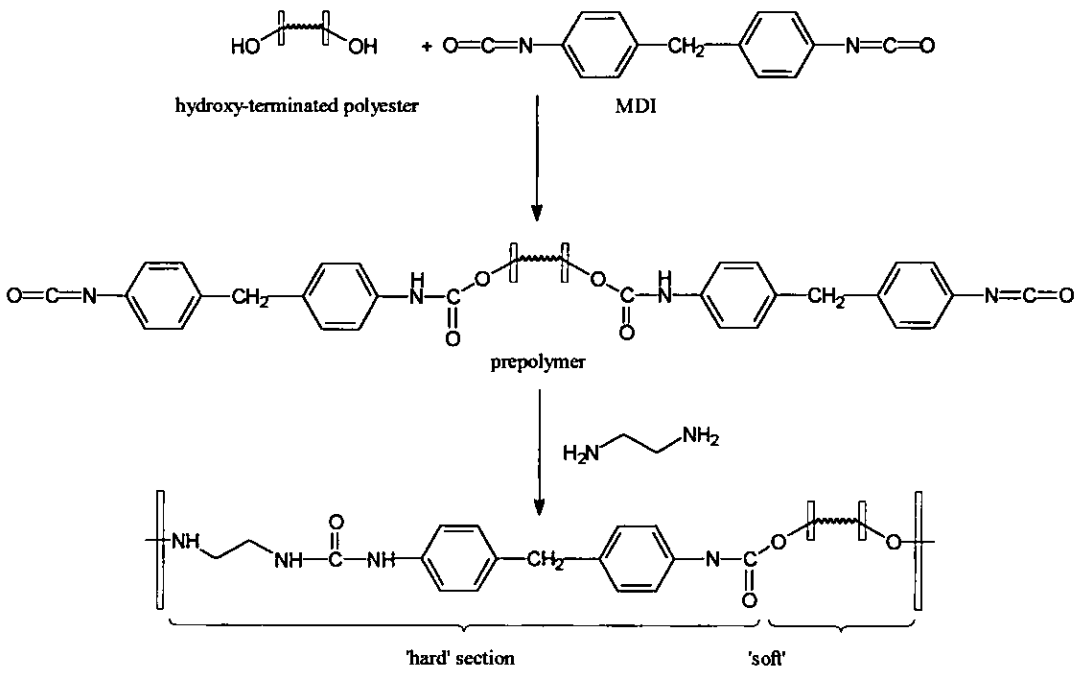

Scheme 2 Synthesis of polyurethane polymer.

These polyester urethanes are used as solid elastomers, in shoe soles and print rollers. They are used extensively in the manufacture of foamed polyurethane, which is used in components in cars, shoes and garments.[4] Special types of polyester urethanes are used in high performance surface coatings and adhesives. The form of the polyester (which is termed the 'soft segment'), controls the physical properties of the polyurethane polymer to a large degree because it forms the bulk of the polymer. Although it is the di-isocyanate that forms the 'hard segment' of the polyurethane, the actual frequency of hard segment formation is controlled by the molecular weight of the polyester.[5]

The reactions of the diacids and diols are thermodynamically unfavourable and it requires the elimination of water to push the reaction to completion. The common reaction

conditions are a temperature in excess of 220°C and either a reduced pressure or a rapid sparge of inert gas to remove the water of condensation. In the case of the high molecular weight polyesters the reaction temperature is over 270°C and the pressure may be as low as 1-5mmHg.[6]

In addition to the cost of the energy used, there are several other disadvantages to the process. Heat labile monomers cannot be used at the temperature at which the reaction is carried out. In the case of the adipate polyesters the reaction is reversible, this limits the molecular weight of the polyester to a maximum of approximately 4000 Daltons.[7] In addition, at 270°C undesirable side products start to form, such as macrolactones, which can cause deterioration in the physical properties of the final polymer.

Most of the original work on these polyesters was carried out in the 1930's by famous names such as Carothers,[8] and Winfield and Dickson.[9] Over the intervening years much process and application development has been done, but very little novel work has been carried out since those early days.

In the period between 1965-1970 the potential biosynthesis of polyesters was recognised and ICI developed a semi-commercial fermentation process to a polybutyrate polyester; however, this process was abandoned after several years of development.

1.2 Enzymatic synthesis.

In the late 1970's Klibanov and his co-workers pioneered the use of enzymes as catalysts in non-aqueous systems [10] and by 1980 this work had been extended to the use of lipases

in organic synthesis.[11]

In the 1980's it was discovered that a lipase could act as an esterase in a non-aqueous system, however, the reactants were limited to activated acids or alcohols or to the transesterification of divinyl adipate in solvent.[12]

At Baxenden Chemicals it was decided to explore the lipase catalysed reaction of un-activated intermediates such as adipic acid and butane-1,4-diol. Using di-*iso*-propyl ether as the solvent, the lipase from *Rhizomucor miehei* catalysed the reaction of these starting materials: the water of reaction being removed by molecular sieves.[13]

Subsequent work showed that it was possible to synthesise polyesters in excellent yield, without the use of solvent by using the lipase B (CALB) from *Candida antarctica*.[14] The polyesters produced were superior to conventional polyesters as they had a much narrower molecular weight distribution, typically 6000 Daltons with a dispersity of 1.5. These polyesters produced adhesives with much improved physical properties.[15]

In order to explain why the enzyme produced such low dispersity polyesters, the polymerisation process was investigated in detail. It was found that in the early part of the reaction the diol monoadipate, 6-carboxy-11-hydroxy-7-oxaundecanoic acid (AB), was the principal intermediate and that the polyesters were formed primarily by the polymerisation of AB.[16]

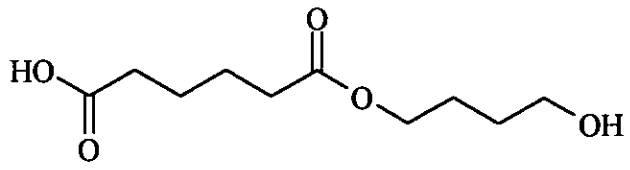

AB

It was also found that while the intermediate, 1,6-hexanedioic acid di-(4'-hydroxybutyl)ester BAB was formed, the species ABA, and other acid terminated oligomers, were never found and, furthermore, transesterification did not appear to occur.[16]

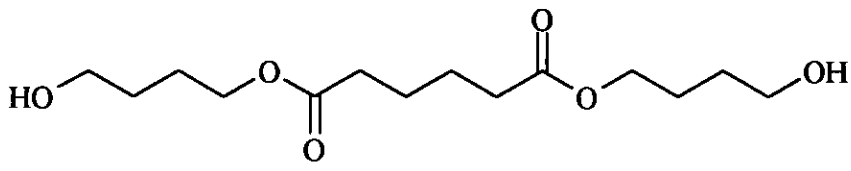

BAB

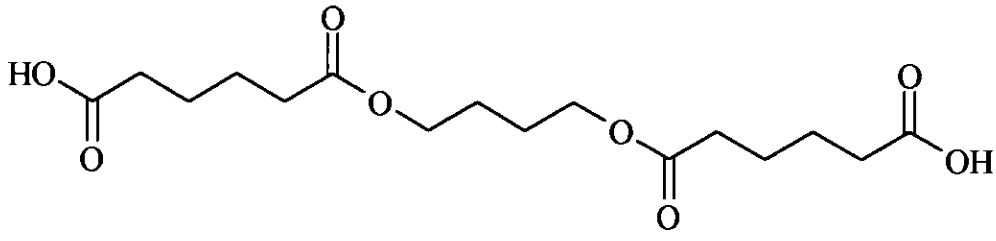

ABA

However, when the reaction was carried out in toluene as solvent, transesterification did occur and the polyesters produced had a much broader molecular weight distribution with consequently inferior physical properties.

As the development of the process continued a number of observations were made which could not be explained readily. Deactivation of the enzyme occurred to a much greater extent when hydrophilic diols such as butane-1,4-diol were used, compared to more lipophilic diols such as hexane-1,6-diol.[17] It was also observed that the reaction with high molecular weight diols, such as α,ω–polytetramethylene ether diol, was comparatively fast in spite of the size of the reacting molecule and that there was no de-activation of the enzyme during the reaction. The apparent selectivity of the enzyme to what appeared to

be structurally similar substrates was surprising. Insofar as a number of diacids and diols had been tried as substrates with varying success, maleic acid, fumaric acid, itaconic acid and hex-3-ene-dioic acid were all found to be un-reactive in the solvent free system. The C3 to C6 diols were also tried and found to give significantly different degrees of oligomerisation with adipic acid under similar conditions.[17]

1.3 Mechanism of the enzyme catalysis.

The mechanism by which lipases produce such dramatic rate enhancement on the hydrolysis and synthesis of fatty acid esters and related compounds has been the subject of extensive work for many years. It was Pauling,[18] in 1946, who first proposed that enzymes catalyse their specific reactions by the stabilisation of a transition state of the compound. Then in 1969 work by Blow, *et al.*,[19] on serine proteases identified the nature and function of the serine (Ser), histidine (His) and aspartate (Asp) catalytic triad as the key to the active site of the protease. Subsequent work by Brady, *et al.*,[20] showed that the lipases also worked by an identical active site containing the Ser-His-Asp catalytic triad. For a number of years this mechanism was accepted as the explanation for most, if not all, of the rate enhancement produced by the lipase family of enzymes. In recent years, however, it became obvious that this was not the complete explanation and more sophisticated theories have since been developed. It was proposed initially that the geometry of the active site exerted a steric force on a molecule in the site that reduced the activation energy by destabilising the ground state of the substrate.[21] Warshel,[22] has shown that theoretically the catalytic contribution caused by steric effects is in effect minimal; this is almost certainly due to the fact that the enzyme is quite flexible and

undergoes changes in conformation due to the presence of the substrate, without any significant increase in free energy. Experimental work has been done by Raines, *et al.*,[23] to modify the shape of the substrate or the conformation of the enzyme in the region of the active site. However, in all cases there was a decrease in enzyme activity compared to the natural state. While this work proves that steric effects can damage enzymatic activity, it does not prove the converse that steric effects can cause rate enhancement.

A number of authors, notably Crosby [24] and Dewar and Cohen [25] have proposed that the basis of enzyme catalysis is their ability to desolvate ground states which are strongly solvated in solution, thereby reducing the solvation energy of both the ground and transition states. Warshel,[26] however, has shown by thermodynamic considerations that enzymes do not use a desolvation mechanism, because enzymes that enhance the k_{cat}/K_m, do not benefit from destabilising the ground state, but rather from the stabilisation of the transition state.

In 1971, it was proposed by Page and Jencks [27] that the substrate having entered the reactive site, became fixed in a configuration that limited both the rotational and translational degrees of freedom so that the molecule was fixed in the optimum orientation for the reaction to take place. Storm, *et al.*,[28] extended this work by the development of the theory of an orbital steering mechanism, which proposed that the enzyme keeps the reactive group on the substrate in the optimum orientation for the formation of the transition state. This was tested by Bruice,[29] who reacted a series of model compounds in solution and showed that restriction of the rotation about a bond could lead to large increases in the reaction rate of the compounds. It requires a major leap of imagination to extrapolate his work on the ring closure reactions of diacids and diesters in solution, to the reactions that take place in the active site of an enzyme. While

it is possible that entropic factors may not have a major role in enzyme activity when small molecules are involved, intuitively when one considers the size of the molecules with which we are working, these factors must be significant. A simple consideration of statistical thermodynamics would lead to the conclusion that the probability of either the carboxyl or hydroxyl group at the end of a molecule, which may be 2000 Daltons, coming close enough and in the correct orientation to react at 60°C, would be quite small.

It is now becoming obvious that the enzyme does not have just one means of enhancing the reaction rate, but several, which may or may not be used in concert depending on the substrate and the media in which the reaction takes place. In the case of our lipase, we can break down the explanation of the enzymatic activity into a number of different factors. When we do this the explanations for the behaviour of the enzyme in non-aqueous media also becomes more understandable.

1.4 Hydrophobic/hydrophilic attraction.

Enzymatic processes usually take place in water, which is essential to all biological processes and to the forces that govern protein folding. The proteins typically fold in such a way that apolar residues form the core whereas the polar residues tend to be on the surface where they are hydrated. In 1990 Dill, *et al.*,[30] showed that it is hydrophobic forces that control protein folding. However, this is an over-simplification and non-polar amino acid residues may cover up to 50% of the enzyme surface, where they are organised into clusters that form hydrophobic areas of the surface. The distribution and extent of the hydrophobic regions may be critical to the performance of the enzyme. X-Ray studies on a number of lipases by Brady [20] identified a loop of hydrophobic

protein, which formed a lid over the active site making it inaccessible to the substrate. While this lid formation is common to most lipases, it was shown by Cygler and Schrag [31] not to be present in *Candida antarctica* lipase B.

In the case of most lipases, it is the variation in surface hydrophobic/hydrophilic properties between enzyme and substrate that gives rise to the oil/water interfacial activation, which is necessary for the hydrophobic lid to open, allowing the substrate access to the active site.[32] However, the attraction of hydrophobic molecules to each other, like the breaking of an oil in water emulsion, brings the typically hydrophobic fatty substrate into contact with the lipase, which in water will cleave the fat into its components. Lango and Combes [33] modified the hydrophobic surface of lipases by glycosylation and showed that as the surface becomes more hydrophilic there is a decrease in lipase activity. When chymotrypsin is made more hydrophilic, the rate of hydrolysis is halved, but in the case of *C. rugosa* lipase, all activity is lost. However, when the lipase is made more hydrophobic on the surface the rate increases by more than 50%. This work is particularly relevant to the use of lipases in non-aqueous media because it was shown that increasing the hydrophilicity of the enzyme surface helped the enzyme retain its activity in polar solvents, probably by helping the enzyme retain its loosely bound water. Increasing the hydrophobicity of the enzyme increased activity in non-polar solvents probably by helping the solubilisation of the enzyme in the non-polar solvent.

The attraction of non-polar fatty substrates to the hydrophobic parts of the enzyme is best understood when we think of these as oils in water being surrounded by layers of water, with a large decrease in entropy when the oil in water emulsion is formed. When the substrate enters the site and forms the Enzyme-Substrate complex, ES, there is a

corresponding large increase in entropy, which is the driving force for the first part of the binding process.[34] The low solubility of the fatty substrate in water has been correlated with its high affinity for the corresponding non-polar parts of the active site. It is obvious that these hydrophobic interactions will be affected when the enzyme is operating in non-aqueous media. Maurel,[35] has shown that the higher the solubility of the substrate in the medium the lower its affinity for the enzyme site and the higher its Michaelis constant, K_m. The Michaelis constant can be considered to give a measure of the affinity of an enzyme for its substrate and is derived from Michaelis-Menten kinetics. It was shown that the greater the contribution of hydrophobic interactions in the binding process, the greater the effect of organic solvents on the reaction.

1.5 Electrostatic Factors.

Having reached the active site of the enzyme, we may now consider the impact of short range electrostatic forces and hydrogen bonding. It was Jencks [36] who first proposed in 1975 that enzymes use electrostatic binding interactions away from the catalytic triad to enhance the catalytic power of the enzyme. This effect was confirmed by Fersht,[37] who showed that by changing or removing polar amino acid residues remote from the active site, it was possible to destroy all activity, even though the active site itself was unchanged. It is proposed that direction into the site and the positioning of the substrate molecules, with respect to each other and to the active site, is controlled largely by electrostatic forces.[30,38,39] This effect has been proven in a number of different enzymes, including the triad in the serine proteases. This concept is particularly relevant to enzymatic activity involving large molecules as substrates, or the assembly of large

molecules such as RNA and our aliphatic polyesters.

Once the substrate has entered the site and been positioned by electrostatic forces so that the requisite orbitals are aligned optimally, other electrostatic binding interactions come into play. They may act to desolvate or destabilise the substrate ground state or stabilise the transition state. The binding of the substrate does not enhance the reaction rate, whereas stabilisation of the transition state does increase the rate.[40]

In the last few years, the concept of the low barrier hydrogen bond (LBHB) has been introduced into enzymology. The LBHB is nothing more that a short, very strong hydrogen bond: an average hydrogen bond has a bond energy of 5 kcal mol^{-1}, whereas the LBHB may have a bond energy as high as 20 kcal mol^{-1}. It is surprising that this has only been considered recently. It has been known for many years, that in polar polymers such as polyamides most, if not all, of the strength of the polymer comes about because of the strong hydrogen bonds that form between amide groups when aligned in the optimum conformation.[41] It is not surprising therefore that many strong hydrogen bonds form between the peptide groups of the enzyme and between the peptide groups and the polar parts of a substrate. It is possible to have ordinary hydrogen bonds form with many of the amino acid side chains, but most will not have the polarity of the amide groups required to form a LBHB.

The strength of the hydrogen bond depends on its length, its geometry and the nature of its environment. In water, the hydrogen bonds to the oxygen atoms are 2.8 Å long and the bond energy 5 kcal mol^{-1}. They are weak because of the difference in the pK of the two oxygen atoms in H_3O^+ and H_2O, therefore the proton in H_2O—H-OH is tightly bound to the OH^- as a water molecule. In solvents, however, strong hydrogen bonds can form with bond energies of up to 20 kcal mol^{-1}. It is obvious therefore that the properties of

hydrogen bonds in organic solvents are extremely relevant to our work. In the serine protease γ-chymotrypsin a LBHB has been identified by NMR spectroscopy between histidine 57 and aspartate 102, this LBHB is related to the formation of the acyl chymotrypsin.[42] It has been proposed by Cassidy, *et al.*,[43] that this LBHB in the active site stabilises the transition state and lowers the activation energy for its formation. When the substrate enters the site it causes conformational changes in the enzyme which bring the His-57 and Asp-102 closer together, which in turn enhances its ability to remove a proton from the serine, Ser-195, and lowers the energy of the transition state, or tetrahedral intermediate.

Similar low field protons indicating LBHB formation have been found in a number of serine proteases [44,45] and there is no reason not to suppose that the same effect occurs in lipases. It has been calculated by Cleland, that the bond energy of the LBHB of 18 kcals mol^{-1} corresponds to a rate enhancement of 13 orders of magnitude.[46]

1.6 The Catalytic Triad.

The next and most quoted aspect of lipase activity is the mechanism of the catalytic triad that is shared with the serine proteases.

The early work of Blow [19] on proteases demonstrated the significance of the catalytic triad Asp-His-Ser, these three residues occur in the active site of a whole family of eponymous proteases, the aspartic proteases and the serine proteases. Polgar, *et al.*,[47] found that the aspartic residue remains ionised in the active site and Hunkerpillar [48]

introduced the notion of a charge relay system, see Figure 1.1, whereby the ionised aspartate pulls a proton from the histidine, which in turn activates the serine hydroxyl by the removal of a proton.

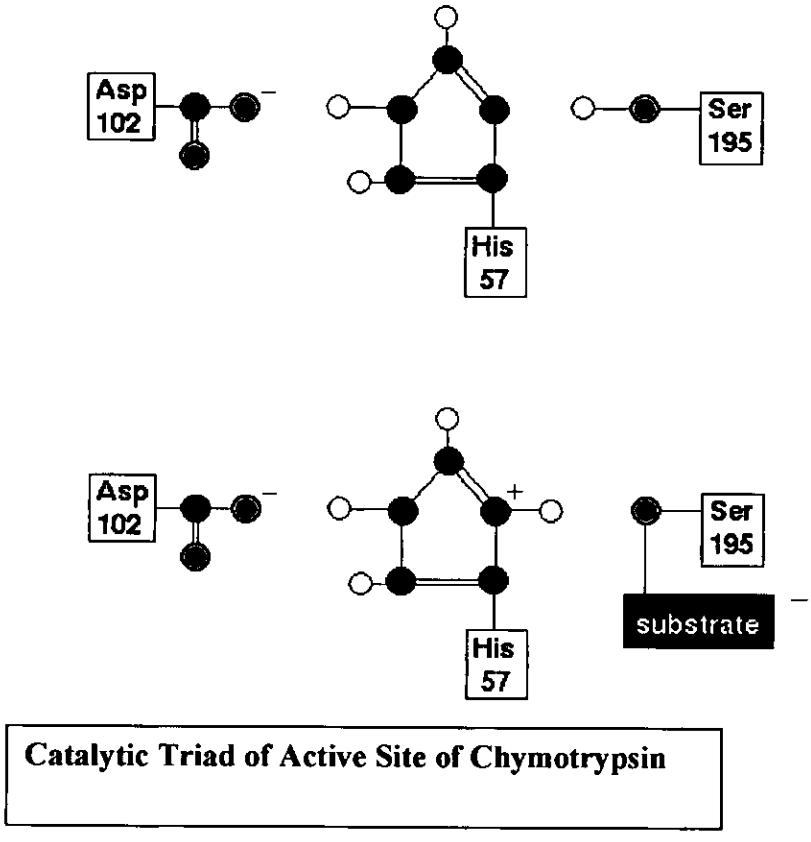

Figure 1.1 The Charge relay system of proteases and lipases.

Carbon - black, Nitrogen – blue, Oxygen - red

More recently, this theory has been modified by Kossiakoff,[49] who has shown by NMR studies that a proton is not transferred to the histidine from the serine. Naray-Szabo, *et al.*,[50] state, that the role of the aspartate residue when ionised is to increase the stability of the ion pair formed by the protonated histidine and the transition state of the substrate (tetrahedral intermediate). Either way it has been shown by site directed mutagenesis that the removal of the aspartate residue from the active site reduces the activity of the enzyme by several orders of magnitude.[51,52] Recent work,[53] has confirmed the theory of

Derewanda that the His residue of the triad has an additional hydrogen bond between the $C^{\varepsilon 1}$-H of the histidine and a carbonyl of the backbone. Derewanda,[54] proposed that this H-bond has three possible roles: (i) to pre-align the His in the optimum position to activate the Ser; (ii) to increase the electronegativity of the $N^{\varepsilon 2}$ and (iii) to facilitate deprotonation of the His to form the imidazolium ion. However, a fourth role has been proposed that involves the H-bond causing the His to flip through 180° during the reaction, so that it can catalyse both formation and decomposition of the acyl tetrahedral intermediate.

It should be noted that while the most common catalytic triad in proteases and lipases is that of the Ser-His-Asp there are occasions in both types of enzyme where the aspartate is replaced by glutamate and in some cases the serine might be replaced by threonine. The three members of the triad lie in close proximity, but they do not lie near to each other in the peptide chain, nor is there any commonality in their position in the chain.

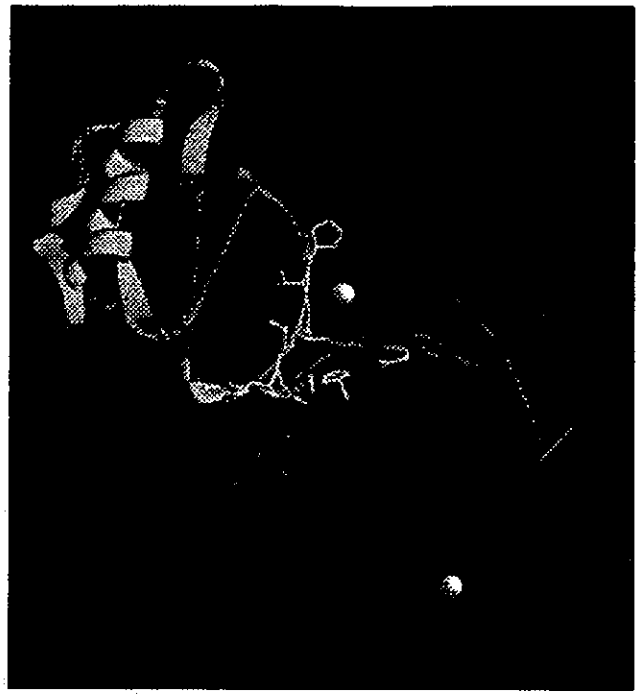

Figure 1.2 γ-Chymotrypsin from the ExPASy database.[55]

The catalytic triad is in orange, bound ligand in magenta and Calcium in white
The histidine residue can be seen in the centre of the picture, with the aspartate on its right and the serine just discernible on its left.

The mechanism of the aspartic protease was shown to be common to the acyl lipases and the phospholipases by the work of Rubin [56] and Brzozowski, *et al.*,[57] this may be seen in the list of proteases and lipases together with their catalytic triads given below.

Table 1.1 The positions of the relevant amino acids in the active sites of the following enzymes.[58,59]

Rhizomucor miehei lipase	Asp 203	His 257	Ser 144
Candida antarctica lipase	Asp 187	His 224	Ser 105
Candida rugosa lipase	Glu 341	His 449	Ser 209
γ-Chymotrypsin	Asp 102	His 57	Ser 195
Subtilisin	Asp 32	His 64	Ser 221
Geotrichum candidum lipase	Glu 354	His 463	Ser 217

Figure 1.3 is taken from the ExPASy protein database and shows the detail of the active site of γ-chymotrypsin with the catalytic triad shown clearly. The other residues marked, form the limits of the oxyanion hole, which will house the tetrahedral intermediate of the enzyme-substrate transition complex.

All of the above mechanisms and molecular behaviour are affected in differing ways by changes in the media which surround the enzyme molecule. The greatest change, which is relevant to our work, is the change in enzymatic activity that occurs when the surrounding aqueous medium is replaced by an organic solvent. Other more subtle changes may occur, depending on the physical properties of the specific organic medium.

Other factors such as pH also affect the activity of the enzyme, but none approach the significance of the aqueous medium and the concentration of water in the organic solvent in non-aqueous media.[60]

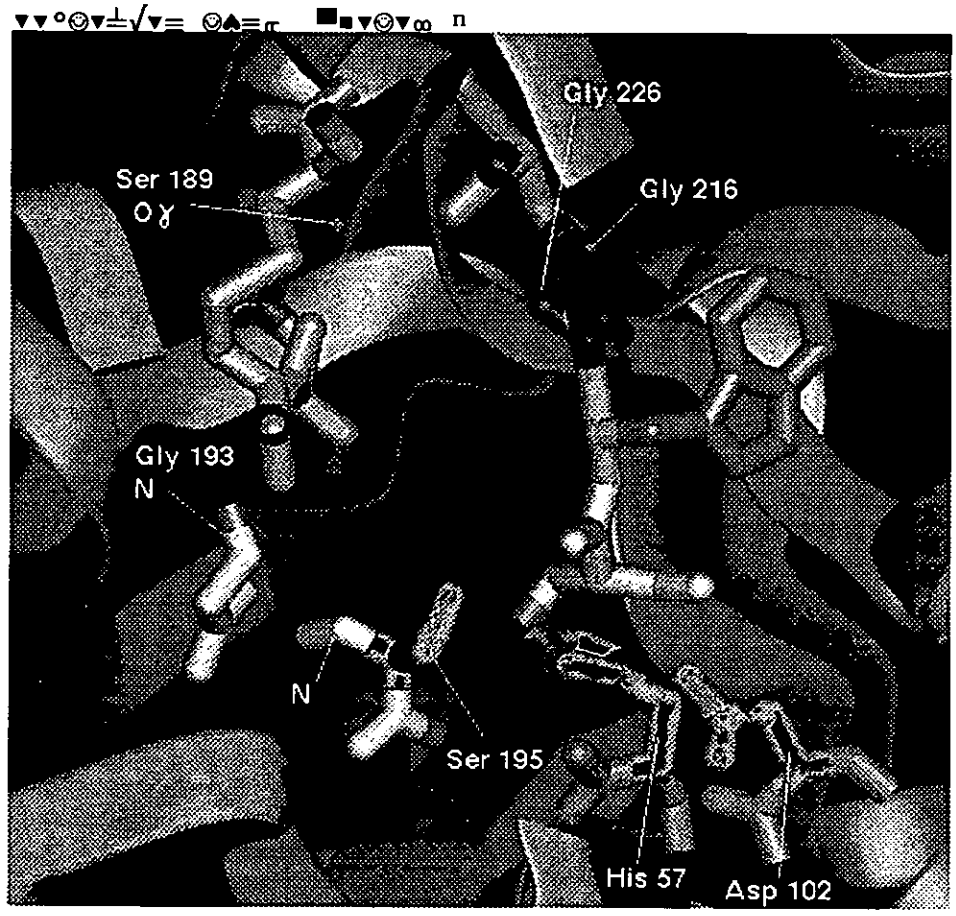

Figure 1.3 Active site of γ-chymotrypsin.

Showing the key residues and the catalytic triad (in red) of Asp102, His 57, and Ser 195

1.7 The role of water.

It has long been realised that enzymes, which have evolved to function in water need water for optimum activity and there is a fall in activity of many orders of magnitude when the enzyme functions in non-aqueous media. Furthermore, the conformation of the protein depends on the presence of water; in anhydrous conditions, enzymes become more rigid and more resistant to heat. It is often stated that water acts as a lubricant within the enzyme molecule, allowing flexibility and movement which is necessary for the changes in conformation that are thought to occur during the change from enzyme-

substrate binding to enzyme-transition state binding.[61] However, we believe that this interpretation is an over simplification, which does not give the true picture of the role of water in the enzyme.

It has been shown by Parker, *et al.*,[62] and Lee, *et al.*,[63] that the water associated with the enzyme molecule exists in three states, tightly bound water, less tightly bound water and a reservoir of free water. It is proposed that each type of "bound water" is fulfilling a different function within the enzyme.

Firstly the tightly bound water:

This water is bonded by LBHB to the extremely polar peptide units of the enzyme. If we consider the analogy with polyamides, they absorb 2-5% of their weight of water readily, which causes a dramatic fall in physical properties of the polymer.[64] Absorption of 2-3% by weight of water corresponds to 25% of all amide cross-linking sites being blocked by hydrogen bonded water. In a polyamide, there are sufficient sites for hydrogen bonding still remaining to form a crystalline polymer of outstanding physical properties. In the protein, the polarity of a peptide unit is identical to the amide unit and these form extremely strong hydrogen bonds with water on the protein. This water does not lubricate the protein, as is often stated, but by analogy to a polyamide it actually stops it becoming an unfavourable rigid molecule, with most of the peptide groups cross-linked to each other by hydrogen bonds. The absorption of this water on to various peptide units is an integral part of the folding process of the protein and is essential for the maintenance of enzyme activity.

Less tightly bound water.

Other water molecules are bound by conventional hydrogen bonds to the less polar side chains of the hydrophilic amino acids. There is also an excess of water associated with the protein, more than is required for the formation of all the hydrogen bonds, the "less tightly bound water". These water molecules are in equilibrium with those bound to the less polar sites. They can in effect change from being inter-molecularly bonded with water to being intra-molecularly bonded, forming new cross-link sites and allowing the protein to change conformation within the limits of the folding process and to hydrogen bond to the substrate. The proposal is that these hydrogen bonds are continually being broken and reformed in equilibrium, as the water molecules move on and off the polar side chains of the protein.

Once the protein has folded to its correct conformation, with its water hydrogen bonded to the appropriate polar sites, we can look on it as a closed system. Any changes in movement of water to a site or away, providing there is no increase in cross-linking or folding, does not involve any further change in entropy. Once the protein is folded, it does not require any further input of energy, while it may change shape, this does not increase or decrease the order of the molecule, therefore there is no overall change in the entropy of the system.

When the substrate molecule approaches the enzyme and enters the site, it has all the degrees of freedom as if it were in dilute solution. However, once it becomes bound, first by hydrophobic attraction and then by the electrostatic attraction, there is a significant loss of entropy as it loses all or most of its translational and rotational degrees of freedom. The remaining energy can now only be vibrational energy, but with the orbital steering due to the geometry of the site and the electrostatic forces, all this energy is directed to the formation of the covalent bond of the enzyme transition complex. However, the

hydrogen bonding of the substrate occurs only to polar sites that were previously hydrogen bonded with water. Once the transition state becomes the product, the water then re-associates with the polar side chains of the enzyme. In the course of the reaction the enzyme may have changed conformation and been temporarily bound to substrate instead of water, but at no time has the enzyme become more or less ordered. Therefore, the entropy of the system has not changed, but for the substrate and transition state there has been a large decrease in entropy until such time as it leaves the enzyme site as product.

Therefore, we may consider the remarkable efficacy of the enzyme as a catalyst to be due to the following factors.

1. A physical attraction between enzyme and substrate in aqueous media.

2. An electrostatic attraction, which pulls the enzyme and substrate into close contact in the optimum spatial arrangement to enter the active site.

3. Within the active site, binding gives orbital steering and the focussing of the molecule's energy into only one degree of freedom with the transition state being stabilised by preoriented dipoles.

4. In the case of the serine proteases and lipases, the remarkable proton transfer mechanism of the triad, which activates the serine hydroxyl group.

In our particular system, we believe there is a further mechanism that will be developed in our later discussions.

Since all enzymes evolved to catalyse reactions in dilute aqueous solutions, we need to consider how the transition to operating in a non-aqueous system, with high concentration of substrates, affects each of these individual rate enhancing mechanisms.

Overall, it has been shown that the activity of an enzyme such as a protease can decline by many orders of magnitude when it functions in a non-aqueous solvent. Zaks and Klibanov [65] demonstrated that the activity of subtilisin Carlsberg declined by 6 orders of magnitude when used in acetonitrile compared to its activity in water. This fact used to be explained by stating that the enzyme changed conformation in solvent, or became less flexible in solvent. However, the reality is far more complex.

Several authors, including Fitzpatrick [66] and Xu, *et al.*,[67] have shown that the overall structure of the enzyme does not change when transferred from water to solvent, but there is always the massive drop in activity. Schmittke,[68] investigated these different factors using subtilisin Carlsberg. They also observed a fall in activity, of 7 orders of magnitude, when the enzyme was in solvent.

Of this difference, approximately 2 orders of difference were attributed to the change in the activity – pH profile when the enzyme was changed from water to solvent.

The desolvation energy of the substrate is much higher in non-aqueous media than in water, this affects the binding energy that is required for catalysis. It was estimated that this would also cause a drop in activity of 2 orders of magnitude.

The third cause is the reduced flexibility of the protein due to the solvent dehydrating the enzyme by displacing some of the less tightly bound water molecules on the enzyme. Though this cannot be seen by any difference in secondary structure of the enzyme, there are subtle differences in the tertiary structure that may be picked up by NMR and Far UV

spectroscopy. This effect has also been attributed to an expected fall in activity of approximately 2 orders of magnitude.

The above work leaves just one order of magnitude unexplained. This may possibly be due to the lack of hydrophobic interaction between the enzyme and substrate, which was not considered in the above work.

It has been shown by Halling [69] that for many non-aqueous enzyme systems, it is the water content which is the single most important parameter. This affects the activity of the enzyme and the thermodynamic water equivalent (a_w) is the best way of measuring the availability of the water in the system. It must be remembered that the importance of the water content as measured by a_w is not due to the fact that it is a reactant, but rather because of its effect on the free water/less tightly bound water equilibrium within the enzyme.

There are some enzymes; our *Candida antarctica* lipase B (CALB) is one, where the activity of the enzyme is largely independent of the water activity of the system,[70] though why this should be is not clear at present.

1.8 Outline of the research project.

After consideration of the above, it is obvious that in our work on the kinetics of the esterification using CALB we must consider the following.

1. The effect of the hydrophobicity of the system, including both reactants and medium; its impact on enzyme substrate binding and on the electrostatics within the enzyme and on its surface.

2. The solubility of the substrates in the medium in which the reaction is being carried out and the changing solubility as the reaction proceeds.

3. The effect of pH on both the pK_a of the key components of the catalytic triad and on the electrostatic forces within the enzyme and between the enzyme and substrate.

4. What structural changes, if any, occur within the enzyme under the conditions of the reaction in the different media and during the course of the reaction?

In particular, we wish to determine why transesterification occurs under some conditions and not others? Knowledge of the conditions required for optimum enzyme activity will lead to shorter reaction times and improved enzyme recyclability.

2 Development of methods.

In order to decide on the experimental techniques that we might use to follow the kinetics of the polyesterification reaction we need to consider the mechanisms of the reactions most likely to be involved.

The reaction of the diacid with the diol in our system is a typical esterification reaction. As an enzyme catalysed reaction, it is complicated by the fact that it is a 'ping-pong' reaction;[71] nevertheless, like all esterifications the reaction rate is affected by the concentration of both acid and diol.

$$\text{Rate} = k[A][B]$$

The actual progress of the reaction is best shown as a Cleland plot;[72] see Scheme 3.

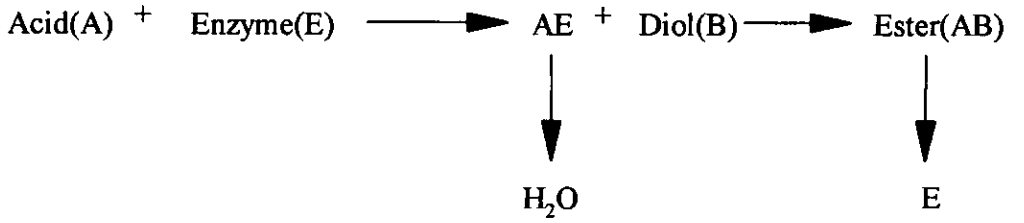

Scheme 3 Cleland plot for the esterification reaction.

In our case, the rate considerations are complicated, by the complex and changing nature of the polymerisation reaction, which involves a number of steps, *viz.*:

$$A + B \rightarrow AB$$

$$AB + B \rightarrow BAB$$

$$2\,AB \rightarrow ABAB$$

The only possible reaction which might be expected, but which has been shown not to occur is:[16]

$$AB + A \rightarrow ABA$$

In addition to the number of possible reactions, there are changes in the rate caused by the changing concentration of the reactants. In addition, the rate becomes diffusion controlled and finally as the polymerisation proceeds there is a significant increase in the viscosity of the medium, which adversely affects the rate according to the Stokes-Einstein equation.[73]

In order to overcome these problems and to simplify the reaction being studied we chose only to investigate the reaction of A + B in a vast excess of diol B. The reaction then becomes independent of [B] and the only reaction of consequence is:

$$A + B \rightarrow AB + H_2O$$

When studying the kinetics of a reaction it is necessary to decide first, on what is to be measured. The rate of increase of formation of product, the rate of decrease of substrate or the change in some physical property such as viscosity, pH or absorbance that may be related directly to the rate of reaction.

In the esterification reaction it was thought feasible that we could measure the decrease in diol or acid substrate or the production of product, in particular the water produced during the reaction. It was then necessary to decide between a continuous and a stopped assay of the reaction. Most studies of enzyme kinetics use some form of stopped assay either by sampling from the continuing reaction or by stopping the reaction at specific times during

A stopped assay using chromatographic techniques such as HPLC or GCMS was considered so that the decline in substrate and increase in product could be followed, however, we did not have regular continuous access to these instruments. It was considered that having to take samples and store them until such access was available would introduce significant unknowns, particularly as the enzyme is active at a temperature only slightly above ambient. Also the substrates were known to absorb water from the air, this would cause distortion of the results or at worse, reversion of the esterification reaction.

There is an inherent attraction in a continuous assay, in that there is a sense of being able to watch the reaction as it proceeds. We were interested in the initial rate of reaction, but were reluctant to use a technique which involved extrapolating a later rate back to zero time. It is the initial rate that gives all the information about the affinity of the enzyme for the substrate. Therefore, the uncertainties that would arise from the back extrapolation of data would create doubts about the validity of any conclusions resulting from such data.

Therefore, having reviewed all available techniques, it was decided to attempt to develop methods that would enable one to carry out a continuous direct measurement of the rate of reaction, with sufficient sensitivity that the initial rate data would be meaningful.

2.1 Spectrophotometry.

Spectrophotometric techniques have been used for many years to follow the kinetics of enzymatic reactions, however, they do require one of the reactants or the product to absorb light, most commonly in the ultraviolet or visible regions of the spectrum.

Spectrophotometry is most useful in enzyme kinetics, when one of the products is a naturally occurring chromophore like NADH, a co-enzyme to some of the dehydrogenases.[74] In the case of the lipases and esterases, much work has been done using artificial substrates such as *p*-nitrophenyl esters, because the *p*-nitrophenolate ion absorbs strongly at 400 nm.[75] These methods become impractical when the reactants do not have a chromophore, are present at high concentrations or the system is not homogenous, all of which apply in our lipase system. In addition, it is known that both the reaction profile and the products formed in our system vary according to the reaction media and conditions. We therefore considered that the use of an artificial chromophore in the system would give results that would not be relevant to the studies on the polyesterification of diols and diacids.

When considering other possible spectroscopic methods that might be used to follow the reaction kinetics of the polyesterification reaction, it seemed obvious that the choice was to follow either the conversion of the carboxylic acid to ester, the concomitant formation of water or the conversion of the hydroxyl to ester. The OH stretch from water and both types of hydroxyl overlap in the mid-infrared region, as do the carbonyl bands of the ester and carboxylic acid. Therefore, it was decided to explore the possibility of using near infrared (NIR) spectroscopy to differentiate between these compounds.

2.2 Introduction to near infrared spectroscopy.

The NIR region of the electromagnetic spectrum covers the range of wavelength between approximately 780-2500 nm. NIR spectroscopy has been used by a number of workers to measure the hydroxyl content in alcohols, albeit in simple laboratory conditions.[76,77,78]

More recently, several authors have developed NIR methods for following the process of the manufacture of polyether and polyester polyols by monitoring the hydroxyl number as the reaction proceeds.[79,80,81]

The principle behind all infrared spectroscopy is that by using radiation of a specific wavelength it is possible to excite a chemical bond from its vibrational ground state to its fundamental state. The measurement of the absorbance at a specific wavelength gives a fingerprint of the different types of chemical bonds within the molecule. Generally, in the mid infrared range the spectra exhibit sharp and narrow peaks that are essentially the fundamental modes of vibration of specific bonds. In the near infrared region, in essence, too much energy is put into the bond and so like any harmonic oscillator the vibrational energy, which is made up of many forms of bending and stretching moments, creates significant overtones of the fundamental vibration. In addition, when a bond absorbs a quantum of energy, thereby increasing its own overtone and combination vibrational energy, it can share some of this energy in a non-quantised manner with adjacent bonds. Therefore, the absorbance seen is due to the infrared energy absorbed by the principal bond plus that shared with adjacent bonds; this absorbance is termed a combination band. The NIR region contains numerous bands, especially those related to the fundamental C-H, O-H and N-H vibrations. Such vibrations are particularly significant because of the anharmonicity of these vibrations, which arises due to the light hydrogen atom in the bond.

In the near infrared spectrum the merging of many combination bands with the 1st, 2nd and 3rd overtones produces broad bands, which are the result of many individual overlapping peaks, this usually gives a hopelessly complex spectrum. The apparent impossibility of obtaining meaningful results from such a spectrum is overcome by the use of

sophisticated computational methods such as: multiple regression analysis of selected wavelengths, or global methods such as principal components regression (PCR) or partial least squares (PLS), which use the whole spectrum.[82] In order for such mathematical techniques to produce useful results, two criteria must be met. Firstly, a large number of scans should be taken at a constant temperature and averaged by the software. Secondly, many samples of differing known composition should be available so that using the statistical techniques available in the software it becomes possible to set up a good calibration curve.

As mentioned above, the bonds with the greatest anharmonicity (e.g. those involving hydrogen) vibrate at high energy with large amplitude and have the greatest intensity. In the specific system being considered there is a strong absorbance of the 1st hydroxyl overtone at 1450 nm, unfortunately there is the possibility of confusion with water, which produces an overtone at 1410 nm. However, amongst the stretching/bending combination bands, there is a significant separation between the water combination band at 2250 nm and the hydroxyl combination band at 2075 nm. Furthermore, in the mid infrared, the carbonyl stretch differs little between an ester and a carboxylic acid, but in the near infrared, there is a reasonable separation by the time we get to the 2nd overtone of the carbonyl stretch. In the NIR, the ester absorbs at *ca.* 1950 nm (wavenumber 5128 cm^{-1}) and the carboxyl absorbs at *ca.* 1900 nm (wavenumber 5263 cm^{-1}) (see Figure 2.1).

Initially, we looked at these carboxyl carbonyl overtones, over a range of concentrations, in the NIR spectra of decanoic acid in *n*-heptane, Figure 2.2. We found a good correlation of about 0.99 between absorbance and the concentration of decanoic acid at 1999 nm (5002 cm^{-1}), the OH combination region, but not at the expected carbonyl overtone position of 1901 nm (5260 cm^{-1}).

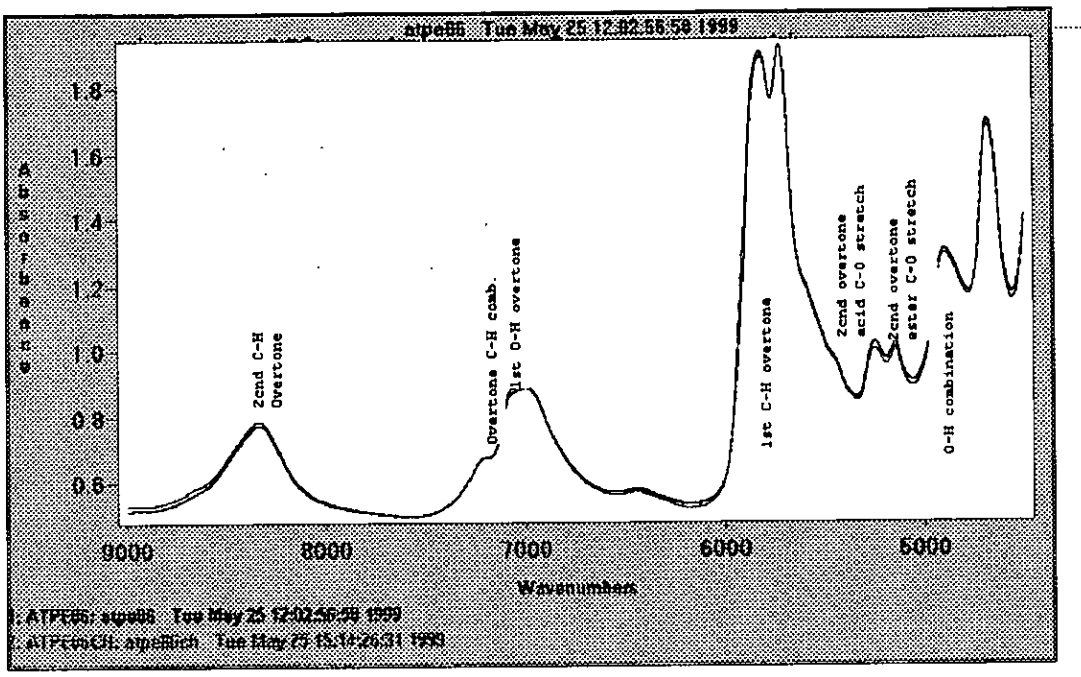

Figure 2.1 Typical Near Infrared spectra of polyesters.

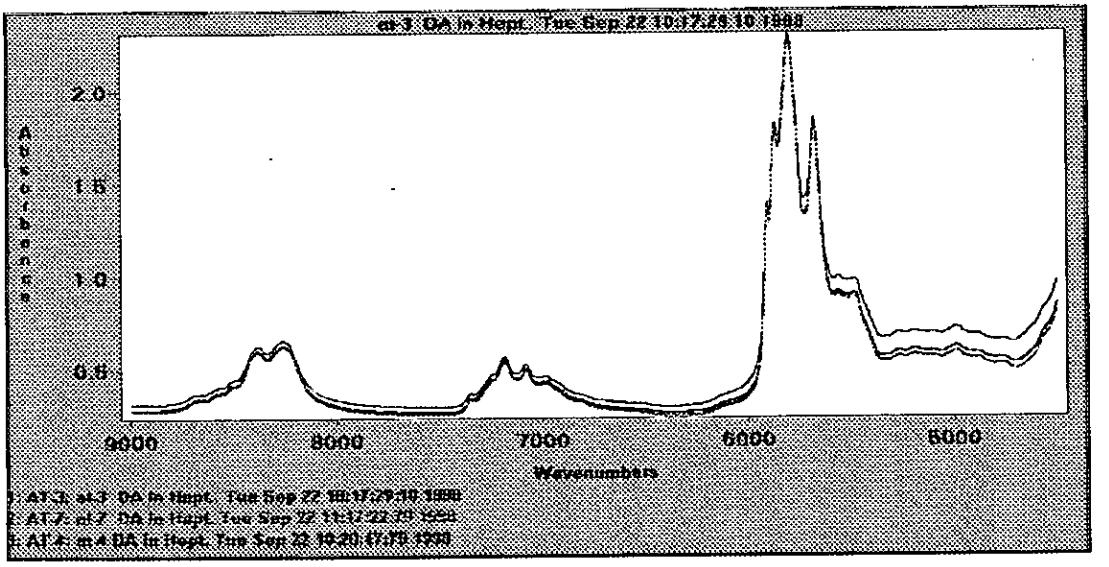

Figure 2.2 NIR spectrum of decanoic acid in *n*-heptane.

This experiment was repeated using decanoic acid in 1,4-butanediol; however, it was found that the correlation at *ca.* 2000 nm had disappeared, even though there appeared to be a reasonable separation and correlation at other parts of the spectrum. When the NIR

spectra of adipic acid in 1,4-butanediol were studied, a reasonable but non-linear correlation between acid concentration and total absorbance at 1960 nm was seen. However, this method might not be relevant when both ester and acid carbonyls are present at the same time. It was attempted therefore to add polyester to the solution in proportion to the reduction in adipic acid concentration in the 1,4-butanediol, in order to simulate conversion of acid to ester. We had great difficulty in getting the polybutane adipate polyester to dissolve in the 1,4-butanediol/adipic acid solutions. The addition of co-solvents such as toluene/IPA and tetrahydrofuran were tried, but no useful correlation between acid concentration and absorbance under these conditions could be obtained.

2.3 Development of NIR method for following reaction kinetics.

Due to the specialised requirements of the proposed enzyme kinetics study, we then looked at developing a method for the determination of the acid concentration in diol at much lower concentrations than would be used in the actual commercial polyester synthesis. A number of standards were prepared of adipic acid in solution in 1,4-butanediol with concentration of acid varying from 0.06% to 5.0% $^{w}/_{w}$. The near infrared spectra were obtained at 60°C; initial examination of the spectra found a clear separation of the spectra across a wide range of wavenumbers. However, it proved impossible to obtain a good correlation between absorbance and the concentration of adipic acid. We then re-examined the spectra using the PLS Quant software. Because of our success in determining the acid values using the specific regions 1850-2080 nm and 1430-1540 nm, we selected these bands for the calibration. The method PLSQ2 used was: Bands 1850-2080 nm and 1430-1540 nm, 6^{th} dimension, cross validate × 10. Using this method for the unknowns gave the results in Table 2.1

Table 2.1 Determination of adipic acid in 1,4-butanediol.

Solution	Titration $\%^{w}/_{w}$	NIR Determined $\%^{w}/_{w}$
AaBd-11	0.32	0.34
AaBd-3	0.59	0.55
AaBd-7	0.91	0.91

A further set of standards was prepared and the calibration curve was rechecked. The fit was not as good as we had hoped, therefore we re-examined the spectra. It was decided that the optimum spectral bands for the polyester determinations were not necessarily the best for the adipic acid in 1,4-butanediol determination. Examination of different regions of the spectrum and relating these to the accuracy of the PLS prediction led us to select the bands 1820-2000 nm and 1470-1670 nm.

The unknowns: AaBd2-4, 2-9 and 2-10 gave the results shown in Table 2.2.

Table 2.2 Determination of adipic acid in 1,4-butanediol.

Unknown	Titration $\%^{w}/_{w}$	NIR Determined $\%^{w}/_{w}$
AaBd 2-4	2.034	2.031
AaBd 2-9	0.222	0.174
AaBd 2-10	0.246	0.262

The spectra were then re-run at 120°C to determine the effect of changing the hydrogen bonding in this system. The results are shown in Figure 2.3.

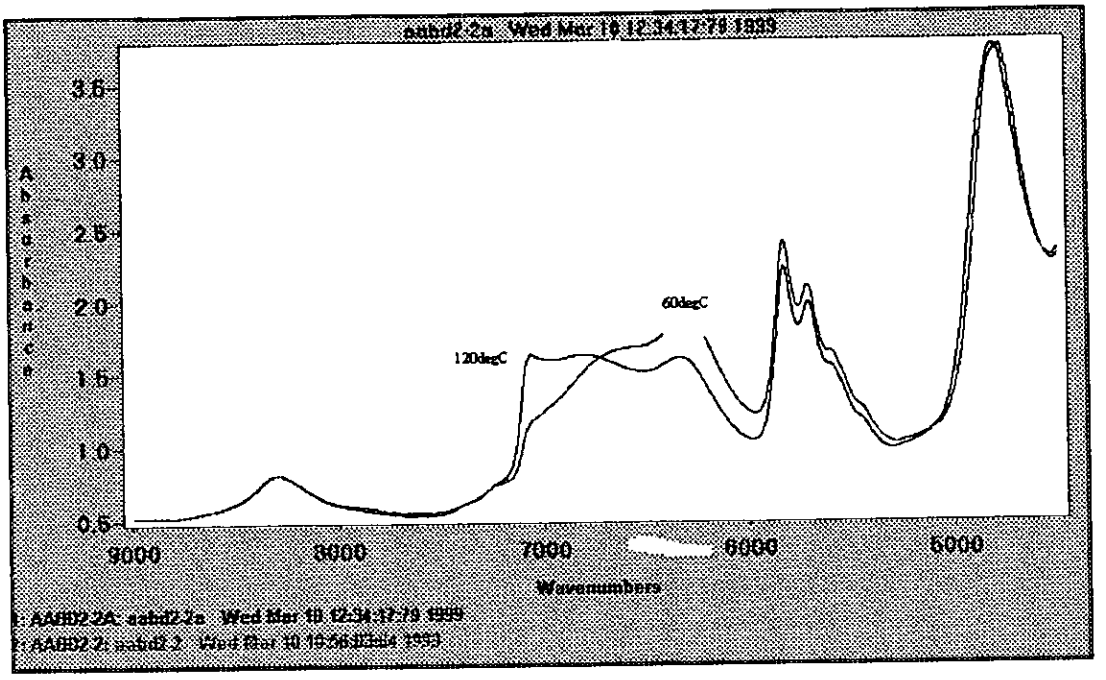

Figure 2.3 NIR spectrum of adipic acid in 1,4-butanediol at 60°C and 120°C.

The very large peak at 2060 nm (4850 cm^{-1}) is the hydroxyl combination band; surprisingly this does not change much between 60°C and 120°C. This is probably due to the large excess of hydroxyl groups overwhelming the influence of the carboxyl H-bonding. The C-H overtones at 1725-1785 nm changed very little, but unsurprisingly, there was a marked change in the O-H overtone at 1430 nm (7000 cm^{-1}). Although there was an improvement in the correlation at 120°C, the method was still not sufficiently accurate at low concentrations.

Due to the poor correlation between absorbance and the adipic acid content, even when using the power of the PLS software, it was necessary to develop a method that would give the accuracy required by the kinetic studies. We have seen the effect that the hydrogen bonding between the carbonyl and hydroxyl groups has on the accuracy of the hydroxyl number determination of polyesters (See Section 10). It can be assumed that the association of the relatively low concentration of carboxyl groups, compared to the vast

excess of hydroxyl groups, prevents an accurate correlation between carboxyl content and absorbance. Therefore, methods by which the hydrogen bonding could be disrupted were studied. The addition of several solvents both polar and non-polar was tried without effect until chloroform was tried, this has the advantages of being almost completely miscible with both the polyesters and the aliphatic diols and it has a relatively clean, simple spectrum in the NIR region. It has four distinct peaks (Figure 2.4), the CH combination at 1850 nm (5400 cm^{-1}), the 1st C-H overtone at 1690 nm (5920 cm^{-1}), the 1st overtone of the C-H combination at 1410 nm (7090 cm^{-1}) and the 2nd C-H overtone at 1150 nm (8695 cm^{-1}).

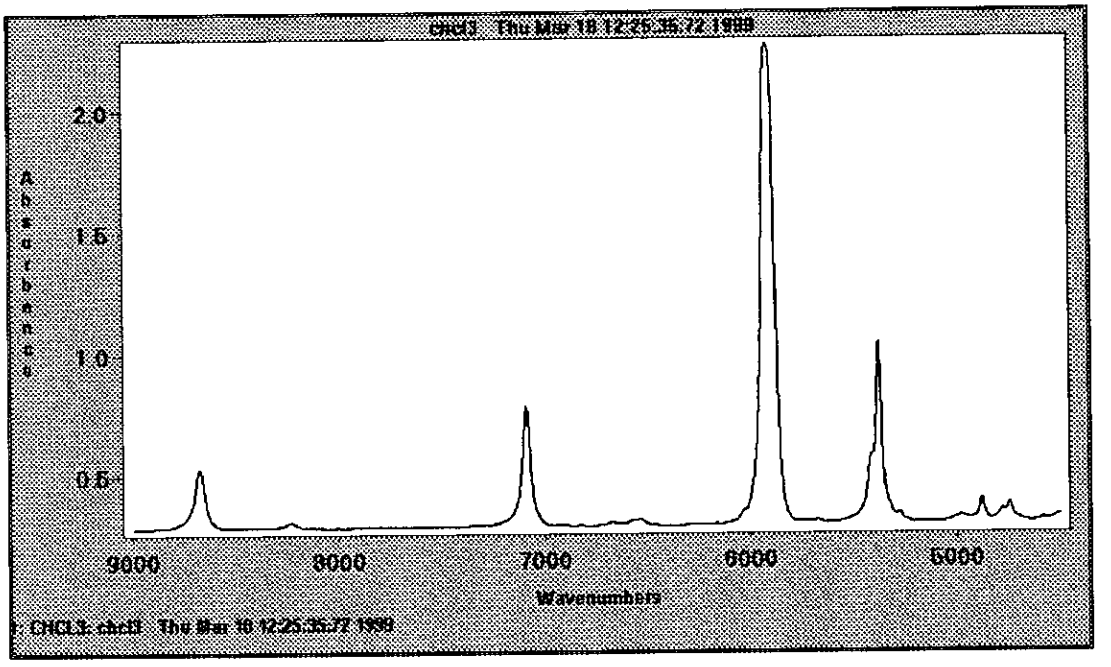

Figure 2.4 Near Infrared spectrum of chloroform.

It was hoped that the polarity of the $CHCl_3$ molecule would disrupt the hydrogen bonding between the carbonyl of the carboxylic acid and the hydroxyl groups of the diol. One drop, about 0.5%$^{v}/_{v}$, was added to the cuvette containing the solution of adipic acid in diol and the NIR spectrum was retaken (Figure 2.5). It was obvious that in addition to the

$CHCl_3$ absorbance, a new peak had appeared at 1938 nm (5200 cm^{-1}) in all the samples. This we attributed to the 2nd overtone of the carbonyl stretch.

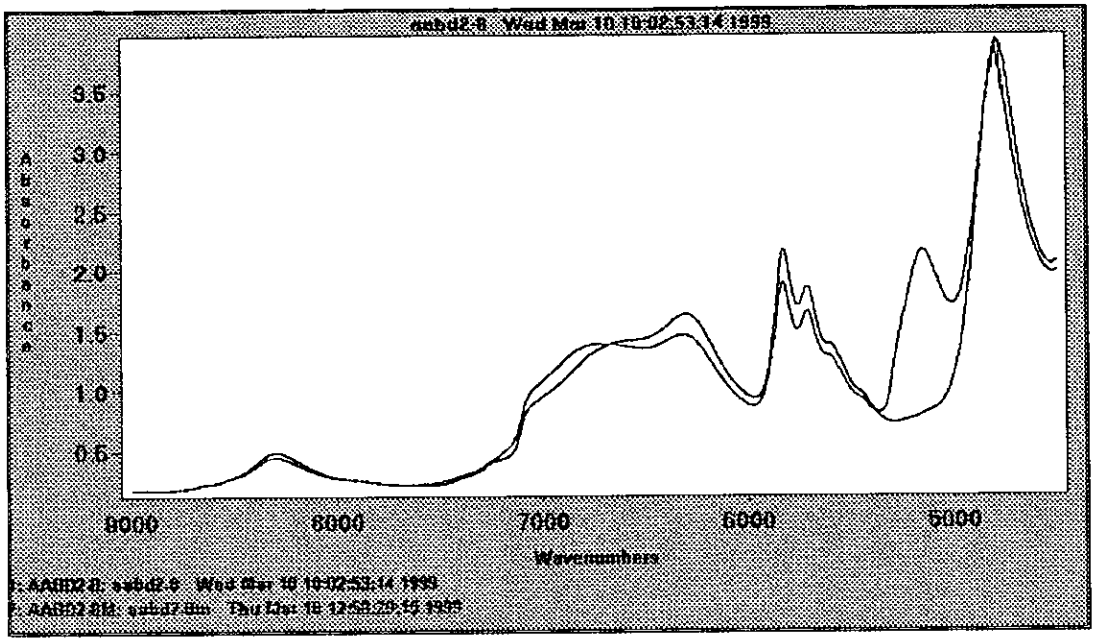

Figure 2.5 NIR spectrum of polybutane adipate + chloroform, (polybutane adipate - blue, polybutane adipate + chloroform - red).

Because the new peak was so clear, we decided to look for a correlation between the absorbance and the concentration of acid without resorting to the use of PLS. After inspection, it was found that the net absorbance at 1938 nm, relative to a base-point at 1887 nm, gave a correlation coefficient R^2 of 0.985 to the concentration of acid. In order to find out if the amount of $CHCl_3$ added was critical, we ran the spectra with increasing amounts of $CHCl_3$ up to 5%$^v/_v$ of the acid/diol solution. No change was observed in the relative size or shape of any of the peaks other than those attributed to the chloroform.

In order to confirm our theory that the chloroform disrupts the hydrogen bonding we repeated the experiments using carbon tetrachloride as the solvent. The carbon tetrachloride has no absorbance in the NIR region. No observable changes occurred, no

relative size or shape of any of the peaks other than those attributed to the chloroform.

In order to confirm our theory that the chloroform disrupts the hydrogen bonding we repeated the experiments using carbon tetrachloride as the solvent. The carbon tetrachloride has no absorbance in the NIR region. No observable changes occurred, no carbonyl peak emerged and the spectra overlapped completely. The polarity of chloroform is far greater than that of carbon tetrachloride; therefore, the latter does not have the ability to form strong polar interactions with the carbonyls of either the ester or the acid groups. It is believed that this confirms that the effect is not a simple solvent effect, but is in fact due to the disruption of the hydroxyl/carboxyl hydrogen bonds, possibly via hydrogen bonding through the chloroform hydrogen (see also Chapter 5).[83]

In confirmation, the effects of addition of similar amounts of chloroform on the spectra of polyesters were investigated. No observable difference in the spectra on addition of 0.5-5.0%$^{v}/_{v}$ of $CHCl_3$ to polyhexane adipate polyesters was seen. However, it is only when looking at the correlation between absorbance and substrate concentration, that subtle differences in the sensitivity of the method can be seen. The calibration of the absorbance of the polybutane adipate polyesters against concentration was then repeated after the addition of approximately 1% of chloroform. The correlation coefficient improved from 0.997 to 0.999. This increase was expected to be small because these were commercial polyesters and the acid numbers were all below 1%, so there was only a small hydroxyl concentration to be freed from association with the carbonyl groups of the acid ends.

The correlation between acid number and the absorbance at the hydroxyl overtone region was then looked at. An excellent inverse correlation between the acid number and absorbance at 2028-2050 nm was noted. This confirmed the above point that the method

is able to detect the additional hydroxyl groups that have been freed from association with carbonyl groups. However, this is not a satisfactory method for the measurement of the actual acid number of the polyester, as it depends on the relative amount of hydroxyl in the polyester and requires the measurement of the absorbance both before and after the addition of chloroform. A similar increase in the correlation between the absorbance at 2028-2050 nm and hydroxyl number, from 0.997 to 0.999, was observed with a series of polyhexane adipate polyesters using the same technique. The net absorbance, at the carbonyl overtone at 1937 nm to a base-point at 1886 nm, gave a poor correlation of 0.80 to the acid number. However, as these were all commercial polyesters with very low acid numbers the correlation was not expected to be very good, as the titrimetric method does not have the accuracy to give a better correlation.

It was hoped therefore to use this technique to follow the initial phase of the reaction in the cuvette in the NIR spectrometer by taking regular spectra as the reaction proceeds.

5-10 mg of the lyophilised *Candida antarctica* lipase B was weighed accurately into NIR cuvettes and the cuvettes filled with a 0.4 M solution of adipic acid in 1,4-butanediol just above its melting point and below the temperature at which the reaction is measurable. The contents were mixed mechanically and the cuvette placed into the Peltier cell of the NIR spectrometer where it was heated to 60°C over 2 minutes. At this point, a NIR spectrum was obtained every minute for 10 minutes. A distinct difference in the spectra was seen, the peak at 5155 cm^{-1} was quite clear so the absorbance at 5155 cm^{-1} was plotted against time (see Figure 2.6).

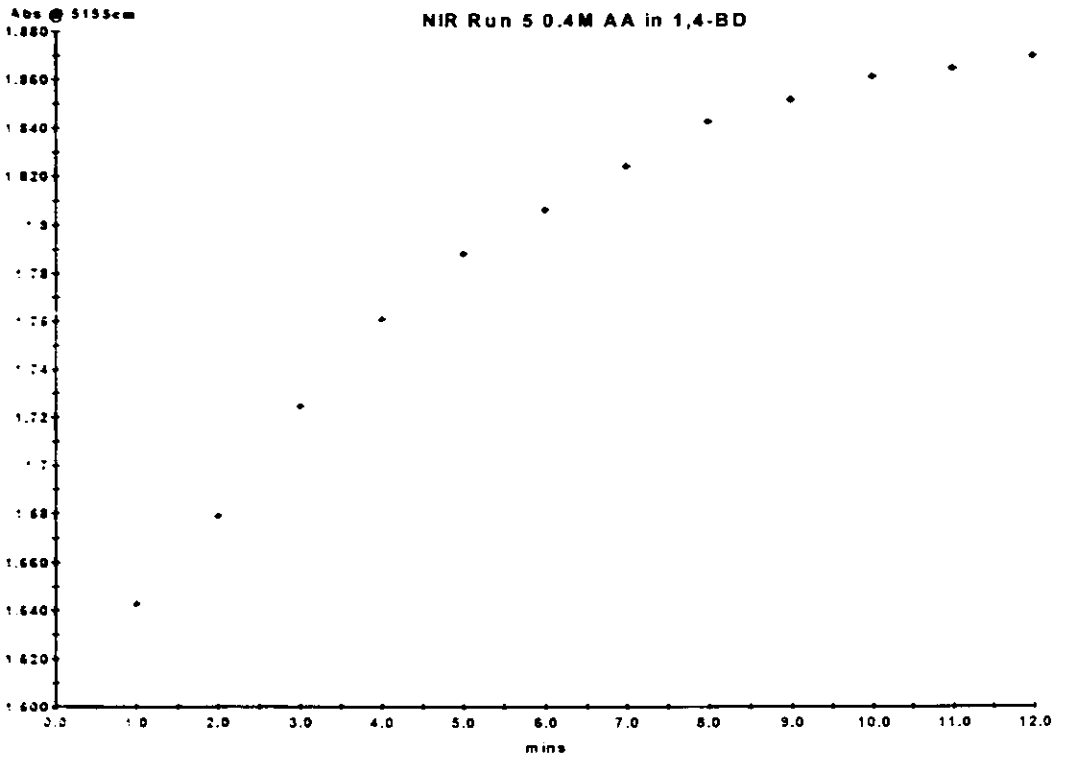

Figure 2.6 Reaction of adipic acid and 1,4-butanediol by NIR.

The rate of change in absorbance was plotted against the amount of enzyme used in each run. We hoped to see a clear first order relationship, which would enable us to use this technique over a range of substrate concentrations in order to determine the Michaelis-Menten constants.

Unfortunately, there was no correlation between the change in absorbance and the amount of enzyme used.

There are several reasons for this apparent anomaly. Although the Peltier cell can raise the temperature quite quickly, it is difficult to ensure the rate is exactly the same for every experiment. In addition, it is difficult to ensure that the small amount of enzyme is adequately dispersed throughout the cuvette. The light beam passes only through a small

section of the cuvette; it is essential that the contents in this region contain a consistent amount of enzyme in order for accurate rate measurements to be made. It is known that water can affect the NIR spectrum and it is quite difficult to be certain that neither the cuvette nor the reaction medium pick up water during the preparation.

In addition to these difficulties, we were concerned that the addition of a solvent such as chloroform might change the reaction as it had been observed in large scale preparations that differences in the reaction occurred if solvents were added.

2.4 Development of Thermogravimetric Methods for Following Enzyme Reactions.

Thermogravimetric analysis (TGA) techniques have a number of advantages that are relevant to the study of any enzyme reaction where a weight loss or gain may be expected. TGA methods use very small sample weights, typically between 10-40 mg per reaction. This can be a valuable benefit where either the substrate or the enzyme is not readily available in large quantities.

Modern TGA instruments have the ability to control the temperature of the sample more accurately than almost any other technique that may be used to follow a chemical reaction. Due to the small sample size, TGA instruments have the ability to raise the temperature to the chosen reaction temperature very quickly. In the case of an enzymatic reaction, where the enzyme may have some activity at or just above room temperature, this can be most important. When studying enzymatic reactions it is always the initial reaction rate that is used to characterise the enzyme, if the reaction occurs while the sample is being heated to the desired temperature the results obtained may be inaccurate.

TGA instruments are designed to operate so that the reaction may be carried out in a controlled atmosphere with an accurately controlled gas flow. This is particularly relevant, when volatile products or co-products are produced which may need to be removed for the forward reaction to proceed.

The major disadvantage with TGA instruments is that there is no provision for stirring the sample during the reaction; therefore, studies where mass transfer is important cannot be carried out. In the case of an enzymatic reaction, provided that the enzyme can be readily incorporated into the sample, this is not a major problem, as interest is usually in the initial reaction.

As stated previously, it is essential that the reaction studied involve a measurable change in weight in order to use TGA techniques. The synthesis of esters by direct esterification or transesterification, because of the production of volatile co-products such as water or an alcohol, seemed to be potential candidates for study using TGA.

One of the problems that is specific to enzymatic reactions is that different enzymes contain differing amounts of water and more importantly require different amounts of water in order to function,[84] (see Section 1.7). The actual water requirement is usually specified as the thermodynamic water equivalent that gives the optimum activity of the enzyme. The lipases typically require a lower water activity in order to function than other enzymes. *Candida antarctica* lipase B has been shown to require very little water, expressed as water equivalent in order to function.[85] Therefore, we were optimistic that residual water in the enzyme would not have a significant effect on our measurements nor would the low water environment have an adverse effect on the activity of the enzyme.

Experiments were then carried out involving the polyesterification of the diols 1,4-butanediol and 1,6-hexanediol with adipic acid in order to evaluate the utility of TGA for following these reactions. It became obvious that there were several problems, some general and some specific to our system, which had to be considered when using the TGA for this purpose.

In order to obtain consistent, reproducible results it is necessary to remove the water of reaction, this we did by passing dry nitrogen over the sample. We found that if the flow rate varied by more than ± 20% we could easily see the difference in the rate of removal of water. It also became obvious that the surface area to volume ratio of the sample affected the rate of removal of water. However, both of these problems were easily resolved.

The TGA has an accurate gas flow control system so it was decided to control the nitrogen flow at 50 ml min^{-1} for all future experiments. The TGA uses aluminium pans, which are of closely matched size and shape so that the surface area of the sample can be fixed. It was not difficult to develop a technique whereby the sample volume was maintained between 20-25 µl. However, if the sample volume were increased to 40 µl then there was a measurable reduction in the rate of removal of water from the sample. We assumed that this was due to the longer diffusion path for the water to reach the surface and that this was becoming the rate-limiting factor.

We found that some of the substrates, such as 1,4-butanediol and 1,6-hexanediol, although having boiling points of 208°C and 235°C respectively, nevertheless had significant volatility at 60°-70°C with a flow of nitrogen over the surface. It was realised that if the weight loss due to the volatility of the diol was significant compared to the weight loss due to the removal of water, then this would have an adverse effect on the

accuracy of the method. Therefore, the weight loss of 1,4-butanediol, 1,6-hexanediol and polytetramethylene diol (PTMEG 650) was determined both from neat samples and from samples containing dissolved adipic acid under a nitrogen flow of 50 ml min^{-1} (see Tables 2.3 and 2.4).

Table 2.3 Weight loss of diols at 60°C after drying.

Time, mins	1,4-butanediol, mg	1,6-hexanediol, mg	PTMEG 650, mg
0	23.827	25.112	22.382
2	23.819	25.110	22.382
4	23.897	25.105	22.382
6	23.877	25.101	22.381
8	23.856	25.097	22.381
10	23.834	25.093	22.381
12	23.814	25.090	22.381
14	23.795	25.086	22.381
16	23.775	25.082	22.381
20	23.736	25.075	22.381

The 1,4-butanediol was dried over molecular sieves, whereas the 1,6-hexanediol and PTMEG 650 were stored in a desiccator over phosphorus pentoxide and then preheated to 110°C prior to measuring the volatility at 60°C. The experiments were repeated at 50°C and 70°C. The weight losses measured are shown in Table 2.4.

Table 2.4 Volatility of 1,4-butanediol, 1.6-hexanediol and PTMEG at relevant temperatures.

	Volatility, μg min^{-1}		
	50°C	60°C	70°C
1,4-butanediol	2.5	10.0	16.0
0.4M adipic acid in 1,4-butanediol	2.5	9.8	not done
1.6-hexanediol	0.0	2.0	4.0
0.4M adipic acid in 1.6-hexanediol	0.0	2.0	4.0
PTMEG 650	0.0	0.0	0.0

These weight losses were used subsequently as the correction factors to be deducted from the observed weight loss in the relevant experiments.

We were also concerned that the lack of mixing might affect the accuracy of the method adversely. Thus, several procedures were evaluated.

Diacid, diol and enzyme were mixed below the temperature at which the enzyme was expected to be active and then the temperature was raised quickly to the reaction temperature. This method failed, as 1.6-hexanediol is solid below 45°C and the adipic acid is not readily soluble in either of the diols at lower temperatures and does not dissolve readily at the reaction temperature.

Secondly, the enzyme and diol were mixed prior to putting into the TGA and then a known weight of adipic acid was added to the pan at, or just below the reaction temperature. A dispersion of 0.25% $^{w}/_{w}$ *Candida antarctica* lipase B was made in 1.6-hexanediol, this premix was stored refrigerated and solid samples put into the pan of

the TGA and weighed. The sample was melted, by heating to 50°C and then adipic acid added to the pan and weighed. The temperature was raised to 70°C at a rate of 5°C min^{-1} under a N_2 flow of 50 ml min^{-1} and the reaction started within a few minutes as the adipic acid began to dissolve in the diol. The weight loss was monitored over a period of 140 min (see Figures 3.9, 3.17 and 3.18 for examples of raw data), the rate was measured and the weight loss due to the evaporation of 1,6-hexanediol was deducted to give the weight loss due to the loss of water of reaction. The experiment was repeated using a range of adipic acid concentrations from 0.23 M to 1.66 M. The results are shown below in Table 2.5 and Figure 2.7.

Table 2.5 Rate of reaction of adipic acid and 1,6-hexanediol at 70°C.

[adipic acid]	Enzyme	Rate of water loss*		Adipic acid conversion
mol dm^{-3}	mg	µg min^{-1}	µmol min^{-1} mg^{-1}	µmol min^{-1} mg^{-1}
0.23	0.325	9.84	16.9	8.5
0.35	0.245	8.8	20.4	10.2
0.4	0.252	10.4	23.0	11.5
0.49	0.252	13.0	28.5	14.5
0.85	0.662	11.9	10.0	5.0
1.02	0.725	14.5	10.7	5.5
1.07	0.593	9.7	9.1	4.5
1.23	0.751	11.1	8.2	4.0
1.66	0.598	7.9	7.3	3.7

*Correction factor for 1,6-hexanediol loss is 2µg min^{-1}

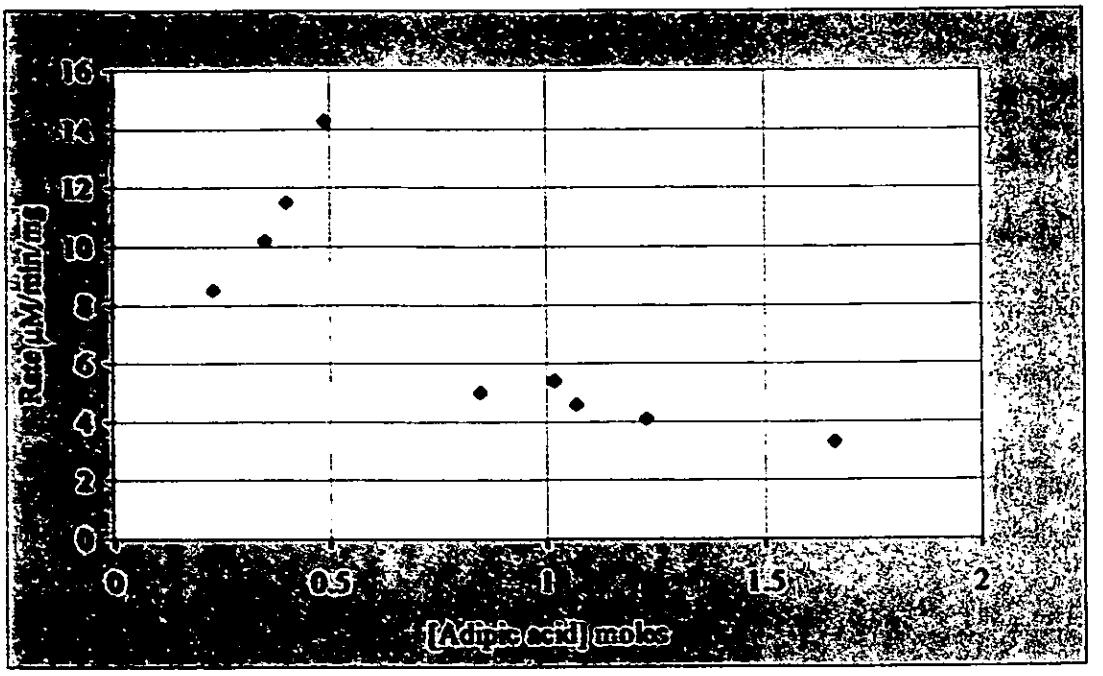

Figure 2.7 Effect of adipic acid concentration on its reaction with 1,6-hexanediol.

The graph in Figure 2.7 shows two quite distinct regions: up to a concentration of 0.49 M the rate increases as expected with the increase in the concentration of the substrate. Above this concentration, we see a marked decline in the reaction rate, which is more or less independent of the substrate concentration at a constant rate of 10 μg min^{-1} mg^{-1}. It was thought that this apparently anomalous observation was due to the limited solubility of adipic acid above 0.5 M when the dissolution of adipic acid becomes the rate-controlling factor. However, this would not explain the decline in rate above 0.5 M. Subsequent work showed that at the higher concentrations of acid, the increased pH of the medium has an adverse effect on the enzyme. In addition, it was considered that at a temperature of 70°C the evaporation errors were becoming significant, thereby decreasing confidence in the results.

The main disadvantages of this technique arise due to the poor solubility of adipic acid in

the diol and the fact that each of the acids to be studied has a different solubility. Because of this, we might not know the concentration of the acid accurately during the key initial stages of the reaction, we decided therefore not to continue using this method.

The third method evaluated involved pre-preparation of a solution of the acid in the diol at an accurately known concentration; approximately 25mg (accurately weighed) were placed in the TGA pan. The enzyme was then added to the solution at just below the temperature at which it becomes active, i.e. 30°-40°C, and then the temperature was raised quickly to the reaction temperature. The obvious problems with this technique were the non-dispersion of the enzyme into the substrate solution and the impossibility of adding exactly the same amount of enzyme to each experiment. We also found subsequently that if the enzyme is added to the mix below its melting point the gas flow in the apparatus may blow some of the enzyme from the surface before it has had a chance to disperse. However, we found that the finely powdered nature of the lyophilised enzyme meant that it was readily absorbed if added to the liquid reactants in the TGA pan. Providing that no lumps or aggregates are added then the enzyme is rapidly wetted by the substrate and the reaction starts immediately at a temperature above 50°-55°C. The problem of not being able to control the exact amount of added enzyme was not considered to be important, providing the exact amount of enzyme was known and that the reaction rate could be shown to be first order with respect to the concentration of enzyme. All things being considered we were confident that this would be the best technique to use.

Using this technique, we looked at the effect of varying enzyme concentration on the reaction rate when the substrate is at a concentration above 0.5 M. We prepared a 1.14 M solution of adipic acid in 1,6-hexanediol by heating to 100°C for 1 hour and then

transferred approximately 25 mg to the TGA pan and weighed accurately. When the TGA had cooled to 60°C some of the adipic acid would fall out of solution. When the mixture had cooled to 50°C, the *Candida antarctica* lipase B was weighed carefully onto the surface of the substrate where it was absorbed rapidly into the solution. The reactants were then heated to 60°C at 5°C min^{-1} whereupon the reaction would start. The results are shown in Table 2.6 and Figure 2.8.

Table 2.6 Rate of reaction of adipic acid and 1,6-hexanediol at 60°C.

[adipic acid]	Enzyme	Water loss*	
mol dm^{-3}	mg	µg min^{-1}	µmol min^{-1} mg^{-1}
1.14	0.043	9.9	3.5
"	0.099	5.4	3.0
"	0.100	6.6	3.7
"	0.160	9.0	3.15
"	0.170	8.8	2.9
"	0.175	10.2	3.2
"	0.295	16.3	3.1
"	0.382	21.1	3.1
"	0.518	29.0	3.1

*Correction factor for 1,6-hexanediol loss 2µg min^{-1}.

The data shown in Figure 2.8 was analysed using the Enzfitter curve-fitting program. The Marquardt-Levenberg algorithm was used to get the best fit and to give the analysis of variance. The fitted data are shown in Table 2.7.

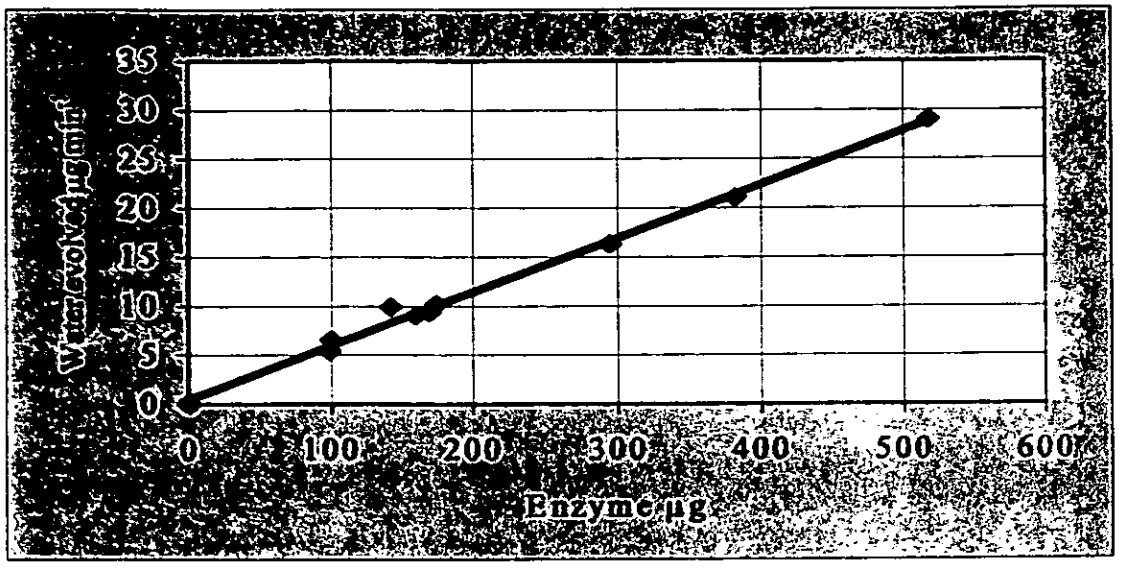

Figure 2.8 Effect of enzyme concentration on rate of reaction.

Table 2.7 Statistical analysis of effect of enzyme concentration on rate.

Enzyme mg	Observed Water µg min^{-1}	Predicted Water µg min^{-1}	Residual	% Residual
0.043	2.7	2.4346	0.2654	9.83
0.099	5.4	5.5931	-0.1931	-3.58
0.1	6.6	5.6494	0.9506	14.40
0.16	9	9.0181	-0.0181	-0.20
0.17	9.3	9.5781	-0.2781	-2.99
0.175	10	9.8579	0.1421	1.42
0.295	16.3	16.541	-0.2412	-1.48
0.382	21.1	21.348	-0.2483	-1.18
0.518	29	28.799	0.201	0.69

The analysis of variance gave a correlation coefficient, R-squared, of 0.9978. This R squared value, is substantially better than anything achieved using the NIR

spectrophotometric methods. On examination of the fitted data it is important to note that the largest percentage residuals (difference between the observed values and the predicted values) are at the low end of the enzyme concentration. This is understandable because of not only the overall sensitivity of the instrument, but the difficulty of determining the exact weight of added enzyme due to minor oscillations of the balance; these errors being of greater significance at the lower weights of enzyme. It was concluded that the optimum weight of enzyme for accurate measurement of the reaction kinetics was between 200-500 µg and that the reaction rate as measured by water loss is in fact first order with respect to the amount of enzyme present.

3. Investigation of the kinetics of the esterification reaction.

3.1 Acid-Diol Esterification.

Using the TGA method developed in Chapter 2 the reaction kinetics were determined for the various substrates of potential interest in the large scale process. While various diacids are available the principal one used in the manufacture of polyesters is adipic acid. Therefore, all of the initial work was done investigating the reaction of adipic acid with various diols. The first system to be investigated was that of adipic acid in 1,6-hexanediol. Solutions of adipic acid in 1,6-hexanediol were prepared, dried, added to the TGA and then an accurately weighed amount of the lyophilised *Candida antarctica* lipase added. After following the pre-programmed heating rate to 60°C the rate of weight loss due to the loss of water was measured. The results for the reaction of adipic acid and 1,6-hexanediol are given in Table 3.1. The Enzfitter program was used to analyse the data and to plot the best fit curve shown in Figure 3.1. The Analysis of Variance gave R-squared (correlation coefficient) as 0.98.

The reaction rate of the intermediate BAB with adipic acid was then determined and compared to the reaction rate with 1,6-hexanediol. The same procedure as the previous experiments was followed. However, when determining the correction factor, the BAB was found to be extremely wet. Thus, it was necessary to develop an alternative procedure so that the BAB could be dried prior to the experiments.

With only a relatively small amount of BAB, insufficient to make up pre-prepared samples, the BAB was weighed directly into the TGA pan before adding the requisite amount of adipic acid. The temperature of the pan was raised at 20°C min^{-1} to 110°C and held for at least 30mins until the rate of weight loss was constant. We assumed that at

this point all the water had been removed and the continuing weight loss was due to the evaporation of the BAB. The sample was cooled to 30°C and re-weighed, we assumed that the weight loss had been due entirely to the loss of water and BAB, i.e. no adipic acid has been lost. The *Candida antarctica* lipase B (CalB) was added to the pan.

Table 3.1 Rate of reaction of adipic acid and 1,6-hexanediol at 60°C.

[adipic acid]	Enzyme	Water loss*	Reaction rate
mol dm^{-3}	mg	$\mu g\ min^{-1}$	$\mu mol\ min^{-1}\ mg^{-1}$
0.74	0.271	15.0	3.06
0.78	0.055	3.1	3.13
0.36	0.094	3.9	2.34
0.51	0.210	10.0	2.68
0.35	0.070	3.0	2.44
0.13	0.550	7.75	0.9
0.21	0.040	1.0	1.39
0.21	0.077	1.75	1.28
0.2	0.260	7.0	1.5
0.74	0.335	19.3	3.2
0.51	0.261	12.4	2.64
0.13	0.165	3.27	1.1
0.1	0.725	7.5	0.7

*Correction factor for loss of 1,6-hexanediol 2$\mu g\ min^{-1}$.

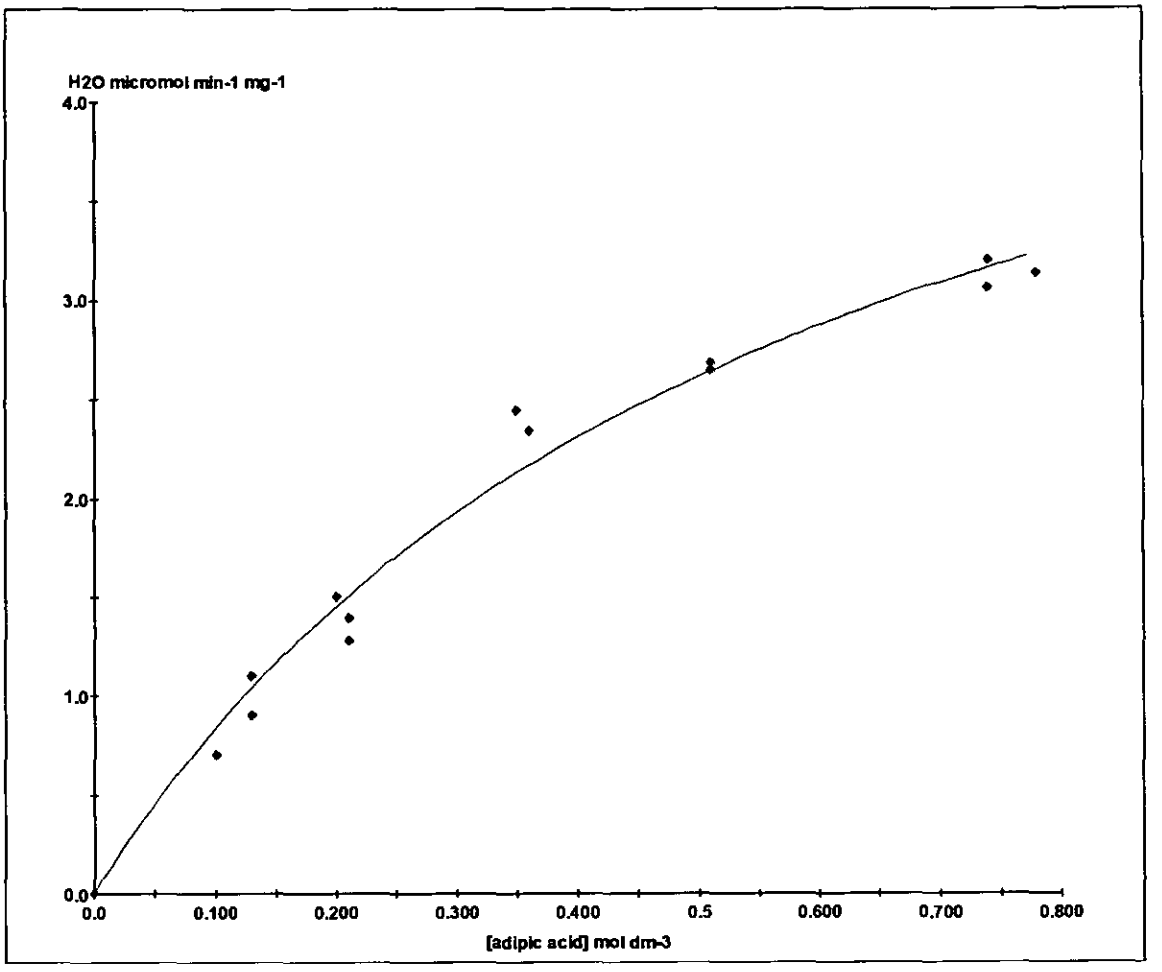

Figure 3.1 Effect of substrate concentration on the reaction rate of adipic acid and 1,6-hexanediol.

In earlier experiments, it was believed that some of the previous inaccuracies were due to the enzyme starting to react while the sample was being heated to the reaction temperature. Therefore, the heating rate was changed to 20°C min^{-1} to 50°C, 7°C min^{-1} to 58°C and 1°C min^{-1} to 60°C. Using this profile we reached 60°C in 100-120s, passed it by 0.5°C and then settled between 59°-60°C. After drying, the weight loss due to the evaporation of BAB at 60°C, was found to be 1 μg min^{-1}, this was then used as the correction factor. The results are shown in Table 3.2 and Figure 3.2

Table 3.2 Rate of reaction of Adipic acid with BAB.

[adipic acid]	Enzyme	Water loss*	
mol dm^{-3}	mg	$\mu g\ min^{-1}$	$\mu mol\ min^{-1}\ mg^{-1}$
0.21	0.215	4.25	1.2
0.36	0.460	9.5	1.9
0.26	0.319	9.0	1.6
0.16	0.203	3.5	1.0
0.24	0.350	9.5	1.5
0.44	0.476	17.0	2.0
0.16	0.160	2.5	0.9
0.1	0.255	2.8	0.6
0.1	0.312	3.7	0.66
0.44	0.287	11.3	2.2
0.57	0.206	8.7	2.34
0.57	0.398	17.0	2.4
0.21	0.401	9.4	1.3

*Correction factor for loss of BAB $1\mu g\ min^{-1}$.

The Enzfitter program was used to analyse the above data and to produce the best fit curve, shown in Figure 3.2. The Analysis of Variance gave R-squared of 0.98.

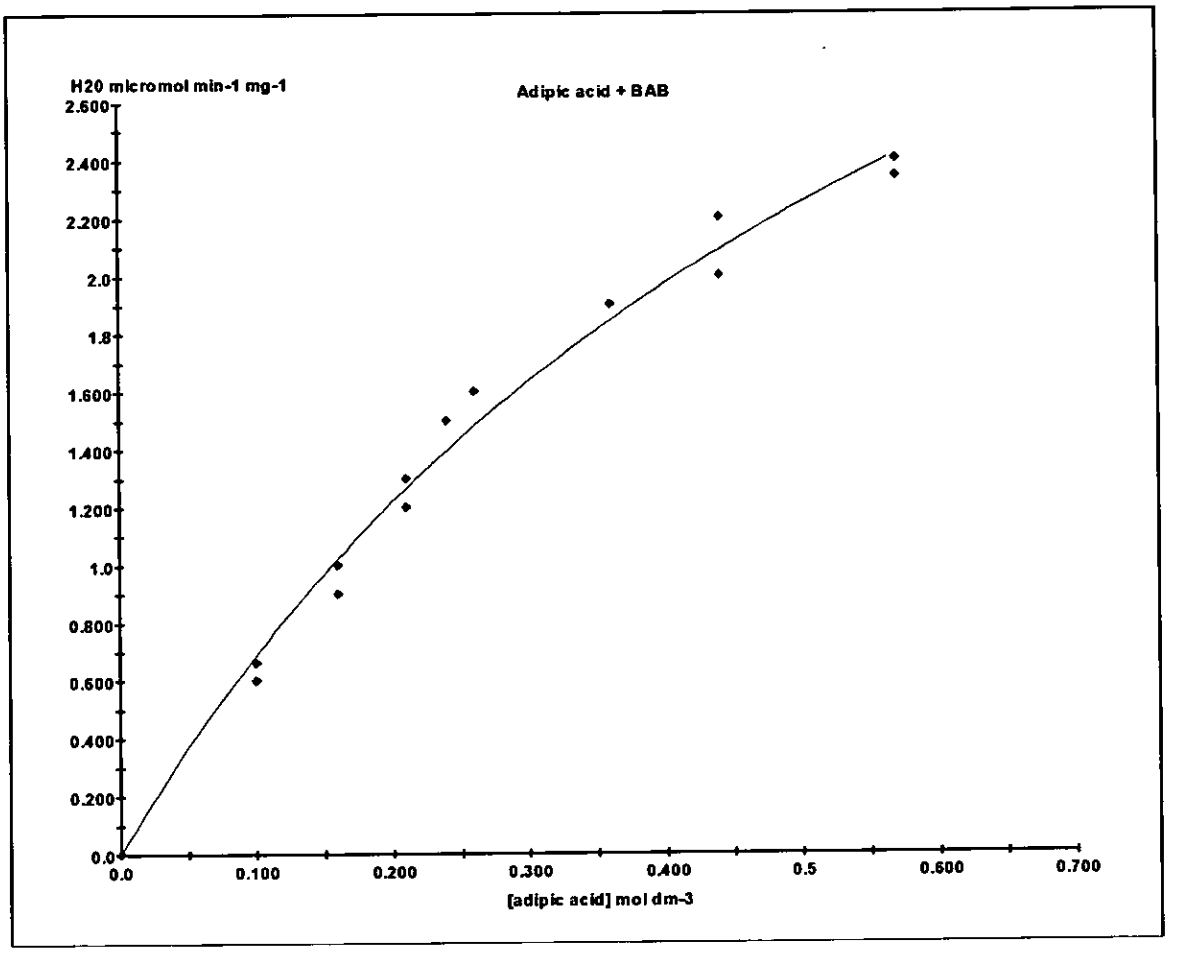

Figure 3.2 Effect of substrate concentration on the reaction of adipic acid and BAB.

Although the rate of conversion of adipic acid was slower with BAB than with 1,6-hexanediol, we were surprised at the comparability of the rate considering the relative size of BAB to 1,6-hexanediol. In order to explore the effect of a significant increase in the size of the diol on the rate it was decided to investigate the reaction of adipic acid with the α,ω–polytetramethylene ether glycol of average molecular mass 650. The procedure followed was the same as that used for BAB. The results obtained are shown in Table 3.3 and Figure 3.3.

Table 3.3 Rate of reaction of adipic acid with PTMEG 650.

[adipic acid]	Enzyme	Water loss*	
mol dm^{-3}	mg	μg min^{-1}	μmol min^{-1} mg^{-1}
0.84	0.120	7.00	3.24
0.3	0.095	3.00	1.80
0.25	0.097	2.80	1.60
0.2	0.103	2.25	1.20
0.45	0.156	6.20	2.20
0.41	0.124	6.50	2.90
0.21	0.180	7.40	2.20
0.36	0.180	7.60	2.35
0.36	0.152	7.00	2.40
0.4	0.269	12.75	2.63
0.4	0.147	6.00	2.27
0.1	0.022	4.00	1.00
0.4	0.345	14.50	2.33
0.1	0.282	4.40	0.90

*No correction factor needed for loss of PTMEG.

The Enzfitter program was used to produce the best fit curve shown in Figure 3.3. The Analysis of Variance gave R-squared as 0.90.

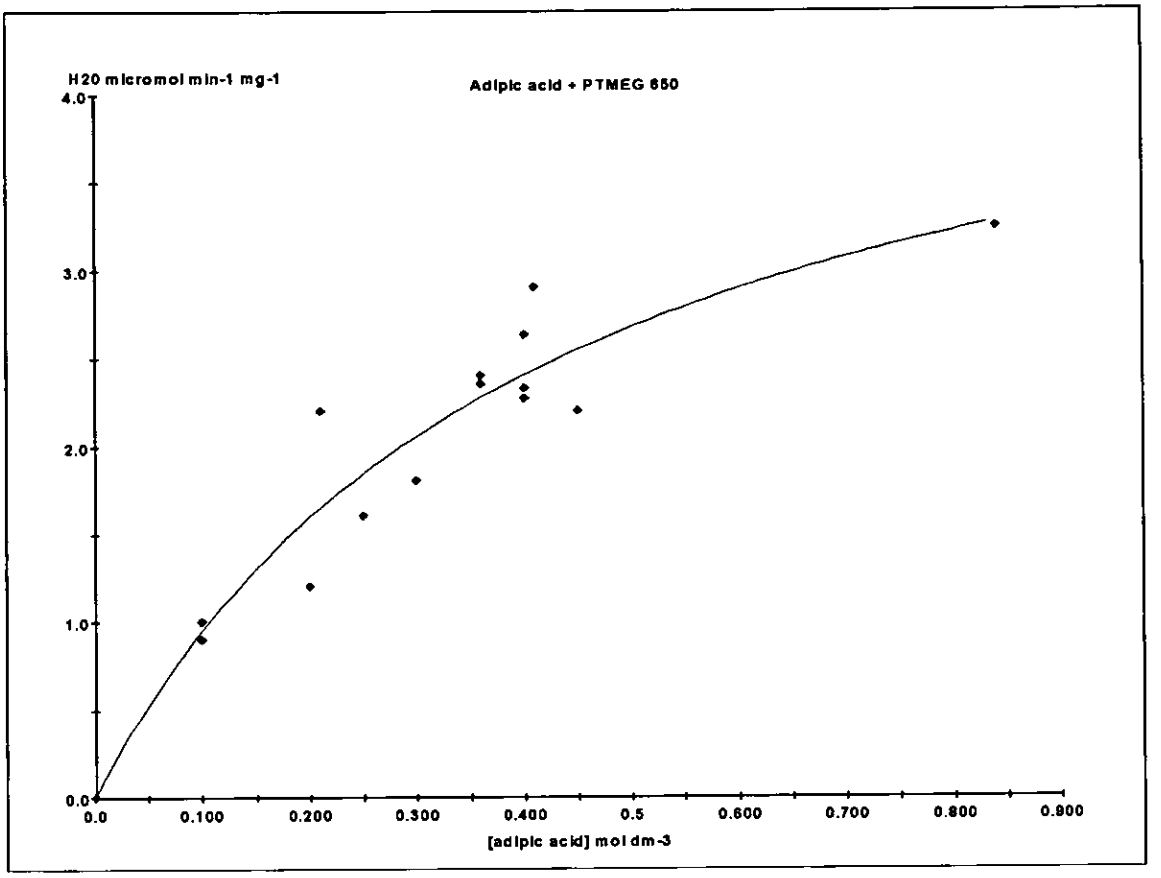

Figure 3.3 Effect of substrate concentration on the reaction of adipic acid with PTMEG 650.

It can be seen that the scatter of the results is greater than for previous series. This may be explained by the limited solubility of adipic acid in the PTMEG. Care had to be taken to ensure that some of the adipic acid did not fall out of solution during the cooling down after the drying cycle, prior to the addition of the enzyme.

The reaction rate was greater than that of adipic acid with BAB in spite of the fact that the excess of hydroxyl groups is significantly lower because of the high molecular weight of the PTMEG 650.

In our earlier work,[13] we had shown the existence of both AB and BAB in the early stages of the polymerisation reaction. Both had been synthesised by the method of Harffey.[16] It

was now logical to look at the rate of reaction of AB under the same conditions as our experiments on adipic acid with the various diols.

The AB was added to the TGA pan and dried by heating for 15min until the weight was constant. It was then cooled and the weight loss at 60°C was measured and found to be negligible. Therefore, weight losses due to AB evaporation were ignored. The sample was then cooled to 30°C and the enzyme added; the temperature was raised to 60°C using the heating profile used for the previous experiments. The results are shown in Table 3.4.

Table 3.4 Reaction rate of AB polymerisation.

Enzyme	Water loss*		AB conversion
mg	$\mu g\ min^{-1}$	$\mu mol\ min^{-1}\ mg^{-1}$	$\mu mol\ min^{-1}\ mg^{-1}$
0.130	11.3	4.8	4.8
0.432	38.5	5.0	5.0
0.246	22.5	5.1	5.1
0.233	17.5	4.2	4.2
Average			4.8

*No correction factor needed for loss of AB.

It was surprising to find the rate to be significantly greater than the reaction rate of adipic acid with 1,6-hexanediol, BAB or PTMEG. Although the AB is not in solution, it must be remembered that the concentration of carboxyl groups is half that compared to adipic acid as it has only the single carboxyl group. In the early stages of the enzymatic polyesterification, we find significant amounts of AB in the reacting mixture,[13] this is surprising in view of the much higher reactivity of the AB, compared to the reactivity of adipic acid with either 1,6-hexanediol or BAB. In order to investigate this apparent anomaly we repeated the AB polymerisation experiments in the presence of adipic acid,

thus simulating the reaction mix in the early stages of the polyesterification. It was assumed that the carboxyl groups of the adipic acid were unlikely to react because of the great excess of AB and the demonstrated much higher reactivity of the AB carboxyl group, see Table 3.5.

Table 3.5 Rate of reaction of AB in the presence of adipic acid.

Adipic acid	Enzyme	Water loss*		AB conversion
$\%^{w}/_{w}$	mg	$\mu g\ min^{-1}$	$\mu mol\ min^{-1}\ mg^{-1}$	$\mu mol\ min^{-1}\ mg^{-1}$
3.9	0.570	19.5	1.90	1.90
5.9	0.544	19.25	1.97	1.97

*No correction factor needed for loss of AB.

As may be seen from these two experiments there is a significant drop in the reactivity of AB when in the presence of adipic acid. This observation parallels that of the decline in reaction rate of adipic acid with 1,6-hexanediol at higher concentrations of adipic acid. Paktar, *et al.*,[86] have shown that pH 7.0 is optimum for the *Candida antarctica* lipase B and that below pH 6.0 there is a dramatic fall in the activity of the enzyme (Figure 3.4).

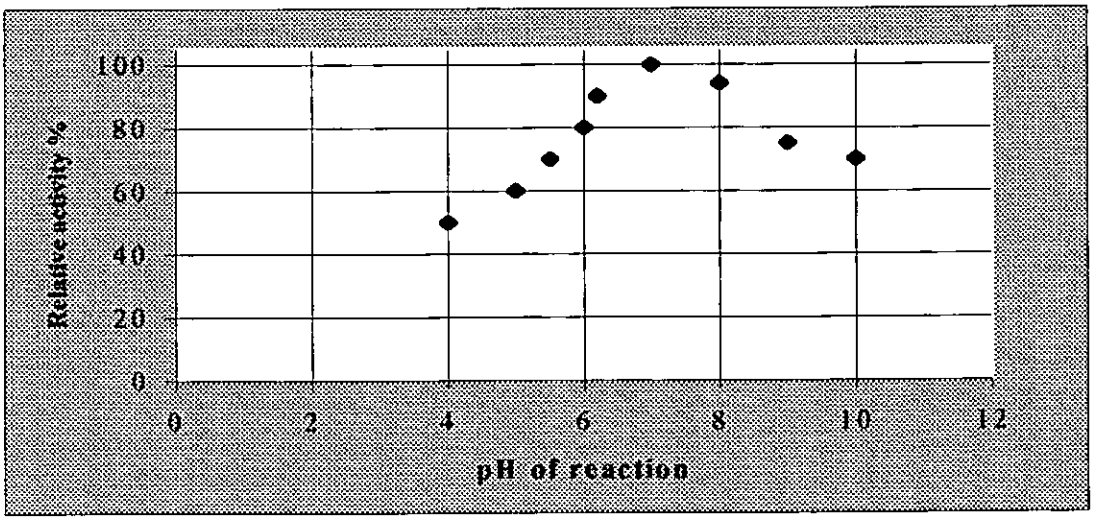

Figure 3.4 The relationship of pH to Activity as determined by Paktar.[72]

The dissociation constants for a series of acids with a range of pK_a's, taken from the Chemical Handbook,[87] are collected in Table 3.6.

Table 3.6 Dissociation Constants of a variety of carboxylic acids.

Acid	pK_a
Aspartic acid	3.9
Adipic acid	4.1 and 4.3
Succinic acid	4.2 and 5.6
Decanoic acid	5.0
Octanoic acid	4.9
Lactic acid	3.1

Unless there are other factors, that might affect the enzyme-substrate reaction, such as steric effects or high concentration, all the acids listed with a pK_a above that of aspartic acid should make suitable substrates for the CALB enzyme. They will not inhibit the dissociation of the proton from the aspartic acid in the catalytic triad. However, these acids will inhibit the protonation of the histidine residue, which has a pK_a of 6.0. By preventing the charge transfer across the histidine ring the media with low pH will slow the reaction rate dramatically as shown in Figure 3.4.

In theory an aspartic lipase should not be able to catalyse the esterification of lactic acid. However, From, *et al.*, have found some small activity with lactic acid although the rate of reaction was very slow.[88]

In addition to the dissociation of aspartic acid, enzymes like all proteins are sensitive to the pH of their environment and their conformation is affected by changing pH. The

dissociation of the proton from the aspartic acid in the catalytic triad. However, these acids will inhibit the protonation of the histidine residue, which has a pK_a of 6.0. By preventing the charge transfer across the histidine ring the media with low pH will slow the reaction rate dramatically as shown in Figure 3.4.

In theory an aspartic lipase should not be able to catalyse the esterification of lactic acid. However, From *et al.*, have found some small activity with lactic acid although the rate of reaction was very slow.[88]

In addition to the dissociation of aspartic acid, enzymes like all proteins are sensitive to the pH of their environment and their conformation is affected by changing pH. The enzyme is held in its optimum conformation by a large number of H bonds, which are altered by changes in pH. In the case of the *C. antarctica* lipase B, Anthonsen has computed the charge distribution around the active site and shown that at pH 4.0 there is a significant difference in the charge distribution and site shape compared to that at pH 7.0 and 9.0.[89] Peterson has shown that the electrostatic potential distribution on the surface of a lipase as a function of pH, determines the pH activity profile of the enzyme.[90] The change in pH affects not only the ionisation of the residues but also the distribution and strength of electrostatic interactions, on or near the surface of the enzyme.

The reduction in the esterification reaction rate of AB in the presence of excess adipic acid implies that the acid is having an adverse effect on the activity of the enzyme. Adipic acid, with its pair of carboxyl groups of similar pK_a, produces a H^+ concentration of between 1.5-1.8 times that produced by a similar mono-carboxylic acid at the same molarity.

In view of these findings it was necessary to learn more about the pH of the various

Table 3.9 pH of adipic acid in water/PTMEG emulsions.

[adipic acid] in water/PTMEG	pH
5ml 0.3 M AA in water + 5ml PTMEG 650, i.e. 0.15 M	2.69
5ml 0.3 M AA in water + 10ml PTMEG, i.e. 0.1 M	2.94
5ml 0.3 M AA in water + 15ml PTMEG 6, i.e. 0.075 M	3.03
5ml 0.3 M AA in water + 25ml PTMEG, i.e. 0.05 M	3.2

The relevance to our system is obvious. Even in non-aqueous media there is a shell of water associated with the enzyme, this aqueous microenvironment is essential for the enzyme to remain active. In a water miscible non-aqueous medium where the water dissociation is suppressed by the organic component, the apparent pH is much higher than when the organic phase at the same concentration is immiscible with the water. With the miscible system, the enzyme experiences a much lower H^+ concentration in its aqueous shell and the pH is much closer to its optimum. This is a simplification of the numerous and complex actual effects that the aqueous/non-aqueous media have on the enzyme.

Some organic solvents that are miscible with water will strip the water from the enzyme, since the water has a greater affinity for the polar solvent than for the enzyme. When this occurs the enzyme loses activity and may be denatured completely.[91] Furthermore, the substrate solubility will differ in various organic media and there will be differences in the partitioning of the acid between the aqueous and non-aqueous phases, which will affect the apparent pH of the enzyme's water shell. Maurel, *et al.*, have shown that in

solvent systems there is a significant perturbation of the pK_a of the ionisable groups of the active site and surface of the enzyme.[92,93]

In order to confirm the effect of pH on the rate of reaction of adipic acid with 1,6-hexanediol, we repeated earlier experiments with and without the addition of *tris*-(2-amino-2-hydroxymethyl-1,3-propanediol) buffer and with part of the acid replaced by the ammonium salt or the amine salt of triethylamine.

A 0.4M solution of adipic acid in 1,6-hexanediol was prepared, the tris buffer was then added; the solution was left at 100°C for 48 hours; then cooled and the lipase added. A very low reaction rate was observed, possibly due to the reaction of tris with the acid or enzyme prior to esterification. A sample of the solution was examined by FTIR and it was found that most of the adipic acid had been converted to the amine salt and rendered inactive. The experiment was repeated without the prolonged heating. The reactants were dried as in previous experiments, the solid tris added and the sample heated to 60°C for 15min until all the buffer material had dissolved. The mixture was cooled, the lipase added and then heated to 60°C (see Table 3.10).

Table 3.10 Reaction rate of 0.4 M adipic acid (AA) + 1,6-hexanediol (HD) + tris buffer.

Substrate	Enzyme	Water loss*	
	mg	$\mu g\ min^{-1}$	$\mu mol\ min^{-1}\ mg^{-1}$
AA + 1,6-HD	0.41	17.0	2.1
AA + 1,6-HD + tris	0.548	28.5	2.9
AA + 1,6-HD	0.389	16.5	2.4
AA + 1,6-HD + tris	0.375	18.0	2.7

*Correction factor for loss of 1,6-hexanediol 2 $\mu g\ min^{-1}$.

Several workers have reported a rate enhancement with the addition of triethylamine to enzymatic reactions. This observation was confirmed in our earlier work.[17] It was suspected that in the case of the synthesis of polyesters, this enhancement was due to a buffering effect, which protected the enzyme from the low pH caused by the ionisation of the adipic acid.

The ammonium salt of adipic acid and the amine salt of triethylamine and adipic acid were prepared. A 0.4 M solution of adipic acid in 1,6-hexanediol was prepared with part of the acid replaced by the corresponding amount of acid as either the ammonium or triethylamine salt. No loss of either ammonia or triethylamine could be detected during the standard weight loss calibration checks. The reaction rates observed with these part neutralised substrates are given in Table 3.11.

Table 3.11 Effect of amine salts on the reaction rate of adipic acid and diol.

Substrate % $^{w}/_{w}$ amine salt	Enzyme mg	Water μg min^{-1}	Rate of water loss μmol min^{-1} mg^{-1}
90% NH_4 AA	0.368	5.4	0.7
62% NH_4 AA	0.487	12.5	1.4
10% NH_4 AA	0.547	17.8	1.4
24% TEA AA	0.801	44.6	3.2

These results appear to confirm that in the case of the triethylammonium salt the presence of the buffer, which increases the pH of the medium, does indeed increase the reaction rate.[94] However, it would appear that the presence of the ionic ammonium salt of adipic acid gives a poorer substrate for CalB. Although triethylamine is the stronger base and therefore the TEA salt more ionised, it may, however, be less polar overall as it has an

organic "sheath" around the N^+, thus it becomes more available as a buffer in the non-aqueous environment. It has been confirmed that buffering can overcome some of the problems caused by the acidity of the adipic acid. The work was discontinued, however, when it was realised that the presence of any of these buffers would have a deleterious effect on the final polyester.

As a result of this work a recommendation was made to change the manufacturing process so the concentration of adipic acid was kept to a minimum particularly in the initial stages of the reaction. Instead of adding the stoichiometric amount of adipic acid at the beginning it was recommended that only the amount of adipic acid be added that could be dissolved in the diol and that this be done prior to the addition of the lipase; the remaining adipic acid being added in stages as the reaction progressed. This procedure was also followed for all the syntheses described in Chapter 9.

3.2 The effect of hydrophobicity of the medium on the enzymatic catalysis of the reaction.

The degree of dissociation of the acid depends on the hydrophobicity of the medium in which it is dissolved and most enzymes are affected significantly by the hydrophobicity of the medium in which they are placed.[95] It is known that most lipases have large hydrophobic regions around the outside of the active site.[96] Some lipases, though not CALB, need a hydrophobic/hydrophilic interface in order to open the 'lid', which is the protein segment covering the active site of the enzyme.[31,97]

Next we investigated the effect of changing the hydrophobicity of the alcohol, effectively the medium, and the second substrate, the acid, and the combination of both of these.

A problem, which affected the choice of alcohols and acids to be studied, is the much higher volatility of the monohydric alcohols and monocarboxylic acids, compared to the di-functional compounds of similar molecular weight. In order to evaluate a much more hydrophobic medium with a relatively low vapour pressure at 60°C we decided to look at the reaction of adipic acid with dodecanol. The dodecanol and adipic acid were dried in a desiccator over P_2O_5 and added to the TGA pan. The solution was heated to 110°C for 15 minutes, cooled to 25°C, the *Candida antarctica* lipase B (CalB) added, the temperature raised to 50°C at 20°C min^{-1}, to 58°C at 7°C min^{-1} and to 60°C at 1°C min^{-1}. The results are shown in Table 3.12 and Figure 3.5.

Table 3.12 Rate of reaction of adipic acid with dodecanol.

[adipic acid]	Enzyme	Water loss*	
mol dm^{-3}	mg	µg min^{-1}	µmol min^{-1} mg^{-1}
0.21	0.309	6.78	1.22
0.21	0.400	8.64	1.2
0.26	0.282	7.91	1.56
0.12	0.275	4.63	0.8
0.44	0.322	10.5	1.8
0.5	0.206	7.19	1.94
0.55	0.358	13.5	2.1

*Correction factor for loss of dodecanol 2.5 µg min^{-1}.

The data was analysed using the Enzfitter program to produce the best fit curve shown in Figure 3.5. The Analysis of Variance gave R-squared as 0.99.

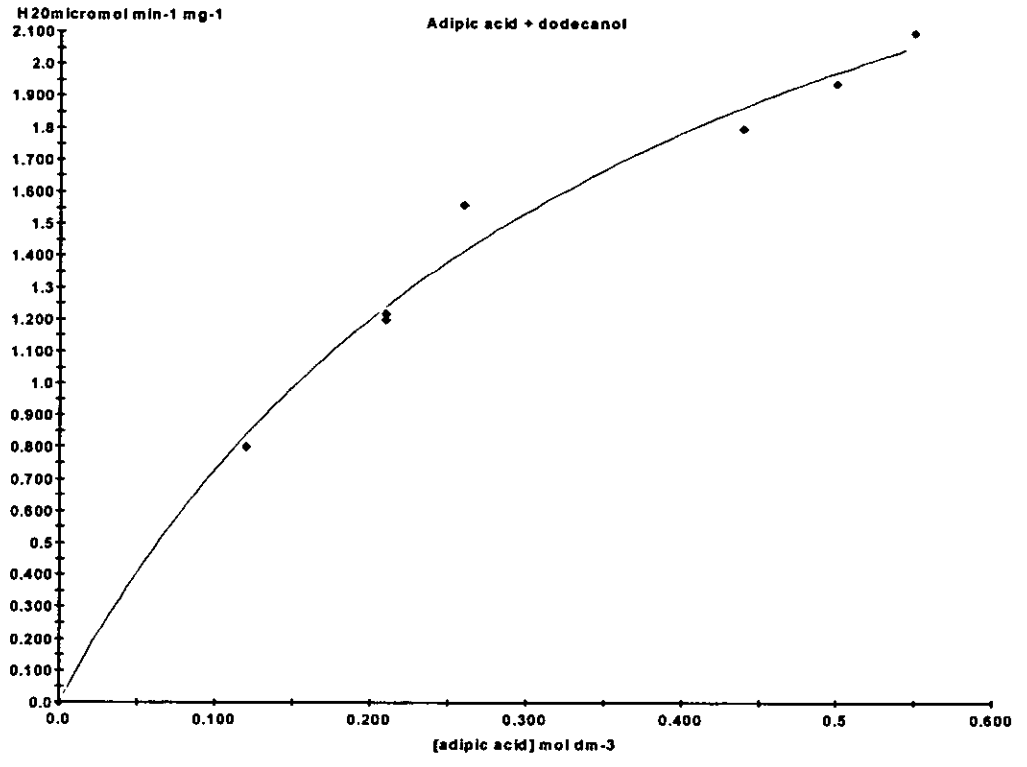

Figure 3.5 Effect of substrate concentration on the reaction rate of adipic acid with dodecanol.

We then repeated the experiments using solutions of decanoic acid in 1,6-hexanediol and decanoic acid in dodecanol. Because of the extremely low vapour pressure of adipic acid it had been assumed that in all previous experiments there was no loss of adipic acid by evaporation; therefore no loss in concentration during the experiments. However, this assumption cannot be made for a monocarboxylic acid like decanoic acid in a monohydric alcohol. Literature [98] vapour pressure data for decanoic acid and dodecanol are compared in Figure 3.6. The two curves are almost identical, so it was assumed that the relative composition of decanoic acid in dodecanol would not change during the drying cycle or reaction. The weight loss correction factors for decanoic and adipic acid solutions in 1,6-hexanediol were the same. The reaction conditions were the same as for the previous experiment and the results are in Table 3.13 and Figure 3.7.

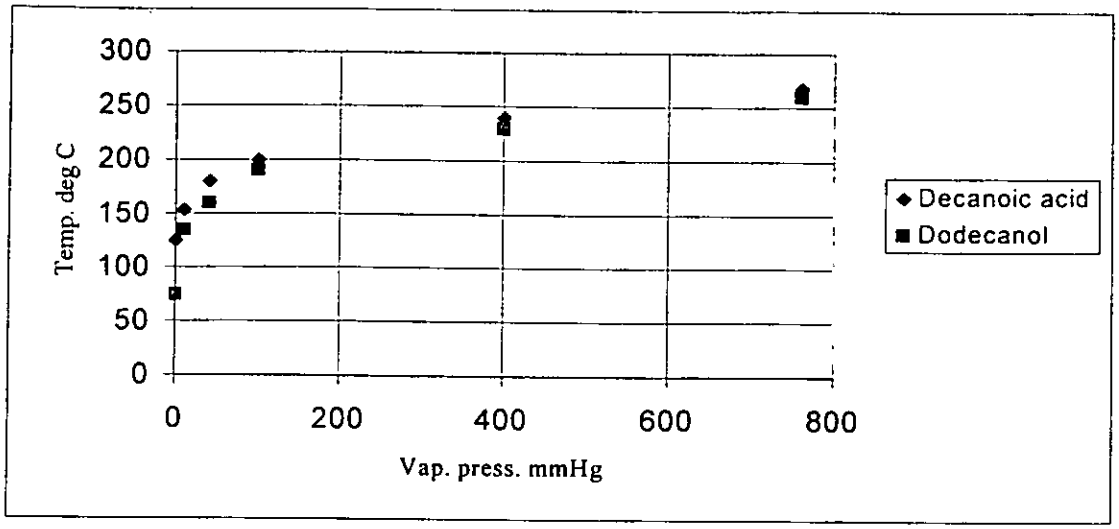

Figure 3.6 Vapour Pressure curves for dodecanol and decanoic acid.

Table 3.13 Rate of reaction of decanoic acid with 1,6-hexanediol.

[decanoic acid]	Enzyme	Water loss*	
mol dm^{-3}	mg	$\mu g\ min^{-1}$	$\mu mol\ min^{-1}\ mg^{-1}$
0.1	0.294	3.44	0.65
0.10	0.410	4.20	0.60
0.21	0.210	3.86	1.03
0.21	0.464	8.50	1.01
0.21	0.354	6.50	1.02
0.22	0.310	6.00	1.1
0.33	0.226	6.25	1.5
0.41	0.355	10.0	1.6
0.6	0.396	12.62	1.77
0.6	0.492	14.5	1.72

*Correction factor for loss of 1,6-hexanediol and decanoic acid 2 $\mu g\ min^{-1}$.

The Enzfitter program was used to analyse the data and to produce the best fit curve shown in Figure 3.7. The Analysis of Variance gave R-squared as 0.99.

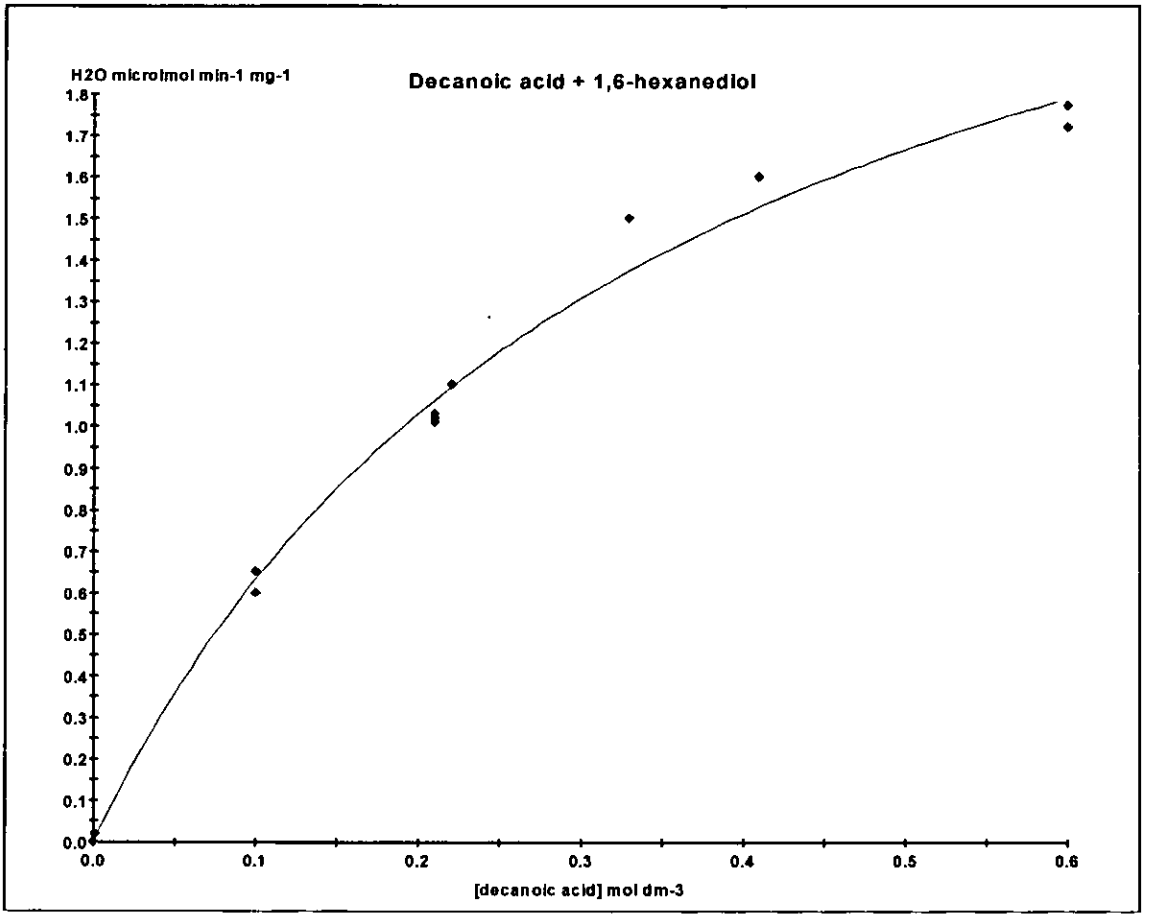

Figure 3.7 Effect of substrate concentration on the reaction rate of decanoic acid with 1,6-hexanediol.

Similar results for the reaction of decanoic acid with dodecanol are given in Table 3.14 and Figure 3.8.

Table 3.14 Rate of reaction of decanoic acid and dodecanol.

[decanoic acid]	Enzyme	Water loss*	
mol dm^{-3}	mg	$\mu g\ min^{-1}$	$\mu mol\ min^{-1}\ mg^{-1}$
0.21	0.381	3.40	0.50
0.44	0.452	4.80	0.6
0.44	0.370	4.35	0.64
0.80	0.441	6.35	0.8
0.80	0.545	7.7	0.78
0.1	0.463	2.1	0.25
0.1	0.341	1.7	0.28
1.21	0.353	5.65	0.89
1.21	0.770	11.73	0.85

*Correction factor for loss of dodecanoic acid and dodecanol 2.5 $\mu g\ min^{-1}$.

Up to this point all of the rate studies had been carried out using a 100% pure sample of *Candida antarctica* lipase B produced commercially. When this was no longer available the work was continued using Chirazyme L-2 lyo supplied by Roche Diagnostics (formerly Boehringer Ingelheim). This is exactly the same enzyme as that used previously, except that it is diluted with a combination of lyoprotectant and inert diluent. In order to be able to compare the results obtained with the two enzymes the relative activities were determined using the lipase assay method described in Appendix 3. Because of the special nature of the enzymatic polyesterification reaction, the activity of the two enzymes was determined in two esterification assays. The results of these are given in Table 3.15.

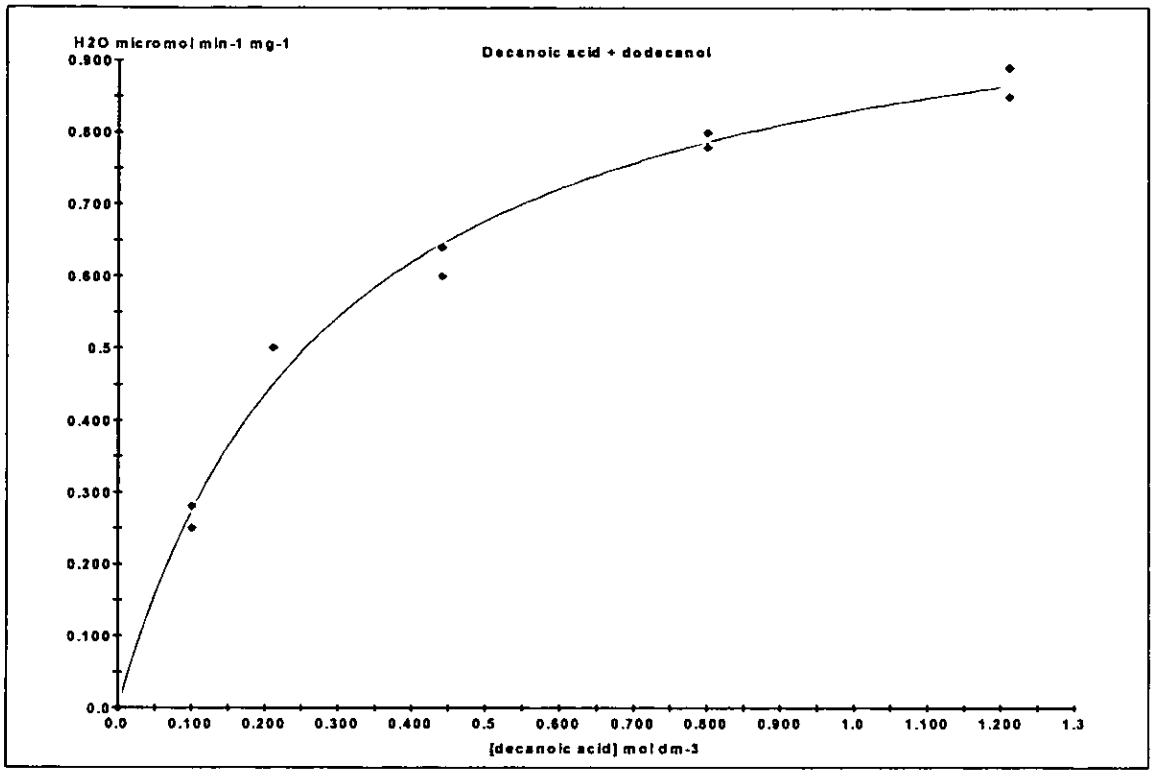

Figure 3.8 Effect of substrate concentration on the reaction rate of decanoic acid and dodecanol.

Table 3.15 Comparison of activity of *C. antarctica* products.

Enzyme	Substrate	V_{max} $\mu mol\ min^{-1}\ mg^{-1}$	K_m $mol\ dm^{-3}$	Lipase units
CalB	AA + HD	4.60	0.52	-
Chirazyme L-2	"	1.46	0.53	-
CalB	AA + PTMEG	4.89	0.41	-
Chirazyme L-2	"	1.89	0.56	-
CalB	-	-	-	485
Chirazyme L-2	-	-	-	165

The results obtained are compatible with the claim by Roche Diagnostics that Chirazyme L-2 contains 33-35%$^{w}/_{w}$ of the active *Candida antarctica* lipase B enzyme. The structural

studies carried out using circular dichroism (Chapter 9) confirm that the secondary structures of the pure CalB and the Chirazyme L-2 are the same. Therefore, it is possible to compare approximately the results obtained using the two enzymes, using a multiple of 3.0 as a correction factor to resolve the difference in activity due to the different active enzyme content. The studies of the effect of hydrophobicity of the substrates and media were continued using Chirazyme L-2 lyo.

The previous experiments using adipic acid in PTMEG 650 had given substantial variability in the results as may be seen in Figure 3.3. The lack of accuracy had been attributed to the low solubility of adipic acid in PTMEG 650 below 35°C. Therefore the series of experiments was repeated using the same reaction conditions as before; except that after the adipic acid solution in diol had been through the drying cycle, the enzyme was added as soon as the temperature in the TGA had fallen to 40°-42°C. The raw data for these experiments are given in Table 3.16 and are plotted in Figure 3.9.

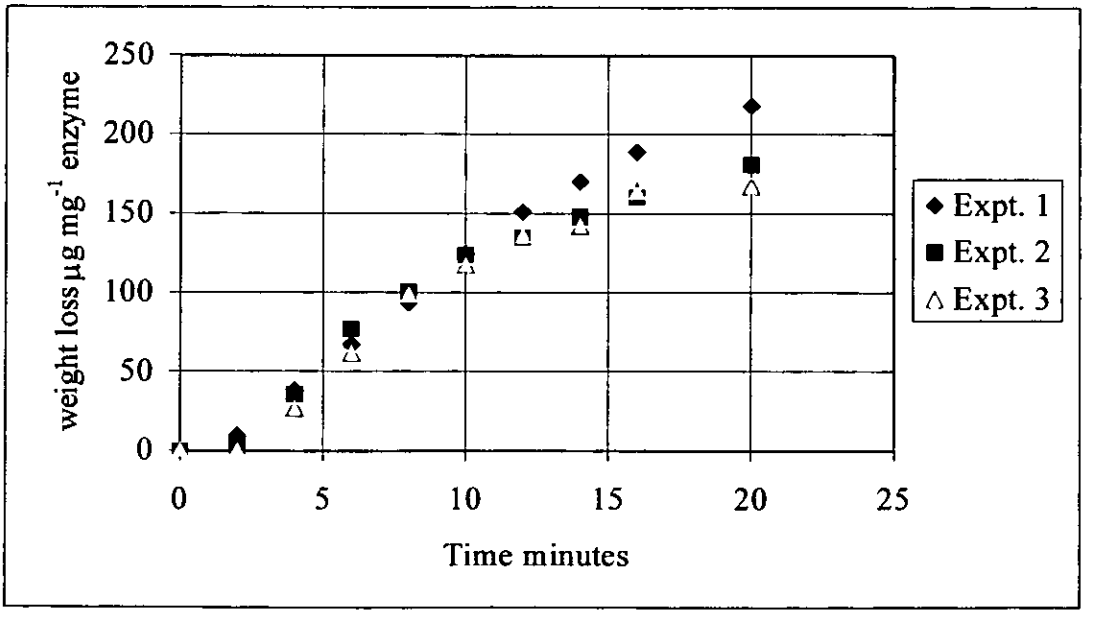

Figure 3.9 Weight loss with time per mg of enzyme for the reaction of 0.4 M adipic acid with PTMEG 650 at 60°C.

Table 3.16 The reaction of 0.4 M adipic acid with PTMEG 650 at 60°C.

	Exp. 1	Exp. 2	Exp. 3
Time mins	Wt. loss* $\mu g\ mg^{-1}$ of enzyme	Wt. loss* $\mu g\ mg^{-1}$ of enzyme	Wt. loss* $\mu g\ mg^{-1}$ of enzyme
0	0.0	0.0	0.0
2	9.6	3.0	0.0
4	38.4	36.0	27.0
6	67.1	77.0	61.7
8	93.5	101.0	98.8
10	124.7	124.0	117.3
12	151.1	135.0	135.8
14	170.3	147.8	142.0
16	189.0	160.4	164.0
20	218.0	180.8	167.0

*No correction factor was required for loss of PTMEG.

The maximum rates were taken between 4-10 minutes and were:-

Experiment 1 0.80 $\mu mol\ min^{-1}\ mg^{-1}$.

Experiment 2 0.81 $\mu mol\ min^{-1}\ mg^{-1}$.

Experiment 3 0.83 $\mu mol\ min^{-1}\ mg^{-1}$.

The reaction between adipic acid and PTMEG 650 did not require the deduction of any correction factor. The results of the reaction between 0.4 M adipic acid and PTMEG 650 are shown in Table 3.17. It is obvious that these results are far more consistent than the earlier series (see Figure 3.3).

Table 3.17 Rate of reaction of adipic acid and PTMEG 650.

[adipic acid] mol dm^{-3}	Enzyme mg	Water loss* $\mu g\ min^{-1}$	Reaction rate $\mu mol\ min^{-1}\ mg^{-1}$
0.1	0.503	3.0	0.33
0.1	0.573	2.9	0.27
0.2	0.236	2.0	0.47
0.2	0.297	2.4	0.45
0.2	0.120	1.2	0.56
0.2	0.282	2.7	0.53
0.4	0.417	6.0	0.80
0.4	0.636	9.3	0.81
0.4	0.162	2.4	0.83
0.6	0.347	6.2	0.99
0.6	0.315	5.7	1.00
0.6	0.240	4.3	1.00
0.8	0.322	6.2	1.07
0.8	0.153	3.2	1.17
0.8	0.387	8.4	1.20

*No correction factor was required for loss of PTMEG 650.

The data was analysed using the Enzfitter program to give the best fit curve shown in Figure 3.10. The Analysis of Variance gave R-squared as 0.99.

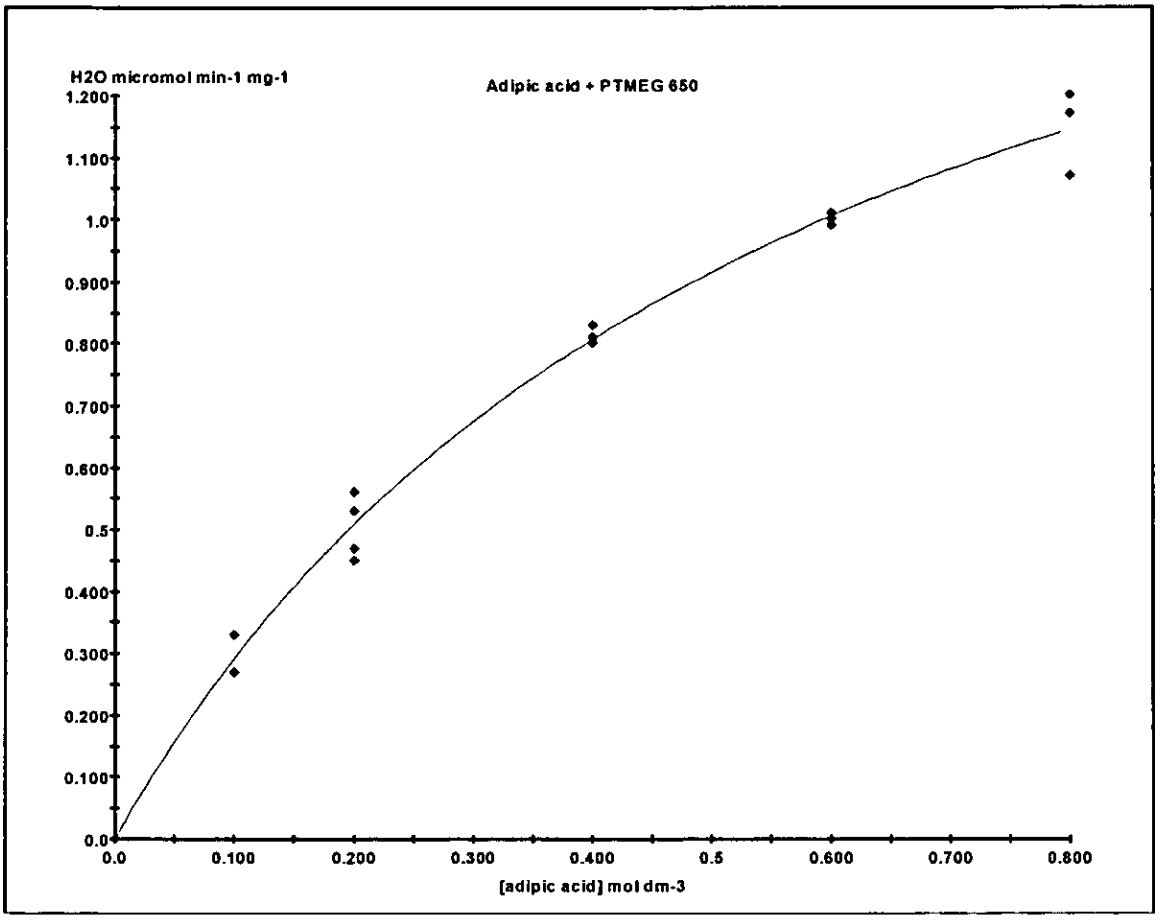

Figure 3.10 Effect of substrate concentration on the rate of reaction of adipic acid and PTMEG 650.

In order to investigate the effect of hydrophobicity of the medium on the reaction rate further, two extremely hydrophilic diols were used as media and substrate. The first, diethylene glycol gave no discernible reaction, measurable with the TGA. This confirmed the unsuccessful attempts to use enzymes to synthesise polyesters based on diethylene glycol on a larger scale. The second hydrophilic diol that was tried was polyethylene glycol 400. The reaction conditions were exactly the same as in earlier experiments and the results are given in Table 3.18.

Table 3.18 The rate of reaction of adipic acid and PEG 400.

[adipic acid] mol dm^{-3}	Enzyme mg	Water loss $\mu g\ min^{-1}$	Rate of reaction $\mu mol\ min^{-1}\ mg^{-1}$
0.1	0.840	7.6	0.5
0.1	0.521	7.2	0.77
0.1	0.173	1.5	0.48
0.2	0.737	12.7	0.96
0.2	0.546	8.5	0.86
0.2	0.738	15.5	1.17
0.4	0.497	15.2	1.7
0.4	0.531	15.3	1.6
0.4	0.687	18.5	1.5
0.6	0.269	10.0	2.06
0.6	0.410	16.2	2.2
0.6	0.511	16.6	1.8
0.8	0.242	9.6	2.2
0.8	0.363	13.7	2.1
0.8	0.392	16.9	2.4
1.0	0.304	13.8	2.52
1.0	0.484	20.5	2.35
1.0	0.506	19.1	2.1

*No correction factor needed for loss of PEG 400.

The Enzfitter program was used to produce the best fit curve shown in Figure 3.11. The Analysis of Variance gave R-squared 0.99.

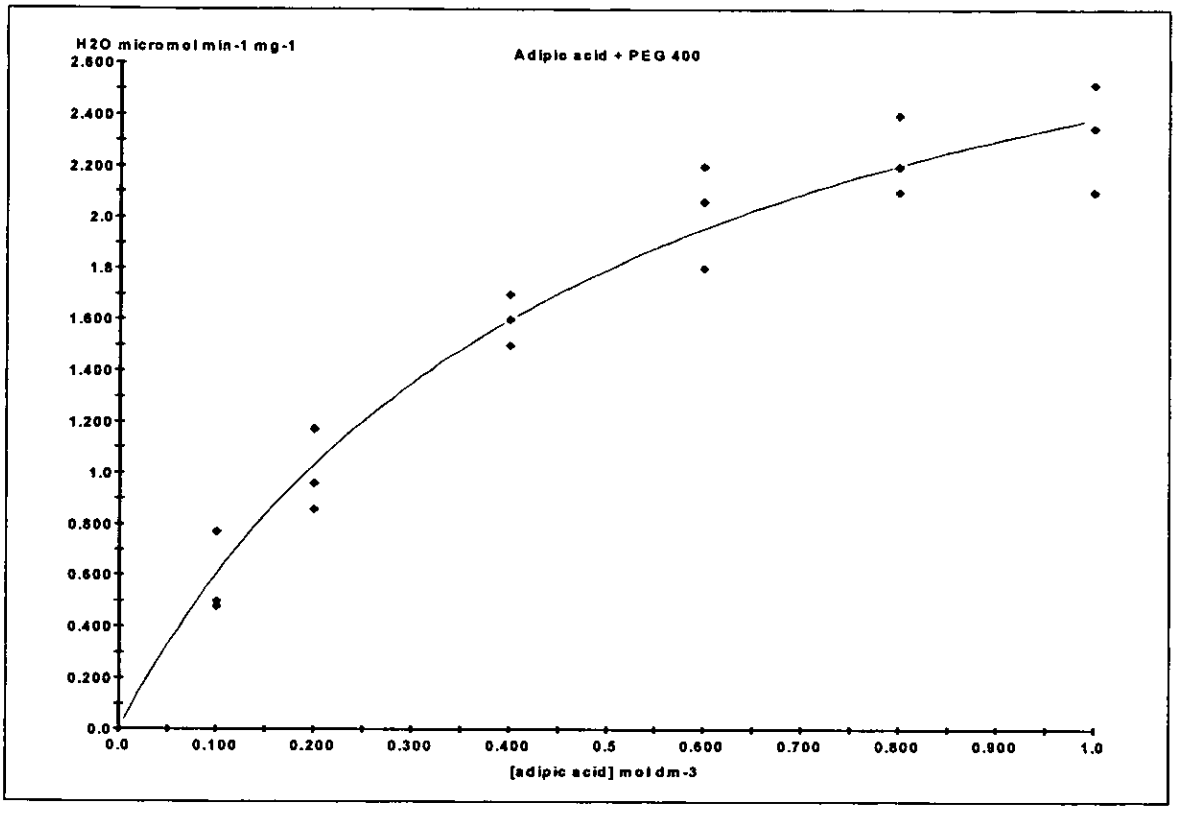

Figure 3.11 The reaction of adipic acid with PEG 400.

When we compare the rates of reaction of the diols: 1,6-hexanediol, BAB, PTMEG 650, PEG 400 and dodecanol (Figure 3.12), a number of interesting conclusions emerge.

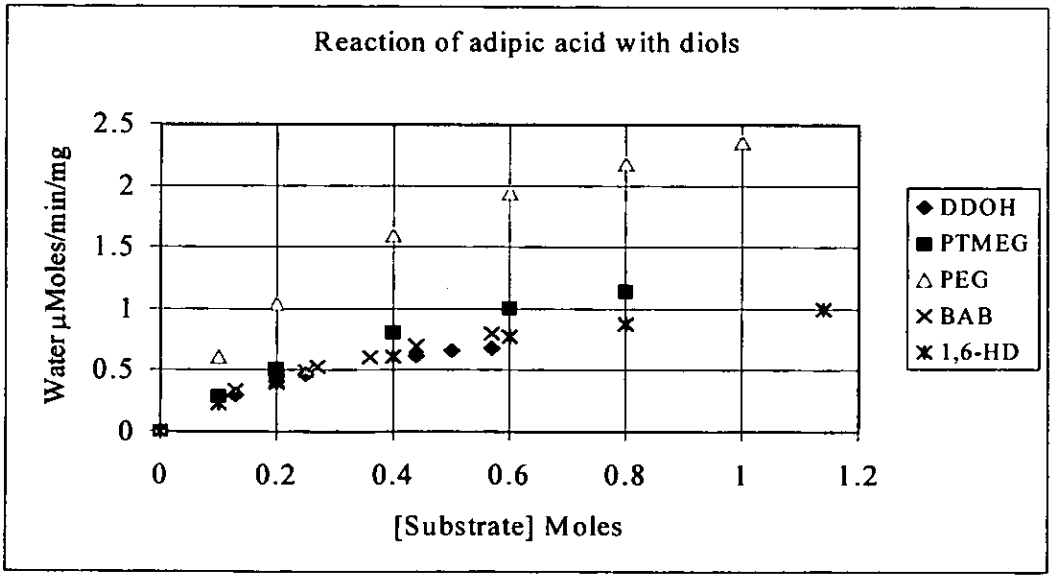

Figure 3.12 Reactivity of adipic acid with various diols.

The reaction rates of adipic acid in 1,6-hexanediol and PTMEG 650 are almost identical; bearing out observations made on large-scale syntheses at Baxenden Chemicals Ltd. The polyesterification of adipic acid and PTMEG is a surprisingly facile and relatively fast reaction. When one compares the relative size of the 1,6-hexanediol molecule at 118 Daltons, with PTMEG at 650 Daltons, it seems surprising that there is no significant difference in rate, bearing in mind the size of the PTMEG molecule. In addition, the molar concentration of hydroxyl groups is almost 6 times less in the PTMEG solutions than in the 1,6-hexanediol solutions.

A 0.4 M solution of adipic acid in 1,6-hexanediol has a 23 times molar excess of hydroxyl to carboxyl groups, whereas in a 0.4 M solution of adipic acid in PTMEG 650 there is only a 4 times molar excess of hydroxyl to carboxyl. Similarly, the polyethylene glycol 400 has a significantly smaller molar excess of hydroxyl groups yet it has the highest reactivity of all the diols used.

The phenomenon of alcohol inhibition is quite common with lipase enzymes,[99] however, there appears to be no relationship between the hydroxyl concentration and the reaction rate in the various diols. The hydroxyl concentrations in descending order are, 1,6-hexanediol, BAB, dodecanol, PEG 400 and PTMEG 650, whereas the highest rate is found with the PEG 400 and the lowest rate with dodecanol.

Both observations seem to point to the fact that under the conditions of our experiments, the reaction of the hydroxyl group of the diol with the acylated enzyme is so fast that it is not the rate controlling factor in the overall reaction. This conclusion is in accordance with observations in other lipase systems.[100]

There does however appear to be an inverse relationship between rate of reaction and the hydrophobicity of the diol used.

We looked initially to see if this relationship could be quantified by using the dielectric constant as a measure of the hydrophobicity of the diol, however, this was not successful.[35] The relationship between the reaction rate and the logP, the partition coefficient of the diol between octanol and water, was studied. In some cases, we had insufficient material to determine the partition coefficient; therefore, we used the Summation of Common Fragment Constants method, also known as 'The Fragment Method', developed by Hansch and Leo,[101] to determine the ClogP. In order to be consistent we then used the ClogP for all comparisons with reaction rate. The ClogP partition coefficients for the relevant substrates are collected in Table 3.19.

Table 3.19 C logP of diols.

Substrate	C logP
1,4-Butanediol	-0.9.
1,6-Hexanediol	0.80
Dodecanol	5.4
PTMEG 650	2.5
PEG 400	-3.2
BAB	1.7
AB	1.04

Although a form of correlation between the reaction rate and the C logP may be seen in the Figure 3.12, it is not very clear. Therefore, using Enzfitter to determine the V_{max} of the reaction of adipic acid with the various diols a study of the effect of the

hydrophobicity as measured by C logP on the rate as measured by V_{max} determined by Enzfitter, was made. The results are shown in Figure 3.13.

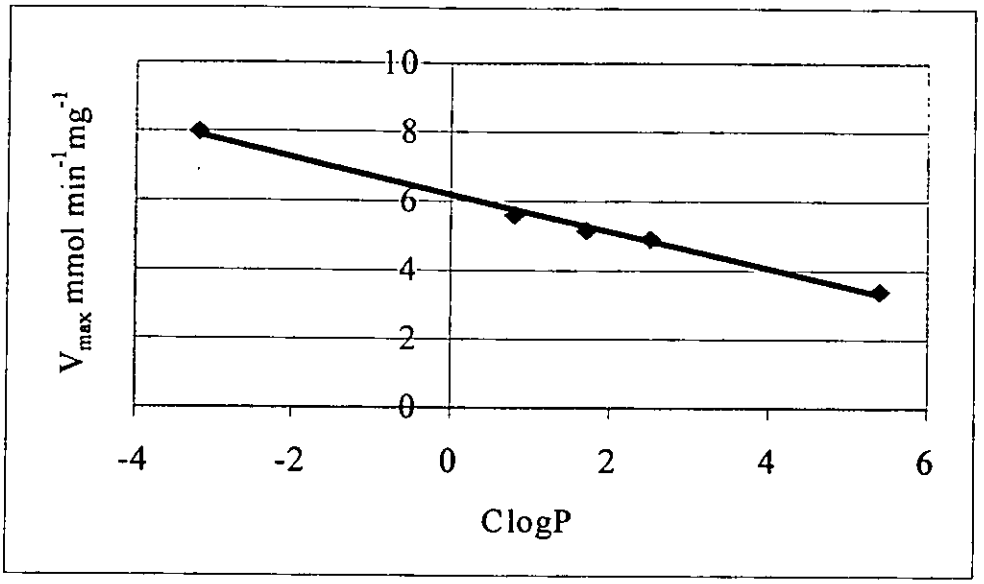

Figure 3.13 The effect of ClogP on the V_{max} of the reaction of adipic acid with diol.

There are a number of possible reasons for the pronounced effect of the hydrophobicity of the medium on the reaction rate. The desolvation of the acid substrate from the diol solution into the enzyme site will depend on the solubility of the acid in the diol, however, the hydrophilic diols are the best solvents for the acid, which means they would require the greatest desolvation energy, the converse of what would be expected. It has been shown in Chapter 6 on structural studies that the enzyme is not affected structurally by changes in the hydrophobicity of its surroundings; therefore it is unlikely that the enzyme is behaving differently in the different media. The most plausible explanation for this effect is the desolvation of the product from the active site. If the rate controlling reaction is the acylation of the enzyme then the product being formed is water. The rate of reaction will be controlled by the rate of removal of water from the active site of the enzyme. The more hydrophilic the surrounding medium, the faster the water will be

removed, however, it is not only the removal of the water from the enzyme that is affected by the hydrophilic surroundings. The mass transport of water through the medium is much faster if it is hydrophilic so that it reaches the surface rapidly where the stream of dry nitrogen removes it.

When we compare the reaction rates of the acids in the different diols it appears that not only does increasing the hydrophobicity of the diol have an adverse effect on the rate, but as will be seen below, the hydrophobicity of the acid substrate also appears to slow the reaction. The hydrophobicity of various acid substrates as measured by ClogP are shown in Table 3.20.

Table 3.20 ClogP of acid substrates.

Substrate	ClogP
AB (AA + 1,4-BD)	1.04
Adipic acid	0.42
Decanoic acid	4.2
Dodecanoic acid	6.0
11-Hydroxyundecanoic acid	3.85
15-Hydroxypentadecanoic acid	4.9

The fastest reacting was the AB hydroxy acid which has a visceral ester group, this makes it an extremely polar compound, but not as polar as adipic acid as it has only one carboxyl group. Thus, the $[H^+]$ derived from the ionisation of the AB is such that the pH of the AB system stays within the optimum range for the activity of the enzyme.

Reaction of AB and two further hydroxy acids, were studied, 11-hydroxyundecanoic acid (11-HUDA) and 15-hydroxypentadecanoic acid (15-HPDA), which are similar to AB, but without the visceral ester group.

The experimental procedure was the same as the earlier experiments, except that the 15-hydroxypentadecanoic acid does not melt until 85°C. Therefore, in this case the acid was heated to 100°C for 10 minutes. No weight loss was observed; it was cooled to 45°C and the *Candida antarctica* lipase B added, after which the temperature was raised to 86°C at 20°C min^{-1}. It is known that CalB, being a thermozyme, is fully active at this temperature and that the enzyme's activity does not start to decrease unless kept above 90°C for some time. In order to make a useful comparison with the reactivity of AB and 11-HUDA the reaction rate at 60°C was estimated using the Arrhenius equation. The results are shown in Table 3.21.

Table 3.21 Comparison of reactivity to C logP for hydroxyacids.

Substrate	Rate $\mu mol\ min^{-1}\ mg^{-1}$	C logP
AB	4.8	1.0
11-HUDA	1.1	4.1
15-HPDA	0.2	4.9

With these limited data, it can be seen that there appears to be a direct inverse relationship between the reactivity of the acid and its hydrophobicity, as measured by its ClogP. These experiments were all carried out using the 100% hydroxy acid and therefore not directly comparable with the results obtained from the solutions of acid in diol.

It has been shown that the hydrophobicity of the diol, which is the overall medium, has a major effect on the activity of the enzyme. We wanted to know if the polarity of the acid substrate would have an effect on the reaction rate even when in a large excess of diol.

Four monocarboxylic acids were selected (see Table 3.22) with differing hydrophobicity and their reactivity determined when in dilute solution in 1,6-hexanediol.

Using the same experimental procedures as before: 0.4 M solutions of the acid in 1,6-hexanediol, were prepared and the solution dried by heating in the TGA at 110°C for 20min, cooling to 25°-30°C, adding the enzyme and heating to 60°C at the standard rate. The weight loss used as the correction factor was determined and found to be 2 $\mu g\ min^{-1}$, the same as for previous 1,6-hexanediol experiments. After several runs had been completed and very erratic results obtained, we realised that both levulinic acid and acetylvaleric acid are quite volatile at 60°-80°C in spite of having boiling points in excess of 240°C. We measured a weight loss of 20 $\mu g\ min^{-1}$ for each acid when heated to 60°C in the TGA. We were concerned therefore, that during the drying cycle up to 110°C there could be a significant loss of the acid from the solution and a large unknown change in the concentration of the acid in the diol. Therefore, we decided to dry the acid and acid/diol solution over P_2O_5 prior to the experiment, dispensing with the drying cycle. This gave a significantly higher reaction rate than the previous experiments; this was assumed to be due to our having lost a significant amount of substrate during the previous drying cycle.

The maximum conversion rates of the four acids as 0.4 M solutions in 1,6-hexanediol were compared to their partition coefficients, ClogP, as shown in Table 3.22 and Figure 3.14.

Table 3.22 Effect of substrate polarity on reaction rate.

Substrate	Initial rate μmol min^{-1} mg^{-1}	ClogP
Levulinic acid	3.5	1.0
Acetylvaleric acid	2.9	2.0
Decanoic acid	1.6	5.0
Dodecanoic acid	0.9	6.0

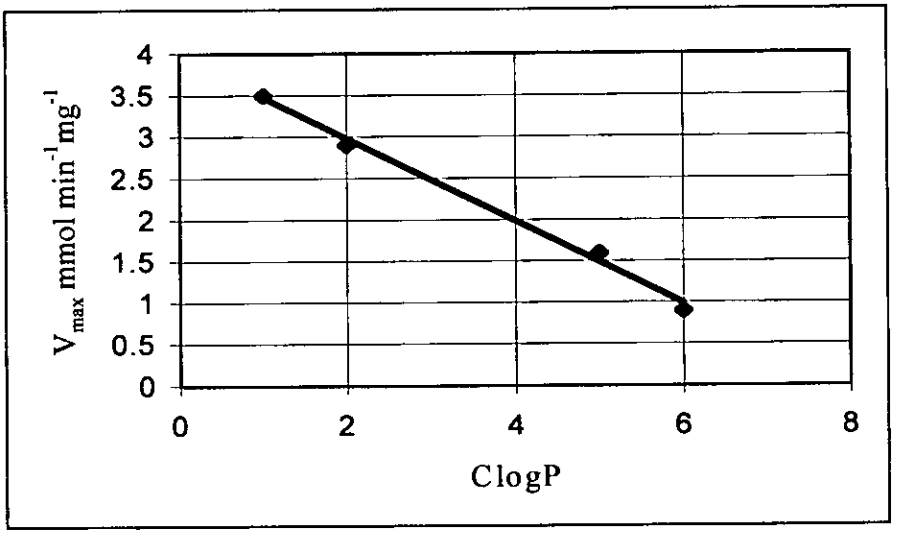

Figure 3.14 Effect of substrate hydrophobicity on initial reaction rate.

The relationship between the substrate polarity and the reactivity with the enzyme is quite clear. The explanation as to how the changes in polarity of the substrate molecule can affect the reaction rate when those changes are brought about by the introduction of a polar carbonyl group remote from the reacting carboxyl is more difficult. In *Candida rugosa* the binding of fatty acids has been shown to decrease with increasing chain length.[102] The rate of transesterification of fatty esters using *Candida antarctica* lipase B has also been found to be dependant on the acyl chain length, the optimum length being a six carbon chain.[103] Therefore, the observation of declining rates with the more

hydrophobic acids has probably more to do with the acyl chain fitting the active site rather than any physical effect due to the increasing hydrophobicity.

3.2.1 Michaelis-Menten kinetics.

In order to investigate the characteristics of the enzyme that have such dramatic effects on its activity with different substrates and in different media, it is first necessary to determine the Michaelis-Menten constants of the enzyme in the various systems. While the graphs of reaction rate against substrate concentration appear to resemble a Michaelis-Menten plot superficially, there is a major problem with this method. The difficulty arises in determining when the rate no longer changes with increasing concentration. Although in theory when all the enzyme sites are filled the rate should not increase with increasing concentration in reality the plot rarely becomes flat. Therefore, there is always a degree of estimation in determining the maximum rate, V_{max}.

There are two problems with the systems studied, which in common with many other systems make it difficult to estimate the maximum rate. Firstly, the substrates used are not very soluble in the diols, which acts as both substrate and reaction medium, therefore high substrate concentrations cannot be used. A further difficulty arises when comparing the acid substrates; their solubility varies considerably in the reaction medium according to the chain length of the particular acid. It is not unusual to find that substrates are also enzyme inhibitors. In the systems studied, the increasing pH at higher concentrations of the acid substrate had a significant adverse effect on the activity of the enzyme.

The rate data was plotted to confirm that a reasonable rate/concentration curve had been obtained and then one of the traditional data manipulation procedures was used to get a

better estimate of the maximum rate. The most common of these techniques is the Lineweaver–Burke,[104] or double reciprocal method, was tried first. This involves plotting the reciprocal of the rate against the reciprocal of the concentration, so that the rate equation becomes:

$$\frac{1}{V} = \frac{K_m}{V_{max}} \times \frac{1}{[S]} + \frac{1}{V_{max}}$$

V = Rate, V_{max} = Maximum rate, K_m = Value of [S] giving $V = V_{max}/2$, [S] = Substrate concentration.

The straight line produced by this method intersects the y-axis at 1/V and intercepts the x-axis at 1/[S].

Although the Lineweaver-Burke method is taught widely and is used commonly, it has some fundamental flaws. The major problem is that the slope of the graph is heavily biased by the rates determined at the lowest concentrations. Any errors are accentuated because for small values of V, small errors give enormous errors in 1/V, whereas, at large values of V the same errors give hardly noticeable errors in 1/V. The data from any kinetic experiment will be less accurate at the lowest substrate concentrations.

An alternative technique is the one developed by Eadie-Hofstee,[105] which attempts to overcome the problems of the Lineweaver-Burke method. The equation above is multiplied on both sides by V_{max} and rearranged. The equation becomes therefore:

$$V = V_{max} - K_m \times \frac{V}{[S]}$$

A plot of V against V/[S] is a straight line with a slope of $-K_m$ and which intercepts V_{max} on the rate axis and V/K_m on the rate/K_m axis.

A straight line plot is obtained which intercepts the y-axis at V_m and the x-axis at V/K_m. Although in principle this method overcomes the errors resulting from measurements at low concentrations, any errors that do occur will be present on both axes of the plot. However, the Eadie-Hofstee method is still generally accepted as a better method than that of Lineweaver-Burke. There are other methods such as the Hanes plot, which uses the slope of the graph obtained when plotting [S]/V substrate concentration over rate against [S] substrate concentration.[104] The intercept on the y-axis gives K_m/V, while the intercept on the x-axis is $-K_m$. The only advantage of this method is that it avoids any problems caused by rate errors influencing the data on the x-axis.

At the end of the work using the lyophilised *Candida antarctica* lipase B the Michaelis Menten constants determined by these methods were found to be as shown in Table 3.23.

Table 3.23 Michaelis-Menten constants for the esterification reactions.

System	Observed	Lineweaver-Burke		Eadie-Hofstee	
	V_{max} $\mu mol\ min^{-1}\ mg^{-1}$	K_m $mol\ dm^{-3}$	V_{max} $\mu mol\ min^{-1}\ mg^{-1}$	K_m $mol\ dm^{-3}$	V_{max} $\mu mol\ min^{-1}\ mg^{-1}$
AA + 1,6-HD	3.2	0.6	6.88	1.1	5.3
AA + BAB	2.8	0.72	6.90	1.02	4.3
AA + PTMEG	3.5	0.84	4.64	0.72	4.7
AA + DDOH	2.4	1.66	2.72	1.10	2.28
DA + 1,6-HD	2.0	0.80	5.88	0.58	4.54
DA + DDOH	0.9	0.38	1.96	0.38	1.82

We were somewhat surprised by the size of the difference of the apparent V_{max} taken from our rate graphs and the V_{max} given by the Lineweaver-Burke plots. For example adipic acid and 1,6-hexanediol had an apparent V_{max} of 3.2 μmol min^{-1} mg^{-1} compared to the Lineweaver-Burke V_{max} of 6.88 μmol min^{-1} mg^{-1}. In addition, in the case of adipic acid in dodecanol, the K_m did not appear to fit in with that of the other systems. The Eadie-Hofstee method,[105] which involves plotting the rate against the rate/[substrate], was then tried as it is generally accepted to give results that are more accurate.

It may be seen that for some systems, notably decanoic acid in 1,6-hexanediol, decanoic acid in dodecanol and adipic acid in PTMEG, there is a reasonably good correlation between the two methods. In other cases, there are significant discrepancies between the two methods.

Although we had some confidence in the constants determined by the Eadie-Hofstee plots we did not like the potential uncertainties inherent in techniques, which are little more than primitive methods of data manipulation to force the information into a straight line. Therefore, we decided to use the curve fitting program together with the analysis program in the Enzfitter software , which is discussed in the Development of Methods Chapter.

One problem with the use of K_m for analytical purposes is that it often underestimates the binding energy of the process. Whereas the specificity constant V_{max}/K_m includes both activation energy and binding energy. We were interested specifically in the affinity or specificity constant of the enzyme with the different substrates. It is the best method to test the relevance of substrate, solvent or enzyme changes in enzymatic catalysis.[106] The rate of formation of the acyl enzyme is governed by the specificity constant, because it is the rate of reaction between the free enzyme with the free substrate. It depends only on the acylation step and is independent of the reaction between acyl enzyme and alcohol. A

summary of the results obtained from the two traditional methods and the powerful Enzfitter software is given in Table 3.24.

Table 3.24 Comparison of methods for the determination of Michaelis constants.

System	Specificity L-B	Specificity E-H	V_{max} Enzfitter	K_m Enzfitter	Specificity Enzfitter
AA+HD	11.46	4.82	5.60	1.14	4.91
AA+BAB	9.56	4.22	5.15	1.29	3.99
AA+PTMEG	5.52	6.53	4.92	0.84	5.86
AA+DDOH	1.6	2.07	3.38	0.71	4.76
DA+HD	7.35	7.83	2.82	0.35	8.05
DA+DDOH	5.16	4.79	1.07	0.29	3.69

In both the case of the hydrophobicity of the medium and the substrate there appeared to be a close relationship between the ClogP and the reaction rate measured by the maximum rate V_{max}. However, it was found that there is no relationship whatsoever between either the hydrophobicity and the K_m or the specificity V_{max}/K_m, which is extremely interesting, as earlier work with decanoic acid and dodecanol had claimed the reverse, the more hydrophobic solvents giving a higher rate of esterification.[107] The higher logP solvents gave a low K_m due to the effect of the solvent on substrate desolvation. The V_{max}, however, did not show any correlation with logP because, as the authors state: "V_{max} is only changed if the enzyme conformation or structure or mechanism is changed".[107] They examined six different solvents, although two were disregarded because of apparently anomalous results! Maurel proposed that the greater the role of hydrophobic interactions the greater the effect the solvent logP has on the binding process (K_m). The higher the solubility of the substrate in the organic media the

lower its relative affinity for the enzyme and the higher the K_m.[35] Although the work was done with subtilisin and not a lipase, Kim, *et al.*,[108] showed that the increased rate of transesterification with polar solvents was due to the polar transition state being stabilised by the medium, this then lowers the activation energy for the reaction. However, they also found no correlation between V_{max}/K_m and hydrophobicity as measured by the dielectric constant.

If we consider the implications based on Michaelis-Menten theory, which states that:

$$K_m = k_2 + \frac{k_1}{k_{-1}}$$

then when we have a reaction like ours, which is a typical ping-pong lipase reaction, and k_2 is always significantly less than k_1, that is:

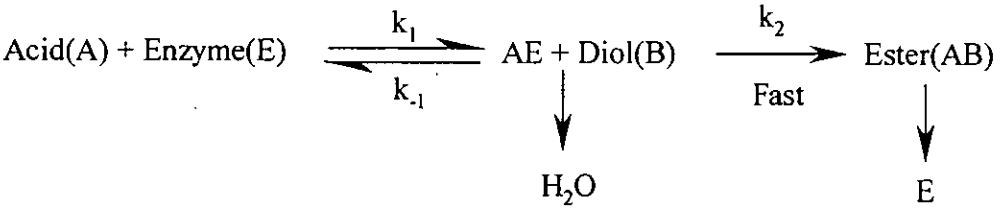

Since the de-acylation step is the faster reaction and a large excess of diol is maintained throughout, when we measure the rate of water produced we are measuring k_1, however, because of the association of the two moieties in AE the determination of k_1 will include an approximation for k_{-1}. Therefore, the determination of K_m will approximate to the dissociation constant K_d for the reaction below.

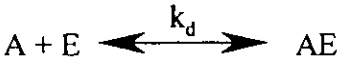

$$K_m = [E]_{free} \times \frac{[A]}{[AE]} = K_d$$

In Michaelis-Menten kinetics the K_m is a measure of how tightly the enzyme binds to the substrate, which means that K_m is a measure of the affinity of the substrate for the enzyme. V_{max} is a measure of how fast the enzyme can go when all the reactive sites are acylated, i.e. all are in the form of the covalent AE complex.

Our results show that changing the hydrophobicity of the medium does not appear to change the affinity of the substrate for the enzyme or, apparently, the nature of the binding between enzyme and substrate.

There are a number of possible reasons for the pronounced effect of the hydrophobicity of the medium on the reaction rate as measured by V_{max}. The desolvation of the acid substrate from the diol solution into the enzyme site will depend on the solubility of the acid in the diol, however the hydrophilic diols are the best solvents for the acid, which means they would require the greatest desolvation energy, the converse of what would be expected. It has been shown in Chapter 6 on structural studies that the enzyme is not affected a great deal structurally by changes in the hydrophobicity of its surroundings; therefore, it is unlikely that the enzyme is behaving differently in the different media. The most plausible explanation for this effect is the desolvation of the product from the active site. If the rate controlling reaction is the acylation of the enzyme then the product being formed is water. The rate of reaction will be controlled by the rate of removal of water from the active site of the enzyme. The more hydrophilic the surrounding medium, the faster the water will be removed, however, it is not only the removal of the water from the enzyme that is affected by the hydrophilic surroundings. The mass transport of water through the medium is much faster if it is hydrophilic so that it reaches the surface rapidly

where the stream of dry nitrogen removes it. It has been proposed that there is a better correlation between the solubility of water in the solvent and enzyme activity than between activity and log P, this intuitively is attractive and is almost certainly relevant but is probably an over simplification.[107] The correlation found over a large number of solvents was tenuous and unconvincing. The truth is probably that the solvent affects substrate desolvation, transition state stabilisation as well as product desolvation from the active site. More hydrophobic solvents will also increase the strength of dipoles and perturb the pK_a of relevant residues in the enzyme. The observed relationship being a summation of all these effects the importance of which will vary from system to system.

3.3 Investigation of the acyl binding site.

In the work of Pleiss [58] and others [31] it was shown that the active site of the lipase is divided into the acyl binding side and the alcohol binding side. The acyl binding side is usually described as being relatively non-specific whereas the alcohol side is far more specific. A considerable amount of work has been published on the stereospecificity of the alcohol side of the lipase binding site.[59] *Candida antarctica* lipase B as an example is highly stereospecific for secondary alcohols because of the geometry of the oxyanion hole, which stabilises the tetrahedral intermediate of the alcohol-acyl enzyme reaction.[109] Apart from work showing the preferences of lipases for different chain lengths according to the overall shape of the active site, as discussed in Chapter 7, very little has been published on the detailed effect of chain length and substitution along the chain.

All previous work has been carried out using monocarboxylic acids,[110] however, because of our interest in polyesterification it was decided to use dicarboxylic acids. Firstly

because they are the acids required for the process but also being short chain acids, such as adipic acid, the ω-carboxyl group is inside the active site of the enzyme when the α-carboxyl group is approaching and acylating the serine of the active site. Because of the abundance of hydrophobic areas at the entrance to the site (See Chapter 7) and electrostatic interactions within the site it was considered likely that the position of the ω-carboxyl could well influence the overall reactivity of the acid and the enzyme.

The dicarboxylic acids chosen for this study were:-

Succinic acid	$HOOC-(CH_2)_2-COOH$
Glutaric acid	$HOOC-(CH_2)_3-COOH$
Adipic acid	$HOOC-(CH_2)_4-COOH$
Pimelic acid	$HOOC-(CH_2)_5-COOH$
2-Oxoadipic acid	$HOOC-CO-(CH_2)_3-COOH$
3-Oxoadipic acid	$HOOC-CH_2-CO-(CH_2)_2-COOH$
3-Methyladipic acid	$HOOC-CH_2-CH(CH_3)-(CH_2)_2-COOH$

The experimental method was exactly the same as described in Chapter 2 for the earlier experiments. The enzyme used in these later experiments was Chirazyme L-2 lyo from Roche Diagnostics. This is commercial purity *Candida antarctica* lipase B that has had lyoprotectant and inert diluent added. The actual structure and activity of the enzyme is exactly the same as the *Candida antarctica* lipase B from Novo which was used in the earlier work (see Chapter 9). The activity per milligram of the 100% *Candida antarctica*

lipase is approximately 3.0 times that of the Chirazyme L-2 lyo. The rate of reaction at 60°C, of the above acids in 1,6-hexanediol was determined.

The results for succinic acid in 1,6-hexanediol are given in Table 3.25. The Enzfitter program was used to analyse these data and to plot the best fit curve as shown in Figure 3.15. The Analysis of Variance gave an R-squared (correlation coefficient) of 0.990.

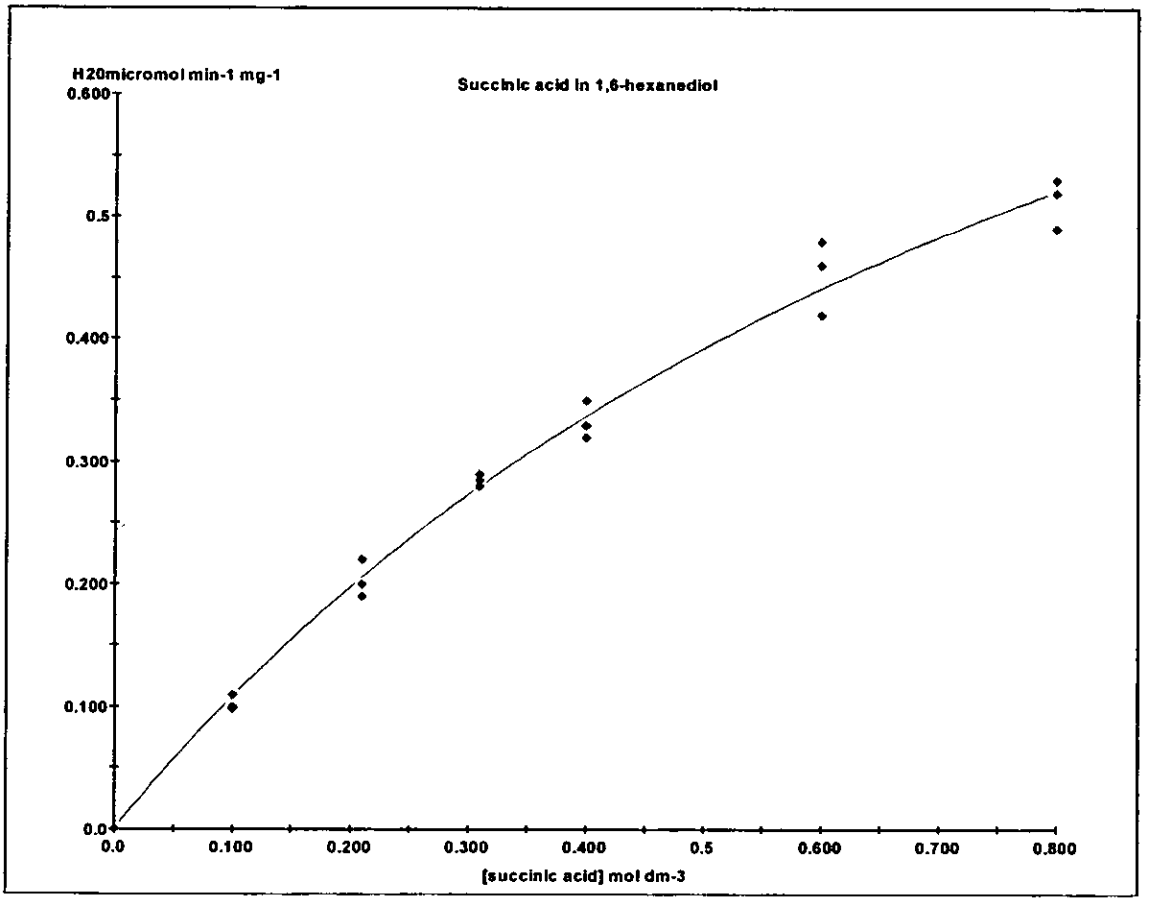

Figure 3.15 The reaction of succinic acid with 1,6-hexanediol.

Table 3.25 Reaction of succinic acid in 1,6-hexanediol at 60°C.

[succinic acid] mol dm^{-3}	Enzyme mg	Water loss* $\mu g\ min^{-1}$	Rate of reaction $\mu g\ min^{-1}\ mg^{-1}$
0.1	0.537	1.0	0.098
0.1	0.871	1.6	0.1
0.1	0.411	0.7	0.99
0.1	0.387	0.8	0.11
0.21	0.635	2.2	0.19
0.21	0.523	1.9	0.2
0.21	0.453	1.8	0.22
0.31	0.511	2.6	0.28
0.31	0.623	3.2	0.285
0.31	0.525	2.7	0.29
0.4	0.566	3.3	0.32
0.4	0.6	3.8	0.35
0.4	0.342	2.0	0.33
0.6	0.382	3.2	0.46
0.6	0.287	2.2	0.43
0.6	0.193	1.7	0.49
0.8	0.438	3.9	0.49
0.8	0.32	3.0	0.52
0.8	0.419	4.0	0.53

*Correction factor for loss of 1,6-hexanediol 2 $\mu g\ min^{-1}$.

The reactions were repeated with glutaric acid in 1,6-hexanediol and the results shown in Table 3.26.

Table 3.26 The reaction of glutaric acid in 1,6-hexanediol at 60°C.

[glutaric acid] mol dm^{-3}	Enzyme mg	Water loss* $\mu g\ min^{-1}$	Rate of reaction $\mu g\ min^{-1}\ mg^{-1}$
0.11	0.499	2.7	0.30
0.11	0.742	3.2	0.24
0.11	0.215	1.0	0.26
0.2	0.368	2.8	0.42
0.2	0.419	2.9	0.38
0.2	0.59	4.3	0.40
0.3	0.418	4.3	0.57
0.3	0.446	4.3	0.54
0.3	0.423	4.2	0.55
0.41	0.558	6.3	0.63
0.41	0.246	2.7	0.60
0.41	0.245	3.0	0.68
0.61	0.428	5.7	0.74
0.61	0.507	5.9	0.65
0.61	0.331	4.7	0.79
0.8	0.405	6.2	0.85
0.8	0.570	8.4	0.82
0.8	0.468	6.7	0.80
1.0	0.291	4.7	0.90
1.0	0.821	12.4	0.84
1.0	0.400	6.0	0.83

*Correction factor for loss of 1,6-hexanediol 2$\mu g\ min^{-1}$.

The Enzfitter program was used to analyse these data and to plot the best fit curve as shown in Figure 3.16. The Analysis of Variance gave an R-squared of 0.978.

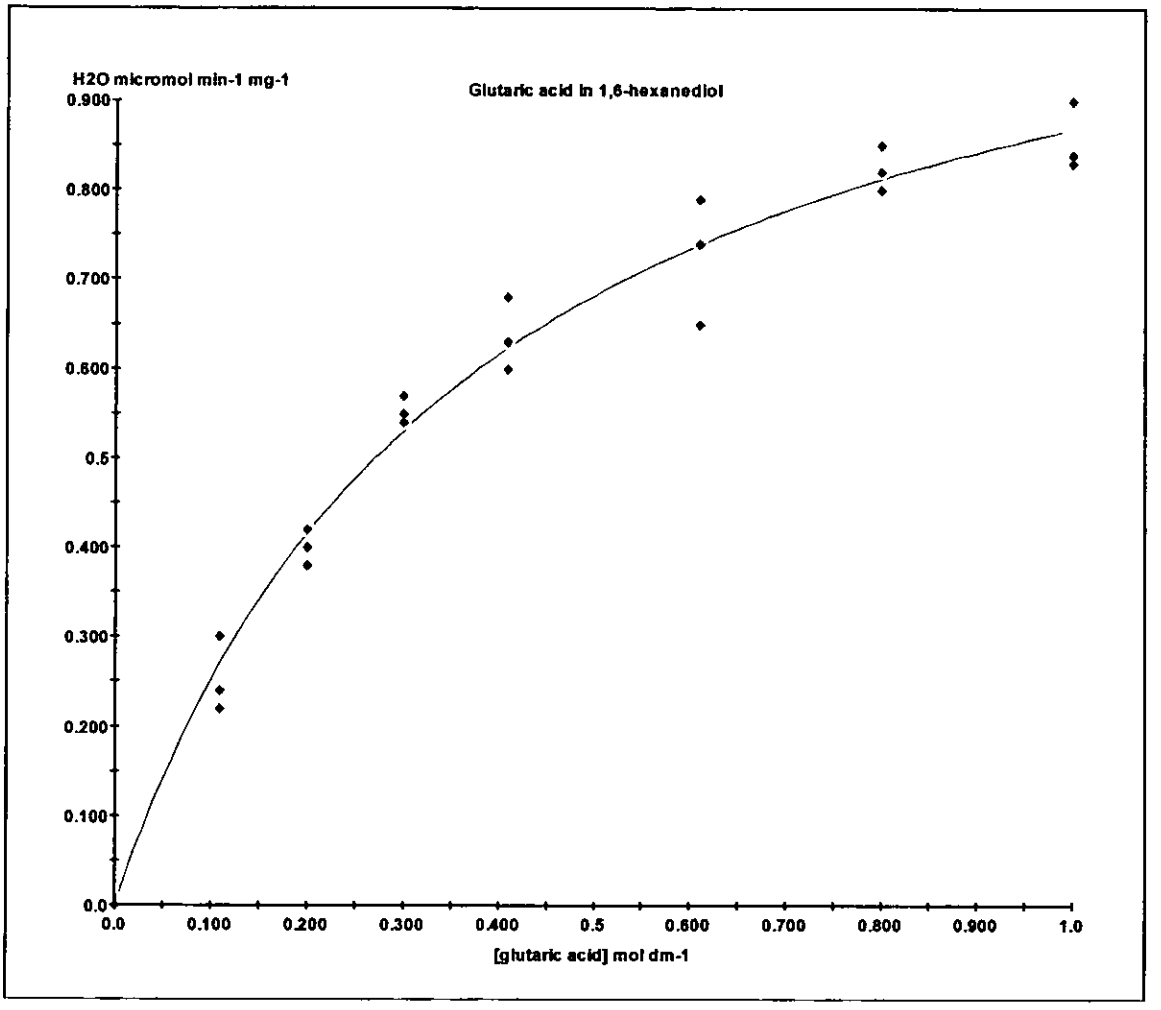

Figure 3.16 The reaction of glutaric acid with 1,6-hexanediol.

The results for the reaction of adipic acid in 1,6-hexanediol are given in Tables 3.27 and 3.28.

Table 3.27 The reaction of 0.4 M adipic acid with 1,6-hexanediol at 60°C.

	Exp. 1		Exp. 2		Exp. 3	
Time mins	Wt. loss $\mu g\ mg^{-1}$ enzyme	Wt. loss ACF.* $\mu g\ mg^{-1}$ enzyme	Wt. loss $\mu g\ mg^{-1}$ enzyme	Wt. loss ACF.* $\mu g\ mg^{-1}$ enzyme	Wt. loss $\mu g\ mg^{-1}$ enzyme	Wt. loss ACF.* $\mu g\ mg^{-1}$ enzyme
0	0.0	0.0	0.0	0.0	0.0	0.0
2	0.0	0.0	0.0	0.0	6.0	2.0
4	17.0	9.0	53.0	45.0	40.0	32.0
6	85.0	73.0	78.0	66.0	69.0	57.0
8	112.0	96.0	111.0	95.0	95.0	79.0
10	145.0	125.0	138.0	118.0	119.0	99.0
12	162.0	138.0	162.0	138.0	140.0	116.0
14	186.0	158.0	184.0	156.0	166.0	138.0
16	208.0	176.0	204.0	172.0	181.0	149.0
20	241.0	201.0	251.0	211.0	224.0	184.0

*ACF: After correction factor for loss of 1,6-hexanediol 2 $\mu g\ min^{-1}$.

In experiment 1 the reaction was slow to start and the maximum rate was taken from 6-12 minutes. In experiments 2 and 3 the rate was measured between 4-10 minutes. The maximum rates obtained, after correcting for the amount of enzyme added, were:-

Experiment 1 0.60 $\mu mol\ min^{-1}\ mg^{-1}$.

Experiment 2 0.68 $\mu mol\ min^{-1}\ mg^{-1}$.

Experiment 3 0.62 $\mu mol\ min^{-1}\ mg^{-1}$.

In all cases the rate plot (e.g. Figure 3.17) was inspected to see if there were any

anomalies, the problems usually occurred in the first 4 minutes because of the slight variations in the time to get the reactants to 60°C. Therefore, the rate was taken from 4-10 minutes unless there was an observed problem. In several experiments the Michaelis Menten plots were drawn using rates taken at 2-6 minutes, 2-8 minutes, 4-10 minutes and 4-12 minutes. The plots were then prepared using the curve fitting program of the Enzfitter software and the correlation coefficient obtained. By far the best correlation was obtained when using the rate measured between 4-10 minutes.

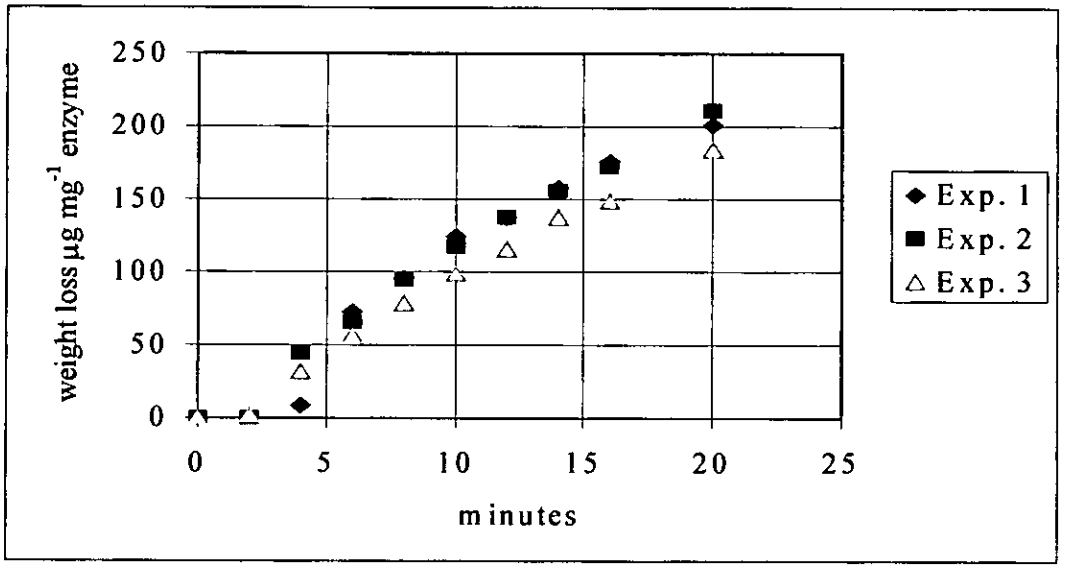

Figure 3.17 Weight loss with time per mg of enzyme for the reaction of 0.4M adipic acid with 1,6-hexanediol at 60°C.

The reaction of 0.8 M adipic acid with 1,6-hexanediol at 60°C is shown in Table 3.28. The rate was measured between 4-10 minutes and the maximum rates obtained were:-

Experiment 1 0.85 µmol min^{-1} mg^{-1}.

Experiment 2 0.84 µmol min^{-1} mg^{-1}.

Experiment 3 0.86 µmol min^{-1} mg^{-1}.

Table 3.28 The reaction of 0.8 M adipic acid with 1,6-hexanediol at 60°C.

	Exp. 1		Exp. 2		Exp. 3	
Time mins	Wt. Loss μg mg^{-1} enzyme	Wt. Loss ACF.* μg mg^{-1} enzyme	Wt. Loss μg mg^{-1} enzyme	Wt. Loss ACF.* μg mg^{-1} enzyme	Wt. Loss μg mg^{-1}	Wt. Loss ACF.* μg mg^{-1} enzyme
0	0.0	0.0	0.0	0.0	0.0	0.0
2	24.0	20.0	25.0	21.0	48.0	44.0
4	92.0	84.0	52.0	44.0	71.0	63.0
6	121.0	109.0	98.0	86.0	92.0	80.0
8	170.0	154.0	127.0	111.0	144.0	129.0
10	196.0	176.0	155.0	135.0	176.0	156.0
12	223.0	199.0	180.0	156.0	200.0	176.0
14	260.0	232.0	201.0	173.0	230.0	202.0
16	318.0	286.0	224.0	192.0	259.0	227.0
20	346.0	306.0	258.0	218.0	307.0	267.0

*ACF: After correction factor for loss of 1,6-hexanediol 2μg min^{-1}.

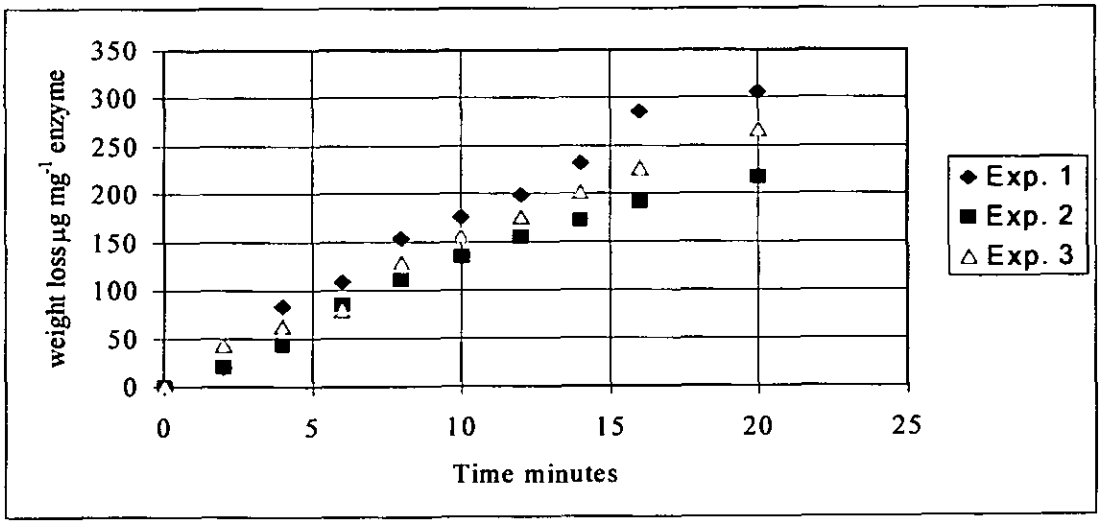

Figure 3.18 Weight loss with time per mg of enzyme for the reaction of 0.8 M adipic acid with 1,6-hexanediol at 60°C.

Table 3.29 Reaction of adipic acid in 1,6-hexanediol at 60°C.

[adipic acid] mol dm^{-3}	Enzyme mg	Water loss $\mu g\ min^{-1}$	Rate of reaction $\mu g\ min^{-1}\ mg^{-1}$
0.1	0.462	2.0	0.24
0.1	0.721	3.31	0.25
0.1	0.708	3.30	0.26
0.2	0.317	2.17	0.38
0.2	0.674	5.0	0.41
0.2	0.512	4.00	0.43
0.4	0.825	8.9	0.60
0.4	0.536	6.0	0.62
0.4	0.550	6.6	0.68
0.6	0.491	6.7	0.76
0.6	0.346	5.0	0.80
0.6	0.559	7.3	0.72
0.8	0.377	6.1	0.9
0.8	0.613	9.4	0.85
0.8	0.667	10.3	0.86
1.14	0.425	8.2	1.07
1.14	0.540	9.4	0.97
1.14	0.365	6.5	0.98
1.14	0.558	10.5	1.05

*Correction factor for loss of 1,6-hexanediol 2 $\mu g\ min^{-1}$.

The Enzfitter best fit curve for these data is shown in Figure 3.19. The Analysis of Variance gave an R-squared of 0.987.

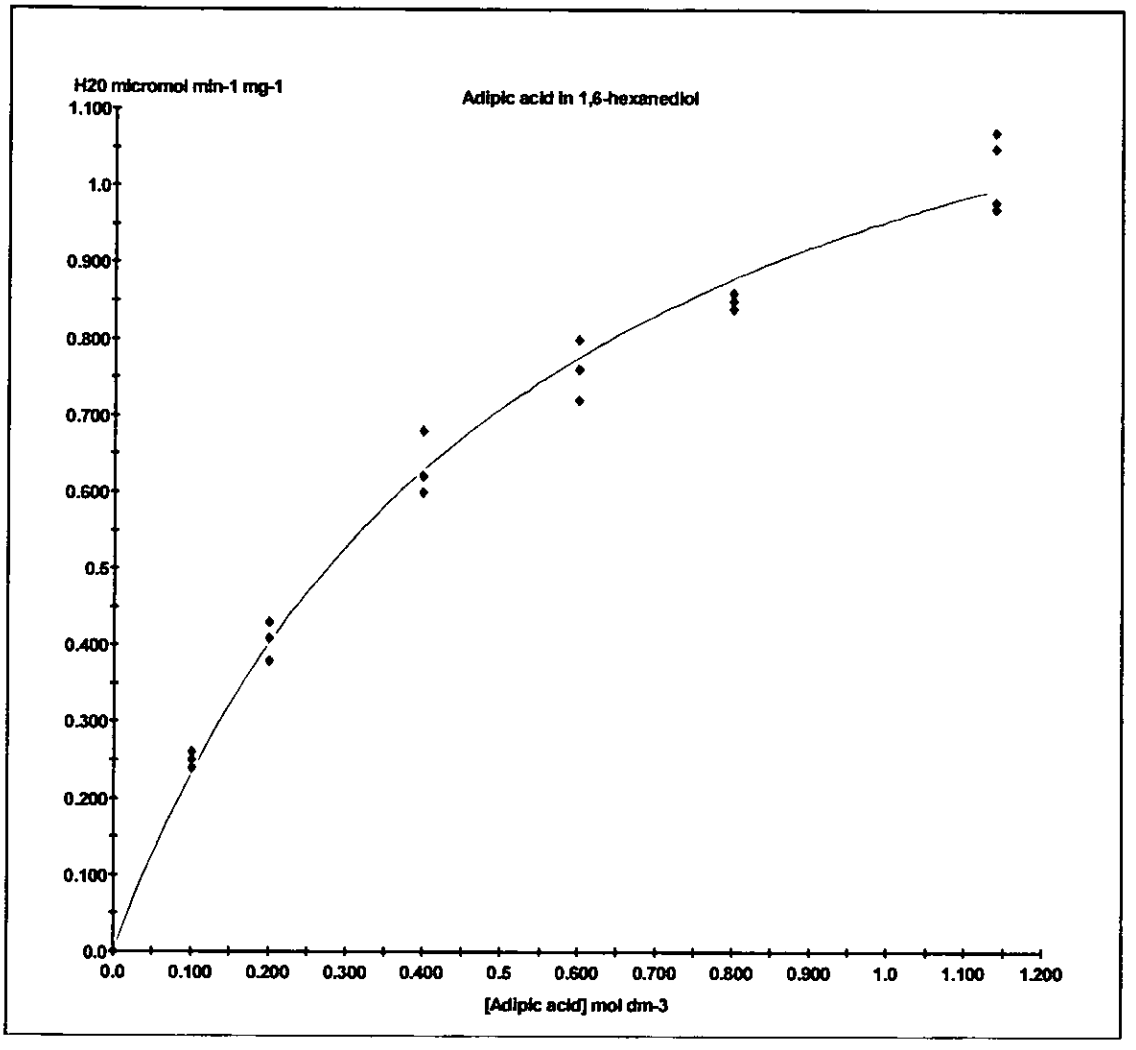

Figure 3.19 The rate of reaction of adipic acid and 1,6-hexanediol.

The results for the reaction of pimelic acid and 1,6-hexanediol are shown in Table 3.30.

Table 3.30 The reaction of pimelic acid and 1,6-hexanediol at 60°C.

[pimelic acid] mol dm^{-3}	Enzyme mg	Water loss* $\mu g\ min^{-1}$	Rate of reaction $\mu g\ min^{-1}\ mg^{-1}$
0.1	0.492	1.8	0.2
0.1	0.438	1.5	0.19
0.1	0.311	1.1	0.19
0.1	0.582	2.1	0.2
0.225	0.483	3.5	0.4
0.225	0.472	3.0	0.35
0.225	0.294	1.6	0.3
0.44	0.298	2.7	0.51
0.44	0.569	5.2	0.51
0.44	0.401	3.7	0.51
0.65	0.357	5.0	0.78
0.65	0.405	4.6	0.63
0.65	0.264	3.1	0.65
0.65	0.310	4.0	0.72
0.85	0.629	9.3	0.82
0.85	0.262	3.8	0.81
0.85	0.231	3.3	0.8
1.0	0.706	10.8	0.85
1.0	0.537	8.0	0.83
1.0	0.578	8.7	0.84

*Correction factor for loss of 1,6-hexanediol 2 $\mu g\ min^{-1}$.

The Enzfitter program was used to analyse the data and to plot the best fit curve shown in Figure 3.20. The Analysis of Variance gave R-squared as 0.981.

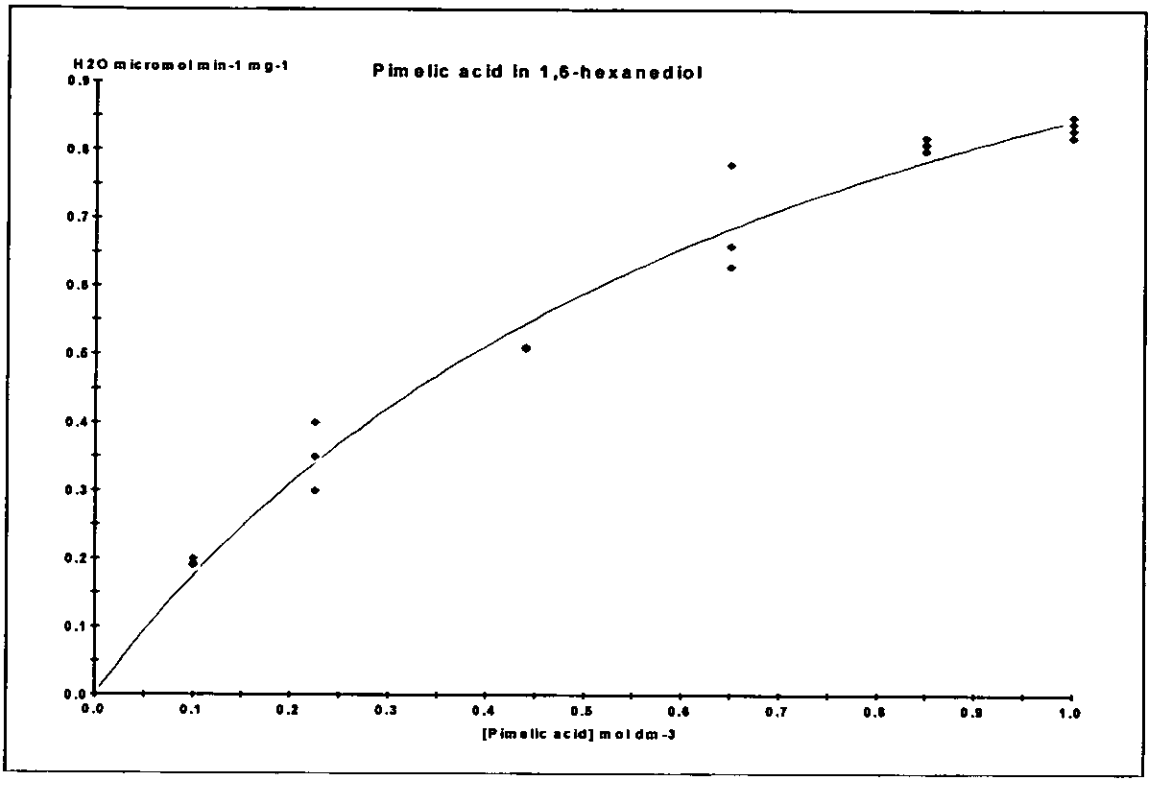

Figure 3.20 The rate of reaction of pimelic acid and 1,6-hexanediol.

Because of the cost and difficulty in obtaining 2-oxoadipic acid it was not possible to determine the reaction rate over a range of substrate concentrations. Therefore, the rate of reaction with 1,6-hexanediol was determined at a concentration of 0.4 M of acid in diol. The results obtained from the reaction of 2-oxoadipic acid and 1,6-hexanediol are given in Table 3.31.

Table 3.31 Reaction of 2-oxoadipic acid with 1,6-hexanediol.

[2-oxoAA] mol dm^{-3}	Enzyme mg	Water loss* $\mu g\ min^{-1}$	Rate of reaction $\mu mol\ min^{-1}\ mg^{-1}$
0.8	0.372	2.2	0.33
0.8	0.349	2.3	0.36
0.8	0.217	1.3	0.34

*Correction factor for loss of 1,6-hexanediol 2 $\mu g\ min^{-1}$.

The average rate of 0.34 μmol min^{-1} mg^{-1} was surprisingly low compared to un-substituted adipic acid. In view of the findings of the molecular modelling exercise, it seemed possible that the 2-oxoadipic acid was acting as an inhibitor for the enzyme. It was thought that if the carboxyl group in the 1-position acylated the serine of the active site then the hydrogen bonding of the 2-oxo carbonyl to the threonine 40 could well stabilise the complex to the extent that the second stage of the reaction would not occur.

In order to test this theory samples were prepared of mixed adipic and 2-oxoadipic acids. A 0.4M solution of adipic acid was prepared in which 15%$^{w}/_{w}$ of the adipic acid had been replaced by 2-oxoadipic acid and a second 0.4M solution prepared in which 1%$^{w}/_{w}$ of the adipic acid had been replaced by 2-oxoadipic acid. The results of these reactions with 1,6-hexanediol are given in Table 3.32.

Table 3.32 Reaction of adipic/2-oxoadipic acids with 1,6-hexanediol.

[diacid] mol dm^{-3}	Enzyme mg	Water loss* μg min^{-1}	Rate of reaction μmol min^{-1} mg^{-1}
0.4 M AA	0.850	8.5	0.55
0.4M AA+15% 2oAA	0.499	4.0	0.45
0.4M AA+1% 2oAA	0.379	3.3	0.48

*Correction factor for loss of 1,6-hexanediol 2 μg min^{-1}.

The above results can be explained by assuming that the 1-carboxyl of the 2-oxoadipic acid is either un-reactive towards the serine of the lipase or the reaction is so slow that it cannot be measured by our method. The rate of reaction of 0.34 μmol min^{-1} mg^{-1} would then be correct, if the carboxyl concentration was assumed to be half of that quoted because of the 2-oxoadipic acid having only one reactive carboxyl group.

The results with the blends of adipic and 2-oxoadipic acids should only be taken as an indication of the rates as they were the result of only one experiment at each concentration. The reduction in rate, if meaningful, could be explained by the un-reactive carboxyl group occupying the active site unproductively, thus reducing the observed rate of reaction.

The results obtained from the reaction of 3-oxoadipic acid and 1,6-hexanediol are given in Table 3.33. The Enzfitter program was used to analyse the data and fit the curve shown in Figure 3.21. The Analysis of Variance gave R-squared as 0.978.

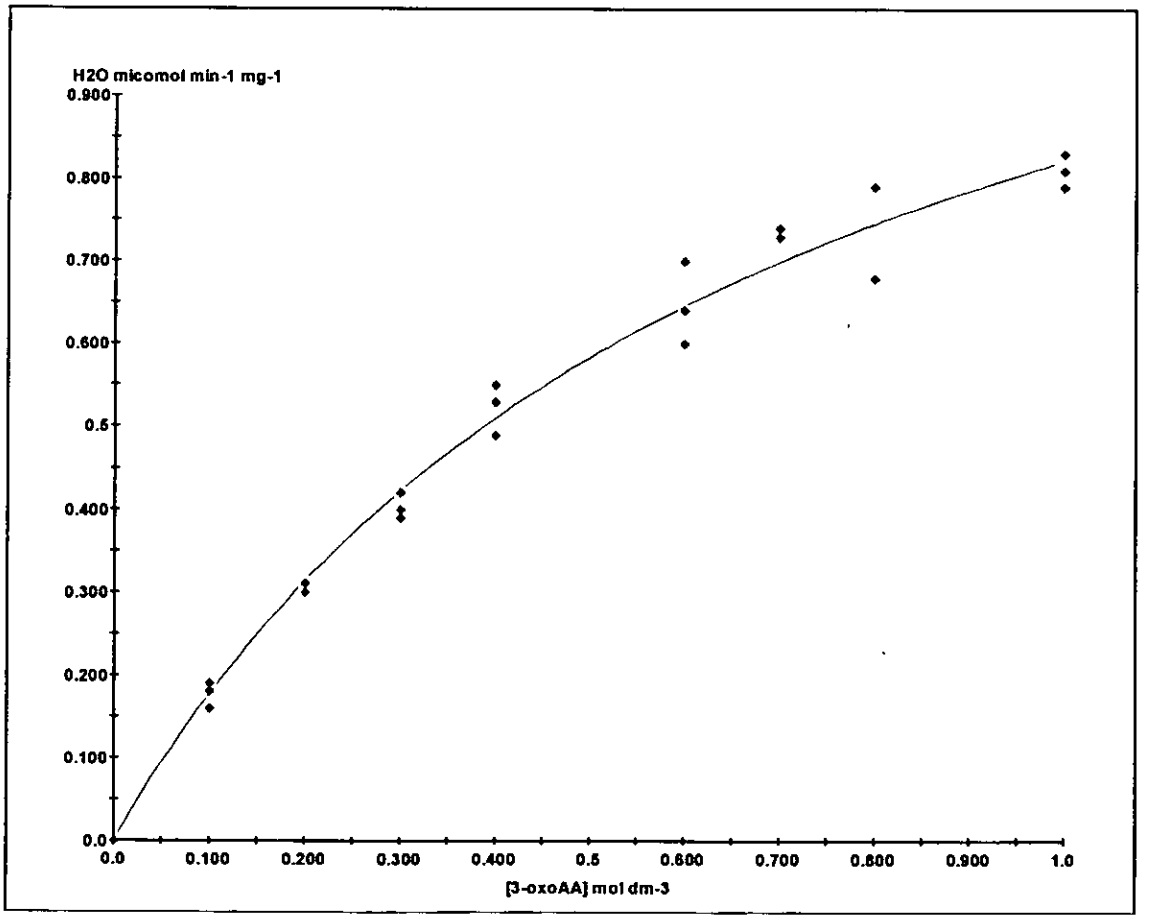

Figure 3.21 The rate of reaction of 3-oxoadipic acid with 1,6-hexanediol.

Table 3.33 The reaction of 3-oxoadipic acid and 1,6-hexanediol at 60°C.

[3-oxoAA] mol dm^{-3}	Enzyme mg	Water loss* $\mu g\ min^{-1}$	Rate of reaction $\mu mol\ min^{-1}\ mg^{-1}$
0.1	0.585	2.0	0.19
0.1	0.488	1.6	0.18
0.1	0.302	0.9	0.16
0.2	0.614	3.3	0.3
0.2	0.528	2.9	0.31
0.3	0.311	2.2	0.39
0.3	0.398	2.9	0.4
0.3	0.352	2.7	0.42
0.4	0.355	3.4	0.53
0.4	0.491	4.9	0.55
0.4	0.417	3.7	0.49
0.6	0.762	8.2	0.6
0.6	0.516	6.5	0.7
0.6	0.332	3.8	0.64
0.8	0.408	5.0	0.68
0.8	0.606	8.6	0.79
1.0	0.228	3.4	0.83
1.0	0.259	3.7	0.79
1.0	0.207	3.0	0.81

*Correction factor for loss of 1,6-hexanediol 2 $\mu g\ min^{-1}$.

The results of the reaction of 3-methyladipic acid are given in Table 3.34.

Table 3.34 The reaction of 3-methyladipic acid and 1,6-hexanediol at 60°C.

[3-MeAA] mol dm^{-3}	Enzyme mg	Water loss* $\mu g\ min^{-1}$	Rate of reaction $\mu mol\ min^{-1}\ mg^{-1}$
0.1	0.231	0.8	0.19
0.1	0.506	1.8	0.2
0.1	0.381	1.5	0.22
0.2	0.337	2.0	0.33
0.2	0.644	3.5	0.3
0.2	0.412	3.0	0.4
0.2	0.362	2.5	0.38
0.4	0.551	5.8	0.58
0.4	0.358	3.7	0.58
0.4	0.596	6.0	0.56
0.6	0.411	5.5	0.74
0.6	0.266	3.4	0.7
0.6	0.345	5.0	0.8
0.8	0.383	5.9	0.85
0.8	0.362	6.0	0.92
0.8	0.403	6.5	0.9
1.03	0.181	3.3	1.02
1.03	0.276	4.3	0.87
1.03	0.259	4.5	0.97
1.03	0.252	4.0	0.88

*Correction factor for loss of 1,6-hexanediol 2 $\mu g\ min^{-1}$.

The Enzfitter program was used to analyse the data and to give the fitted curve shown in Figure 3.22. The Analysis of Variance gave R-squared as 0.98.

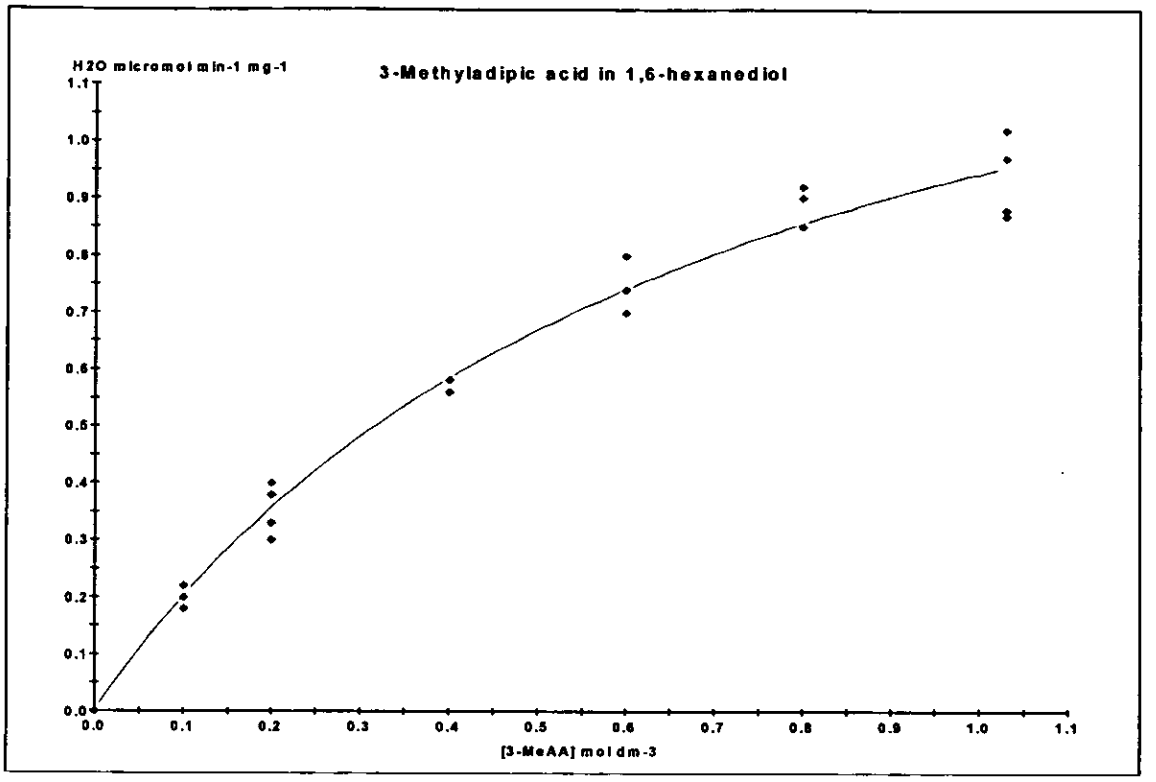

Figure 3.22 The rate of reaction of 3-methyl adipic acid with 1,6-hexanediol.

The Enzfitter program was used to determine the Michaelis-Menten constants V_{max} and K_m for each of the above series of experiments and the results are shown in Table 3.35.

Table 3.35 Michaelis-Menten constants of diacids in 1,6-hexanediol.

Substrate	V_{max} $\mu mol\ min^{-1}\ mg^{-1}$	K_m $mol\ dm^{-3}$	V_{max} 95% confidence limits
Succinic acid	1.15	0.96	0.97-1.33
Glutaric acid	1.2	0.38	1.09-1.3
Adipic acid	1.47	0.53	1.34-1.58
Pimelic acid	1.48	0.76	1.25-1.71

In order to understand better the observed differences in reaction rates the substrate molecules were modelled and energy minimised and their various molecular parameters

calculated (for details of molecular modelling see Chapter 7). These included the overall dimensions of the molecules, the molecular volume, dipole moment, topological symmetry, spatial density and flexibility. All parameters were compared to the specificity constant V_{max}/K_m in order to see if there was any correlation that might explain the differences between the substrates. All the parameters increased as expected with the chain length of the molecule, but no relationship could be seen to the specificity constant.

After minimisation the final total energy of the molecule was measured and when this was compared with the specificity constant there appeared the possibility of a relationship, in that glutaric and adipic acids had the lowest final energy.

The calculated partition coefficients C logP were calculated using the tables of Hansch and Leo.[101] These together with the pK_a of the various acids are shown in Table 3.36.

Table 3.36 Molecular parameters of substrates compared to specificity constant.

Substrate	V_{max}/K_m	C logP	Length Å	pKa_1 - pKa_2	Energy kcals mol^{-1}
Succinic acid	1.19	-0.88	5.23	5.52-4.24	15.43
Glutaric acid	3.12	-0.22	6.80	5.27-4.33	14.38
Adipic acid	2.75	0.44	7.74	5.13-4.49	15.07
Pimelic acid	1.95	1.10	9.14	5.07-4.43	17.11

It is not possible to say with any certainty why the enzyme has the highest affinity for the particular substrates, glutaric and adipic acids. However, when modelling adipate polyesters being formed in the active site it has been observed that a hydrogen bond is formed between the carbonyl of the ester group at the other end of the acid substrate and a threonine residue in the active site. The presence of such a hydrogen bond would

obviously depend on the distance between the two carbonyls of the diacid, too close or too far apart then no hydrogen bond can form. The x-axis (length) of succinic acid is 5.23Å and that of pimelic acid is 9.14Å. Glutaric and adipic acids lie between with lengths of 6.8Å and 7.7Å respectively.

TheMichaelis-Menten constants for the substituted adipic acids are shown in Table 3.37.

Table 3.37 The reaction of substituted adipic acids with 1,6-hexanediol.

Substrate	V_{max} $\mu mol\ min^{-1}\ mg^{-1}$	K_m $mol\ dm^{-3}$	V_{max} 95% Confidence limits
Adipic acid	1.47	0.53	1.34-1.58
3-Oxoadipic acid	1.31	0.6	1.08-1.53
3-Methyladipic acid	1.60	0.69	1.38-1.82

The specificity constant was calculated and compared to the molecular parameters and physical properties, as shown in Table 3.38.

Table 3.38 Molecular parameters of substituted adipic acids.

Substrate	V_{max}/K_m	C logP	pKa_1 - pKa_2	Total energy $kcals\ mol^{-1}$
Adipic acid	2.75	0.44	5.13-4.39	15.05
2-Oxo AA	-	-2.12	4.61-2.53	16.00
3-Oxo AA	2.18	-2.12	4.73-3.13	21.08
3-Methyl AA	2.32	3.29	4.85-4.66	20.75

One possible reason for the lack of activity of the 2-oxoadipic acid is the extremely low pK_a of the carboxyl group with a pK_a of 2.53. This is far below the pK_a of the aspartic

acid of the catalytic triad and as such would inhibit the protonation of that acid; in effect stalling the catalytic mechanism of the enzyme. However, the 3-oxoadipic acid also has a pK_a below that of the aspartic acid with no apparent major effect on the activity of the enzyme. Therefore, the three substrates, 2-oxoadipic acid, 3-oxoadipic acid and 3-methyladipic acid were modelled and compared with adipic acid. The models of the four substrates were energy minimised using MM3 and the molecular dimensions determined.

Table 3.39 Molecular dimensions of some substrates for *Candida antarctica* lipase B.

2-Oxoadipic acid	Molecular weight		160.13
	Dimensions	x	7.786Å
		y	3.437Å
		z	1.211Å
3-Oxoadipic acid	Molecular weight		160.13
	Dimensions	x	7.265Å
		y	2.896Å
		z	2.579Å
3-Methyladipic acid	Molecular weight		160.17
	Dimensions	x	8.286Å
		y	2.772Å
		z	1.961Å
Adipic acid	Molecular weight		146.14
	Dimensions	x	7.520Å
		y	3.100Å
		z	2.003Å

On examination of these properties it is not obvious that any single property can be related to the reactivity with *Candida antarctica* lipase B, although the total energy of the molecule appears to be inversely related to the reactivity. The surface space filled models are shown in Figure 3.23.

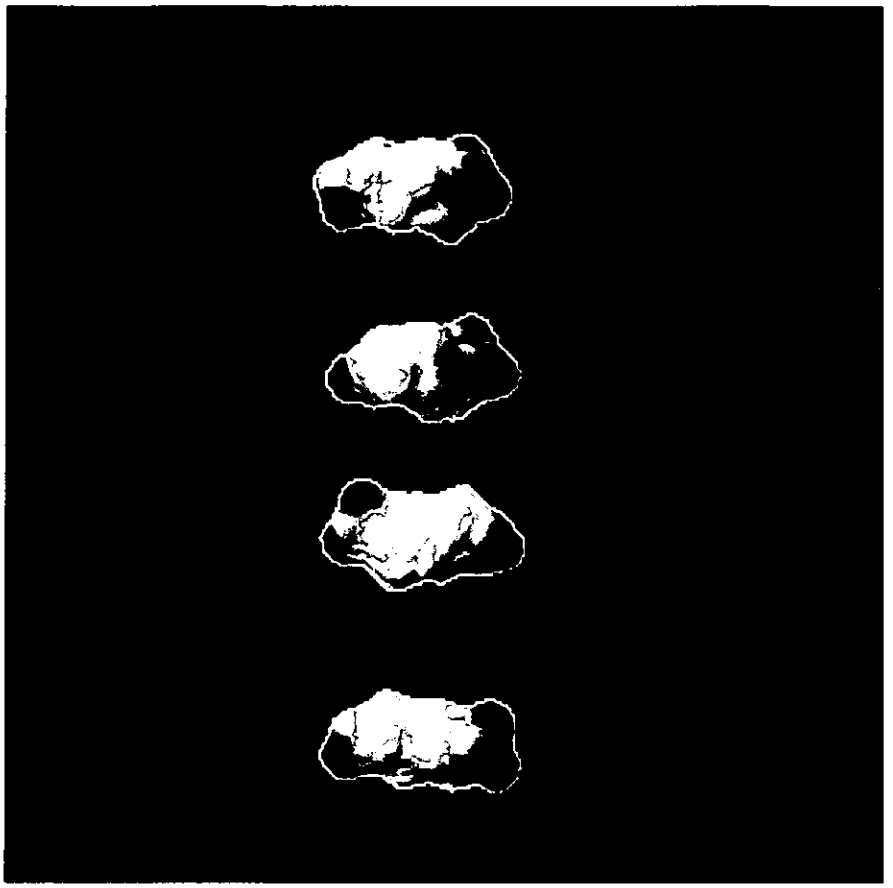

Figure 3.23 Substituted adipic acid substrates modelled in Sculpt. From top to bottom: 2-oxoadipic acid, 3-oxoadipic acid, 3-methyladipic acid and adipic acid.

The models are space filled surface models to show the relative size and shape of the substrates. It can be seen that only the 3-methyladipic acid is noticeably bulkier than the others, however the enzyme still accepts this substrate readily. This observation together with the model of the macrolactone discussed later (see Figure 4.15) confirms that *Candida antarctica* lipase B is relatively unselective as to the acylating substrates that it will accept. However, the fact remains that carbonyl substitution in the 2-position gave a

dramatic reduction in reactivity; therefore, it was decided to look at the possibility of electrostatic interactions in the active site which might disrupt the reaction mechanism.

A model of 2-oxoadipic acid was drawn in ISISDraw, converted to 3D and then copied into a model of *Candida antarctica* lipase B (1tca) in Sculpt (Figure 3.24). The substrate molecule was then docked manually and the whole assembly of protein and ligand minimised using both electrostatic and van der Waals forces. During the minimisation process the conformation of the enzyme pocket changes, initially the His 224 is aligned close to the Ser 105 and the carbonyl in the 2-position on the 2-oxoadipic acid is directed towards the His 224. However, on prolonged minimisation the His 224 moves away and the 2-oxo carbonyl moves round to hydrogen bond to the Thr 40 at a distance of 3.1Å. If this were an accurate simulation of the active site, then such a strong hydrogen bond would undoubtedly interfere with the stability of the tetrahedral intermediate.

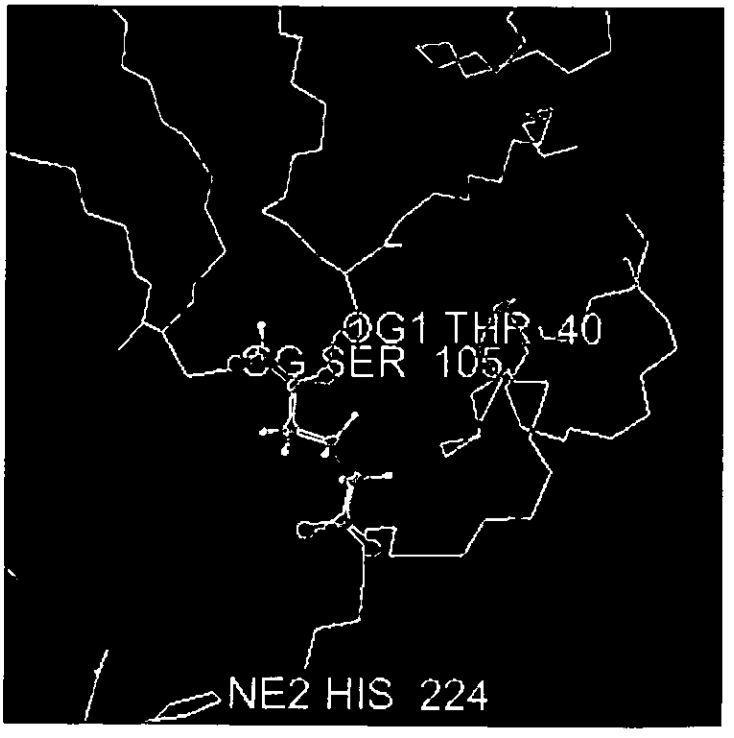

Figure 3.24 2-Oxoadipic acid docked in *Candida antarctica* lipase B.

In the above model the electrostatic and van der Waals interactions have been hidden so that the hydrogen bond may be seen clearly, however, in Figure 3.25, the 3-oxoadipic acid is shown with all interactions visible. It is obvious that the 3-carbonyl of the 3-oxoadipic acid points away, ("South West") from the Thr 40 and there are no interactions between this carbonyl and any part of the enzyme.

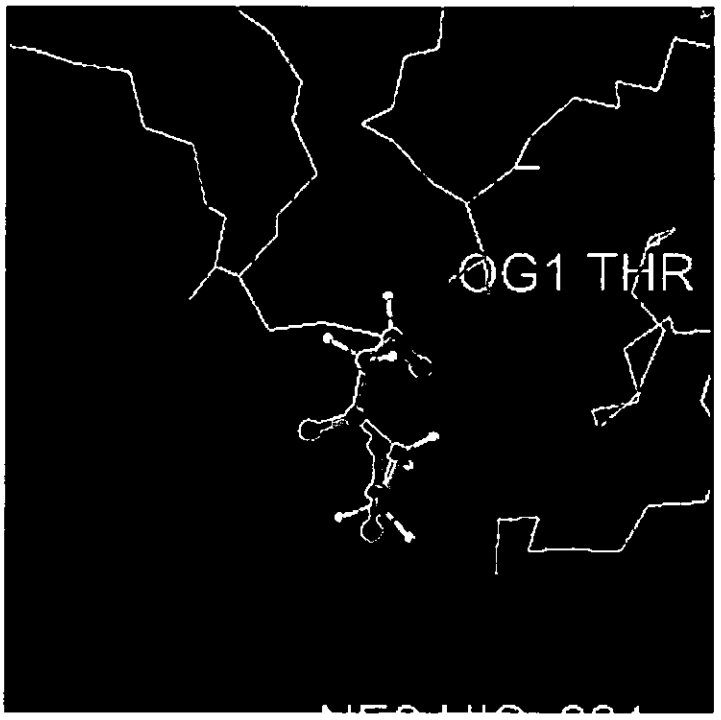

Figure 3.25 3-Oxoadipic acid docked into *Candida antarctica* lipase B.

The exercise was repeated with the 3-methyladipic acid and as with the 3-oxoadipic acid, there were no obvious interactions (see Figure 3.26).

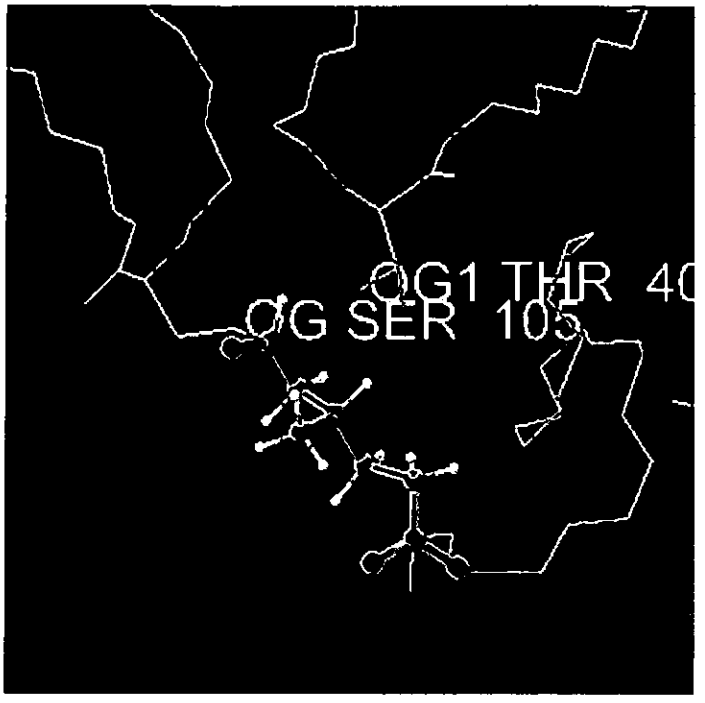

Figure 3.26 3-Methyladipic acid docked into *Candida antarctica* lipase B.

The 3-methyl group is pointing towards the observer and has no van der Waals or electrostatic interactions with residues within the active site other than those due to the acylation of the Ser 105. The slight observed difference in the rate of reaction between this substrate and adipic acid is probably due to small differences in desolvation and diffusion as a result of the methyl substituent.

Therefore, the lack of activity of the 2-oxoadipic acid appears to be due to the unfavourable hydrogen bonding of the 2-carbonyl in the active site.

3.4 Transesterification reaction kinetics.

The transesterification kinetics became more important as a result of the transesterification studies in Chapter 4 and the Isothermal Titration calorimetry described in Chapter 5; a comparison of the rates of transesterification with the rates of

esterification being particularly relevant. The obvious ester to consider for the study of transesterification reactions relevant to the polyesterification process was dimethyl adipate. However, the vapour pressure of this ester at 50°-60°C is such that the weight losses due to evaporation were too large compared to the weight losses from the esterification reaction to give any meaningful results. Also, in the large scale process the transesterification reaction occurs simultaneously with the esterification reaction because both ester and carboxyl groups are always present, at least until the final stages of the polyesterification process.

In order to overcome both of the above problems the monoethyl ester of adipic acid (MEAA) was chosen as the substrate to be studied. The vapour pressure of the MEAA is such that the volatility at 60°C only requires a correction factor of 1 $\mu g\ min^{-1}$ in the TGA. The ethanol, if produced, is sufficiently volatile for its weight loss to be measured by the TGA. The presence of both visceral ester and terminal carboxyl groups in the MEAA, simulates the polyester oligomers in the polyesterification process. The enzyme having the choice of acylation by either group as they are present in equal concentrations in the substrate.

The monoethyl ester of adipic acid (MEAA) was dried over P_2O_5 and solutions in 1,6-hexanediol were prepared. These were pre-dried in the standard drying cycle up to 110°C in the TGA, cooled to approximately 40°C and the enzyme added. The results are given in Table 3.40.

Table 3.40 Reaction of monoethyl adipate and 1,6-hexanediol.

[MEAA] mol dm^{-3}	Enzyme mg	Water loss* $\mu g\ min^{-1}$	Rate of reaction $\mu mol\ min^{-1}\ mg^{-1}$
0.1	0.521	4.2	0.45
0.1	0.221	1.8	0.44
0.1	0.288	2.2	0.43
0.1	0.568	3.5	0.34
0.2	0.483	6.3	0.73
0.3	0.318	4.8	0.83
0.3	0.814	14.7	1.00
0.3	0.491	7.5	0.85
0.4	0.388	7.0	1.00
0.4	0.234	5.3	1.26
0.4	0.281	6.0	1.18
0.5	0.456	11.5	1.40
0.5	0.694	13.7	1.10
0.5	0.431	9.5	1.22
0.5	0.522	11.7	1.25
0.7	0.426	11.7	1.53
0.7	0.424	10.2	1.34
0.7	0.412	10.5	1.41
1.0	0.438	14.3	1.81
1.0	0.491	14.8	1.67
1.0	0.316	11.0	1.93
1.22	0.293	10.0	1.90
1.22	0.656	24.8	2.10
1.22	0.524	17.9	1.90

*Correction factor for loss of 1,6-hexanediol 2 $\mu g\ min^{-1}$.

The results were analysed using the Enzfitter program and the best fit curve is shown in Figure 3.27. The Analysis of Variance gave R-squared as 0.9.

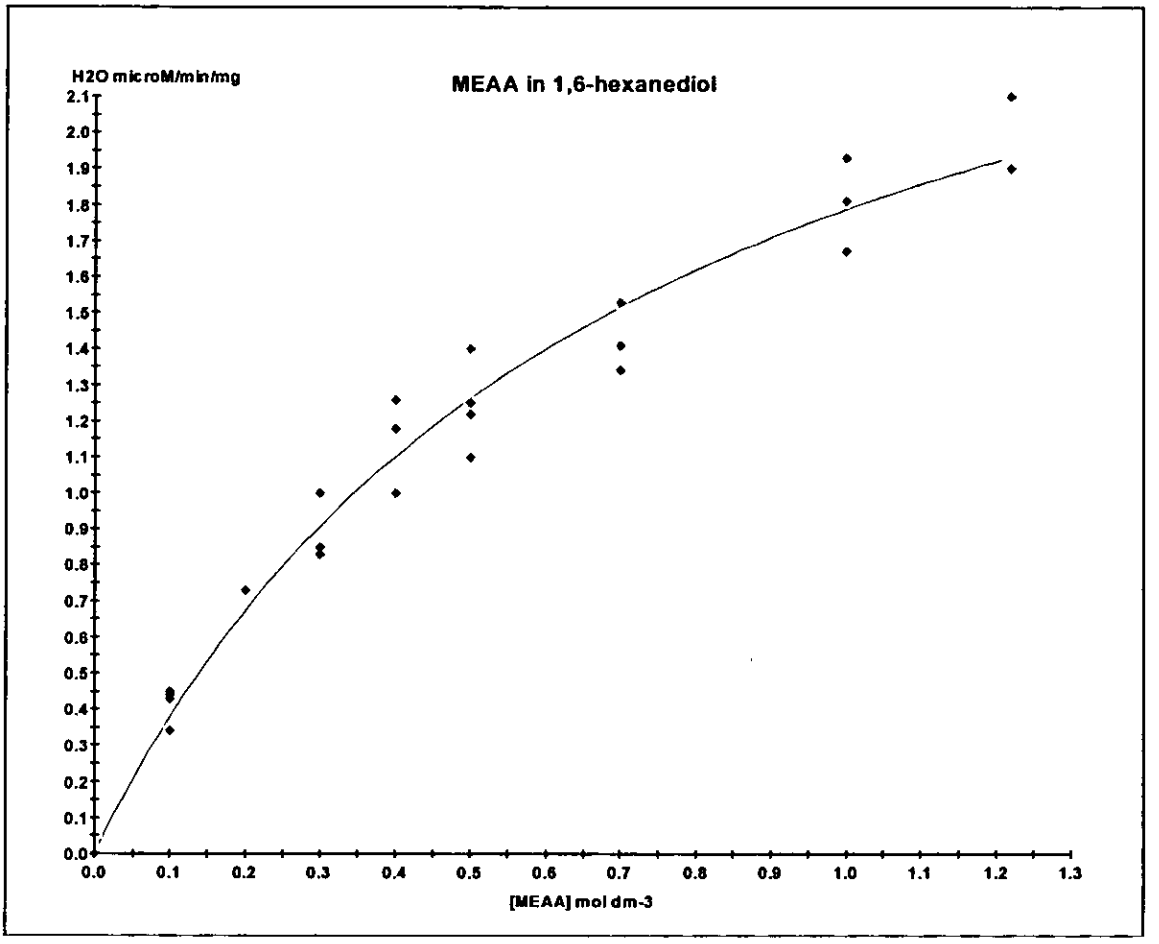

Figure 3.27 The rate of reaction of MEAA with 1,6-hexanediol.

It is obvious from these results that the MEAA substrate is significantly more reactive than any of the previous acid substrates. In several earlier experiments the reactions had been left in the TGA for several hours and the total weight loss measured. When this was done for adipic acid and 1,6-hexanediol the estimated yield was between 70-85% of theoretical. This procedure was repeated using the monoethyl adipate ester with 1,4-butanediol.

22.726mg of 0.8 M MEAA in 1,4-butanediol were heated to 50°C in the TGA with 0.796

mg of Chirazyme L-2 for 200 minutes. The total weight loss due to volatiles was 1.777 mg, after deducting the correction factor of 0.750 mg; the weight loss due to reaction products was 1.027 mg. If one assumes complete reaction of the acid carboxyl group the theoretical loss of water would be 0.327 mg. Therefore, it is obvious that a substantial amount of ethanol has been removed as the product of the transesterification reaction. The theoretical amount of ethanol produced, assuming complete reaction would be 0.836 mg giving a total weight loss of 1.163 mg.

A similar procedure was applied to 1,6-hexanediol. 21.855 mg of 0.8 M MEAA in 1,6-hexanediol was heated to 50°C in the TGA together with 0.780 mg of Chirazyme for 180 minutes. The total loss of volatiles was 1.039 mg, which, less the correction factor of 180 μg, gives a total weight loss of reaction products of 0.859 mg. In both cases it is apparent that substantial amounts of ethanol from the transesterification reaction have been evolved. If the amount of water produced by the carboxyl groups of 0.8 M adipic acid in 1,6-hexanediol is deducted from the rate of weight loss from the MEAA at the same concentration then it is estimated that the difference in the reactivity is 3:1 between the ester carbonyl and the acid carbonyl. These results confirm the results found in both the transesterification studies and the isothermal titration calorimetry that the transesterification reaction is significantly faster than the esterification reaction. This observation is understandable if one considers the chemistry of the carboxyl group. The diagram below shows the nucleophilic attack of the serine OH on an ester carbonyl.

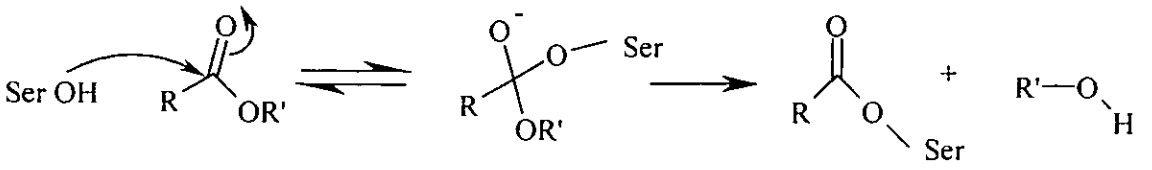

When a nucleophile such as the serine OH attacks the carbonyl of a carboxylic acid

derivative such as an ester, the tetrahedral intermediate expels one of the substituents as a leaving group, leading to a net nucleophilic acyl substitution. The ease by which the leaving group can be removed controls the rate of reaction. In descending order, acid chlorides are the most reactive then anhydrides, esters, amides and then acids.[111] The reason that the carboxylic acids are so much slower reacting than the esters is that the actual reaction mechanism is different. The nucleophile acts as a base and converts the acid to the corresponding carboxylate ion.

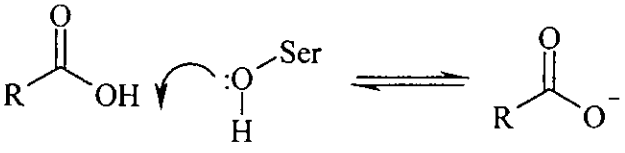

The carboxylate ion is un-reactive to the nucleophilic attack because it is carrying a negative charge already. Therefore the reaction of adipic acid under essentially neutral conditions is predominantly an acid-base reaction rather than a nucleophilic attack on the carbonyl.[112] In order to carry out a nucleophilic attack on the carbonyl carbon of the acid it is necessary to have acid conditions in order to suppress the formation of the carboxylate ion in order that the OH^- leaving group can leave as H_2O. The pK_a of adipic acid of 4.3 is such that only the presence of strong acid, which suppresses the formation of the carboxylate ion, can catalyse the nucleophilic reaction.

3.5 Effect of temperature on the activity of *Candida antarctica* lipase B.

The effect of temperature on the reaction was studied for a number of reasons:

i. If the enzymatic synthesis could be accelerated by carrying out the reaction at a temperature higher than 60°C, then the batch time would be shortened;

thereby favouring the economics of the process.

ii. If the process could be carried out at higher temperatures then the viscosity of the reactants would decrease, higher molecular weight polymers could then be synthesised as the higher viscosity of the higher molecular weight polyesters would not be rate limiting.

iii. Determination of the effect of temperature on reaction rate would allow the calculation of the activation energy of the rate controlling step. The logical system on which to base the rate/temperature studies was the adipic acid - 1,6-hexanediol system. However, it soon became apparent that there were fundamental difficulties in carrying out this reaction at higher temperatures.

The melting point of the adipic acid solutions in 1,6-hexanediol is approximately 50°C. Either because of the proximity to the melting point or the reaction rate being very slow at 50°C, no reaction was observed below 55°C. Furthermore, the onset of the reaction below 58°C was variable so that no reliable results could be obtained below 60°C. At temperatures higher than 60°C the volatility of the 1,6-hexanediol became a problem. The correction factor at 60°C was 2μg min^{-1}; this became 4μg min^{-1} at 70°C, 10.5 μg min^{-1} at 80°C and 20.5 μg min^{-1} at 90°C. The typical weight losses per minute due to the loss of water formed in the reaction were between 5-10mg min^{-1}; therefore, such large correction factors would render the results unreliable. It was necessary to look at relevant alternative systems where the volatility of the substrates would not be a problem. The reaction of monoethyl adipic acid (MEAA) ester with 1,6-hexanediol was studied, while the problems associated with the volatility of the diol still applied, the freezing point of the solutions was approximately 40°C. Also the reactivity of the ester was such that

meaningful weight losses could be observed. Therefore the opportunity arose to look at the rate of reaction at lower temperatures. The reaction of a 0.4 M solution of MEAA in 1,6-hexanediol was carried out at 50°C, 55°C and 60°C. The results are in Table 3.36.

Table 3.36 The reaction of MEAA and 1,6-hexanediol between 50°-60°C.

Temp. °C	Enzyme mg 100% protein	Weight loss* $\mu g\ min^{-1}$	Rate of reaction $\mu mol\ min^{-1}\ mg^{-1}$
50	0.293	12.4	2.35
50	0.298	12.5	2.33
50	0.174	7.6	2.42
55	0.140	6.5	2.58
55	0.187	8.7	2.58
55	0.134	6.5	2.69
60	0.106	5.8	3.04
60	0.271	14.0	2.87
60	0.163	8.3	2.83

*Correction factors for loss of 1,6-hexanediol at 50°C 0$\mu g\ min^{-1}$, at 55°C 1 $\mu g\ min^{-1}$ and at 60°C 2 $\mu g\ min^{-1}$.

These results were plotted as an Arrhenius Plot as shown in Table 3.37 and Figure 3.28.

The Arrhenius equation governs the effect of temperature on the rate of a reaction as shown in Equation 1.

$$K = A\, e^{\frac{-Ea}{RT}} \qquad \text{Equation 1}$$

K is the rate constant, A is the pre-exponential frequency factor, E_a is the activation energy, R is the Gas Constant and T is the temperature in K.

The equation may be re-arranged to Equations 2 and 3. Equation 3 is the equation for a straight line plot, therefore, the activation energy E_a can be calculated from the slope of the graph as shown in Equation 4.

$$\ln K = \ln A - \frac{Ea}{RT} \qquad \text{Equation 2}$$

$$\ln K = \ln A - \frac{Ea}{R} \times \frac{1}{T} \qquad \text{Equation 3}$$

$$Slope = \frac{-Ea}{R} \qquad \text{Equation 4}$$

$$\therefore\ Ea = R \times Slope$$

Table 3.37 Calculation of Activation Energy by Arrhenius plot.

Temp. °C	$^1/_T$ K x 10^{-3}	Rate µmol min^{-1} mg^{-1}	Rate constant K	ln K
50	3.10	2.37	14.8	2.69
55	3.05	2.62	16.4	2.8
60	3.00	2.91	18.2	2.91

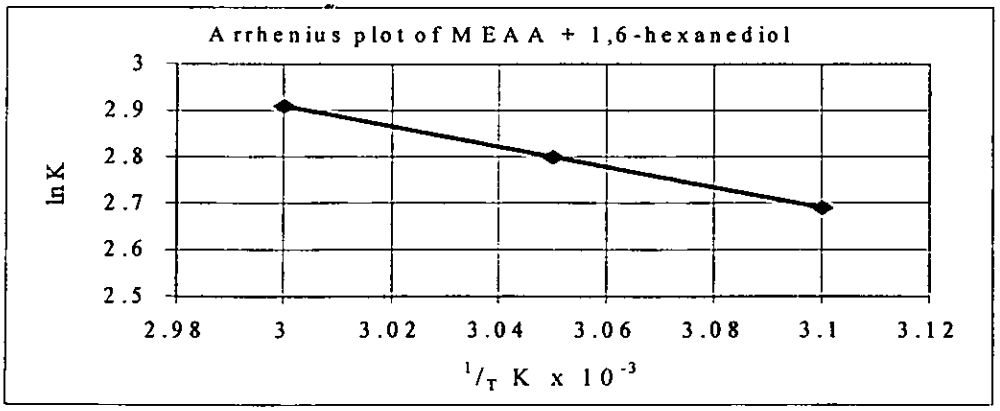

Figure 3.28 Arrhenius plot for MEAA + 1,6-hexanediol.

The slope of the plot was 0.22×10^{-3} K. Therefore, the activation energy is 18.3 kJ mol^{-1}.

The only diol that does not have an appreciable weight loss at elevated temperature is the 650 molecular weight polytetramethylene ether diol (PTMEG 650). Therefore, the rate of reaction of a 0.4 M solution of adipic acid in PTMEG 650 was determined at 60°C, 70°C and 80°C. Because of the earlier observation of declining rates above 80°C only the first 10 minutes of the reaction were considered. The results are given in Table 3.38.

Table 3.38 Reaction of adipic acid and PTMEG 650 between 60°-80°C.

Temp °C	Enzyme mg 100% protein	Weight loss* μg min^{-1}	Rate of reaction μmol min^{-1} mg^{-1}
60	0.212	8.1	2.13
60	0.054	2.1	2.22
60	0.139	5.8	2.28
70	0.139	7.1	2.82
70	0.117	5.3	2.70
70	0.155	7.2	2.79
80	0.078	8.3	3.72
80	0.182	10.5	3.30
80	0.108	8.3	4.29

*No correction factor required for weight loss of PTMEG 650.

The results were converted for an Arrhenius plot as shown in Table 3.39.

Table 3.39 Calculation of Activation energy by Arrhenius plot.

Temp °C	$^1/_T$ K x 10^{-3}	Rate µmol min^{-1} mg^{-1}	Rate constant K	ln K
60	3.0	2.2	13.7	2.6
70	2.9	2.8	17.5	2.9
80	2.8	3.8	23.8	3.2

The slope of the plot of the above data (Figure 3.29) was 3.0 x 10^{-3}K, giving an activation energy of 24.9kJ mol^{-1}.

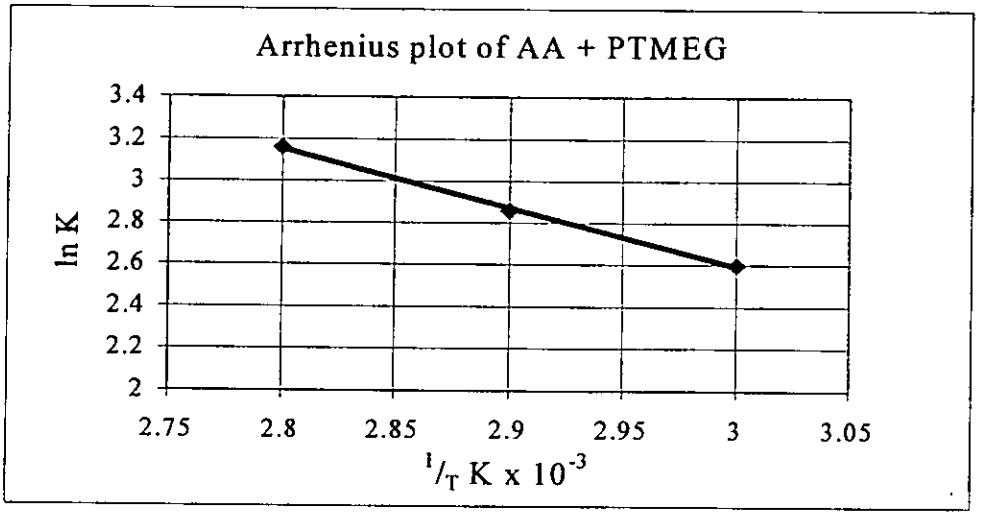

Figure 3.29 Arrhenius plot of adipic acid and PTMEG 650.

Therefore the activation energy of the acylation of the enzyme by adipic acid is measured as 24.9kJ mol^{-1}, whereas that of the acylation by the monoester is 18.3kJ mol^{-1}. The measurement of the activation energy of the monoester reaction undoubtedly contains a contribution from the acylation of some of the enzyme by the monocarboxylic acid end group, therefore, it is possible to say that the activation energy for the ester acylation reaction is less than 18.3kJ mol^{-1}. This explains the observations reported in the rate

studies (Chapter 3.6) and the results of the isothermal titration calorimetry (Chapter 5) that the enzyme is more readily acylated by the ester carbonyl. Because the activation energy of the transesterification reaction appears to be significantly less than that of the acid acylation reaction, the ester acylation will be the preferred reaction.

The activity of the enzyme at high temperatures was of interest for two reasons. It was important to know the upper limits of useful activity in the process for the reasons explained previously. However, it is necessary that any enzyme remaining in the polyester at the end of the process be deactivated. Traces of residual enzyme would lead to hydrolysis of the product at room temperature, which would cause deterioration of the product in service.

In order to probe the temperature denaturation of the enzyme, the activity was determined after heating to temperatures significantly higher than used previously. In order to overcome the problems of diol volatility, the system studied was a 0.8 M solution of adipic acid in PTMEG 650. Because of the relevance to the manufacturing process the enzyme used in these experiments was the *Candida antarctica* lipase B supported on acrylic beads and sold as Novozyme 435. The results obtained are shown in Table 3.40.

It is apparent that the enzyme retains some activity at these elevated temperatures and that 130°-140°C appears to be the point at which activity is lost. However, these are initial rates, no attempt was made to determine how long the enzyme remained active at these temperatures, or if it could be recycled and remain active after exposure to these temperatures.

Table 3.40 The reaction of adipic acid with PTMEG 650 at elevated temperatures.

Enzyme mg	Temp °C	Weight loss* $\mu g\ min^{-1}$	Rate of reaction $\mu mol\ min^{-1}\ mg^{-1}$
2.152	110	15.0	0.39
1.892	110	17.0	0.50
1.702	110	18	0.59
1.914	120	28.0	0.81
2.073	120	26.5	0.71
3.322	130	20.9	0.35
1.989	130	10.7	0.3
2.411	140	4.3	0.10
1.884	140	0	0

*No correction factor required for weight loss of PTMEG 650.

4 The study of transesterification reactions.

Lipase catalysed transesterification reactions in organic media with monoesters have been used to separate racemic mixtures of alcohols and carboxylic acids or to select a specific ester or alcohol group within a molecule as substrate.[113]

Our earlier work had shown that transesterification takes place in the presence of certain solvents, but not in the solvent free system.[16] Our further work on the reaction kinetics of the monoethylester of adipic acid (MEAA) in 1,6-hexanediol (Section 3.4) had shown a 3:1 difference in reactivity of the ester group compared to the carboxyl group. This preference of the enzyme for the ester carbonyl had also been confirmed by the determination of the enthalpy of reaction for the acylation of the enzyme by the acid and ester using isothermal titration calorimetry (Chapter 5).

Therefore, the original question of why the enzyme appears to catalyse the transesterification of polyesters in some circumstances and not in others became more interesting, because one would expect it to catalyse transesterification in all circumstances.

In all our earlier work, the esterification and any transesterification reactions leading to the formation of the polyester would be taking place simultaneously, with the final composition containing the products of both reactions. Therefore, a method was developed whereby the transesterification reaction could be studied independently.

A high molecular weight polyhexane adipate polyester was synthesised using Novozyme 435 as the catalyst. When the polyester had reached a molecular weight of 36000 as measured by GPC we stopped the reaction and measured the acid number and hydroxyl number by titration. The bound enzyme was filtered off and the residual enzyme

deactivated by heating the polyester at 200°C for 15 minutes. This polyester became the standard for all our transesterification experiments and had a M_n of 17500, a M_w of 37000 and Dispersity 1.9. The acid number was measured as 2mg KOH g^{-1} and the hydroxyl number was 13mg KOH g^{-1}. The molecular weights for this and all subsequent transesterification experiments were determined by using a Waters HPLC with a model 510 pump, model 410 refractive index detector and the Waters 717 autosampler. The column was packed with Polymer Labs. 1000Å polystyrene copolymer packing and the eluent used was THF stabilised with 250ppm of butylated hydroxytoluene (BHT) at a flow rate of 1ml min^{-1}. The sample concentration for all experiments was 0.5wt%/vol with an injection volume of 40µl. The data was analysed using the Millennium 32 GPC software. The GPC for this material is shown in Figure 4.1.

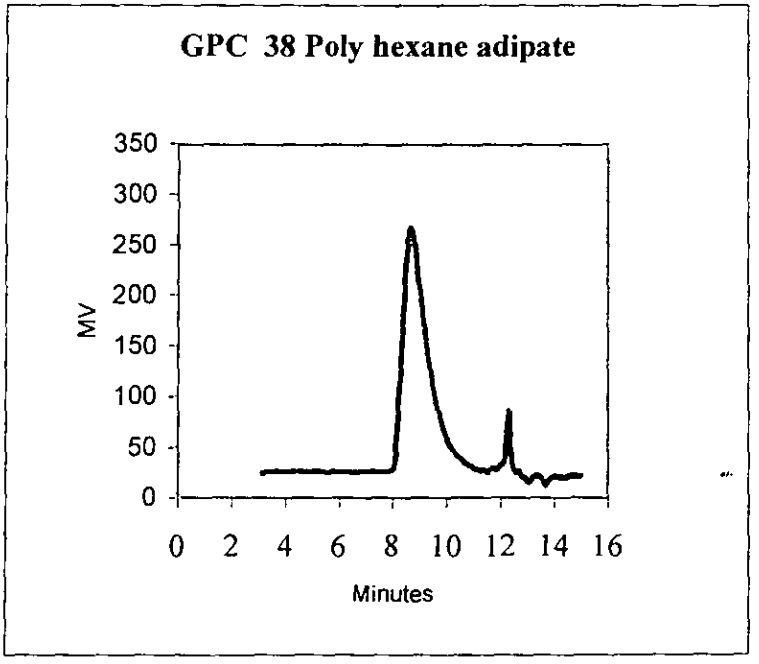

Figure 4.1 GPC of high molecular weight polyester control.

At the beginning we had suspected that it was the enzyme that changed conformation in the presence of the toluene solvent. However, we had shown by CD spectroscopy that it

was unlikely that there was any major change in the geometry of the active site (Chapter 6). Therefore, the possibility remained that solvent molecules were being absorbed onto the hydrophobic regions in or around the active site. It was considered that even one or two bulky solvent molecules such as toluene absorbed in a critical area could easily affect the rate at which the substrate could diffuse into the pocket of the enzyme. Therefore, a standard transesterification experiment was developed, 2 g of the high molecular weight polyester plus 8 cm^3 of solvent, 0.1 g of 1,6-hexanediol and 0.1 g of Novozyme 435 were added to a stirred cell reactor and heated at 60°C for 24 hours. The reaction was then stopped by filtering off the bound enzyme and cooling rapidly to 20°C. In order to simulate the conditions that existed in the earlier syntheses, the solvents chosen were: toluene, 1,4-butanediol, polytetramethylene ether glycol 650 (PTMEG 650) and dioxane. The GPC's obtained are shown in Figures 4.2 to 4.5.

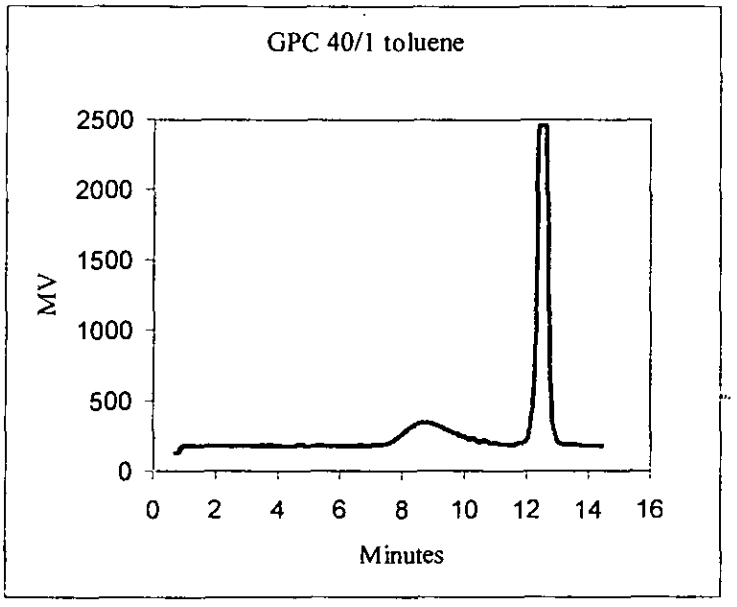

Figure 4.2 GPC of polyester transesterified in toluene.

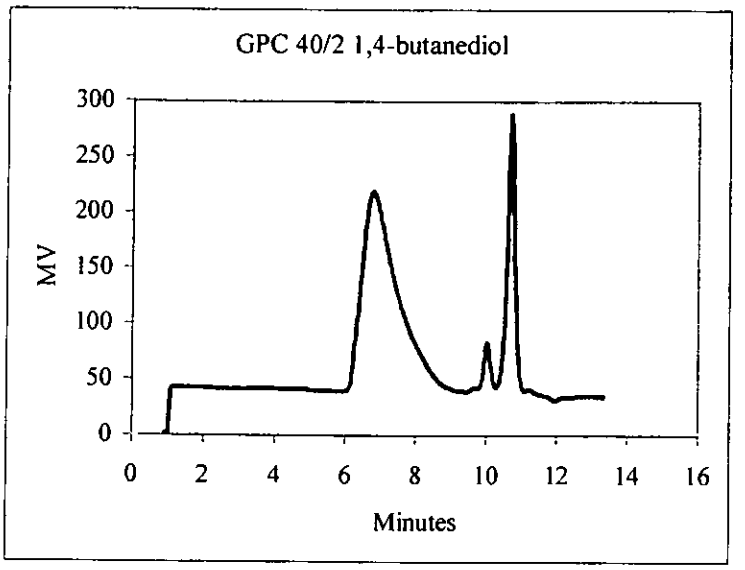

Figure 4.3 GPC of polyester transesterified in 1,4-butanediol.

The high molecular weight polyester has a retention time of 7 minutes, the peaks for the 1,6-hexanediol and 1,4-butanediol are clearly visible.

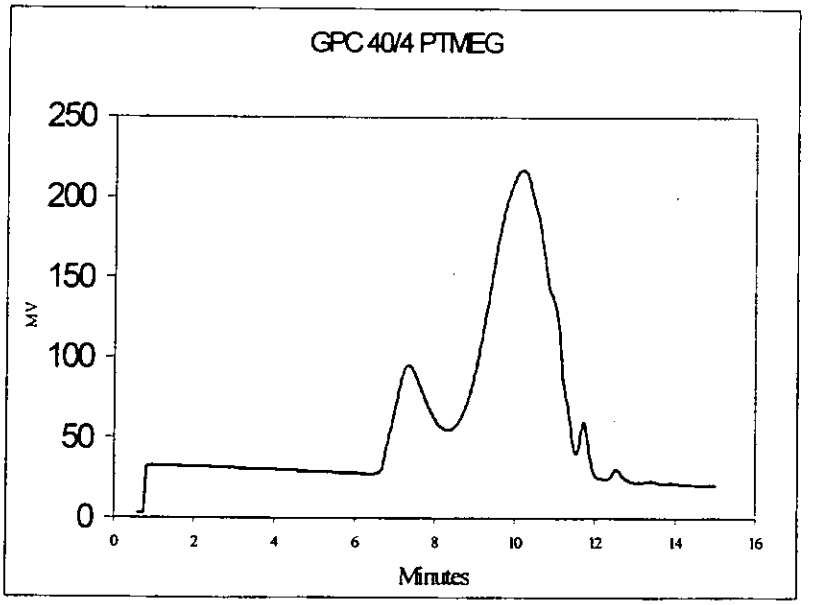

Figure 4.4 Polyester after transesterification in PTMEG 650.

The high molecular weight polyester has a retention time of 7 minutes, the large peak at 10 minutes is the PTMEG 650.

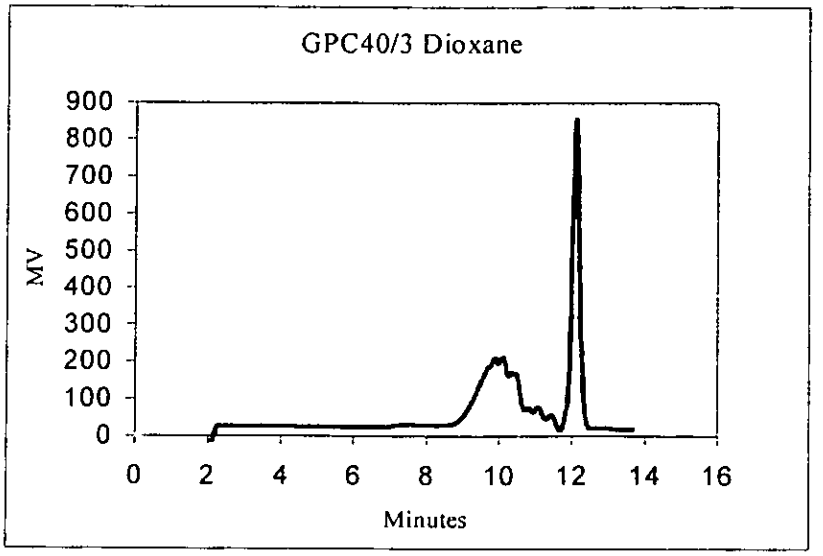

Figure 4.5 Polyester after transesterification in dioxane.

The comparison of the weight average (M_w) and number average (M_n) molecular weight distributions is shown in the Table 4.1.

Table 4.1 Effect of solvent on the transesterification of polyester.

Solvent	M_w	M_n	Dispersity	Comment
PTMEG 650	36000	32000	1.1	Unchanged
1,4-butanediol	26000	-	-	2 phases
Toluene	5800	2898	2.0	
Dioxane	1369	742	1.8	

The hydroxyl of the added diol is involved in the transesterification reaction causing scission of the high molecular weight polyester. However, it appears from these results that the amount of transesterification is independent of hydroxyl concentration. The greatest breakdown of the high molecular weight polyester occurred with toluene and dioxane and not with 1,4-butanediol or PTMEG 650, which have much higher

concentrations of hydroxyls. This appears to contradict the conclusion of Kumar and Gross,[114] who proposed that there is slower transesterification in higher molecular weight polycaprolactones because the higher the molecular weight, the fewer terminal hydroxyls there are to take part in the transesterification reaction.

It had been found by Harffey [115] that the addition of as little as 6%$^{v}/_{v}$ of toluene to the reaction medium gave the same result as when the reaction was carried out in toluene as the reaction solvent. The possibility that toluene was being absorbed from the medium on to the hydrophobic areas of the protein, thereby affecting the mechanism of the reaction, was considered. Therefore, the effect of low concentrations of toluene in 1,4-butanediol on the degree of transesterification was determined. The results are shown in Table 4.2.

Table 4.2 Effect of toluene concentration on transesterification.

Principal solvent	[Toluene] mM	M_w	M_n	Dispersity
1,4-BD	0.11 (0.001%)	26328	14088	1.9
"	1.1 (0.01%)	28232	19232	1.5
"	67 (0.625%)	27060	16892	1.6
"	200 (1.87%)	27708	17836	1.6

The differences between these results are not considered to be significant. It appears that small additions of solvent do not affect the degree of transesterification. It is unlikely, therefore, that absorption of solvent into the hydrophobic areas of the enzyme takes place, as it would be expected that the hydrophobic attraction of the lipase would extract toluene from such a polar medium as 1,4-butanediol, even at these low concentrations.

The effect of the shape of the solvent molecule was then investigated. The standard transesterification experiment was carried out with a number of solvents of different shapes and hydrophobicity. The results are as shown in Table 4.3.

Table 4.3 Effect of solvent configuration on transesterification.

Solvent	M_w	M_n	Dispersity	C logP
Toluene control	5800	2900	2.0	2.7
n-Butylbenzene	5196	2796	1.9	4.0
iso-Butylbenzene	5901	3025	2.0	4.0
tert-Butylbenzene	5864	2909	2.0	4.1
4-Chlorotoluene	5877	2945	2.0	3.3
Hexane	17581	8540	2.0	3.8

Figure 4.6 shows the GPC trace for the polyester obtained after 24 hours in *iso*-butylbenzene. The GPC profiles for all the experiments listed in Table 4.3 are essentially the same for all the aromatic solvents.

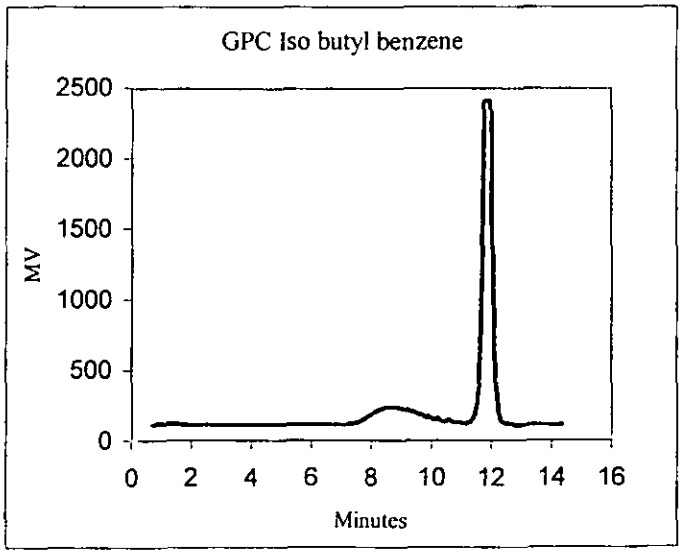

Figure 4.6 Transesterification of polyester in *iso*-butylbenzene.

It is evident from these results that the degree of transesterification as measured by chain scission is not affected by the geometry of the solvent molecule. The differences seen in the experiments with the aromatic solvents are not considered significant; the only significant difference being between the aromatic solvents and the aliphatic hexane. It does not appear, however that the hydrophobicity as measured by C logP is the cause of the difference; there is significant transesterification at a C logP of -0.4 in dioxane and also at C logP of 4.1 in *tert*-butylbenzene. The conclusion to be drawn from these results is that transesterification takes place in any solvent. The only two media in which it does not appear to occur are 1,4-butanediol and polytetramethylene ether glycol. Both of these are very poor solvents for the high molecular weight polyester.

In order to elucidate the mechanism of the transesterification reaction we repeated the experiments with toluene and 1,4-butanediol using 1,1',2,2',3,3',4,4'-octadeutero-1,4-butanediol in place of the 1,6-hexanediol, as the transesterification agent. A 1% solution of d^8-1,4-butanediol in 1,4-butanediol was prepared and the ^2H NMR spectrum obtained (Figure 4.7).

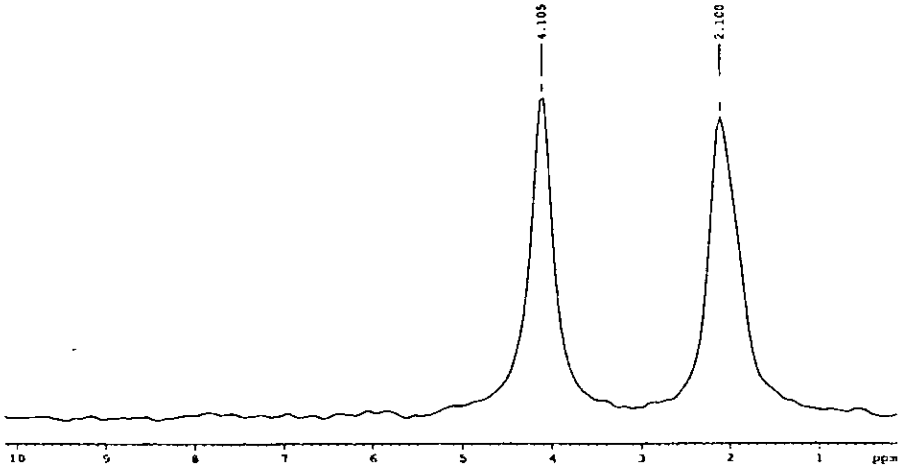

Figure 4.7 ^2H-NMR spectrum of deuterated 1,4-butanediol.

The two peaks of the deuterated diol were δ 4.11 ppm, corresponding to the 1,1'- and 4,4'-deuteriums and δ 2.14 ppm, corresponding to the 2,2'- and 3,3'-deuteriums. The signal to noise ratio was 150:1, therefore we were confident that using this concentration we would be able to see whether transesterification had taken place, by looking for the insertion of the deuterated 1,4-butanediol into the polyester.

A larger scale version of the above reaction was carried out in a cell reactor with stirring at 60°C. Samples were taken at 2 hours, 5 hours and 21 hours and the ^{2}H NMR spectra obtained. No difference could be seen in any of the spectra, thus indicating that in the 1,4-butanediol medium no transesterification had taken place. This experiment was repeated after adding a further ½ volume of toluene and stirring continued at 60°C for 24 hours. When the stirring was discontinued, we realised that the sample was not homogenous and so a few drops of THF were added to act as co-solvent. A ^{2}H-NMR spectrum with excellent signal to noise ratio (2000 scans) was obtained. After 24 hours, there was a small but distinct peak at δ 4.68 ppm due to the increased chemical shift when one end of the diol is incorporated into an ester group. After 48 hours there was a large, distinct peak at δ 4.68 ppm and the peak at δ 2.12 ppm was starting to split, with a pronounced shoulder at δ 2.21 ppm, as a result of the d^{8}-1,4-butanediol now forming a significant part of the ester groups. This indicated that the d^{8}-1,4-butanediol had been incorporated into the polyester and that transesterification had occurred (see Figure 4.8).

In order to maximise the visibility of the deuterated diol in the polyester, the experimental method was changed. A 10%$^{v}/_{v}$solution of the d^{8}-1,4-butanediol in 1,4-butanediol was added to 5 g of the polyester, 4ml of toluene and 0.1 g of Novozyme 435. The mixture was stirred in a cell reactor at 60°C for 24 hours. Filtering off the Novozyme stopped the

reaction and the residual toluene and 1,4-butanediol were stripped off using a Kugelrohr evaporator.

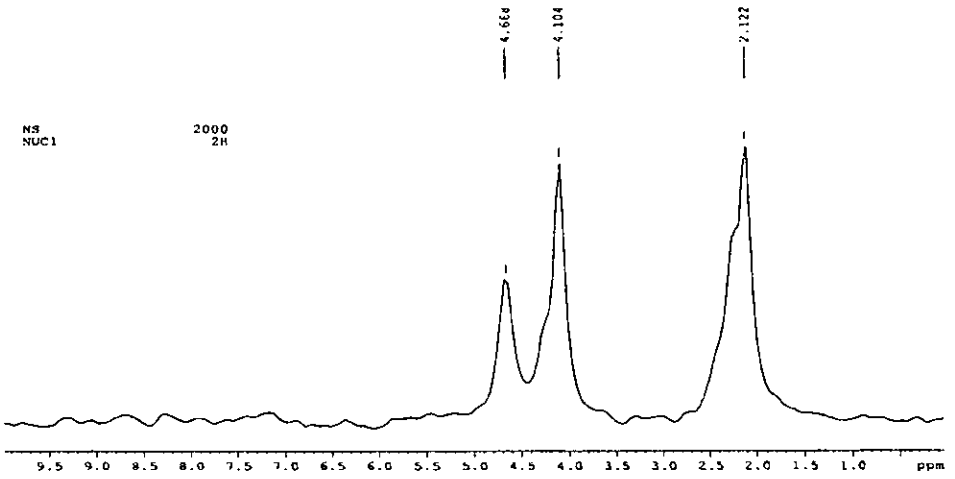

Figure 4.8 ^{2}H-NMR spectrum of polyester + $^{2}H_{8}$- 1,4-butanediol + toluene.

From the ^{2}H-NMR spectrum it could be seen that both of the deuterium resonances had split and the new peaks had moved downfield. The O-$C^{2}H_{2}$ peak had moved in its entirety to δ 4.68 ppm, leaving only a small peak at δ 4.12 ppm. The $C^{2}H_{2}$-$C^{2}H_{2}$ peak had also moved downfield to δ 2.21ppm, which proved that there had been significant incorporation of the deuterated diol into the polyester (see Figure 4.9).

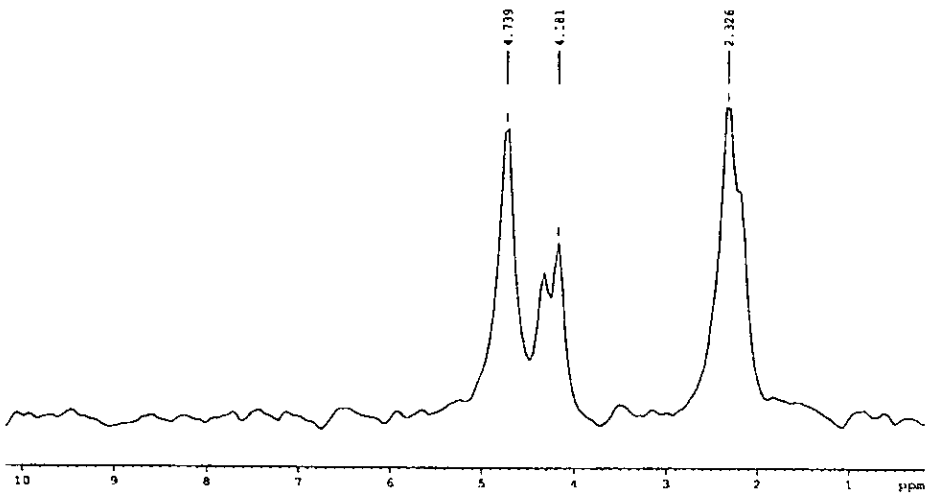

Figure 4.9 ^{2}H-NMR spectrum of polyester + $^{2}H_8$-1,4-butanediol + toluene.

This improved method was then used to repeat the earlier experiment with no added solvent. A sample taken after 24 hours, showed a very small peak at δ 4.68 ppm in the ^{2}H NMR spectrum, which had moved downfield from δ 4.11 ppm, indicating that a small amount of deuterated diol had been incorporated into the polyester. After 48 hours a somewhat larger peak was observed at δ 4.68 ppm, which indicated that transesterification does take place in 1,4-butanediol, but that it is very slow (see Figure 4.10).

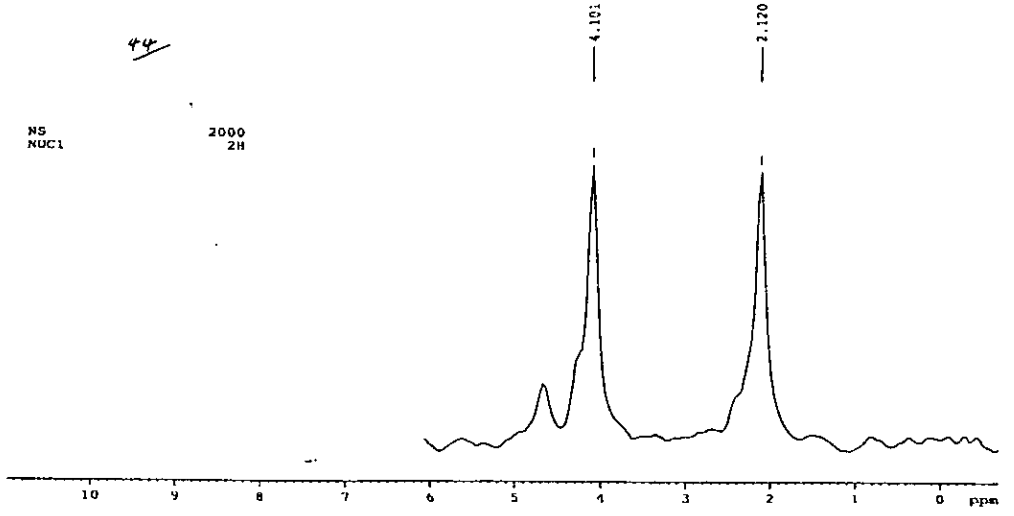

Figure 4.10 ^{2}H NMR spectrum of polyester + $^{2}H_8$-1,4-butanediol after 48 hours.

The conclusion from these experiments seemed to be that the reason for the lack of transesterification in the absence of solvent is the insolubility of the high molecular weight polyester in 1,4-butanediol or PTMEG 650. Only when the polyester is dissolved in solvent is it available to the enzyme and transesterification takes place. It might be that as the polyester reaches a critical molecular weight it starts to drop out of solution in the diol, thus limiting reaction. In order to confirm this point we repeated the above experiment using a polyhexane adipate polyester of 2000 Daltons. The sample taken at 24 hours showed that the HO-C^2H_2 peak at δ 4.11 ppm had split equally with the COO-C^2H_2 peak at δ 4.68 ppm. Similarly, the diol C^2H_2-C^2H_2 peak at δ 2.21 ppm had also split equally with the polyester C^2H_2-C^2H_2 peak at δ 2.12 ppm. This showed that after 24 hours, significant transesterification had taken place and after 48 hours even more transesterification was found (see Figures 4.11 and 4.12).

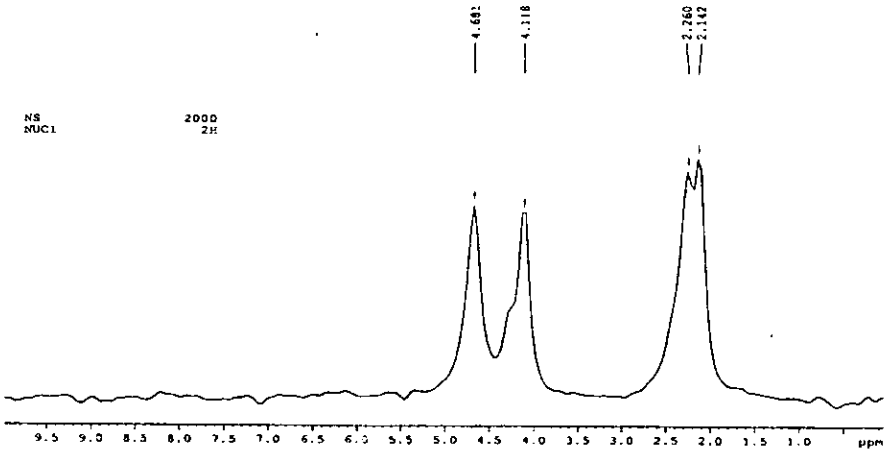

Figure 4.11 Transesterification of 2000 Dalton polyester with $^2H_8$-1,4-butanediol after 24hrs.

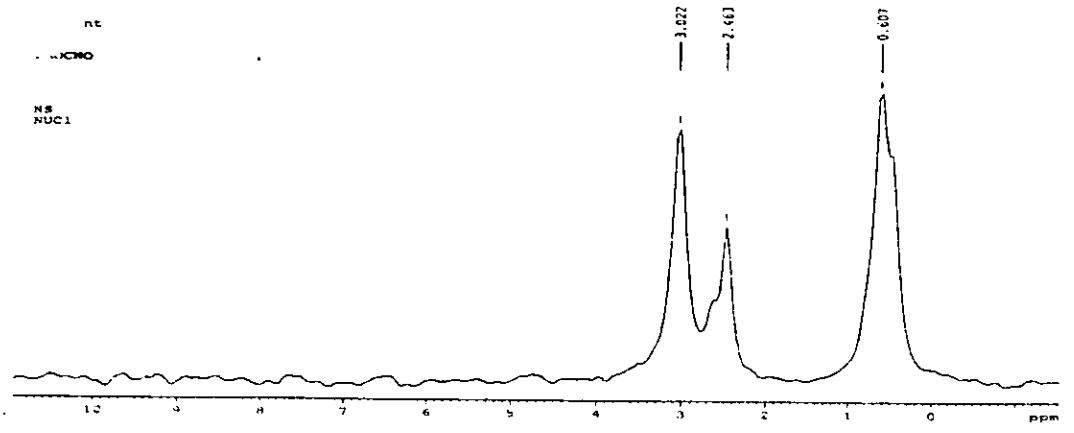

Figure 4.12 Transesterification of 2000 Dalton polyester with $^{2}H_{8}$-1,4-butanediol after 48hrs.

The polyester with the lowest and most uniform molecular weight is the simple oligomer BAB. In order to see if this also was susceptible to transesterification, a sample of BAB was prepared. starting from AB synthesised by the method of Harffey.[16] AB (prepared by Harffey), was reacted with a two fold molar excess of 1,4-butanediol using Novozyme as catalyst. After 24 hours ^{1}H NMR spectroscopy showed that 100% conversion to BAB had taken place. The enzyme and solvent were removed and 10% deuterated diol and Novozyme 435 were added and the mixture heated at 60°C for 24 hours. ^{2}H NMR spectroscopy on the purified sample showed a very small, deuterated ester peak at δ 4.68 ppm, this indicated that some but not very much transesterification had occurred.

Samples from the three experiments above were put through the GPC to see if we could determine the effect of the transesterification on the polyester. Most interestingly, the GPC of the high molecular weight polyester showed that the peak molecular weight, M_w 36000. had declined very little but a number of low molecular weight oligomers had appeared (Figure 4.13).

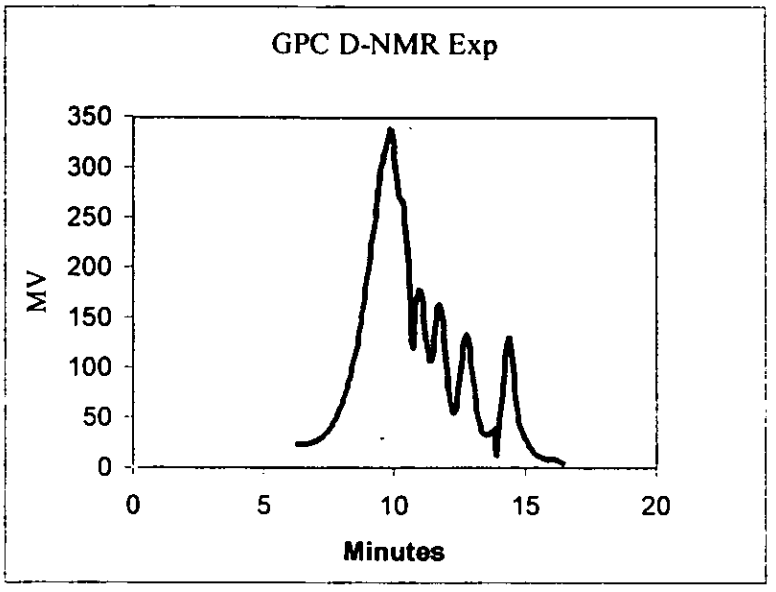

Figure 4.13 Transesterification of polyester with deuterated 1,4-butanediol.

This result shows that the scission is not taking place at random along the polyester backbone, but that it rather takes place at the ester groups near to the end of the polymer chain. This is unlikely to be due to any property of the enzyme because each ester group and its environs are identical and any could fit into the pocket of the enzyme. It is more likely to be a property of the polyester. It is possible that it forms a tight coil in these media and it is only the ends of the chain that are available to the enzyme. It was thought that if a non-reactive solvent similar to 1,4-butanediol could be found, one that would dissolve the monomeric substrates, but not the higher molecular weight polymers, then it may be possible to drive the reaction to give even higher molecular weight polymers.

The standard transesterification experiment was repeated using solvents that were substantially more polar than the previous solvents in order to investigate if the transesterification only occurs in non-polar media. Propylene carbonate, triethylene glycol methyl ether (Triglyme) and tetraethylene glycol methyl ether (Tetraglyme) were chosen as the added solvents. In all cases, extensive transesterification took place and the

molecular weight fell to around 3000 as measured by GPC. There did not appear to be any significant difference in the rate of transesterification between any of these solvents irrespective of their polarity. It would appear that the transesterification reaction takes place in any solvent in which the higher molecular weight polyester is soluble.

From these results, it appears that the rate of transesterification reaction, measured by the rate of insertion of $^{2}H_{8}$-1,4-butanediol into the polyester is ten times faster in toluene than in 1,4-butanediol. The rates of insertion into the high molecular weight polyester and the 2000 molecular weight polyester appear to be approximately the same, however the results of the transesterification are quite different. In the case of the high molecular weight polyester there is nominal reduction in the molecular weight as the chain scission only occurs at the ends of the molecule. In the 2000 Dalton polyester the chain scission occurs at random along the chain with the result that there is a significant reduction in molecular weight.

The transesterification of the oligomer BAB appears to be quite rapid, however BAB cannot polymerise in the presence of excess diol, therefore the deuterated diol can only react at one of its two hydroxyls and this is reflected in the relatively large size of the peak shifted downfield.

One of the main problems that are encountered in the commercial production of polyesters is the formation of macrolactones during the process (e.g. Figure 4.14) during the process.

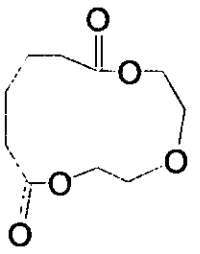

Figure 4.14 Macrolactone of adipic acid and diethylene glycol.

The mechanism of formation and the problems associated with the macrolactone are discussed in our earlier paper.[116] It was thought that if the kinetics of the ring opening reaction could be altered, by using the enzyme under specific conditions, then the ring opening may be favoured, but not the ring formation. This would be a way of using enzymatic transesterification to remove the macrolactone from the linear polyester. It was first necessary to show that *Ca*lB would catalyse the ring opening of the macrolactone. We had shown that the highest equilibrium content of macrolactone produced is during the polyesterification of diethylene glycol with adipic acid and is typically approximately 1.0-1.1%$^{w}/_{w}$.[116]

The DEG/AA macrolactone was heated with Novozyme 435 at 60°C under nitrogen. After 3 days the reaction was stopped, the enzyme filtered off and a sample analysed by GPC, which showed that the macrolactone had been opened and converted to oligomeric polyester of M_w 905 and M_n of 293. The experiment was repeated with toluene added to the reactants. After 3 days GPC showed that the macrolactone had been converted to polyester. However, there was no significant difference between the products of the two reactions (see Table4.4).

Table 4.4 The formation of polyesters by the ring opening of a macrolactone.

System	Molecular weight M_w	Molecular weight M_n	Dispersity
Macrolactone	118	-	-
Macrolactone + enzyme	905	293	3.0
Macrolactone + enzyme + toluene	811	296	2.7

The enzyme activity was somewhat surprising in view of the size and shape of the substrate molecule. Therefore, we modelled the macrolactone substrate into the active site of the enzyme and found that the macrolactone fitted quite nicely into the pocket of the active site (see Figure 4.15). In order to explore the feasibility of removing the macrolactone from the polyester by enzymatic transesterification a series of experiments were carried out using a 2000 Dalton DEG/AA polyester, which had a hydroxyl number of 55 and an acid number of 1.4 mg KOH /g.

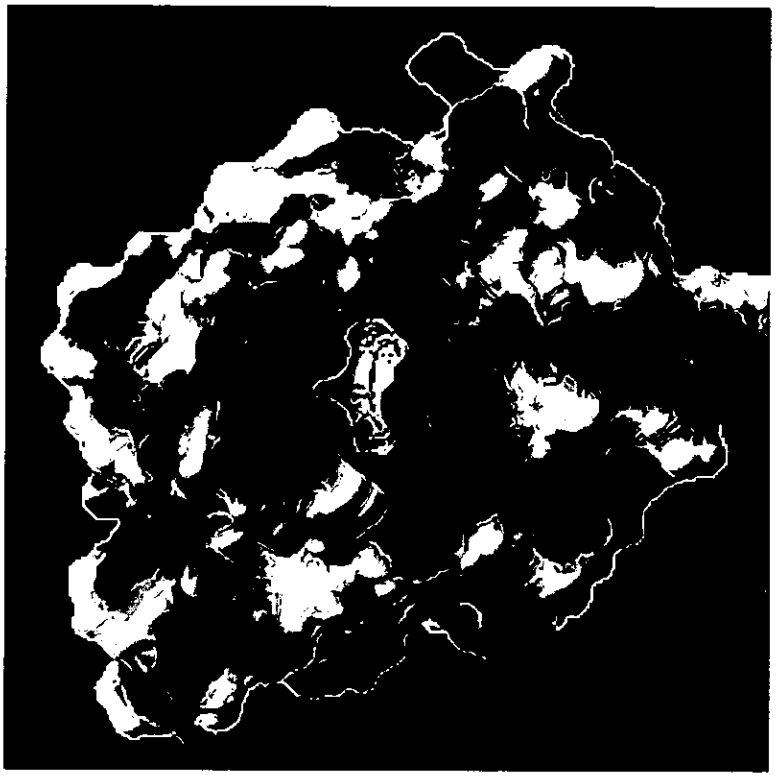

Figure 4.15 *C. antarctica* lipase B with macrolactone docked in the active site.

The polyester was stirred in a cell reactor with Novozyme 435 and 5%$^{v}/_{v}$ of toluene under nitrogen at 60°C. After 24 hours, a sample was taken and any residual enzyme filtered from the sample. After 72 hours the reaction was stopped, the enzyme filtered off and a final sample taken. The samples of the starting material and the 24 hour and 72 hour samples were analysed by Gas Chromatography in order to determine the macrolactone content. The results are shown in Table 4.5.

Table 4.5 Macrolactone content after transesterification

Sample	Macrolactone content %
Control. Starting material	1.1
After 24 hours	0.86
After 72 hours	0.29

This was a most encouraging result, as the lowest macrolactone content that can be achieved by high temperature and high vacuum stripping in a wiped film evaporator is 0.3%.[117] Therefore, a series of experiments were carried out to determine the optimum conditions for the conversion of the macrolactone to polyester (see Table 4.6).

Table 4.6 Reduction of macrolactone by transesterification.

Reactants	Time, hours	Temp, °C	Macrolactone %
Polyester + N435	72	60	1.0
Polyester + N435 + toluene	24	70	0.95
"	72	"	0.98
Polyester + N435 + hexane	24	60	0.99
"	72	"	1.00
Polyester + N435+ 4-chlorotoluene	24	60	1.1
"	72	"	0.97
Polyester + N435 + *n*-butylbenzene	24	60	0.99
"	72	"	0.89
Polyester + N435 + *iso*-butylbenzene	24	60	1.06
"	72	60	1.17

The differences between these results are not considered significant; therefore, it is obvious that there is no detectable reduction in the macrolactone content for any of the above conditions. The initial experiment was repeated twice and on both occasions no reduction in macrolactone was observed. There is no explanation for the initial result. It is unlikely to be analytical error as the reduction was seen in both samples and the observed reduction was in direct relation to the length of time of the reaction.

5 Isothermal Titration Calorimetry

The technique known as isothermal titration calorimetry has only been developed in the last 10 years.[118] It is an ultra-sensitive form of calorimetry, which has resulted from advances in solid-state physics. Using this technique it has become possible to measure the evolution of heat by a chemical or physical process with a sensitivity of 10^{-9} calories. This new technique has opened up many possible fields of research in biochemistry, in particular studies of the thermodynamics of protein-ligand binding, protein-lipid binding and the binding of drugs to receptor sites.[119]

When binding reactions such as these take place a very small amount of heat is absorbed or generated. Measurement of this heat with such a sensitive instrument enables one to make very accurate measurements of binding constants (K_a), reaction stoichiometry (n), enthalpy of formation (ΔH) and change in entropy during the reaction (ΔS).

The principle of the method is that a dilute solution of the ligand is titrated into a cell containing a solution of the protein at a constant temperature, because the cell is stirred it is also possible to use a dispersion of finely divided protein rather than a solution. Alongside the reaction cell is an identical reference cell that contains the neat reaction medium. The major problem in using the isothermal titration calorimeter to follow and determine the thermodynamics of the esterification reaction is that as far as could be ascertained ITC had not been used for non-aqueous enzymology. Of the 200 references in the literature, not one described its use with a non-aqueous system.

Microcal the designers of the instrument were consulted and it was their opinion that the instrument would work with the enzymatic esterification in organic solvent.

When the work started the procedure recommended by Microcal was followed. The reference cell contained water while the reaction cell contained toluene. It was found that the difference in the heat capacity of the two solvents gave substantial problems in obtaining a steady baseline. Instead of getting a steady baseline after a matter of a few minutes it took 40 minutes for a useful baseline to be attained. The water in the reference cell was replaced with toluene after which a steady baseline was obtained after 10 minutes.

A small amount, typically 2-5 μl of ligand solution is injected into the reaction cell held at a constant temperature. As the ligand reacts with the protein, heat is released or absorbed. The instrument measures the amount of energy required to keep the reference cell and the reaction cell at the same temperature. As the protein in the reaction cell becomes saturated with ligand the heat signal diminishes until only the background heat of dilution is seen. When the heat is plotted against the molar ratio of ligand to protein in the cell a complete binding isotherm for the interaction is obtained. The software used by the instrument measures all the experimental parameters including binding affinity, binding stoichiometry, enthalpy and entropy of binding. The ITC isotherms are analysed using a non-linear least squares method to determine the best fit.

We wished to determine the enthalpy of formation of the acyl-enzyme, using (i) adipic acid dissolved in toluene, (ii) decanoic acid and (iii) the monoethylester of adipic acid as the acylating agents. Subsequently, we wished to determine the enthalpy of formation of the ester, by reaction of adipic acid in 1,4-butanediol.

From these measurements it was hoped that we would be able to construct a thermodynamic profile of the reactions.

At the commencement of an ITC experiment it is first necessary to determine the heat of dilution of the ligand as it is injected into the reaction medium. This exotherm or endotherm is then added to or deducted from the heat of reaction of the system being studied. Therefore, when 2 µl injections of 4.2mM adipic acid solution in toluene were injected into toluene a very large endotherm of approximately 20 kcals mol^{-1} was observed, far greater than would be expected from the heat of dilution, which should be approximately 1-2 kcals mol^{-1}. After some consideration, it was realised that the endotherm was due to the dissociation of the adipic acid dimer as it was injected into the toluene (see Figure 5.1).

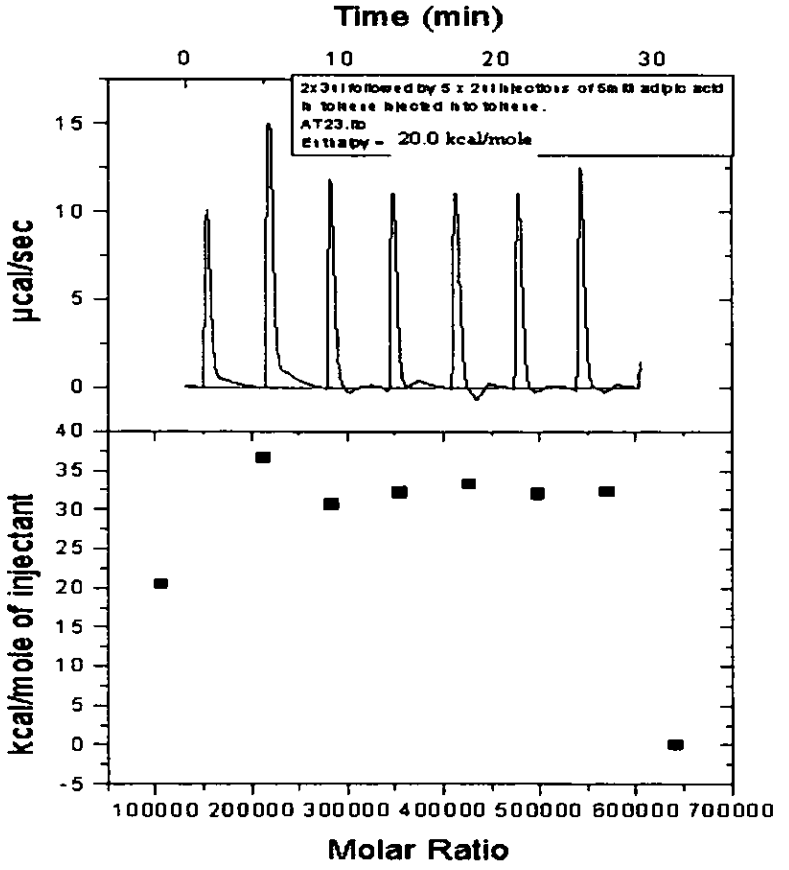

Figure 5.1 Isothermal titration calorimetry of the dissociation of adipic acid dimer.

The problem of hydrogen bonding between adipic acid and hydroxyl groups had been encountered in our NIR studies described in Chapter 2. The formation of dimers by intra molecular hydrogen bonding in carboxylic acids is well known.[120],[121] Adipic acid having two carboxyl groups, forms a particularly stable cyclic dimer, the stability arising from the fact that it requires the simultaneous breaking of four hydrogen bonds for the dimer to dissociate into two monomeric adipic acid molecules.[122] The enthalpy of formation of adipic acid dimer and other dicarboxylic acid dimers has been determined by measuring the difference in the heat of formation in the gaseous and solid phases. In the temperature range 50°-150°C the enthalpy of formation of a monocarboxylic acid dimer was found to be 7.5 kcals mol^{-1}.[123] Adipic acid with its four hydrogen bonds forms a cyclic dimer (see Sculpt model in Figure 5.2) with an enthalpy of formation of at least 15 kcal mol^{-1}.[124]

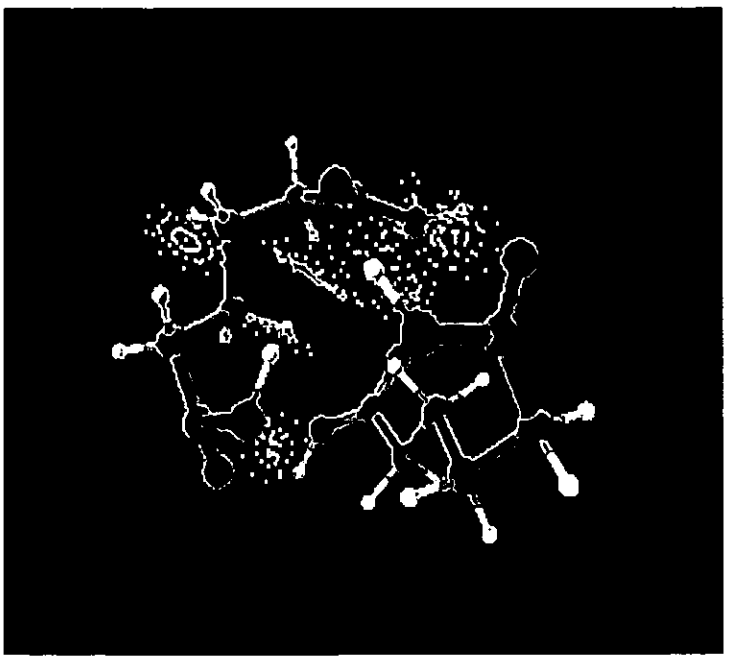

Figure 5.2 Sculpt model of adipic acid dimer showing hydrogen bonds in blue .

In Chapter 2 in the work on the development of NIR methods it had been shown that the addition of chloroform disrupts the hydrogen bonding between the carbonyl of the

carboxylic acid and the hydrogen of the hydroxyl groups. It was proposed that this was due to the formation of a hydrogen bond between the carbonyl and the hydrogen of the chloroform. This mechanism would be equally applicable to the hydrogen bonding responsible for the formation of the adipic acid dimer. This proposal engendered much debate as to whether or not the hydrogen of chloroform can form a true hydrogen bond.

It was thought that H bonds could not form from a C-H bond and that effects seen with chloroform were simply the effects of a polar solvent. The general definition of a specific H bond interaction would require a frequency shift of the C-H stretch and in chloroform; this is ambiguous, particularly with an oxygen atom of an ether or ester carbonyl. However, with pyridine and triethylamine there is a distinct frequency shift of the C-H stretch of 36 and 80 cm^{-1} respectively.[125]

Many authors have published work that confirms the existence of H bonds between chloroform and various reagents. Early work which determined the equilibrium constant and vapour pressures of acetone-$CHCl_3$ mixtures, suggested the presence of H bonds.[126,127] Using both IR spectroscopy and NMR; Lord,[128] Huggins [129] and Huggins and Pimentel,[130] looked at $CDCl_3$ in solvents such as ethers, esters and acetone, measuring the C-D stretch. It appears that the frequency shift is only seen with the strongest bases or that much smaller shifts occur with weaker bonds. The increase in intensity (v_s) with H bonds is more sensitive than the frequency shift and this shows H bonding to occur with chloroform.

Moelwyn-Hughes and Sherman measured the enthalpy of formation of the H bond in 1:1 $CHCl_3$/acetone as +4.1 kcals mol^{-1}.[131]

Staveley, *et al.*,[132] used measurements of heat capacity, volume change and compressibility to confirm the existence of H bonding between $CHCl_3$ and acetone, while Searles used the heat of solution and infrared spectra, to show H bonding between esters and lactones with chloroform.[133]

In "The Hydrogen Bond" by Pimentel and McClellan [134] on page 218 in a discussion of H bonding in carboxylic acid dimers it states, "The equilibrium constant K has not been determined with great accuracy because of solvent effects, for example the equilibrium constant for acid/acid dimer in chloroform is only 1/10 what it is in carbon tetrachloride".

Vinogradov[135] reports that the equilibrium constant for benzoic acid/dimer is: 230×10^3 in carbon tetrachloride, 8.9×10^3 in benzene and 7.2×10^3 in chloroform. These results would appear to confirm that chloroform can indeed disrupt the hydrogen bonding of carboxylic acid dimers.

Boobyer looked specifically at acid dimer-chloroform systems and developed the pulsed charge cloud model.[136,137] In an acid dimer the OH bond vibration pulses the lone pair and gives an induced dipole moment for the OH mode of the dimer. An oxygen sp^2 hybrid orbital is co-linear with the O-H---O axis and is favourable for maximum interaction between the OH bond and the lone pair and forms a dipole which brings them much closer together. This causes a big increase in the intensity of the ν(OH) band in the dimer.

$CDCl_3$ and acetone form a 2:1 complex D bonded together, although the ν(CD) does not shift, its intensity increases by a factor of 8.7. The electronic state of the CD bond is unchanged; the C-D moment induces a moment in the polarisable lone pair of the carbonyl that pulses with the C-D vibration thereby increasing the dipole moment of the

complex. Therefore, there is a significant increase in the intensity of the ν(CD). Several other authors using differing techniques have proved the existence of the chloroform-carbonyl hydrogen bond.[138,139,140] The three chlorine atoms enhance the acidity of the chloroform which then acts as a proton donor enabling the C-H---O hydrogen bond to form.[141]

The results from our isothermal titration calorimetry experiments offered the opportunity to determine the enthalpy of formation of the adipic acid dimer by a novel route and also to confirm the ability of chloroform to disrupt formation of the acid dimer. The previous experiment was repeated. A 5 mM solution of adipic acid in toluene was injected into toluene over a series of 2 μl injections. A pronounced endotherm was observed and the enthalpy of dissociation measured as 22.0 kcals mol^{-1}. The experiment was repeated using a 20 mM solution of decanoic acid in toluene. A smaller endotherm was observed (see Figure 5.3).

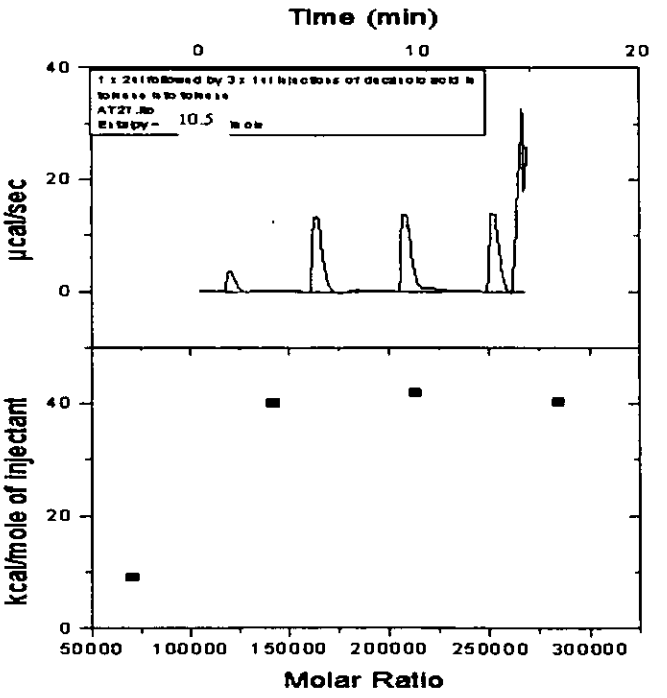

Figure 5.3 ITC of decanoic acid into toluene.

The enthalpy of dissociation was calculated to be 10.2 kcals mol^{-1}. This value, which is equivalent to 5 kcals mol^{-1} per hydrogen bond is reasonably close to the values reported in the literature.[132] It must be remembered, however, that these were determined from the difference of the enthalpy of formation of the acid in the vapour phase and the enthalpy of formation in the solid phase and not in solution as in our case.

Then a 5 mM solution of the monoethylester of adipic acid was injected into toluene in 10 × 2μl injections, the enthalpy of the dissociation was measured as 11.0 kcals mol^{-1}.

A 5 mM solution of adipic acid was prepared in toluene and 10 mM of chloroform added. This solution was injected into toluene containing 10 mM chloroform in the cell. The enthalpy of dissociation was measured as 1.34 kcals mol^{-1} (see Figure 5.4).

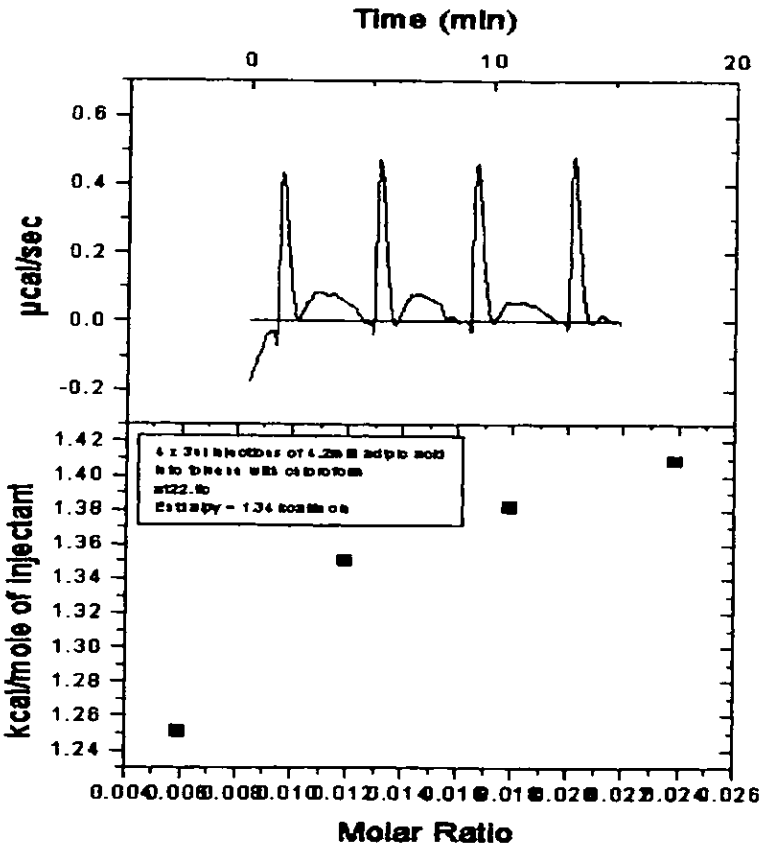

Figure 5.4 Isothermal calorimetry of the dissociation of adipic acid in the presence of chloroform.

It is proposed that the reduction in enthalpy is due to the adipic acid dimer being replaced by the adipic acid chloroform complex. Because there is no difference in the chloroform concentration between the solution in the cell and the injected solution there is no drive for this complex to dissociate. The lower enthalpy of dissociation of decanoic acid and the monoethyl ester of adipic acid are consistent with the hydrogen bond formation of the monocarboxylic acids.

With a more complete understanding of the problems caused by the presence of the adipic acid dimer, the experiments to investigate the thermodynamic parameters of the enzymatic esterification were carried out. A 4.2 mM solution of adipic acid in toluene was injected into toluene containing a 0.15 mM dispersion of Chirazyme lyophilised *Candida antarctica* lipase B, in a series of 2 µl injections. The reaction was carried out at 50°C, with an interval of 2 minutes between each of the injections. As before, the significant endotherm was observed (see Figure 5.5) after each of the initial injections, this decreased and the exotherm due to the acylation of the enzyme became visible.

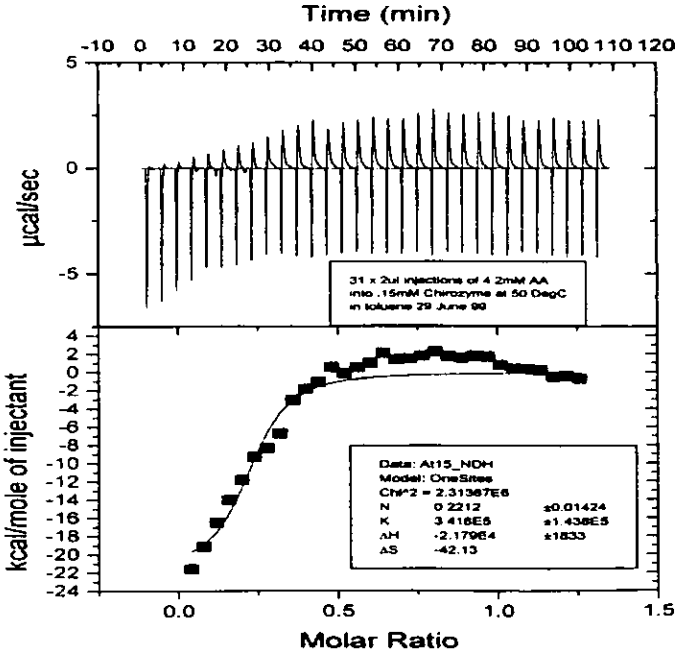

Figure 5.5 Isothermal Calorimetry of adipic acid binding to Chirazyme.

After 31 injections the enzyme had become saturated (fully acylated) and the run stopped. The control was deducted from the measurements and a very good fit observed. The enthalpy of formation of the acyl-enzyme was found to be -21.79±1.8 kcals mol^{-1}. The entropy of formation (ΔS) was calculated to be -42.13 cals $°C^{-1}$ mol^{-1}.

This experiment was repeated using 1,4-butanediol as the solvent. A 8.4 mM solution of adipic acid in 1,4-butanediol was injected into a 0.6mM dispersion of Chirazyme in 1,4-butanediol. The initial profile was the same, however, in this experiment the enzyme could never become saturated, as the 1,4-butanediol is the second substrate in the reaction. Therefore on injection of the acid into the 1,4-butanediol and Chirazyme the reaction goes through to the final stage, which is the synthesis of AB and BAB. In this experiment it is not possible to determine anything to do with the binding, however it is possible to determine the overall enthalpy of formation of the diol-acid ester AB. This was measured as -4.52 kcals mol^{-1}. Therefore the thermodynamic profile of the complete reaction is as shown in Figure 5.6

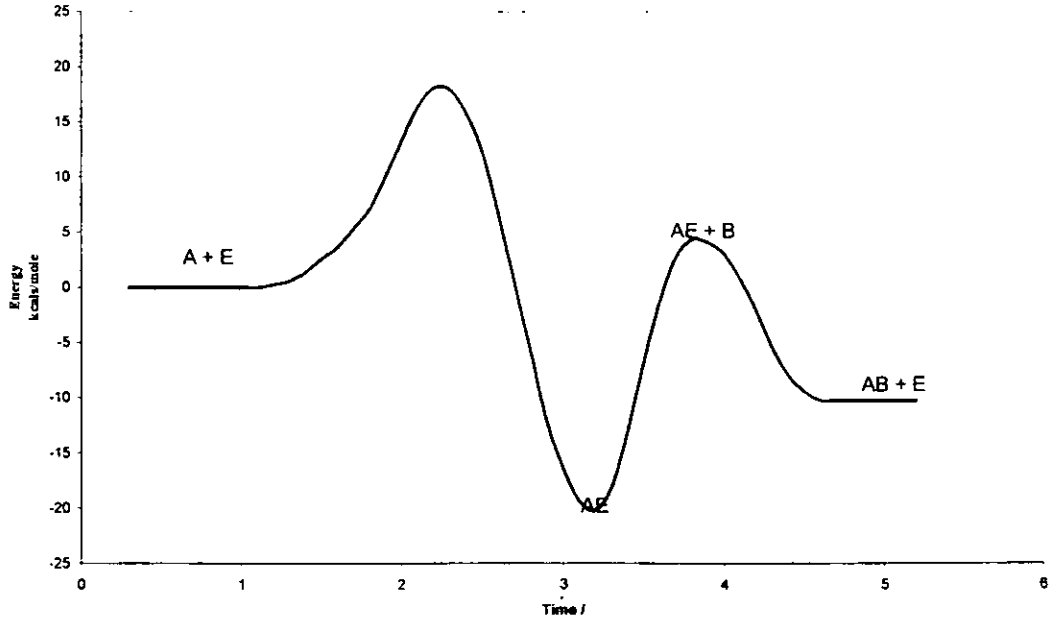

Figure 5.6 Thermodynamic reaction profile of adipic acid + 1,4-butanediol.

This experiment was repeated using the monoethyl ester of adipic acid as the acylating agent (see Figure 5.7). A 4.2 mM solution of monoethyl ester of adipic acid in toluene was injected into a 0.15 mM dispersion of Chirazyme in toluene at 50°C. After 60 × 2µl injections the enzyme was fully saturated and the run stopped. The software again gave a very good fit to the data. The enthalpy of formation was measured as 5.8±0.1 kcals mol^{-1}. The entropy of formation ΔS was calculated to be -42.42 cals $°C^{-1}$.

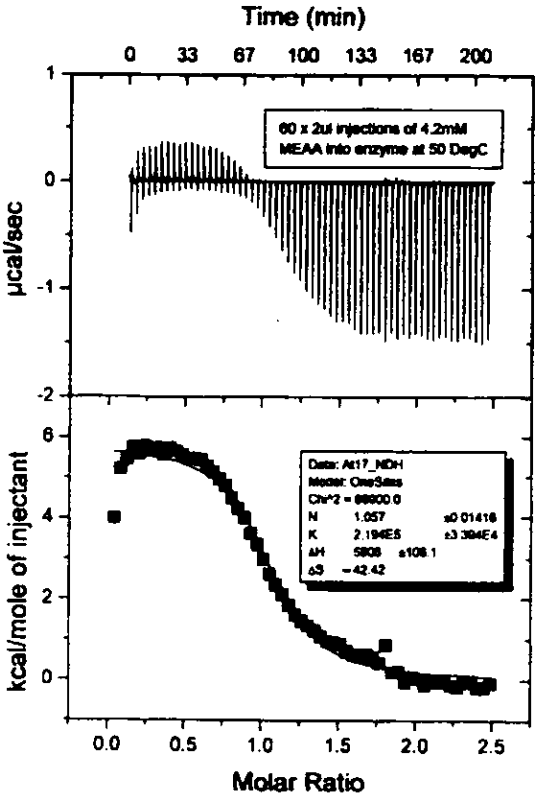

Figure 5.7 Isothermal calorimetry of MEAA binding to Chirazyme.

The conclusions from these experiments are quite interesting. The entropy of formation is, as expected, the same for esterification and transesterification, as the acyl-enzyme product is the same in both cases. The enthalpies of formation are quite different, however, the ΔH from the reaction of the monoethyl ester of adipic acid (MEAA) with the enzyme being significantly less than the ΔH from the reaction of the acid with the

enzyme. This is considered to be due to the fact that the enzyme is being acylated by the ester carbonyl rather than the acid carbonyl. In the case of the MEAA substrate both groups are equally available to the enzyme, however, the ester carbonyl is far more reactive to the nucleophilic attack of the serine than the carbonyl of the acid. This observation confirms the results of the rate studies (Section 3.4), which indicate that the rate of reaction of the ester carbonyl with the enzyme is about three times the rate of reaction of the acid carbonyl. As the knowledge of the extent of dimerisation in adipic acid evolved there was a concern that if, as seems likely, the enzyme was not readily acylated by the dimer then the dissociation of the dimer may be a rate controlling factor in the enzymatic esterification. However, when the injections of adipic acid in toluene were made, into toluene, the endotherm of the dissociation was practically instantaneous. Although this does not prove that the dissociation rate does not control the enzymatic esterification rate it does offer a degree of reassurance.

6 The relationship of Structure and Function in lipases.

While lipases are ubiquitous enzymes, present in microbes, plants and higher animals, they have great structural diversity.[142] Certain structural elements are common to all, but they have large differences in the homology between groups and between individual lipases within these groups.[143] They are frequently divided into microbial and mammalian lipases, however, the homology overlaps and as a whole they are best divided into four groups.

			pdb code
(a)	Pancreatic lipases	e.g. Human pancreatic lipase	1hpl
(b)	Acetyl cholinesterase		1ace
	Cholesterol esterase		1mah
	Candida rugosa lipase		1crl
	Geotrichum candidum lipase		1thg
(c)	*Rhizomucor miehei* lipase		3tgl
	Humicola lanuginosa lipase		1tib
(d)	*Fusarium solani* cutinase		1cus
	Pseudomonas lipase		1esc
	Candida antarctica lipase B		1tca

Although there is little homology in common between the groups, they are structurally and functionally very similar, there are certain elements that run like a thread through all of them.

The lipase structure is made up of predominantly parallel β-strands surrounded by α-helices, in which there is an element termed the α–β hydrolase fold.[144] Between the

eponymous α-helix and β-sheet there is a tight hairpin turn of structure Gly-x-Ser-x-Gly common to all.[145] It is this serine that is the nucleophile of the active site. In lipases, the nucleophile is always a serine, it forms the core of the catalytic triad similar to that found in proteases.[20] The triad of residues is, unlike the proteases, always found in the order Ser-Asp-His in the enzyme molecular sequence.

For example:

Candida antarctica lipase B	Ser105-Asp187-His224
Human pancreatic lipase	Ser153-Asp177-His264
Rhizomucor miehei lipase	Ser153-Asp203-His257
Cutinase	Ser120-Asp175-His188

In the case of *Candida antarctica* lipase B, the serine is found between the helix α4 and the strand β4.

It was shown in 1990 by Winkler,[146] and Brady and Brzozowski,[20] that most lipases have a loop of the peptide chain that normally covers the active site, this is termed the lid. The lid opens only when the enzyme is activated interfacially at an oil-water interface. This is probably the most significant difference between the lipases and the proteases. Not only do proteases not need interfacial activation they are readily unfolded on absorption on to a hydrophobic surface.[147] In the case of *Rhizomucor miehei* lipase the lid is an amphiphilic peptide loop, which rearranges on exposure to an interface (see Figure 6.1). Once open the lid remains in the open position, held in place by a sophisticated lock mechanism made up of an arginine residue, which hydrogen bonds to the backbone to keep the lid open.[148]

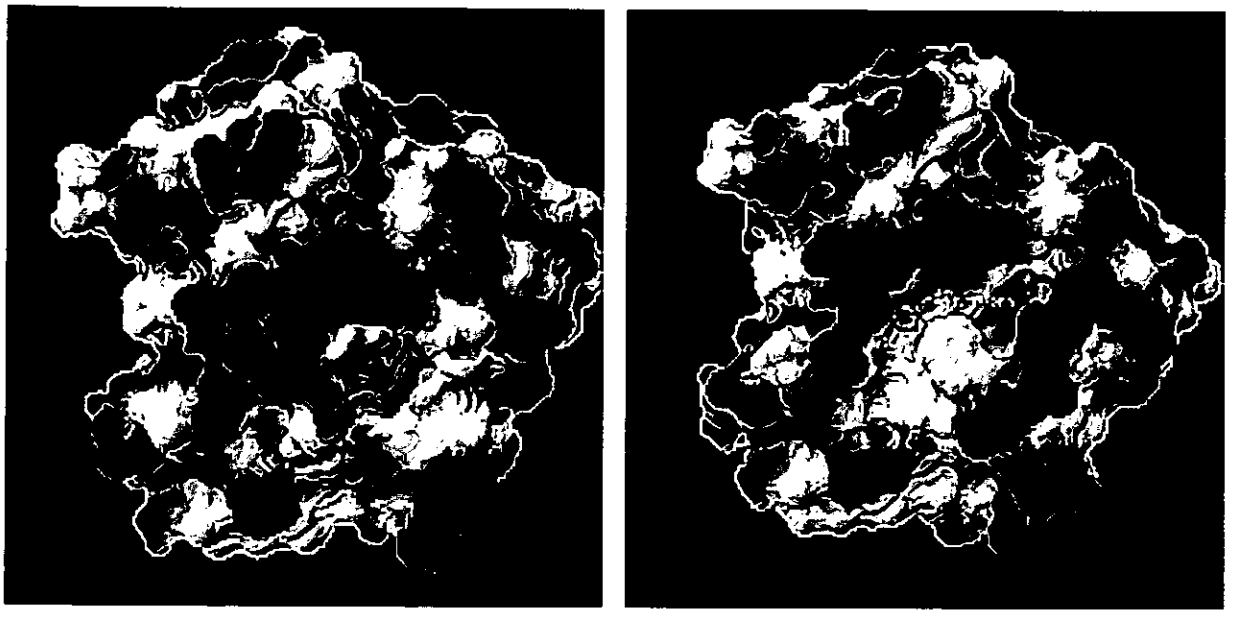

(a) (b)

Figure 6.1 Sculpt models of: (a) *Rhizomucor miehei* lipase in the closed configuration, from pdb file 3tgl, (b) *Rhizomucor miehei* lipase in the open configuration, from file 4tgl; the active site is clearly exposed; shown containing a substrate, diethyl phosphonate DEP in the active site. The hydrophobic regions are shown in blue.

When the lid of the lipase is in the open position, several residues form the oxyanion hole. These residues stabilise the tetrahedral intermediate of the acyl enzyme by hydrogen bonding.[149] Carter and Wells,[52] first identified this mechanism in proteases and it was shown subsequently by Brady and Brzozowski [20] that the same mechanism applied to lipases.

When the lid of the lipase opens the surrounding area becomes significantly more hydrophobic,[110] this is seen quite clearly in Figure 6.1.

When the detailed structure of *Candida antarctica* lipase B was studied it was found to have more in common with cutinase and some of the microbial esterases than the

expected fungal lipases. *Candida antarctica* lipase B like cutinase, does not require interfacial activation in order to be active, nor has it been possible to crystallise the enzyme in a closed form. Uppenberg,[109] found that the short helix α5 in *Candida antarctica* lipase B is highly disordered and that it may well be a putative lid, however, in common with all lipases this region contains two hydrogen bond donors Glu 106 and Thr 40, which form part of the oxyanion hole of the active site. This structure is common to all lipases, the actual residues may vary, but there are always two hydrogen bond donors in the same position, the residues on each side of the proton donor have no side chains, which could interfere with the formation of the hydrogen bonds.[150]

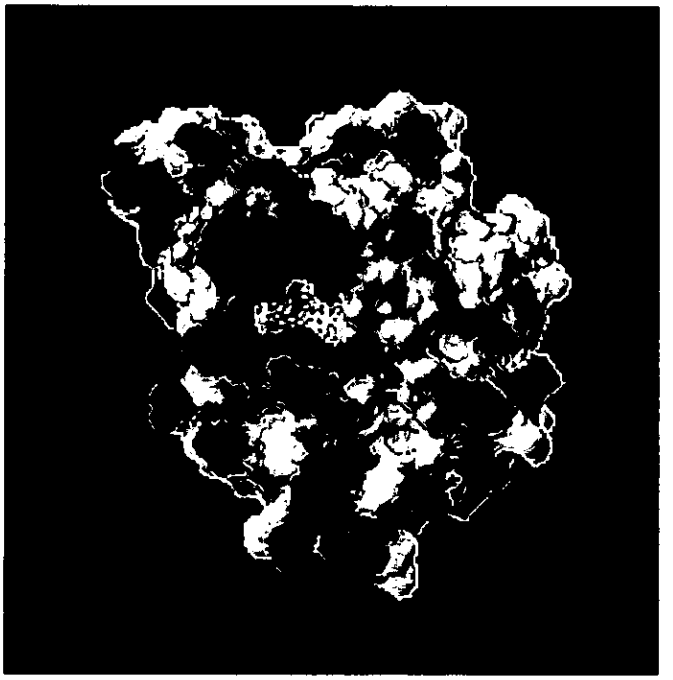

Figure 6.2 *Candida antarctica* lipase B showing active site and hydrophobic regions in blue.

It is thought that the purpose of the lid is to protect the enzyme from agglomeration caused by the hydrophobic attraction between these large hydrophobic areas of the enzyme.

The shape and the size of the actives sites differ from lipase to lipase and this plays a major role in determining the activity of the enzyme and its affinity for different substrates.[151] In the case of *Candida antarctica* lipase B, the pocket seen in Figure 6.2 is 10Å long x 4Å wide x 12Å deep. The base of the pocket is hydrophilic with residues Asp 134, Ser 105, Thr 40 and Glu 157, it is fairly narrow up to C7 from the Ser 105 above that the pocket is smooth and hydrophobic with residues Val 154, Iso 285, Leu 144 and Val 149.

The pocket shown in the model of *R. miehei* lipase from pdb file 4tgl in Figure 6.1b is a hydrophobic crevice, of size 18Å long, 4.5-6Å wide and 10Å deep, whereas in *C. rugosa* lipase, the pocket is in the form of a tunnel some 22Å long.

All lipases will accept C_4-C_{16} fatty acid esters,[110] but their activity varies according to the geometry of the active site. *R. miehei* with its very long hydrophobic crevice has great affinity, measured by its specificity constant K_{cat}/K_m for long chain C_{16}-C_{18} fatty acid esters. Whereas *Candida antarctica* lipase B has a much shallower pocket with only a small hydrophobic area on the wall and so prefers shorter chain fatty acid esters.[152] Rangheard demonstrated that the specificity constant depends more on the fatty acid substrate than either the solvent or the alcohol substrate.[153] While Kirk showed that it is the fatty acid side of the active site that is the primary determinant of the enzyme's affinity for specific chain length substrates.[152]

One of the important features of *Candida antarctica* lipase B is that it is highly stereospecific for secondary alcohols [109] and Orrenius, *et al.*,[154] have shown that it is the geometry of the pocket on the alcohol binding side that controls the stereospecificity. In essence, the geometry affects the binding and stability of the alcohol-acyl enzyme tetrahedral intermediates because of the ease with which the oxyanion residues can

hydrogen bond to the different intermediates. The resulting differences in the reaction rates of the enantiomers will give significant enantiomeric excess, which may be used to synthesize and isolate a specific enantiomer.

The enantioselectivity of a lipase changes in different solvents, the changes being explained by the different desolvation properties of the enantiomers in the different solvents.[95] However, Luque, Tao Ke and Klibanov have shown that differences in desolvation energies can not affect the enantioselectivity and that it is changes in the conformation of the enzyme that cause the enantioselectivity to change.[155]

It can be seen that not only is the structure of the enzyme key to the activity of the enzyme, but that the properties of the enzyme may change if the conformation of the enzyme changes.

When we started work on the enzymatic synthesis of polyesters from simple aliphatic diacids and diols, our initial work, which proved the feasibility of the polymerisation of adipic acid and 1,4-butanediol, used the lipase from *Rhizomucor miehei* in di-*iso*-propyl ether.[13] This was changed subsequently, to using the immobilised lipase B from *Candida antarctica* (Novozyme 435™), which was found to be a superior catalyst both in terms of activity and recyclability. In addition, it was found to be possible to synthesise polyesters using this enzyme without the need for a solvent.[14] The polyesters produced using this system were found to have physical properties such as molecular weight distribution, crystallinity and melt viscosity, which were significantly different from their analogues produced by conventional high temperature polymerisation.[15] It was thought that the observed differences in physical characteristics might well be due to differences in the actual polymerisation reaction mechanism.

It was shown subsequently by Harffey that the polymerisation mechanism was indeed different and that it proceeded via the key intermediate AB, in a step growth mechanism,[17] as opposed to the random condensation of the two monomers. It was also shown by a combination of gel permeation chromatography and Maldi-Tof Mass Spectrometry that at no stage of the reaction is any diacid terminated oligomer (ABA) observed. These observations may be explained if one assumes that interesterification (i.e. transesterification with itself) does not occur within the polyester. It was thought that there might be a structural component of the enzyme that prevents the entry of AB to the active site once it has been acylated by the adipic acid. In the course of that work, it was found that the mechanism of polymerisation also varied depending on whether or not it was carried out in solvent. In toluene, transesterification was found to occur and as a result, the polymers formed had a broad molecular weight distribution and were of limited molecular weight compared to the polyesters produced in the solvent free system.

It was decided therefore to take a detailed look at the reaction kinetics and to determine rates of reaction of the intermediates and related substrates in different media in order to explain some of the observations. We have seen differences in activity depending on the individual substrates in various media, but have found that some compounds that are closely related to the substrates are not at all acceptable to the enzyme as substrates.

We decided to look at the secondary structure of the enzyme in the different media to see if there were any changes that might help to explain the different behaviour of the enzyme. It was known from our kinetic work that the concentration of the acid substrate has a significant effect on the activity of the enzyme (see Chapter 3). Paktar has shown that the optimum pH is 7.0 with a rapid fall in activity below pH 6.0 and above pH 8.0,[86] this is usually explained by the effect of the pH on the ionisation state of the aspartate

residue in the catalytic triad. We have also observed a permanent fall in enzyme activity after exposure of the enzyme to low pH, which affects the recyclability of the enzyme. Because of the known effect of pH of the medium on the hydrogen bonding within the protein, we decided to see if any observable changes in the secondary structure could be linked to the pH of the medium by the determination of secondary structure in a range of aqueous buffers. Once we had sufficient information on the structure of the enzyme in its native form in aqueous buffer we would then look at the secondary structure of the *C. antarctica* lipase B in 3 or 4 solvents of differing polarity. In particular, solvents in which the enzyme produces differing polymers, to see if any correlation could be found between structure and function and to examine also the acylated form of the enzyme in the same solvents and then to compare the structures.

Fortunately, the principal structure of the *Candida antarctica* lipase B enzyme has been explored by a number of workers, notably Uppenberg, *et al.*,[97] Cygler, *et al.*[96] and Pleiss, *et al.*[58] Therefore, there was a published foundation on which we could base our studies of the secondary structure of the enzyme.

The use of circular dichroism (CD) spectroscopy for the determination of protein secondary structure is quite common;[156] it is however used mainly with aqueous systems, but not very much with other solvents. There are a number of problems that are specific to CD spectroscopy in organic solvents; firstly, it is difficult to obtain true solutions of protein in organic solvents and secondly most solvents have a significant absorbance in the UV region.

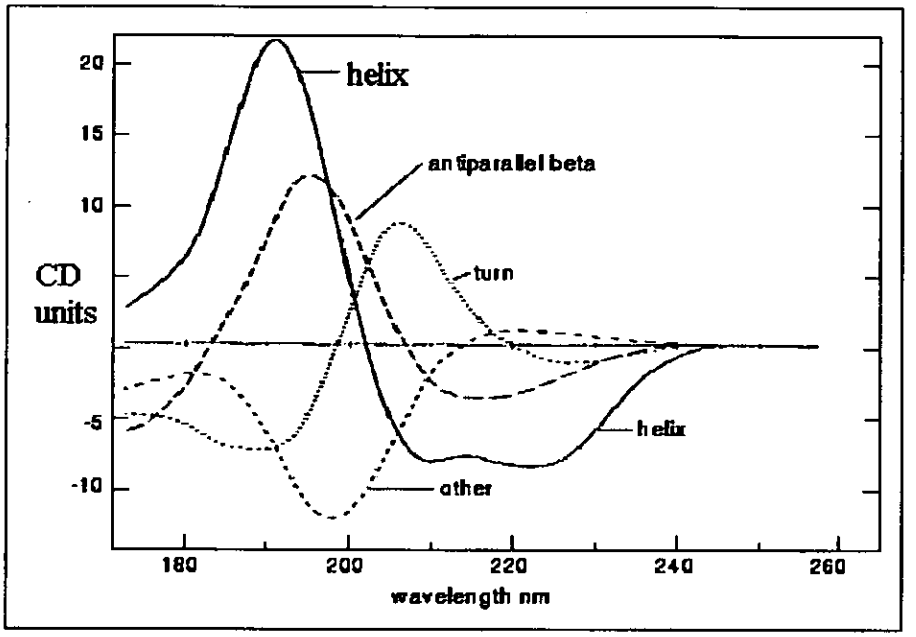

Figure 6.3 A typical CD spectrum of a protein showing the CD absorbance of the different structural elements.

The UV absorbances of the relevant solvents in a 1 cm cell are collected in Table 6.1.

Table 6.1 UV absorbance of solvents at various wavelengths.[87]

	Wavelength, nm	Absorbance compared to water
Hexane	195	1.0
	225	0.05
	250	0.01
Toluene	200	>1.0
	250	>1.0
1,4-butanediol	215	>1.0
	225	0.5
	250	0.04
Water	190	0.01
	250	0.01

At an absorbance of 1.0, 90% of the light is absorbed by the solvent, which means that that solvent cannot be used for normal UV spectroscopy because of the inherent errors caused by the loss of light in the medium.

It is quite obvious that the UV absorbance of the solvents and substrates would make it difficult if not impossible to obtain meaningful CD spectra unless we used an extremely intense source of UV light, particularly as we were looking for relatively small changes in the protein structure. In solvents of such high UV absorbance, it became obvious that we needed the power that can only be obtained from synchrotron radiation light.

When looking at the acylated enzyme, we anticipated that the changes in the secondary structure in the region of the binding site might be small compared to the overall secondary structure of the enzyme. Therefore, we needed the increased precision of an extended wavelength CD, which one gets from a synchrotron radiation source (SRS). This has a typical range of 165-270 nm compared to 190-270 nm obtainable from a conventional CD spectrometer.

We wanted to use the pure *C. antarctica* protein for this work, but because of the preparative difficulties, this was only available in small quantities as a gift from Novo. Therefore, a high photon flux would be needed to give a large signal to noise ratio, which is necessary for accurate measurements on the small samples. In order to overcome all these problems we needed the enormous photon flux that one can only obtain from an SRS such as the one at Daresbury.

The scale and principle of the Daresbury instrument is shown in Figure 6.4. The electron beam is generated in the 100,000 MeV linear accelerator and accelerated to 600,000 MeV in the smaller synchrotron. In the main ring, the electron beam is accelerated to 2 GeV

and this then acts as a storage ring, the beam having a useful life of approximately 8 hours. The electromagnetic radiation, mainly X-ray and ultra violet, is taken off the circulating beam through the side ports, which can be seen in the diagram.

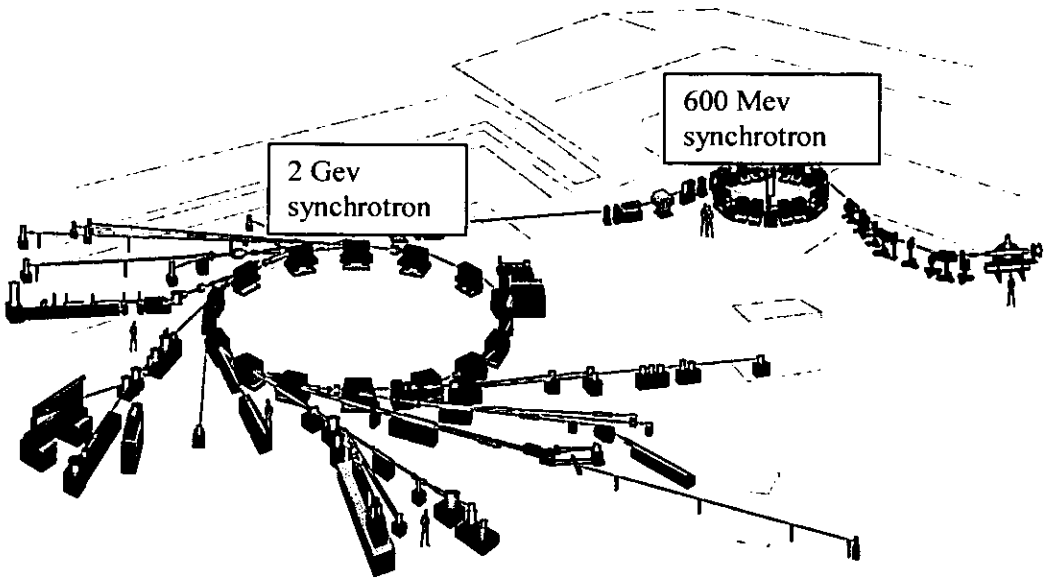

Figure 6.4 The Daresbury synchrotron.

In order to gain experience with the necessary techniques and to develop confidence in the use of the fitting programs, we first measured the CD spectrum for α-chymotrypsin in pH 5.0 KAc buffer and in hexane. The protein was partitioned from the buffer solution into hexane using the method of Dordick,[157] whereby the ion pair is formed between Aerosol OT and the enzyme, which then becomes much more hydrophobic and thus soluble in the organic phase.

The CD spectrum and the secondary structure of α–chymotrypsin has been studied extensively by a number of workers and the spectrum is used as a standard in Curtis Johnson's CDSSTR program [158] so that it gave us the chance to check our methodology.

For this work, we used a conventional Jasco CD spectrometer to obtain the CD spectrum from 180-270 nm. The results obtained using CDSSTR to determine the secondary structure are shown in Table 6.2.

Table 6.2 Secondary structure of a-chymotrypsin.

Structure	KAc Buffer pH 5.0	Hexane	CDSSTR Standard
α-helix	8%	7%	8%
B-strand	38%	34%	35%
Turns	11%	16%	15%
Other	43%	43%	42%

These results, which compared well with the published results, gave us confidence in the methodology chosen to investigate the structure of *Candida antarctica* lipase B.

Figure 6.5 shows the secondary structure of the enzyme derived by using the Sculpt modelling program from the Brookhaven pdb co-ordinates for the file 1tca.

It is obvious from this that the enzyme has a fairly extensive α-helix content compared to the α-chymotrypsin structure given in Table 6.2.

We measured the CD spectra of the pure *C. antarctica* protein (ex Novo) in a number of aqueous buffers ranging from a pH of 4.0 to 9.0, using the synchrotron radiation source at Daresbury. The spectrum obtained is shown in Figure 6.6.

Figure 6.5 The secondary structure of *Candida antarctica* lipase B. Sculpt model based on pdb file 1tca.

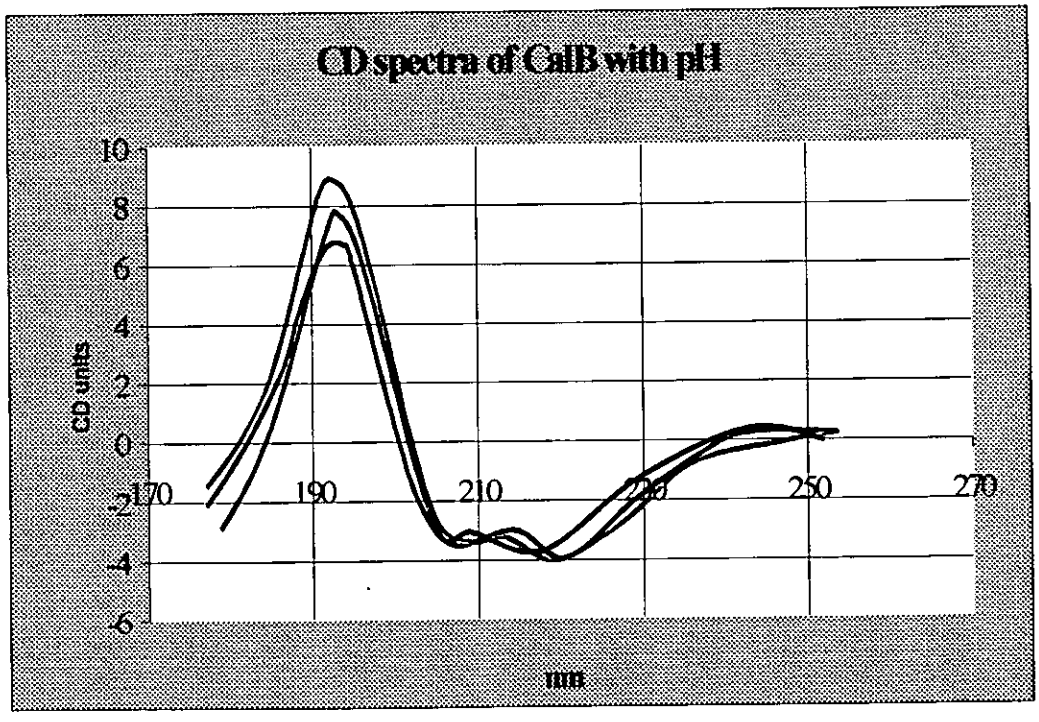

pH 5.0 shown in red, pH 4.0 shown in blue and pH 9.2 shown in black

For these spectra we chose to use the SELCON fitting program developed by Sreerama and Woody,[159] rather than CDSSTR because the standards in the latter were obtained using conventional CD (190-270 nm) whereas the standards used by Sreerama were all obtained using SRS light (165-270 nm).

The results are given in Table 6.3 and compared to the prediction of secondary structure given by the DSSP/STRIDE algorithm from the E.M.B.L. The DSSP algorithm is a "knowledge based" program, which uses the Brookhaven pdb co-ordinates and assigns each amino acid residue to its most likely form of secondary structure.[160]

Table 6.3 Structure of *C. antarctica* lipase B in differing pH buffers.

Structure	PO_4 Buffer pH 4.2	KAc Buffer pH 5.0	PO_4 Buffer pH 6.0	Cacod Buffer pH 7.0 #*	PO_4 Buffer pH 9.0	DSSP
α-Helix	32%	38%	37%	38%	30%	37%
B-Strand	21%	20%	22%	20%	25%	18%
Turns	15%	14%	11%	18%	15%	26%
Other	31%	28%	30%	24%	30%	19%

This result was obtained using conventional CD with Chirazyme ™

There is some loss of helix at the extremes of pH, but the remaining structure does not appear to change over the pH range studied. While the main loss of activity at the extremes of pH is undoubtedly due to the effect of the pH on the ionisation of key residues, i.e. the Asp 187 and His 224 of the triad, the permanent loss of activity that occurs after exposure to extremes of pH may be explained by this loss of helix. CD studies on the enzyme creatine kinase also found that there was minimal change in the secondary structure between pH 6-9, with little loss of activity, after exposure to this range

of pH.[161] Below pH 4.8 and above pH 9.6 there was significant loss of α-helix and of the loss in activity 80% was irreversible.

Because most of our kinetic studies have been done using the unsupported commercial enzyme Chirazyme™, and the supply of the pure enzyme is limited, we repeated the CD spectra in KAc pH 5.0 buffer using commercial Chirazyme. No significant difference was seen between the structures of the two enzymes, however the spectrum obtained using Chirazyme was noisier, due probably to the presence of extraneous protein and the lyoprotectant used in its preparation. The spectra obtained are shown in Figure 6.7.

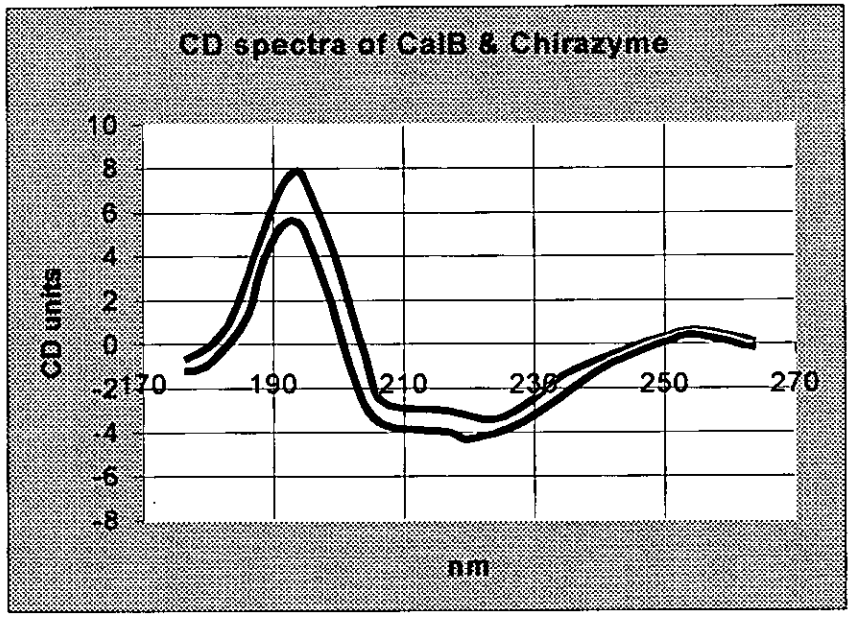

Black – Chirazyme, magenta - pure *Candida antarctica* lipase B

Figure 6.7 The CD spectra for Chirazyme and pure *Candida antarctica* lipase B in buffer.

Then using the method of Dordick,[157] we transferred the protein from solution in pH 5.0 KAc buffer to hexane and to toluene. It is not possible to use exactly the same method with the 1,4-butanediol because of the miscibility of water and the diol. Therefore, instead

of partitioning the protein from the aqueous phase to the organic phase, we used the minimum amount of aqueous buffer necessary to solubilise the protein and added this to the diol. The spectra are shown in Figure 6.8.

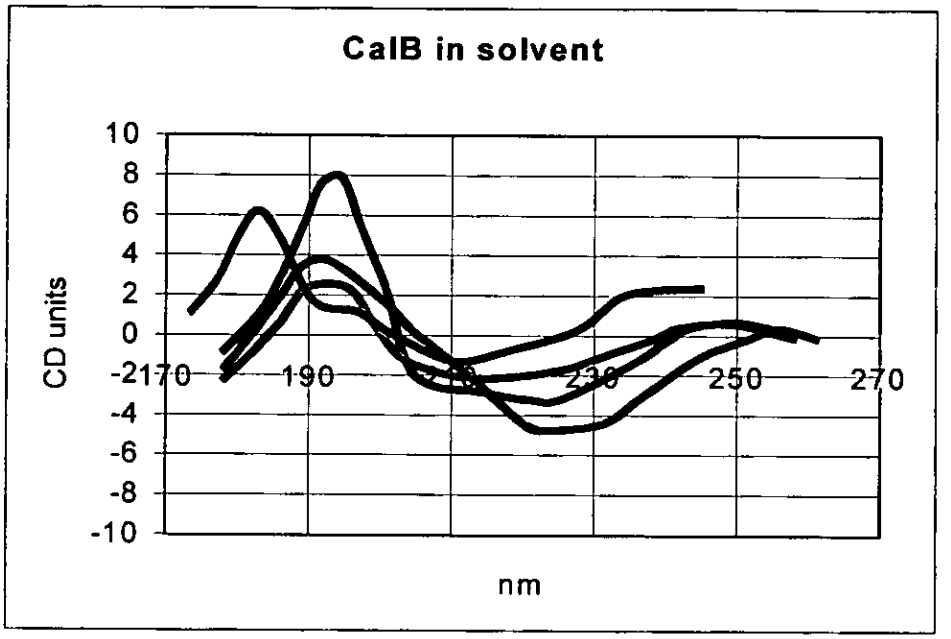

Blue - *Candida antarctica* lipase B in pH 5.0 aqueous buffer as a control, red - *Candida antarctica* lipase B in 1,4-butanediol, magenta – hexane, black – toluene.

Figure 6.8 The CD spectra of *Candida antarctica* lipase B in different media.

The results calculated from the spectra are shown in Table 6.4 with the structure in pH 5.0 buffer for comparison.

Table 6.4 Structure of *C. antarctica* lipase B in solvents

Structure	Hexane	Toluene	1,4-Butanediol	pH 5.0 Buffer
α-Helix	35%	8%	11%	37%
B-Strand	30%	31%	36%	18%
Turns	15%	32%	14%	26%
Other	20%	29%	36%	19%

It must be remembered that the reported structures are based on a fitting program that uses 50 reference spectra from a wide diversity of protein structures. We have seen with α-chymotrypsin, which is one of the standards, a very close correlation between our CD spectra and the published results, whereas *C. antarctica* lipase B does not have any proteins of close homology among the reference spectra. Therefore, when comparing spectra obtained in solvent compared to reference spectra obtained in aqueous buffers a similar degree of accuracy cannot be expected. The measurement of the distinct circular dichroism of the α-helix at 190 nm gives a reasonable confidence in the amount of α-helix quoted, however other structures are not so easy to determine. All spectra were fitted to a correlation R^2 of 0.95 (RMS 0.4) or better, nevertheless the structures other than α-helix should be taken as a guide only.

A number of authors have reported that when the secondary structures of enzymes in solvent are determined by CD spectroscopy there does not appear to be much difference between the structure in solvent and the native form in aqueous buffer.[162] While one might expect the protein to unfold in most solvents because of the hydrophobic inner, the stability of the protein may be increased in hydrophobic solvents because of the reduced mobility of the protein chain in the absence of water.[163] This certainly appears to be the case with α-chymotrypsin, as may be seen from the results in Table 6.3. It also appears to be true for *Candida antarctica* lipase B when partitioned from buffer into hexane as shown in Table 6.4. While this structure was obtained by SRS CD, the result was confirmed subsequently by conventional CD.

The structure obtained for the enzyme in toluene (Table 6.4), therefore, is somewhat surprising, particularly as the enzyme is still active in both solvents. Because of the

unique problems of trying to obtain CD spectra in toluene, which is absorbing up to 99% of the light at certain wavelengths, the sample has to be in the beam for a very long time. The normal procedure used with the aqueous samples and the other solvents, is to take three scans each of 20 minutes duration. In the toluene experiment, we took 60 × 20 minute scans in order to obtain the toluene background and a further 60 × 20 minute scans for the enzyme in toluene. The latter experiment was then repeated using 55 scans. It is possible that the protein lost some α-helix for reasons other than the effect of the solvent alone. Although there was no appreciable drift in the spectrum over the 20 hours it was in the instrument and the temperature was kept constant at 25°C, the protein might still have been affected by the beam. This is almost certainly the first time that a protein structure has been determined in toluene and it could well be the last because it is not easy to justify 3 days of synchrotron time for one experiment.

The spectrum in toluene needs to be interpreted with care, the SELCON program and for that matter any similar program, bases the α-helix content on the CD absorbance at 190nm. If for some reason the CD spectrum in toluene had shifted to the blue, as it appears from the spectrum, then the protein has not actually lost α-helix content. This interpretation would be more consistent with the function of the enzyme in toluene. The loss of helix structure in the 1,4-butanediol is also surprising because of the excellent activity of the enzyme in this medium, which is of course also the substrate for the acylated enzyme.

We then decided to investigate the structure of the enzyme after it had been acylated by the substrate to see if there were any observable changes in the secondary structure. The enzyme was transferred from buffer to dimethyl adipate, which acts as both solvent and

substrate. The CD spectrum obtained when the enzyme is in dimethyl adipate is most interesting (see Figure 6.9). We were unable to obtain a meaningful CD spectrum because we observed an enormous induced circular dichroism, some 10 times larger than we would expect from the protein alone.

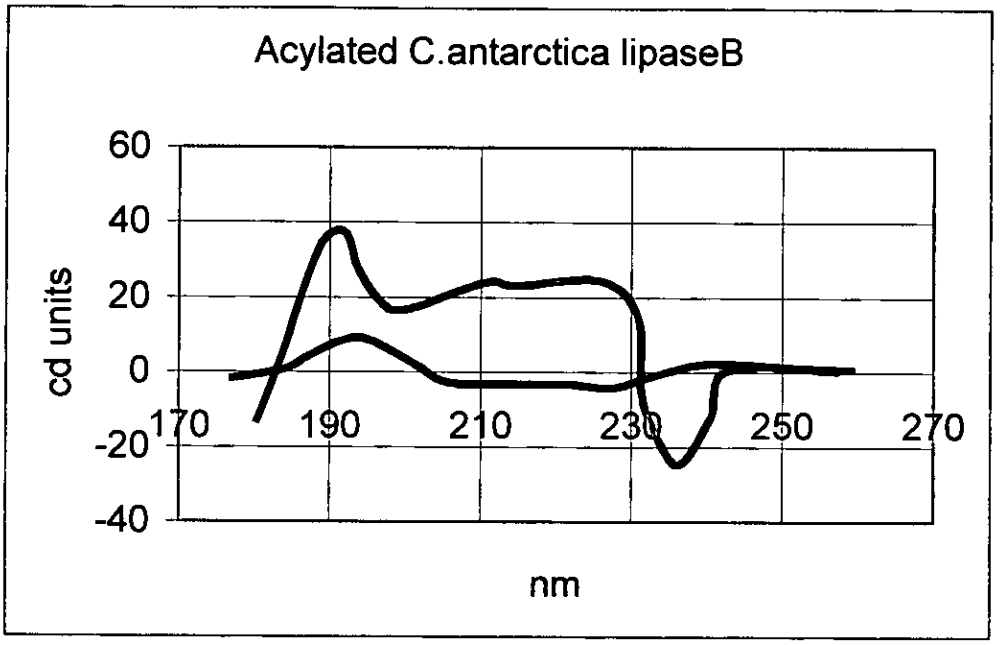

Red - acylated enzyme, magenta – un-acylated enzyme in hexane.

Figure 6.9 CD spectra for *Candida antarctica* lipase B after acylation with dimethyl adipate.

The large induced circular dichroism was not expected though it can be explained because of the binding of the substrate to the enzyme.

Very little has been published on the phenomenon of induced circular dichroism (ICD). In all published cases of ICD occurrence, it has been observed that the ligand must be bound to or very close to an α-helix. The length of the helix being important, there appears to be an optimum length of helix for ICD, too long or too short and the ICD declines.[164] The

magnitude of the ICD is also directly proportional to the amount of binding in the sample.[165] Finally, the observation of the ICD in our experiment appears to confirm that the acyl substrate is bound to the enzyme in a fixed conformation; otherwise, the ICD would not be seen. We have seen a similar effect with *Candida antarctica* lipase B (Chirazyme), which has been acylated by vinyl butyrate, using a conventional CD spectrometer, however the spectrum obtained was very noisy and would be difficult to use quantitatively. The power of the SRS would appear to be essential for this work.

The use of ICD to investigate the binding of substrates to an enzyme seems to be worthy of further study, both in terms of the extent and geometry of the binding.

6.1 Conclusions.

It would appear that the secondary structure of *Candida antarctica* lipase B in aqueous buffer at pH 5.0-7.0 is very close to the natural structure determined by X-ray crystallography. The isoelectric point, pI, for the enzyme is 6.0.[166] At the extremes of pH 4.0 and 9.2 there are significant differences in the α-helix content. In solvents, we see some very interesting effects. In hexane there appears to be little difference in the secondary structure of either α-chymotrypsin or *Candida antarctica* lipase B to that obtained in aqueous buffer. This confirms the work of Yennawar who also found that α-chymotrypsin did not change structure when dissolved in hexane.[167] The result in toluene is an enigma and is most likely to be due to the problems of obtaining a CD spectrum in such a strong absorber of UV light. The physical properties of toluene are not that different to hexane yet there is a very large difference apparently in the degree of unfolding that is caused. All the experiments were very noisy because of the very low

levels of light passing through the sample, however, when we averaged the spectra from the first ten scans and compared this to the average of the last ten scans, no significant difference was seen. Therefore, it is highly unlikely that the sample has deteriorated over time due to the effect of radiation or heat. It can be seen from the spectrum that the principal peak has moved to a shorter wavelength than the typical helix peak absorbance. The SELCON program only assigns helix to the CD absorbance at 190 nm, therefore if for whatever reason the helix absorbance has been shifted then the SELCON will give an erroneous result. The results in 1,4-butanediol are more surprising. Diols such as pentanediol are used in protein folding experiments, where they are added to the aqueous medium to enhance the formation of the correct protein structure. It seems strange that when they are used as the total medium they cause the unfolding of α-helix.

When one examines the secondary structure of *Candida antarctica* lipase B, shown in Figure 6.10 it may be seen that there are several large helices away from the active site of the enzyme. Long helices in proteins may be metastable; therefore, it is possible that the unfolding can occur away from the active site without changing the structure of the site and affecting the activity of the enzyme.

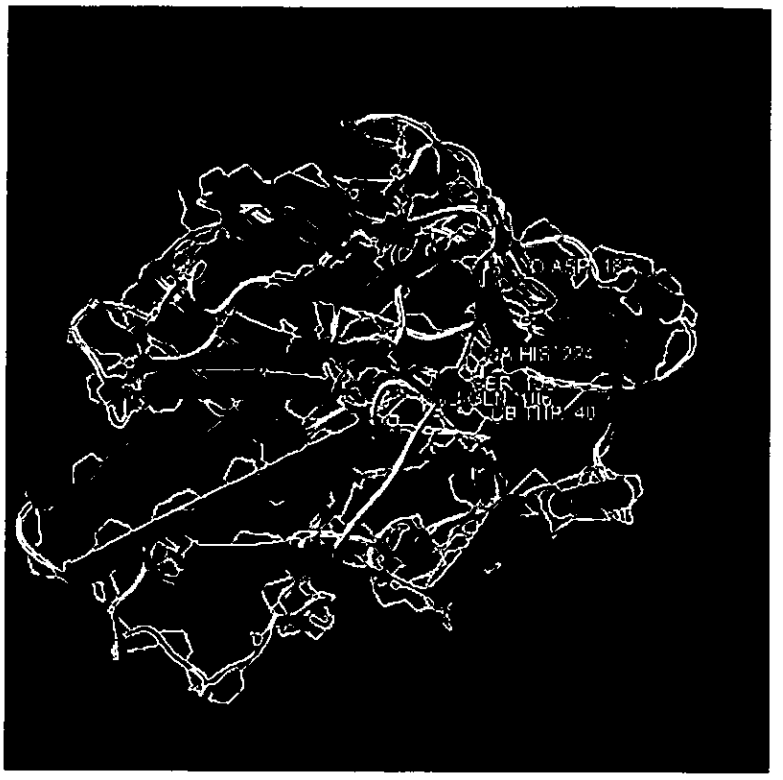

Figure 6.10 The secondary structure of *Candida antarctica* lipase B. Sculpt model based on pdb file 1tca.

7 Molecular modelling.

In order to understand better, the processes taking place within the enzyme active site and the interaction between the enzyme and various substrates we decided to look at the use of molecular modelling programs for this purpose. We looked at a number of programs such as Hyperchem, Spartan and Gaussian 98. All programs give models that are as geometrically accurate as the input knowledge and are capable of manipulation. In order to obtain a good model the whole structure must go through an optimisation process called energy minimisation. Where the programs differ is the level of sophistication used in the quantum mechanics (QM) or molecular mechanics (MM) calculations used to determine the conformational energies used in the minimisation process.

The calculation of molecular energies using QM involves solving approximations to Schrodinger's equation in order to determine electron density, energy and other properties. When used on large molecules such as proteins QM modelling requires a great deal of computing power.

The principle of MM treats the molecule as a series of balls and springs and the energies are determined using Hooke's law. Each atom is moved slightly and a new structure generated in which the energy is lowered, the process is repeated until the whole molecule is in its lowest energy state when the structure is said to be minimised. While this is still an extremely complex task for a protein molecule, nevertheless MM modelling is a simpler method than QM modelling and requires a lot less computing power.

One program seemed to be ideal for the modelling of proteins; this was the Sculpt program from Molecular Dynamics in the USA. It had a number of features that made it ideal for our purposes. It was written specifically for the modelling of proteins and

accepted pdb X-ray diffraction crystallography files readily from the Brookhaven database, with which to create the model. Also it accepted small molecules such as ligands, which if modelled in ISISDraw and converted to 3D, could be pasted into Sculpt. Sculpt allows manipulation of the molecule in real time using MM force field calculations, embodying van der Waals or electrostatic interactions or both. It has good ligand docking facilities; a ligand may be docked into the flexible receptor molecule and the effect of the docking on the enzyme observed readily. The program runs a local energy minimiser so that covalent bond lengths, bond angles and single value dihedrals may be constrained to their original values. Potential energies are used to model explicit hydrogen bonds, variable dihedrals, electrostatic and van der Waals interactions. The latter are modelled using a modified Lennard-Jones function between atoms within 6Å. Electrostatic interactions are modelled using a Coulomb model with a distance depending on dielectric up to 10Å of each other.

Before starting the modelling of the protein, if there is more than one pdb file, it is necessary to decide which of the pdb files to use. In the case of the *Candida antarctica* lipase B there are seven files, each determined by different authors under slightly different conditions and resolutions. Therefore, we ran the Sequence Finder [168] program from Swissprot in order to check the homology of the seven proteins listed under *Candida antarctica* lipase B. Sequence Finder detected no difference in the homology of the the seven files, therefore we selected pdb file 1lbs.[109] This file was copied and pasted into Sculpt and several models created. Fortunately, one of these was seen fairly early, by A. Svendsen of Novo, who spotted an anomaly in the structure. It was discovered that if the grammar of the pdb co-ordinates is not perfect, Sculpt sees a break in the peptide chain and only models the first part of the protein. Therefore, we changed to pdb file 1tca,[97] which gave a complete model of the protein, all subsequent work was done using the co-

ordinates for 1tca, which had been obtained at the higher resolution of 1.55Å compared to the 2.2Å resolution of 1lbs.

A study was carried out of the overall structure of *Candida antarctica* lipase B and this compared to other lipases such as *Rhizomucor miehei* in both the closed pdb 3tgl and open pdb 4tgl configurations [i] (see Figure 6.1 in Chapter 6).

Other lipases studied included *Candida rugosa* lipase and *Geotrichum candidum* lipase shown in Figures 7.1 and 7.2.

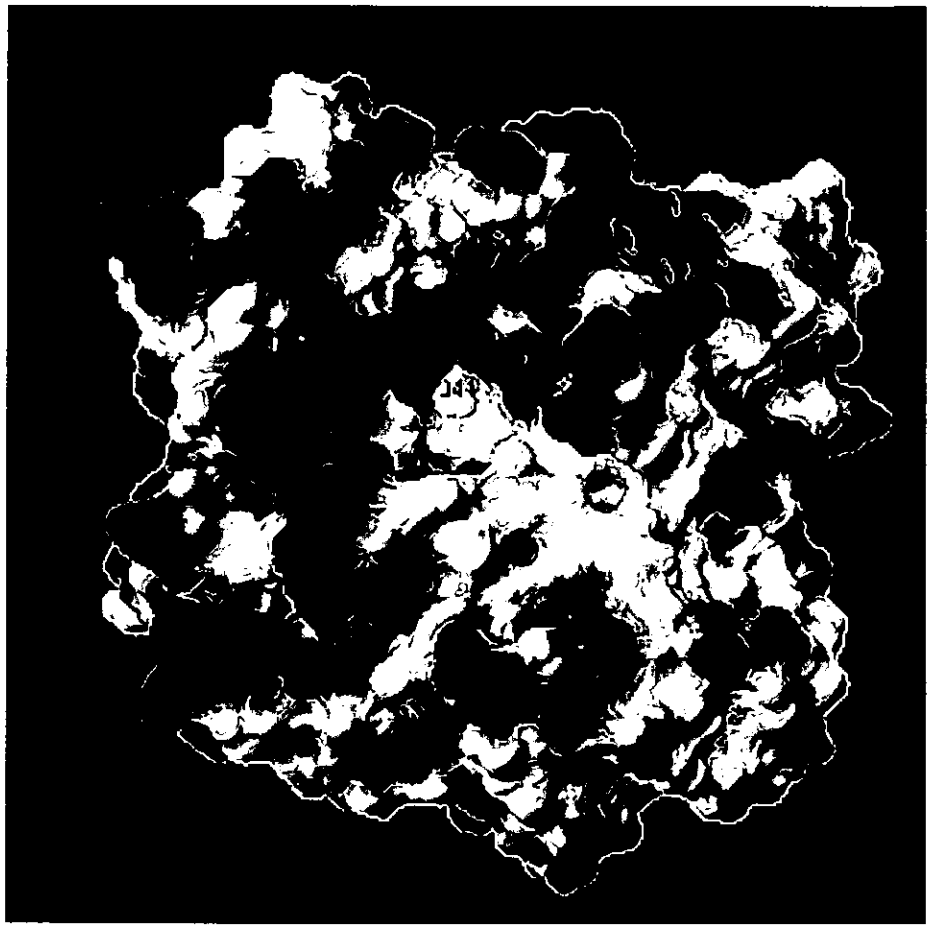

Figure 7.1 *Candida rugosa* lipase modelled from pdb file 1crl.[ii]

The hydrophobic surfaces are shown in blue, the tunnel shaped entrance to the active site is clearly visible in the centre of the model.

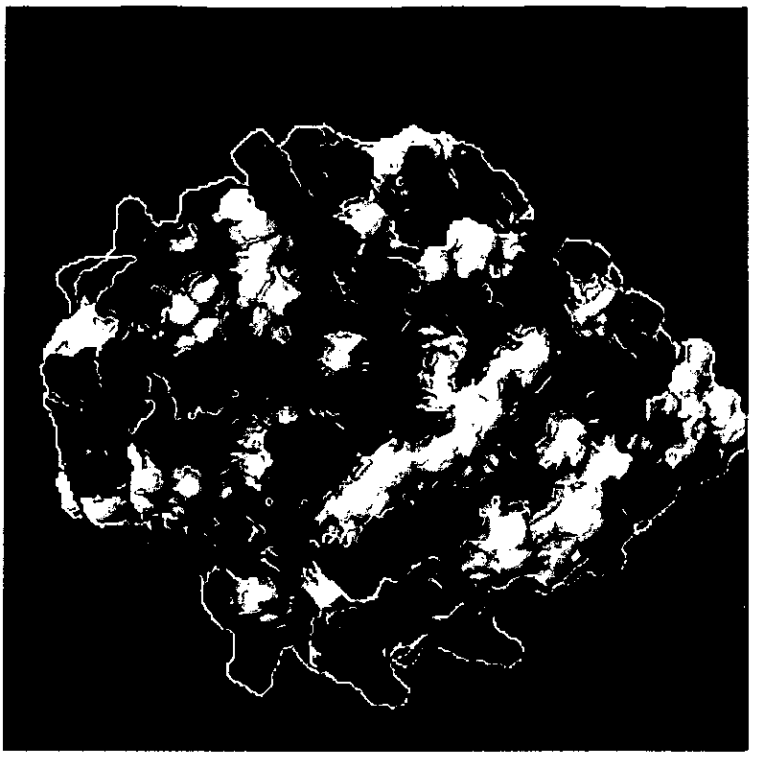

Figure 7.2 *Geotrichum candidum* lipase modelled from pdb file 1thg,[171] showing hydrophobic surfaces in blue.

The model of *Geotrichum candidum* lipase is the closed form so that the active site is not visible. It is obvious that in the closed form there is substantially less hydrophobic surface than any of the other lipases studied. This protein is one of the largest lipase molecules for which the structure has been determined, it consists of 544 amino acids in a single peptide chain folded into one domain, this is one of the largest ever proteins observed.

Geotrichum candidum is unusual in that the lid over the active site is made up of two helices rather than the usual single helix, these are made from residues proline 66 to alanine 76 and serine 294 to phenylalanine 310. These may be seen clearly, over the active site in Figure 7.3.

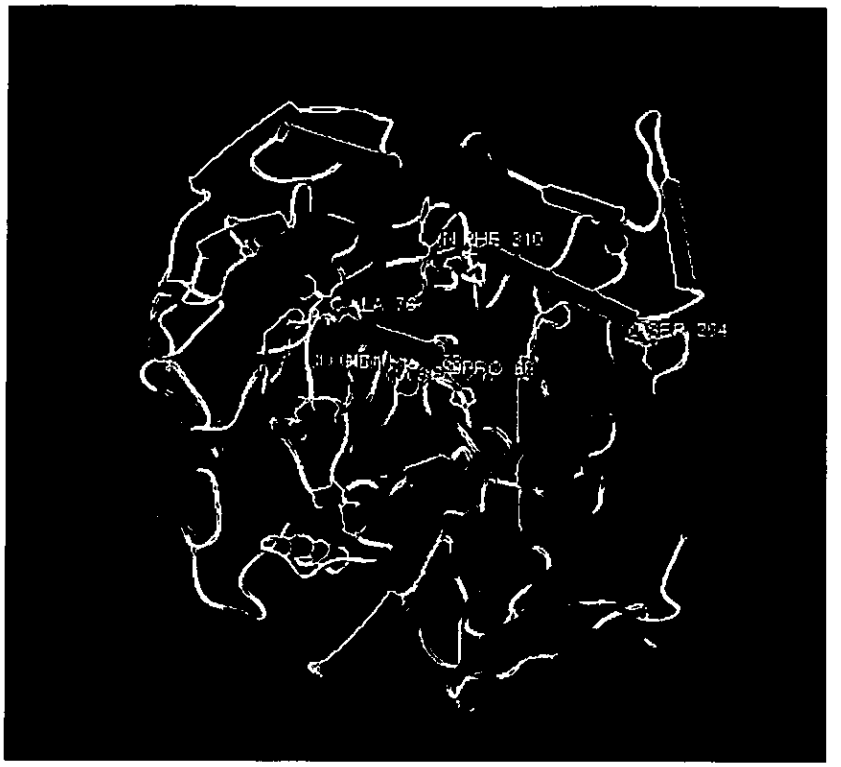

Figure 7.3 Secondary structure of *Geotrichum candidum* showing helices of the lid.

The catalytic triad of this lipase is different to that of *Candida antarctica* in that the aspartate component is replaced by glutamate.

The discussion on the secondary structure of the lipases and the impact of differences in secondary structure on the function of the enzyme is to be found in Chapter 6.

The modelling of the enzymes was then extended to cover the details of the active sites of the various lipases and to compare these with the active sites of common proteases.

The active site of *Candida rugosa* with the catalytic triad of glutamate 341, histidine 449 and serine 209 is shown in Figure 7.4.

Figure 7.4 The active site of Candida *rugosa* lipase.

It should be noted that the *C. rugosa* follows the standard lipase consensus with the serine of the active site in the pentapeptide Gly-X-Ser-X-Gly this is situated on the tight turn between the β sheet and the α helix, the α–β hydrolase fold.

It is interesting to compare the typical lipase active site with the active site of γ-chymotrypsin a typical protease, this was modelled using pdb file 1gmd [167] (see Figure 7.5).

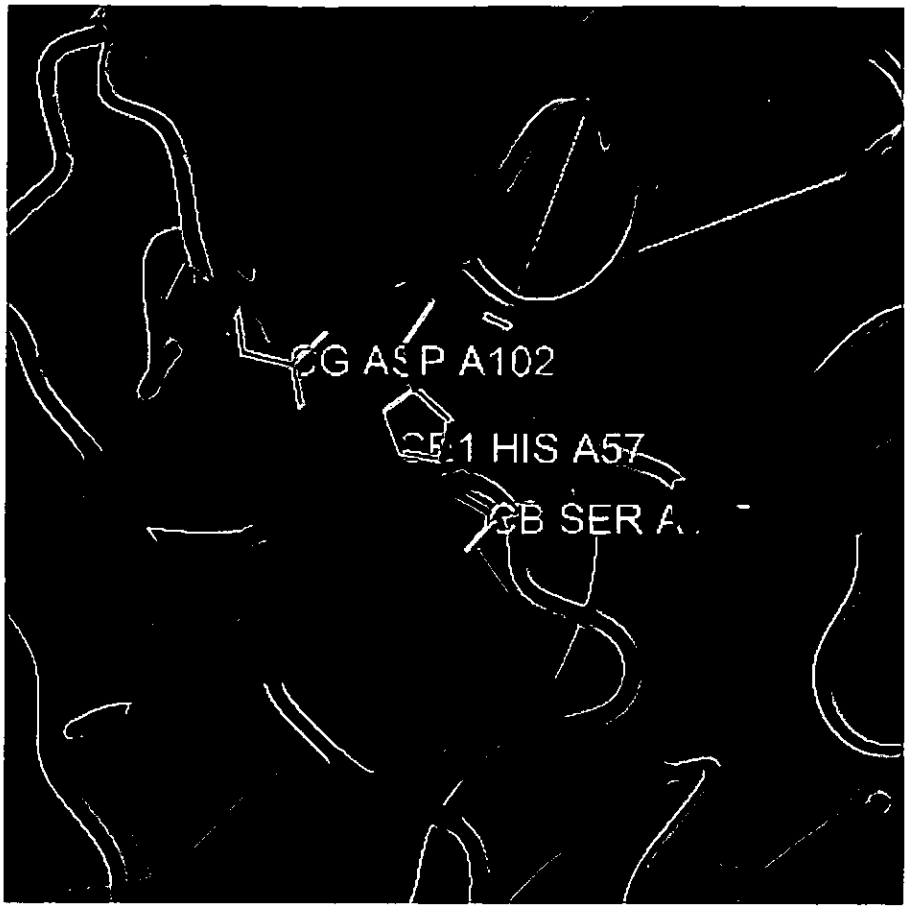

Figure 7.5 The active site of γ-chymotrypsin from pdb file 1gmd.

Although the catalytic triad looks superficially like that of the *C. rugosa* lipase, there are several important differences. The three residues of the triad do not have the same order as the lipase sequence, i.e. serine, aspartate, histidine. The hydrolase fold is missing, there is no α-helix in the environ of the Ser 195 although the β-sheet is in place. Thirdly on close inspection it is obvious that the orientation of the three residues is quite different to that in lipases, in particular, that of the histidine, although the proximity to the aspartate and serine residues is such that the catalytic mechanism is still the same.

The active site of *Candida antarctica* is shown in the Figure 7.6.

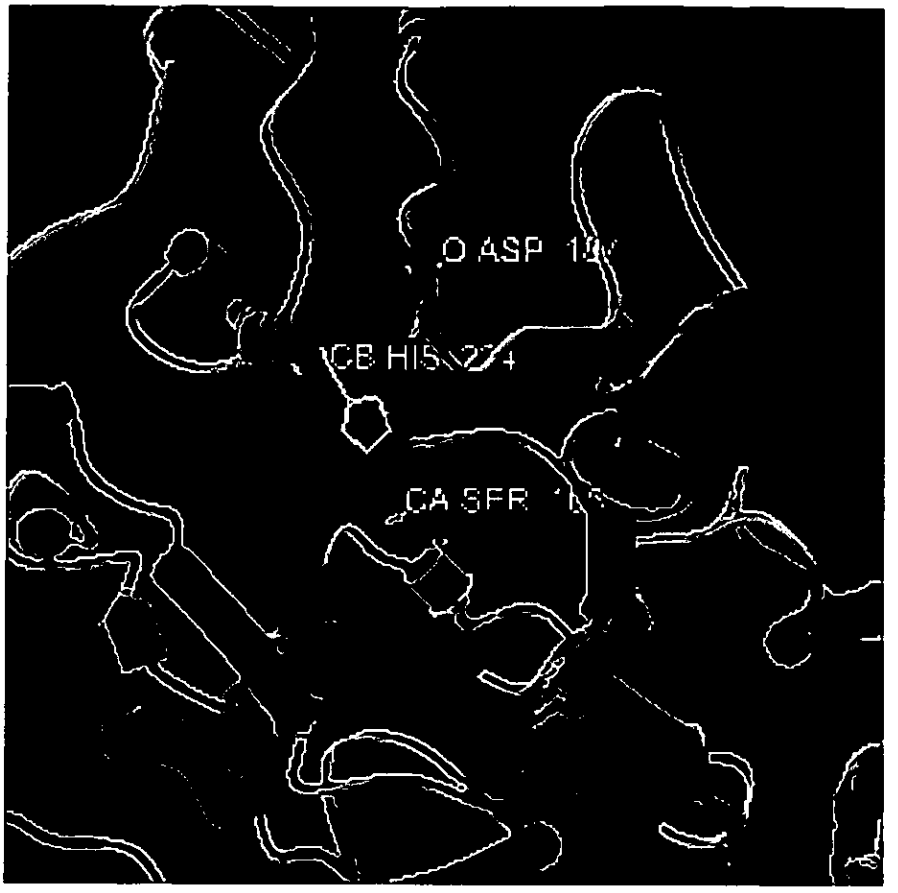

Figure 7.6 Active site of *Candida antarctica* from pdb file 1tca.

The triad is made up of Ser 105, Asp 187 and His 224. The serine 105 can be seen at the end of the short helix in the loop to the β-sheet forming the α–β hydrolase fold. *C. antarctica* lipase B is unusual that the lipase consensus Gly-X-Ser-X-Gly is changed to Thr-X-Ser-X-Gly, the orientation of the residues however is that of the typical lipase.

The Sculpt modelling facility was then used to investigate the interaction of various substrates with the enzyme.

The acylated enzyme was modelled with adipic acid; the diol substrates used included 1,4-butanediol, 1,6-hexanediol and α,ω–polytetramethylene ether glycol 650.

In Figure 7.7, *C. antarctica* lipase B is shown with the substrate AB (adipic acid + 1,4-butanediol) bound to the Ser 105 in the active site.

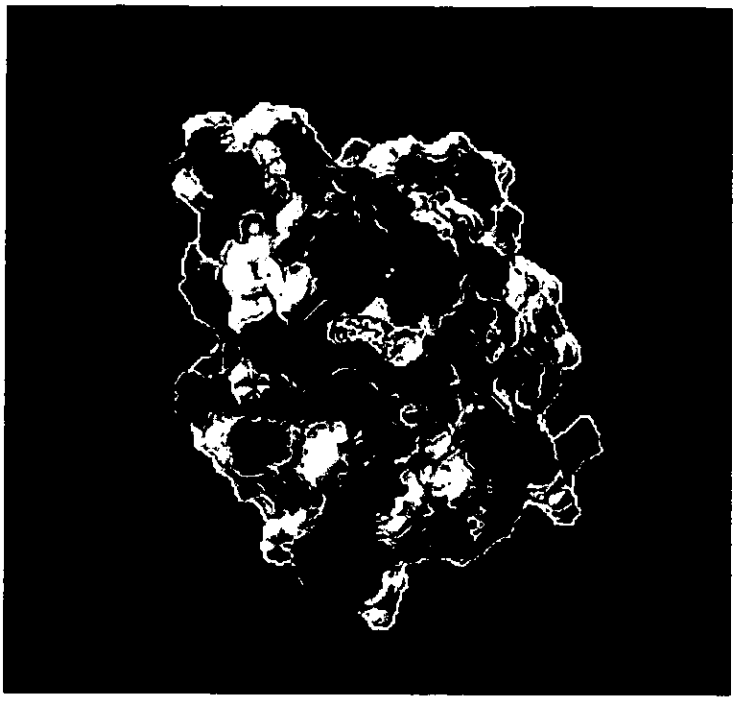

Figure 7.7 The active site of *Candida antarctica* lipase B containing the substrate AB.

Although the above shows the substrate in the active site, it is not particularly informative so it is necessary to model the binding of the substrate into the isolated structure of the pocket. In Figure 7.8 we have attempted to produce a cross section of the active site showing the hydrophobic entrance to the site that is formed by the residues Leu 144, Ile 285, Val 149 and Ala 281. Other hydrophobic residues such as Ala 282 and Leu 278 have been omitted for the sake of clarity. At the bottom of the pocket where the substrate is bound to the Ser 105 there is a strongly hydrophilic region made up of His 224, Asp 134 and Asp 187 together with Thr 40 and Thr 138 and Gln 157. All of these residues play some part in the catalytic process either in the catalytic triad or the stabilisation of the tetrahedral intermediates by the formation of hydrogen bonds in the oxyanion hole.

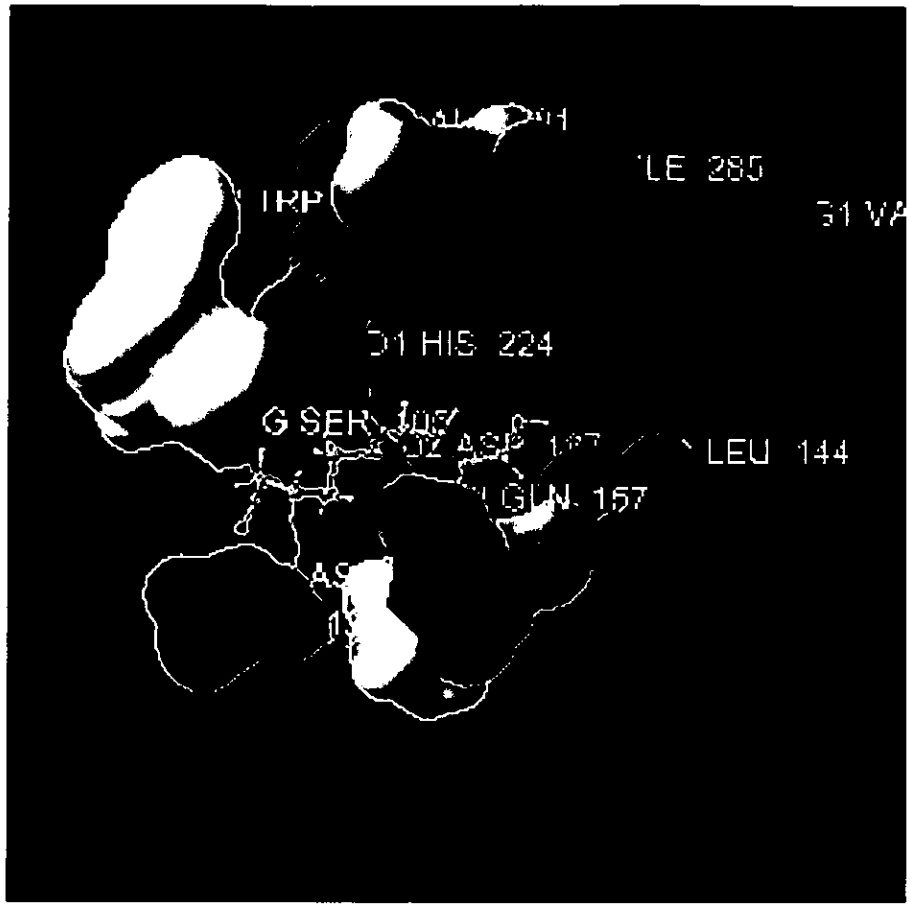

Figure 7.8 The key residues of the active site of *Candida antarctica* lipase B.

It is tempting to try to use modelling to explain some of the effects, seen in the kinetic studies; therefore various substrates were docked into the site to see if there were any observable effects. In the Figure 7.9, the substrate acetylvaleric acid has been docked on to the serine 105 and is in the process of minimisation using both electrostatics and van der Waals forces. The electrostatic attraction between the acetyl carbonyl and the hydrogen of the peptide bond of Asp 134 may be seen. The red umbrellas are the regions where the computation is being carried out.

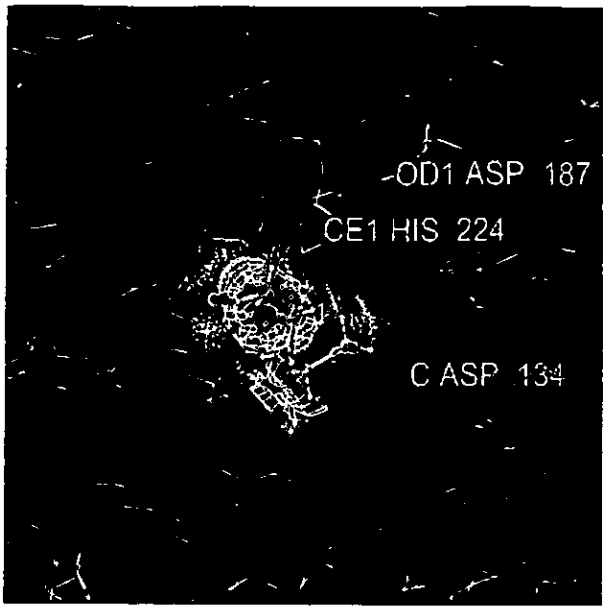

Figure 7.9 Energy minimisation of acetylvaleric acid docked in *C. antarctica* lipase B.

The size of the substrates involved and the apparent ease with which they are accepted by the enzyme is quite surprising. Figure 7.10 shows the AB_4 oligomer docked into the active site with a molecule of 1,4-butanediol entering on the alcohol side to form $B(AB)_4$.

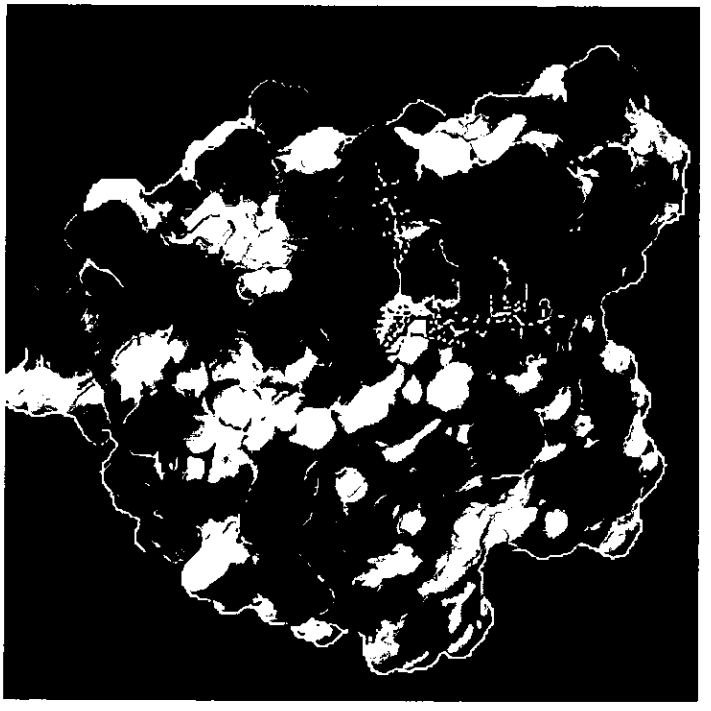

Figure 7.10 The oligomer $B(AB_4)$ docked into *Candida antarctica* lipase B.

The apparent problem of how an extremely long polyester such as a 5000 Dalton or higher polymer molecule can find and enter the active site seemed quite perplexing. We developed the theory that maybe the polymer never leaves the enzyme surface, but in fact creeps over surface while the growing end, whether it is acyl or hydroxyl terminated, remains close to the active site. In order to see if this could be modelled we looked at a 2000 Dalton oligomer of adipic acid and 1,4-butanediol bound to the enzyme and minimised to see what configuration was adopted. This is shown in Figure 7.11.

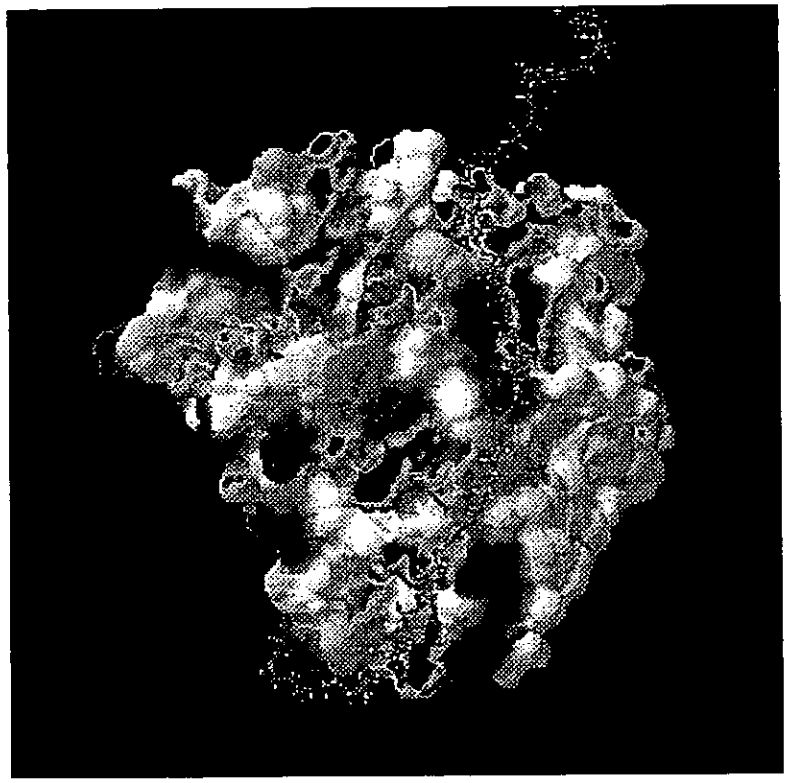

Figure 7.11 High molecular weight polyester on the surface of *Candida antarctica* lipase B.

After many hours of minimisation it appears that the polyester chain wraps itself around the enzyme as a result of the formation of many hydrogen bonds (shown in light blue) with polar residues on the surface. There seems to be an understandable preference for a

vague line of hydrophilic residues shown in red, on the surface of the enzyme. This mechanism, if correct, is similar to that of RNA synthetase where the growing RNA is bound to the enzyme some distance from the active site.[37] The latter mechanism was proven by site directed mutations, which removed key polar residues with the result, that the rate of assembly of the RNA was reduced dramatically. A similar technique could be used to prove our hypothesis if the resources were available. If the surface of the enzyme were made substantially less polar without affecting the active site then the esters could be synthesised, but the rate of polymerisation should decline rapidly as the molecular weight builds. This mechanism would also explain the observation reported in Chapter 4, that on transesterification of high molecular weight polyesters, it is the near terminal ester groups, which are attacked first.

Other modelling was carried out to confirm that the enzyme would accept certain unusual substrates, in particular the macrolactone of adipic acid and diethylene glycol was of interest because of the problems it causes in commercial polyesters.[116] This molecule is a 13 membered ring, which would seem to be a difficult substrate for a lipase (see Figure 4.15 in Chapter 4). In this model the macrolactone can be seen in the active site bound to the Ser 105. The molecule appears to fit into the site quite nicely and as would be expected from the model the enzyme was found to catalyse the ring opening of this lactone very effectively.

8 Evaluation of proteases as esterification catalysts.

There have been several references describing the use of proteases as catalysts for esterification reactions. Park used subtilisin from *Bacillus licheniformis* to synthesize sucrose adipate from divinyl adipate and sucrose,[172] while Akkara and Bruno claimed the use of protease BPN to catalyse the synthesis of polyesters.[173]

The possibility of being able to use a protease as catalyst in the enzymatic polyesterification process has several attractions. There is a wide choice of available proteases; many of these are commercially available in quantity and at a lower price than *Candida antarctica* lipase B. Although many of the available proteases have an alkaline optimum pH there are some that have an optimum in acid conditions.

Therefore, it was decided to evaluate a range of commercially available proteases. The enzymes chosen for evaluation were:-

Protease N from *B. subtilis*, subtilisin Carlsberg, γ–chymotrypsin and papain. The latter was chosen because it has a pH optimum of 4.8 and interestingly, it is the only protease or lipase where the nucleophile of the catalytic triad is not the hydroxyl of a serine or threonine residue, but the SH group of a cysteine residue.

The substrate chosen for the evaluation of these enzymes was 0.4M adipic acid in 1,6-hexanediol. The results are summarised in the Table 8.1.

Table 8.1 Activity of proteases as esterification catalysts.

Enzyme	Enzyme mg	Weight loss $\mu g\ min^{-1}$	Rate of reaction $\mu mol\ min^{-1}\ mg^{-1}$
Subtilisin Carlberg	0.717	-	No reaction
"	0.373	-	No reaction
γ-chymotrypsin	2.502	-	No reaction
Papain	1.533	1.7	0.06
"	2.452	2.2	0.05
Protease N	0.532	-	No reaction

The possible activity of papain in this system is interesting because of its optimum pH of 4.8. In the polyesterifcation of a strong carboxylic acid such as adipic acid the low optimum pH could be a distinct advantage. In view of the slight activity observed with papain, it was decided to investigate the performance of the enzyme in larger scale experiments.

Adipic acid was heated in 1,6-hexanediol to 100°C for 2 hours to maximise the solvation of the acid in the diol. The reactants were then cooled to 60°C and the papain added, the reaction was maintained at this temperature and a pressure of 200mmHg for 48 hours. Samples were taken after 24 and 48 hours for analysis by gel permeation chromatography. In both cases a small amount of AB was seen, but no higher oligomers were present.

The experiment was then repeated using a much larger quantity of enzyme, the temperature and pressure were maintained at 60°C and 200mmHg for 5 days. Samples

were taken after 24 hours and 5 days and analysed by gel permeation chromatography. Once again only a small amount of AB was observed.

Because the enzyme had the ability to catalyse the formation of AB, but no higher oligomers, it was considered that irrespective of its pH optimum it might be being deactivated by the reaction conditions. Either the acidity of the medium, or possibly the 2 phase system, which suits lipases but not proteases, may be deactivating the enzyme. Therefore, the reaction was repeated using dimethyl adipate in place of the adipic acid.

1,6-Hexanediol was dissolved in dimethyl adipate at 60°C and 1gm of papain added. The reaction was maintained at 60°C and a pressure of 200mmHg. After 24 hours the clear solution contained a considerable amount of a white precipitate, which was found to be adipic acid. The reaction conditions were maintained for 3 days. Analysis of the final mixture by gel permeation chromatography showed the presence of adipic acid, 1,6-hexanediol and the dimer AB.

The conclusions reached after these experiments were, papain can catalyse the hydrolysis of dimethyl adipate to adipic acid and can to an extent catalyse the formation of AB, however, it cannot catalyse the esterification of AB or the formation of any higher oligomers. At this stage the work with proteases was abandoned.

9 Enzymatic synthesis of novel polyesters.

The majority of enzymatic syntheses reported in the literature that use lipases, are either concerned with the synthesis of polyesters or the synthesis of stereospecific esters where the enantioselectivity of the enzyme steers the reaction product to a particular isomer. Apart from the synthesis of sugar esters and the work of Harffey with epoxide esters, the low temperature aspect of enzymatic synthesis has not been exploited to full advantage.

Polyester based polyurethanes are well known and used for applications such as surface coatings, textile coatings, adhesives and elastomers. These materials are manufactured from hydroxy terminated polyester resins made by the high temperature condensation of a diacid and diol, followed by further reaction with a di-isocyanate to produce a polyurethane polymer. To date the only practical synthesis of polyurethane polymers has involved the use of di-isocyanates, these are prepared by the phosgenation of the corresponding diamine. The production of the toxic isocyanate involves the use of an even more toxic reactant. Understandably the production of di-isocyanates is limited to only a few companies in the world who are capable of operating the process safely and limited to a select group of diamines. Perforce these limitations mean that most di-isocyanates are expensive.

While there have been many attempts to synthesise di-isocyanates by an alternative route to phosgenation, or to synthesise polyurethanes by a non-isocyanate route, none of these has ever been successful commercially.

With the advent of the enzymatic synthesis of polyesters an alternative route was considered which reversed the conventional process. In the conventional process the addition of the isocyanate must occur after the esterification reaction because the

carbamate group is heat labile, it starts to decompose at 150°C, well below the esterification temperature.

Instead of creating the urethane polymer after the synthesis of the polyester, the low temperature enzymatic synthesis presents the opportunity to synthesise the urethane component first and then and then build the polymer by polyesterification.

9.1 Synthesis of *bis*-carbamate esters.

It was known from the work of Delaby,[174] in the 1950's that the carbamate group could be synthesised by the ring opening addition of a cyclic carbonate such as ethylene carbonate with a primary amine; the product of this reaction being a *bis*-hydroxyethyl carbamate.

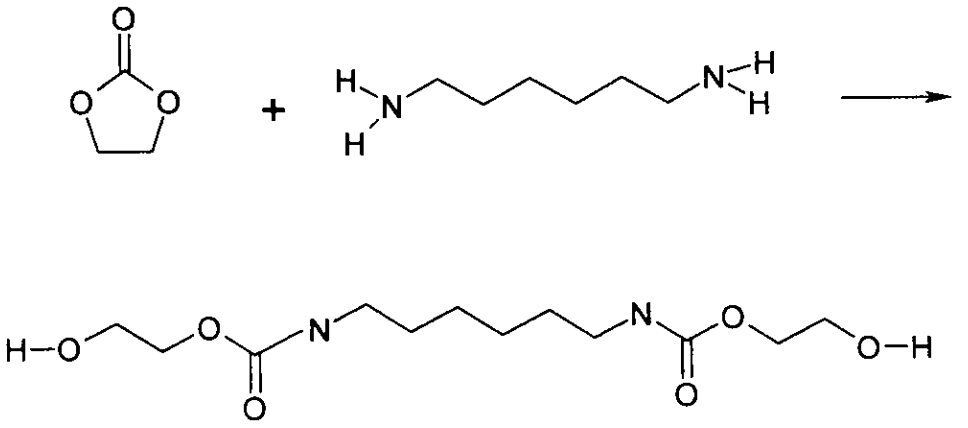

Scheme 4

These reaction products had been used to form polymers by further reacting the *bis*-carbamates with methylol melamine to form cross-linked polyether polymers containing urethane groups. The resulting polymer had some of the properties of a polyurethane, but the need for high temperature stoving meant that some degradation took place.

The use of the enzymatic low temperature synthesis presented the possibility that the polyurethanes could be synthesised without the use of di-isocyanates, such a process

would allow the use of readily available diamines that were not available as the corresponding di-isocyanate. This idea led to two possible applications, firstly to synthesise polymers that were analogues of existing polymers, but without the use of a di-isocyanate, secondly to synthesise polyurethanes where the requisite diamine was available but the di-isocyanate was not available. For example, ethylene diamine is readily available, but ethylene di-isocyanate is not available because of its volatility and extreme toxicity.

In the first objective the work concentrated on the use of aliphatic diamines because the aliphatic di-isocyanates are much more expensive than their aromatic counterparts.

The method of Delaby,[175] for the synthesis of *bis*-carbamates involved carrying out the reaction in ice, this is not practical for large scale syntheses, therefore we developed an alternative synthesis whereby the amine was added slowly to the carbonate and the reaction followed by controlling the exotherm.

The Delaby synthesis using ethylene carbonate and hexamethylene diamine was repeated using the new method. The product, *bis*-hydroxyethyl hexamethylene carbamate, had a melting point of 94°C compared to the 93°C quoted by Delaby.[175] The product was analysed by GPC and ^{1}H NMR spectroscopy and found to be pure. The yield was 70% of theoretical.

Some of this *bis*-carbamate was dissolved in 1,4-butanediol at 90°C under nitrogen, cooled to 60°C and reacted with adipic acid using Novozyme 435 as catalyst. The resulting polyester containing *bis*-hydroxyethyl hexamethylene carbamate groups was analysed by gel permeation chromatography. It was found to have a molecular weight of 9350 Daltons compared to the polystyrene standard and a dispersity of 1.75.

This polyurethane ester was the analogue of a polybutane adipate polyester that had been partially chain extended with hexamethylene di-isocyanate and which could be further chain extended by the addition of hexamethylene di-isocyanate or any other di-isocyanate.

The method was then extended to synthesise a urethane polyester for which no equivalent isocyanate is available. Using ethylene diamine instead of hexamethylene diamine *bis*-hydroxyethyl ethane carbamate, identical to a carbamate based on ethylene di-isocyanate, was prepared. The m.p. of the white crystalline compound was 93°C. The yield was 60% of theoretical; the losses mainly due to the slight solubility of the product in cold ethanol. Chromatography showed that we had a single product free from starting materials.

A 1,4-butanediol adipic acid co-polyester was synthesised using this *bis*-carbamate as part of the diol component. After 48hrs the reaction was stopped and the resulting polyester analysed by GPC. The molecular weight was found to be 4500 Daltons, compared to the polystyrene standard, with a dispersity of 2.4.

This polyester was found to be extremely water soluble, which is explainable by the preponderance of ethane groups in the polymer. Such a water soluble polymer could well have applications in water soluble polyurethane coatings or adhesives.

One of the major problems associated with the commercialisation of a novel process using novel intermediates is the need for costly toxicological testing of the compounds. The EINECS regulations are relaxed if the novel compound does not leave the reactor and if the final product is a high molecular weight polymer. A further problem associated with the above process is the need for recrystallisation from hot ethanol and drying.

Therefore an alternative process was considered. One of the major reasons for the purification process was the need to use toluene as an inert diluent during the reaction. The desired physical properties of the finished polyurethane polyester meant that the *bis*-carbamate was unlikely to be used as the sole diol component of the polyester; this was the reason for the incorporation of the 1,4-butanediol component in the second stage of the esterification process. Therefore, as 1,4-butanediol could not react with either the ethylene carbonate or the diamine reactants, the toluene was replaced with 1,4-butanediol.

The reaction of ethylene carbonate and hexamethylene diamine was repeated replacing the added toluene with 1,4-butanediol. Upon completion of the reaction the product is a clear solution at 60°C, which rapidly crystallises on cooling to a white waxy solid. Gel permeation chromatography and IR spectroscopy showed that the reaction had gone to completion and there were no starting materials remaining.

To this reaction product was added Novozyme 435 and the requisite amount of adipic acid to give a polyester with a molecular weight of 1500 daltons. After heating under reduced pressure for 48 hours the reaction was stopped and the resulting polyester analysed. The molecular weight by GPC was 2200 M_n, 4640 M_w with a dispersity of 2.1. The acid number was found to be 0.7mg KOH g^{-1} and the hydroxyl number 78mg KOH g^{-1}; this end group analysis gave a molecular weight of 1488 Daltons. There is no reason why this principle of using a diol from the second stage esterification as the diluent in the formation of the *bis*-carbamate cannot be extended to the synthesis of any *bis*-carbamate.

The procedure was repeated using propylene carbonate and isophorone diamine.

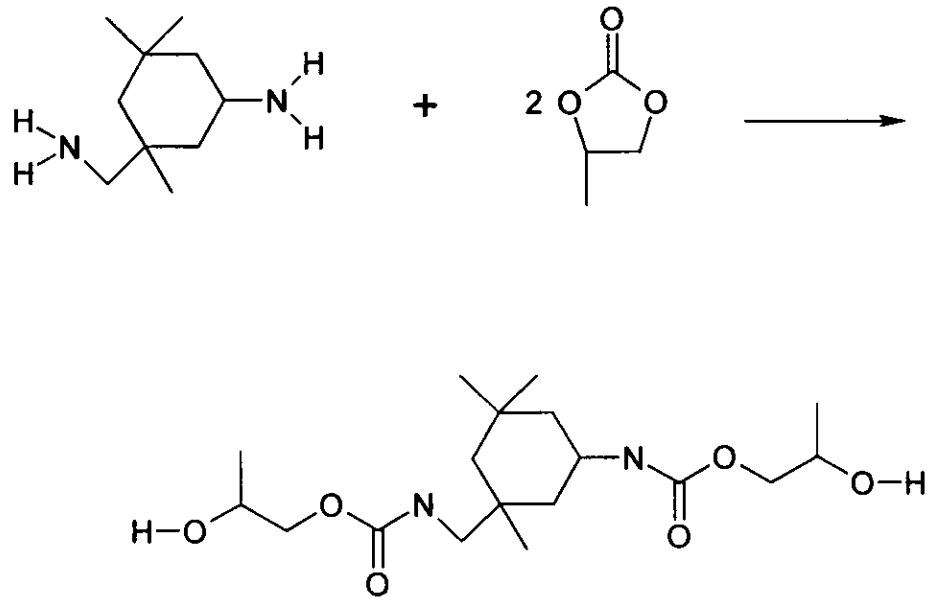

Scheme 5

GPC analysis showed that the reaction had gone to completion and there were no reactants remaining. This *bis*-carbamate was converted to polyester with the addition of 1,4-butanediol and adipic acid at 60°C and reduced pressure using Novozyme 435 as catalyst. After 48 hours the reaction was stopped and the product analysed. The molecular weight was determined by gel permeation chromatography, using a 1000Å column compared to a polystyrene standard. The molecular weight M_w was 6000 and the dispersity 2.14. The acid number was determined by titration as 2.0mg KOH g^{-1}.

The α,ω–polytetramethylene ether diol is used extensively in the manufacture of high performance polyurethane elastomers and coatings. There is no similar di-isocyanate available, however, the related diamine is available by the reaction of the diol with acrylonitrile and hydrogenation to give the *bis*-(3-aminopropyl) polytetramethylene ether of molecular weight 350. The *bis*-carbamate of this diamine was synthesised using the reaction in Scheme 6.

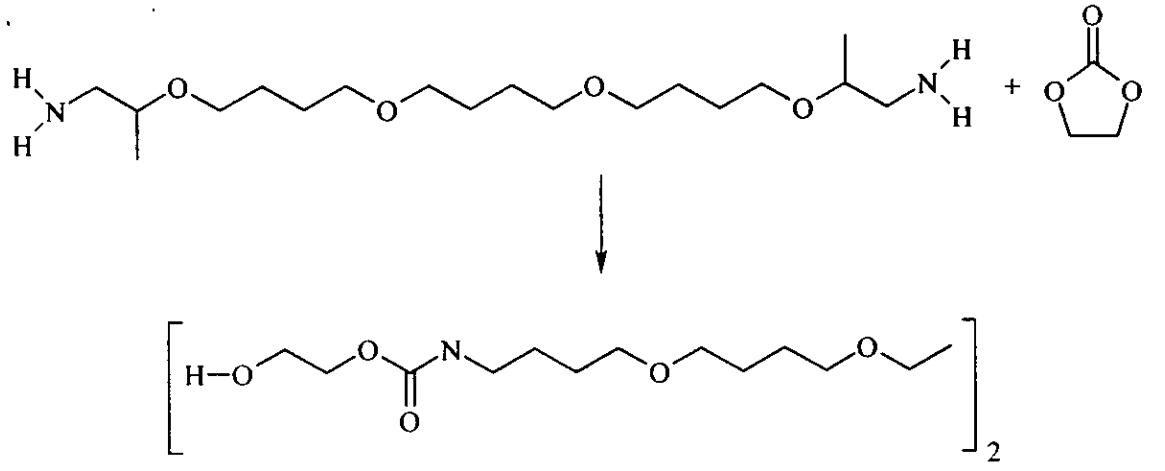

Scheme 6

The product was a reddish viscous liquid. NMR analysis showed that all the ethylene carbonate had reacted, however there was a trace of un-reacted amine remaining. Because of the substantial polyether backbone of the diamine it was not thought necessary to add any 1,4-butanediol to the *bis*-carbamate in order to form a useful urethane ester. Therefore adipic acid was added and Novozyme 435 after heating at 60°C under reduced pressure for 48 hours the final polymer had a molecular weight of 6500 by GPC and an acid number of 5.0mg KOH g^{-1}. The combination of the ester groups and the ether backbone gave a polymer that was not soluble in any of the common solvents. It was thought that this material would make an excellent intermediate in the manufacture of solvent resistance coatings.

The above reaction was extended to the related polyoxypropyleneamine, Jeffamine D230. The amine was added to the ethylene carbonate as before, however the exotherm was substantially less than with any of the previous amines. After all the amine had been added the reaction was maintained at 80°C overnight. TLC and ^{1}H NMR spectroscopy indicated that the reaction had gone to completion with only a trace of residual amine remaining. This *bis*-carbamate was also converted to polyester in the same manner as the

others, the finished polyester was a brown viscous liquid the molecular weight was 6500 daltons by GPC and the acid number was 2mg KOH g^{-1}.

This series of compounds is novel and the reaction principle is capable of being extended to use any diamine and cyclic carbonate to give a novel *bis*-carbamate on which to base an enzymatic urethane ester. A patent has been filed on this reaction and the resulting compounds.

9.2 Synthesis of Oxazolidine esters.

One of the best examples of the utility of enzymatic synthesis in catalysing reactions that cannot be accomplished by any other route is the synthesis of substituted oxazolidine diesters. An oxazolidine ring is formed by the condensation of an alkanolamine with an aldehyde, as in the reaction scheme in Scheme 7.

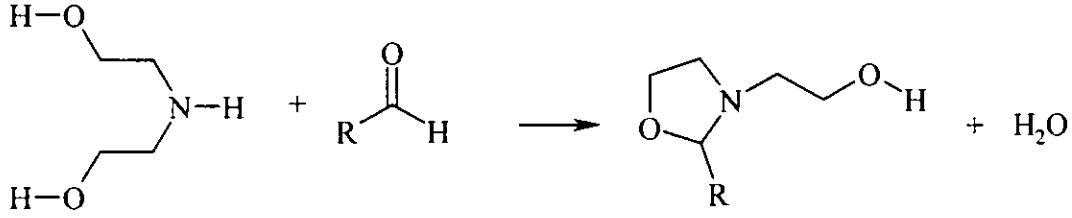

Scheme 7 Synthesis of an oxazolidine.

The oxazolidine ring is extremely water sensitive, the oxazolidine rapidly reverting back to the alkanolamine and aldehyde in the presence of water. This reaction is used to produce high performance moisture curing polyurethane coatings.[176]

Traditionally, moisture curing coatings have been made from urethane pre-polymers containing free isocyanate end groups.[177] When atmospheric moisture is absorbed into

the coating it reacts with the isocyanate to form carbon dioxide and an amine, which then reacts with further isocyanate to form a high molecular weight polymer. There are two problems with this process. Firstly, the carbon dioxide produced forms bubbles in the coating, which has a deleterious effect on physical properties, secondly the rate of reaction of the water and the isocyanate is the rate controlling factor, particularly if the isocyanate is an aliphatic compound. In areas of low atmospheric humidity, this can be a major problem.

The substituted oxazolidine made from diethanolamine and *iso*-butyraldehyde is used in moisture curing coatings in order to give a rapid rate of reaction with the atmospheric moisture.[176] The oxazolidine is reacted with hexamethylene di-isocyanate as shown in Scheme 8.

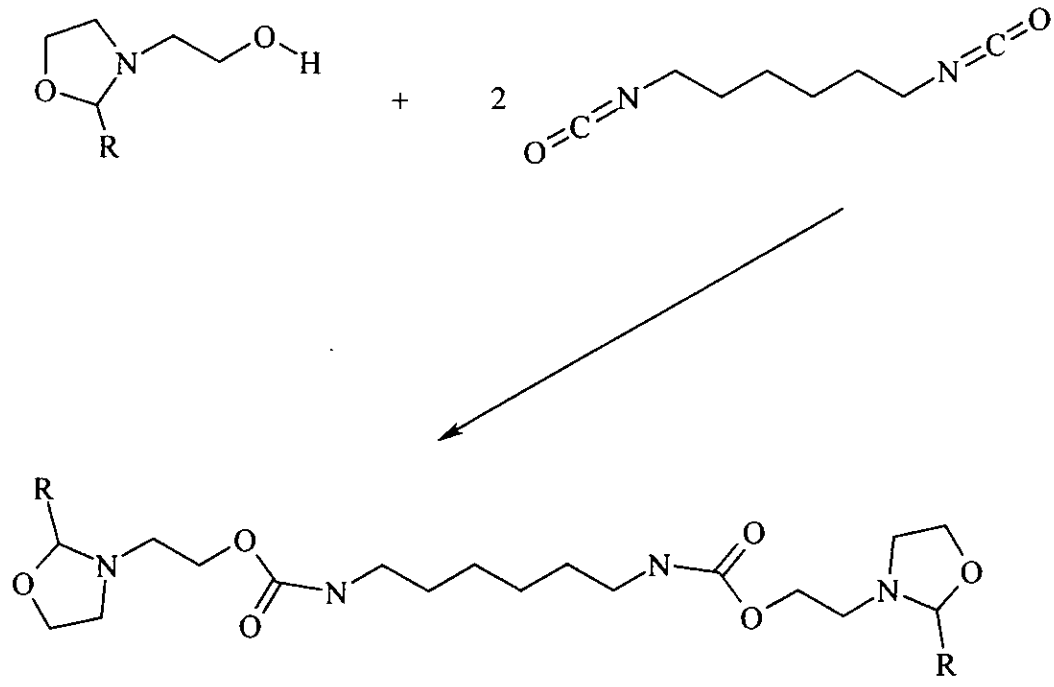

Scheme 8 Reaction of oxazolidine and di-isocyanate.

This diurethane is used as an additive in moisture curing coatings containing an excess of free isocyanate groups in the form of a prepolymer. When a molecule of atmospheric

water is absorbed into the coating it reacts rapidly with the oxazolidine ring which, when opened, forms two reactive sites, the secondary amine and the primary hydroxyl (see Scheme 9) with which the isocyanate reacts rapidly. This mechanism forms an efficient and fast method for the moisture curing of coatings.[176]

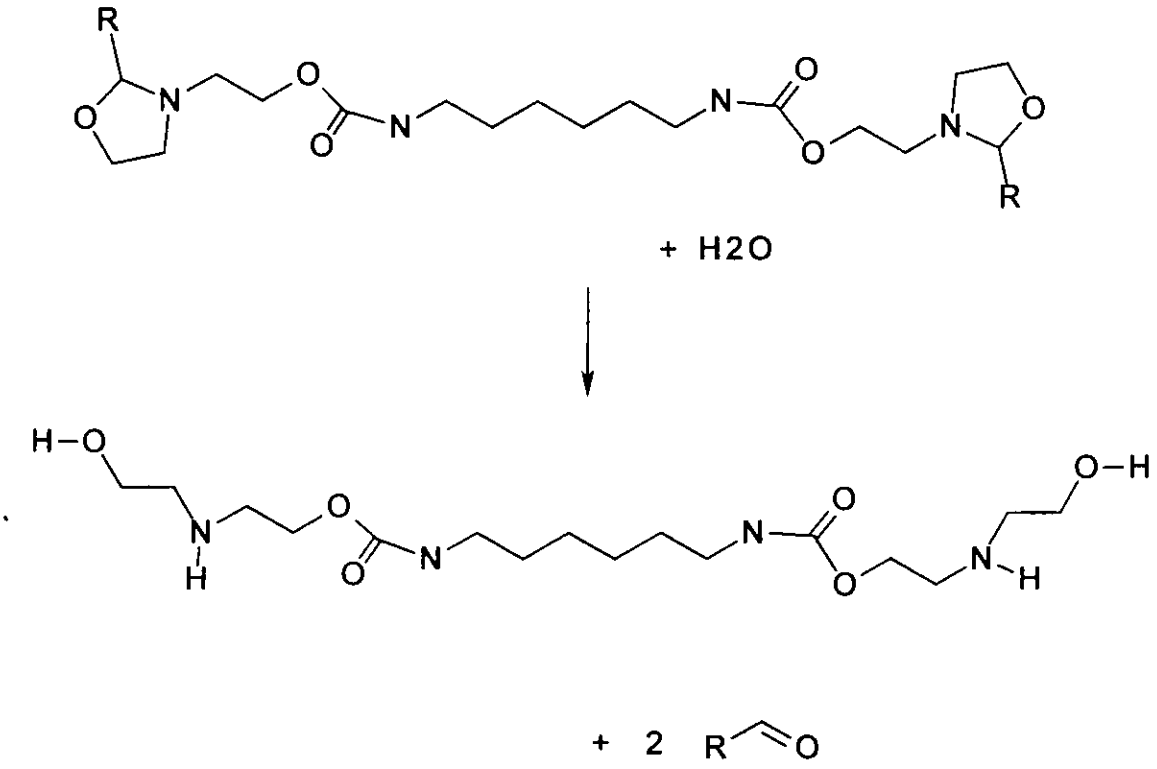

Scheme 9 Mechanism of the oxazolidine curing reaction.

In the past, the only oxazolidine cross-linker to be used is the one based on the diurethane formed with the hydroxyethyl oxazolidine and hexamethylene di-isocyanate, not only is this isocyanate expensive, but it is also extremely toxic.

The diester based on the hydroxyethyl oxazolidine and adipic acid, though similar in structure to the diurethane, could not be synthesised because of the rapid rate of reaction either with the water from the esterification or the alcohol from a transesterification reaction, at the oxazolidine ring.

The advent of the low temperature, enzymatic esterification process offered the opportunity to manipulate the various reaction rates so that the ester might be formed keeping the oxazolidine ring intact.

It was decided to use the dimethyl ester of adipic acid, rather than the adipic acid itself for the esterification. The reaction rate studies (see Section 3.5) had shown clearly that the enzyme preferred the acylation by the diester; therefore, transesterification would be much faster than the esterification reaction. It was considered that the rate of attack on the oxazolidine ring by methanol would be slower than the rate of attack by water. The rate of reaction of the ring opening not being accelerated by the enzyme, whereas the rate of the transesterification would be increased significantly, particularly at the low temperature of the enzymatic esterification.

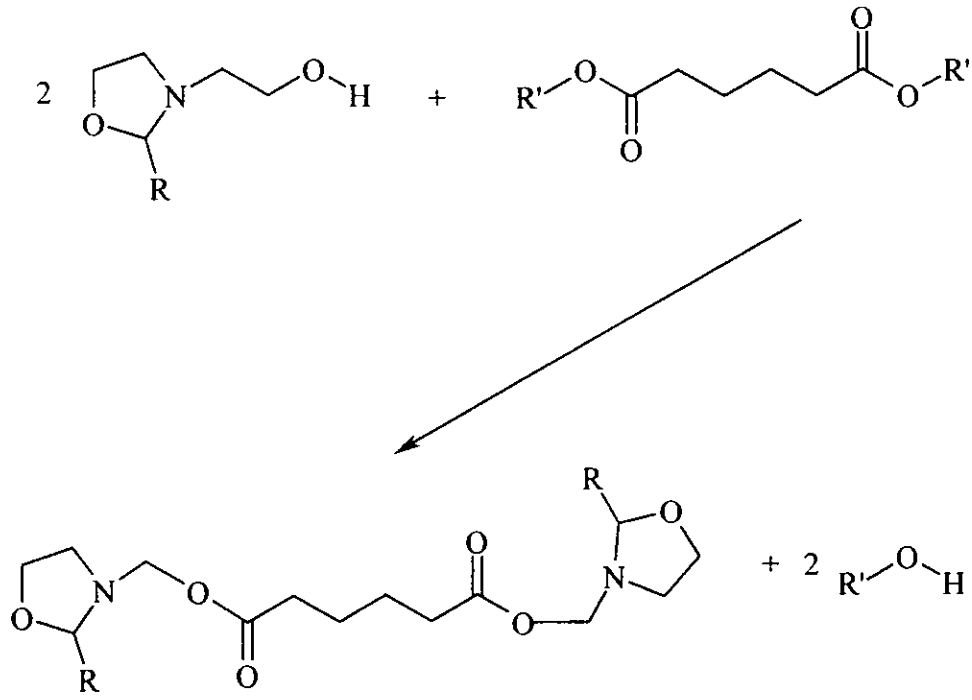

Scheme 10 The enzymatic esterification of hydroxyethyl oxazolidine.

Analysis by ^{1}H NMR spectroscopy and GPC showed that there had been complete esterification of the hydroxyethyl oxazolidine with no discernible opening of the oxazolidine ring. A sample was submitted to Baxenden Chemicals Ltd. who confirmed that the oxazolidine diester did in fact moisture cure urethane coatings.

10 Characterisation of enzymatic polyesters.

The polyesters formed by the polycondensation of diacids and diols are usually characterised by the determination of the number of acid and hydroxyl end groups. Both values are important in the subsequent reactions of the polyester. The hydroxyl value is important because it quantifies the stoichiometry of the polyester for the subsequent reaction with a di-isocyanate to give polyester polyurethane. The acid value is also important because the terminal carboxyl group may react with an isocyanate other than to form a urethane polymer. These other reactions usually cause a decrease in the desired physical properties of the polymer. Acid terminated polyesters may be synthesised, but not for use with di-isocyanates, the secondary polymerisation involves functionality other than isocyanate in the co-monomer.

From knowledge of the end group analysis of a polyester, it is possible to determine the number average molecular weight M_n, but not the weight average molecular weight M_w and no information on the molecular weight distribution may be determined. There are several methods of determining the accurate molecular weights and distribution such as by ultra-centrifugation, vapour pressure osmometry, which determines M_n, and light scattering, which determines M_w. All such methods are time consuming and involve specialised instrumentation. However, no information is determined about the molecular weight distribution. The ratio of M_w/M_n gives the Dispersity Index which is an indication of molecular weight distribution, the theoretical minimum of M_w/M_n is 1, the larger the Dispersity Index the broader the molecular weight distribution.

The most common method used for the determination of molecular weight and molecular weight distribution of polymers is Size Exclusion Chromatography otherwise known as Gel Permeation Chromatography (GPC). The principle used in GPC is that the

chromatographic retention time in the column is related to the hydrodynamic volume of the polymer molecule. The higher the molecular weight the smaller the elution volume, the peaks of the higher molecular weight material appear first.

Gel Permeation chromatography gives an accurate and reproducible characterisation of the molecular weight distribution. The actual molecular weights M_n and M_w are determined by comparison to a known standard, usually polystyrene. Gel Permeation chromatography does not give an absolute molecular weight because factors other than size may affect the retention time in the column. However, as a comparative tool to determine the relative molecular weights and relative molecular weight distribution of similar polymers such as polyesters it is an excellent method.[178]

The determinations of acid value and hydroxyl value are carried out by acid-base titration. The carboxyl groups are titrated and the acid value expressed as mg KOH g^{-1} of polyester. The hydroxyl groups are determined by back titration, after the acylation of all reactive groups using acetic anhydride. Details of both methods are given in Appendices 1 and 2.

While the determination of the acid value is easy the method for the determination of the hydroxyl value is tedious and time consuming. In the past spectroscopic methods have not given the desired accuracy. Early work with NIR to determine hydroxyl content involved the acquisition of spectra at temperatures of over 160°C. At this temperature the reactants continue to react so it can only be done in line, which is not always practical. Also the analysis of finished polyesters at such temperatures is not very easy.

Therefore, we decided to develop NIR methods for the measurement of hydroxyl and carboxyl functionality that would be suitable for use with low temperature production

processes, below the temperature at which the hydroxyls and carboxyls react, and for the characterisation of finished polyesters, under modest laboratory conditions.

Since most spectroscopic methods are secondary techniques the inaccuracies of the chemically determined values are perforce carried over to the spectroscopic calibration curves, the spectroscopic method cannot therefore be more accurate than the chemical method. However, as the existing chemical method is the minimum acceptable standard it was necessary to determine the reasons for any additional inaccuracies in the NIR method and to overcome them.

It was decided therefore, to try to develop methods for the determination of the hydroxyl number and acid number of the polyester, using these parameters to follow the course of the polyester polymerisation and to characterise the finished polyesters.

As the determination of hydroxyl number is the more time consuming by the conventional titrimetric method, it was decided to concentrate on the development of a method for this determination first. Heikka, *et al.*,[179] have published work on the determination of acid value and hydroxyl value using NIR spectroscopy and non-linear partial least squares regression analysis. However, their method was not applicable to our system because of the high temperatures which they used and the accuracy of the results obtained were insufficient for either our purposes or for industrial use.

A range of polyesters of known hydroxyl number was examined, looking specifically at the absorbance of the hydroxyl combination band at 2060-2070 nm and the 1st hydroxyl overtone at 1430 nm. The whole spectrum was screened for regions of maximum separation and the OH combination region around 1925 nm was chosen for further study. Not surprisingly, differences in the backbone of the polyester were found to affect the

absorbance in these regions.[180] In particular a clear difference was seen between polyesters based on aliphatic acids and those based on aromatic acids such as phthalic and isophthalic. A significant proportion of fatty acid in the polyester also affected the absorbance in the regions studied. Most surprisingly, however, it was found that the type of diol used in the polyester had a dramatic effect on the absorbance in the regions that had been thought specific to the hydroxyl group. Even changing from 1,6-hexanediol to 1,4-butanediol or diethylene glycol gave major changes in the NIR spectra. It was thought that these differences may be due to the extremely strong absorbance of the C-H bonds in the NIR and that both bending and stretching absorbances of these bonds have many overtones. Therefore, apparently small differences in methylene content can give large differences in their NIR spectra. While it may have been possible to develop an overall method for the determination of the hydroxyl number of polyesters in general, the accuracy would not have been what was required. In order to get the desired accuracy and reproducibility it was found necessary to prepare specific calibration curves for each type of polyester, *viz.* polyhexane adipate, polybutane adipate, polyDEG adipate and polyhexane phthalate/adipate.

Some hundred or so different examples of these four types of polyester were examined. The acid and hydroxyl numbers had been obtained previously by the classical titrimetric methods (see Appendices 1 and 2 for details).

Correlation of the measured hydroxyl number with the absorbance throughout the spectrum, followed by manipulation of the data using the Mattson Quickquant software to maximise the correlation, made us decide to concentrate on the hydroxyl combination band at 2040 nm. In order to avoid inaccuracies caused by slight changes in the wavelength of the peak, peak absorbance in the range 2028-2050 nm was selected. It was

also found that far greater correlation could be obtained if the net absorbance between the peak and a base-point was used, which after inspection was selected as the absorbance at 2500 nm.

In common with usual NIR practice, the use of internal reference peaks was examined. Several peaks within the spectrum were assessed as reference, however no benefit was obtained, so it was decided that an internal reference was not necessary.

Using the method described in Section 12.3 the hydroxyl number of the polyhexane adipates was determined. The results of which are shown in Table 10.1 and Figure 10.1. A 0.997 correlation between the net absorbance and the hydroxyl number was obtained.

Table 10.1 Net absorbance of polyhexane adipate polyesters at 2040-2000 nm.

Hydroxyl No.*	Absorbance	Hydroxyl No.*	Absorbance
140	0.338	114	0.287
138	0.335	111	0.278
114	0.285	55	0.147
40	0.105	61	0.156
108	0.275	38	0.095
76	0.198	31	0.080
106	0.272	Correlation	0.997

* mg KOH g^{-1}

A range of samples of polyhexane adipate/phthalate polyesters, that is polyesters derived from phthalic anhydride as well as adipic acid were studied. The calibration curve in Figure 10.1 was used, however there was only a poor correlation with the hydroxyl number.

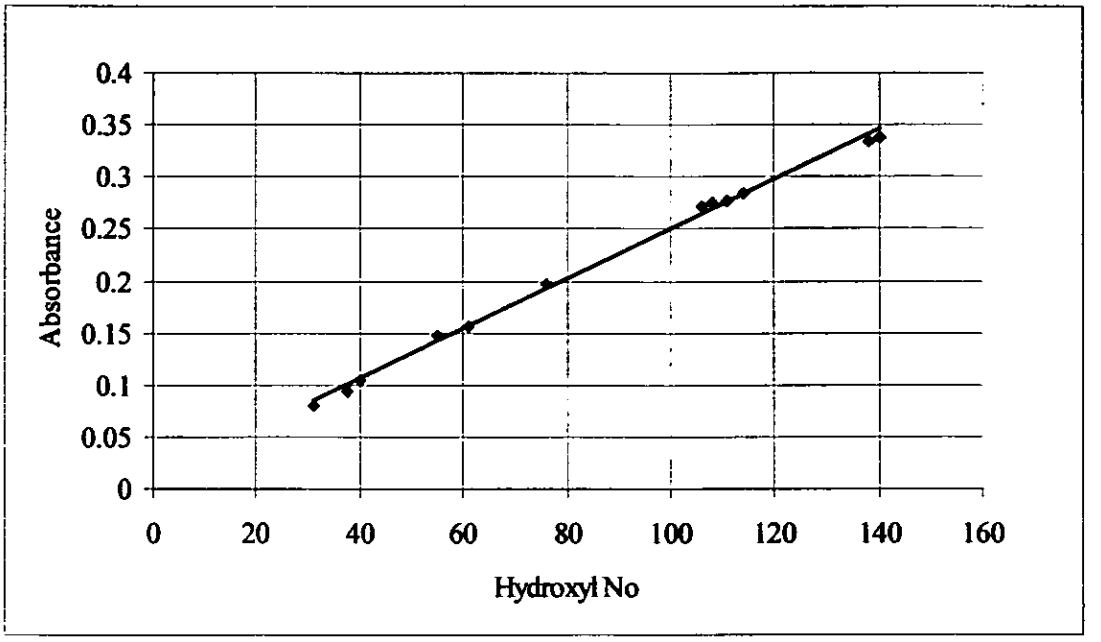

Figure 10.1 Net absorbance of polyhexane adipate polyesters.

It was found necessary to prepare a calibration based only on the mixed adipate/phthalate polyesters. The results of the polyesters containing both adipic acid and phthalic anhydride are shown in Table 10.2 and Figure 10.2, a 0.998 correlation between the absorbance and the hydroxyl number of the polyesters was found.

Table 10.2 Net absorbance of polyhexane adipate/phthalates at 2040-2000 nm.

Hydroxyl No.*	Absorbance	Hydroxyl No.*	Absorbance
72.0	0.1971	94.0	0.2262
73.0	0.1983	108.0	0.2430
75.0	0.2007	111.0	0.2496
80.0	0.2089	114.0	0.2460
94.0	0.2259	114.0	0.2479
94.0	0.2261		
94.0	0.2271	Correlation	0.994

* mg KOH g^{-1}

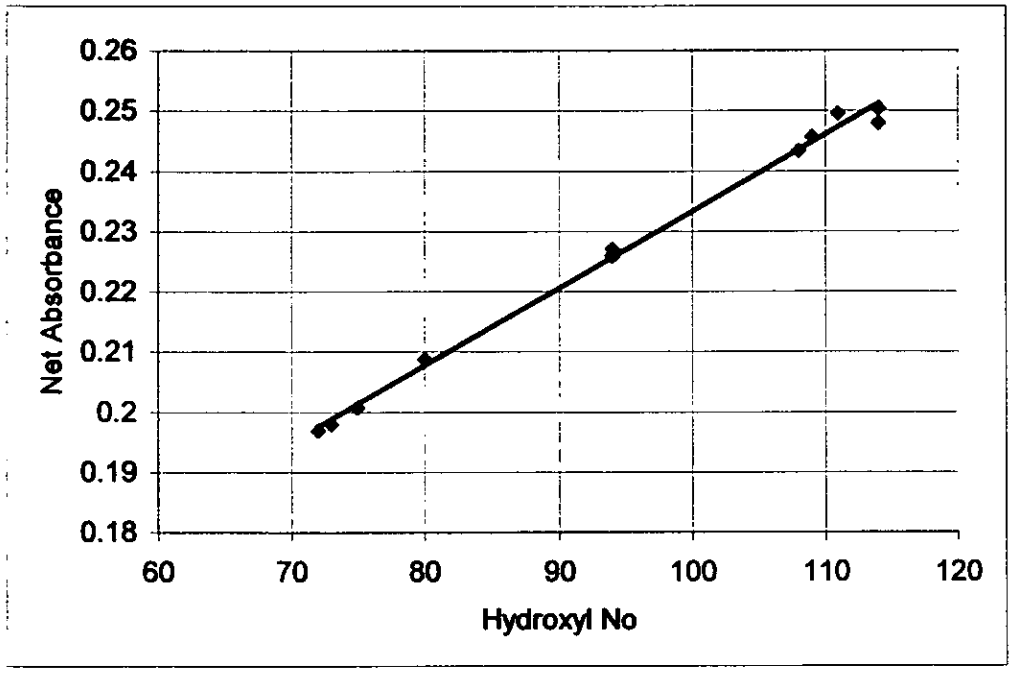

Figure 10.2 Net absorbance of polyhexane adipate/phthalate polyesters.

This method was then used for a range of polyDEG adipates, the results for which are shown in Table 10.3 and Figure 10.3. A range of polybutane adipates was also analysed using this method, the results for which are collected in Table 10.4 and Figure 10.4. The correlation between the hydroxyl number and the net absorbance for these polyesters was 0.998 and 0.997 respectively.

Table 10.3 Net absorbance of polyDEG adipates at 2040-2000 nm.

Hydroxyl No.*	Absorbance	Hydroxyl No.*	Absorbance
62.9	0.245	45.6	0.180
56	0.220	41.9	0.170
78.2	0.300	222.6	0.750
71.4	0.270	75.6	0.280
68.2	0.260	Correlation	0.998

* mg KOH g^{-1}

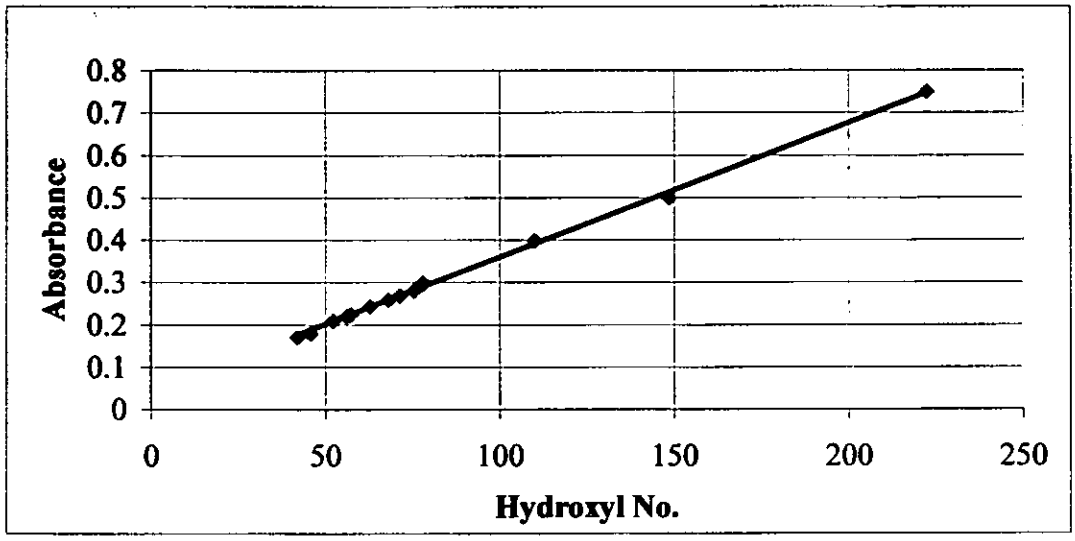

Figure 10.3 Net absorbance of polyDEG adipates.

Table 10.4 Absorbance of polybutane adipates at 2040-2000 nm.

Hydroxyl No.*	Absorbance	Hydroxyl No.*	Absorbance
26.0	0.0814	51.8	0.1486
26.0	0.0794	110.0	0.2830
40.0	0.1161	118.0	0.3054
40.4	0.1211		
49.8	0.1425	Correlation	0.997

* mg $KOH\ g^{-1}$

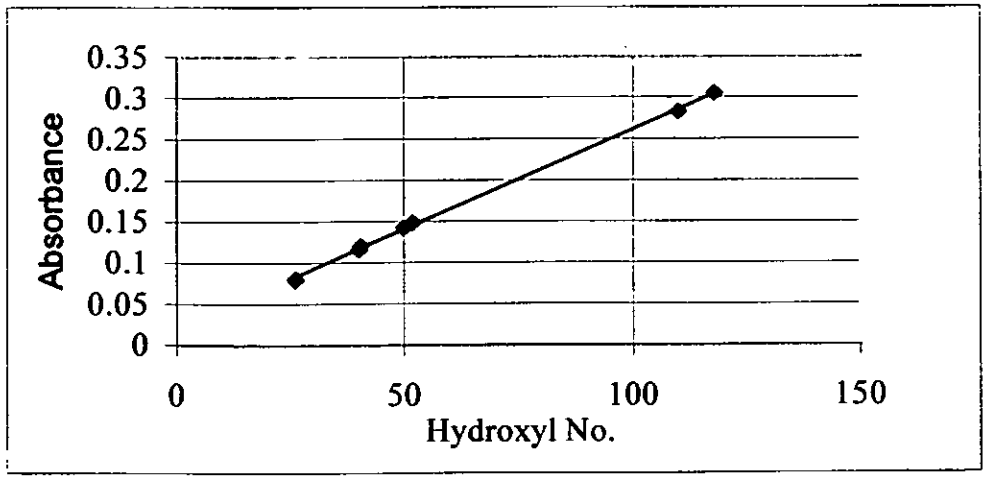

Figure 10.4 Net absorbance of polybutane adipate polyesters.

Up to this point, calibration curves between the NIR absorbance and the hydroxyl number as measured by the method given in Appendix 2 had been prepared. Since the hydroxyl O-H combination band was being studied it seemed logical to look for a correlation between absorbance and the difference in hydroxyl number and acid number, this would eliminate any consideration of the carboxyl O-H bond. To our surprise, we found that the correlation of 0.998 for the absorbance to hydroxyl number, i.e. total O-H, decreased to 0.98 for the correlation between absorbance and hydroxyl O-H alone. This observation led to the conclusion that the carboxyl O-H bond is absorbing in the same region of the spectrum as the hydroxyl O-H bond. This contribution is almost certainly due to the hydrogen bonding between the carboxyl O-H and the carbonyls of the ester and acid groups. In practical terms, however, it does mean that the calibration for the hydroxyl number is influenced to some extent by the acid value. Therefore, polyesters of similar hydroxyl number, but very different acid value, may show differences in their NIR spectra.

We then attempted to develop a similar simple method for the determination of the acid number. The polyesters of adipic acid and diethylene glycol were used for the calibrations because we had a number of samples for which the acid numbers had been determined previously. As with the method for hydroxyl determination, the whole NIR spectrum was scanned for regions of maximum separation and for an absorbance that increased with increasing acid number of the polyester. The one area of the spectrum that seemed to be worthy of further investigation was the carboxylic acid O-H combination band at 1898-1900 nm (~5265 cm^{-1}). After much searching, it was discovered that if the net absorbance of the peak at 1928 nm was measured relative to the baseline between 1895-1980 nm, a correlation of 0.865 was obtained. This was not good enough for industrial quality control purposes, so the method of Brush,[180] was tried which used the

derivatives of the spectrum in the region of 1898 nm. The best correlation was found to be only 0.625, by using the 2nd derivative at 1904 nm. It was then realised that Brush had measured the absorbance at 260°C, whereas our measurements were made at 60°C, which would allow far greater intermolecular hydrogen bonding. In an attempt to overcome the effects of hydrogen bonding it was decided to re-run all the above spectra at 100°C. The samples were preheated in the oven at 100°C for 30 minutes before being transferred to the Peltier cell where they were allowed to stabilise at 100°C for 2 minutes before starting the scan. As may be seen from the spectra (Figure 10.5) there was a dramatic increase in absorbance of the carbonyl overtone at 1904 nm (7000 cm^{-1}), this effect was common to all of the polyesters examined. There appeared to be little difference in any other region of the spectrum, certain peaks had shifted slightly or increased in height, but nothing of any significance. Due to the major change that occurred in the region of the carbonyl overtone, we were optimistic that the change was due to the removal of the carboxyl hydrogen bonding. However, when the method that had been used at 60°C was used at 100°C, no reasonable correlation was found. After examining all the regions of the spectrum, still no correlation between net absorption and acid value was found. Using the spectra taken at 100°C, the method for the determination of hydroxyl number was rechecked, i.e. using the net absorbance at 4900 cm^{-1} to the base-point at 5000 cm^{-1}. It was found that a 0.998 correlation was still obtained, which demonstrates that our method is not particularly sensitive to variation in temperature. This fact could be important when it is used in a chemical plant environment.

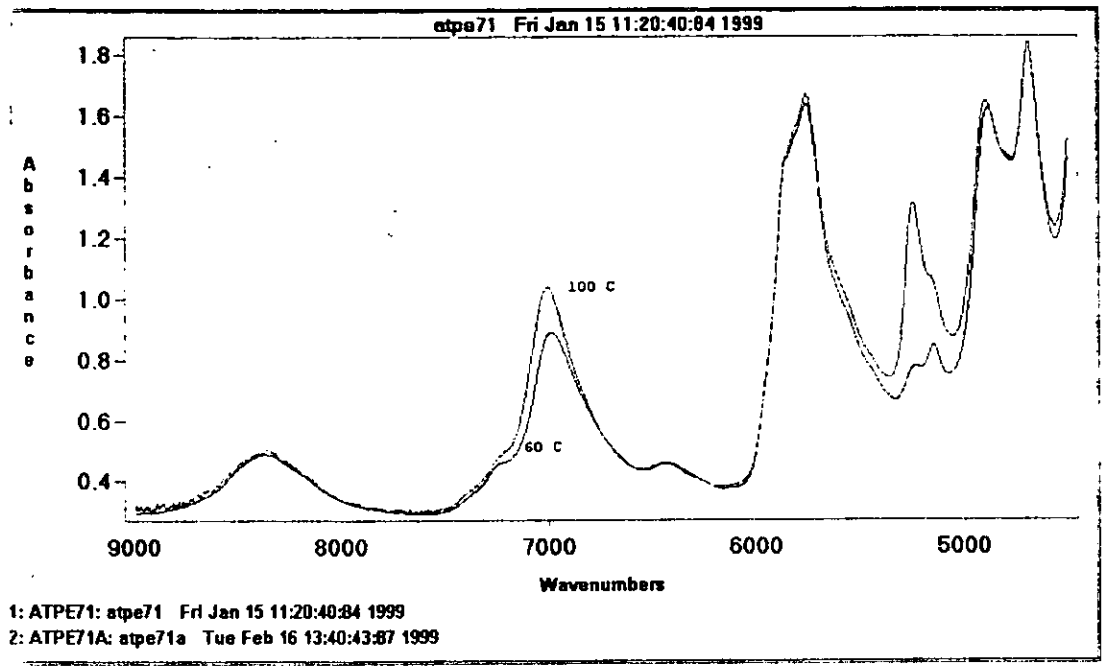

Figure 10.5 Near Infrared spectra of polyester at 60°C and 100°C.

Because of the lack of success in finding a direct relationship between a single peak absorbance and acid value it was decided to look at different regions of the spectra obtained at 60°C using non-linear partial least squares analysis. The software known as PLS Quant by Mattson was used for the analysis. The regions examined initially were those recommended by Mattson for the determination of hydroxyl number in surfactants and polyols. For surfactants with hydroxyl numbers between 85-250, they used the bands between 1980-2120 nm. Resolving to the 8^{th} dimension, they obtained a correlation of 0.999 between hydroxyl number and absorbance. Similarly, for polyols with hydroxyl numbers between 75-300 they obtained a 0.999 correlation, using the bands between 1110-1430 nm and resolving to the 6^{th} dimension. However, none of the samples tested by Mattson were polyesters and none contained carboxyl groups as well as hydroxyls. When these methods were tried, only a poor correlation of approximately 0.60 was obtained between absorbance and hydroxyl number. It was considered that this is almost certainly due to the extensive hydrogen bonding in the polyester systems at 60°C.

The specific regions of interest, 1925±50 nm and 2040-2080 nm were studied further. These are the most relevant overtone and combination bands, no correlation whatsoever was found with the acid value. The whole spectrum was examined, using the 2nd and 3rd overtone regions as likely regions, however none gave any correlation with acid value, despite the computing power of the software. It was found that when the combined OH number and acid value of the polyesters was compared with both the OH and carboxyl overtones and the combination bands between 1850-2080 nm plus the hydroxyl overtone band at 1430-1540 nm, a correlation started to appear. The mathematics involved taking the PLS to the 8th dimension and each measurement was cross-validated up to 23 times. The results obtained are shown in Table 10.5.

Table 10.5 Correlation of acid value and hydroxyl number to absorbance using PLS

Poly-ester	Acid value				Hydroxyl value			
Atpe	Actual*	Method 1	Method 2	Method 3	Actual*	Method 1	Method 2	Method 3
60	23.3	22.9	23.2	22.5	78.8	78.7	78.6	78.8
71	0.3	0.23	0.24	0.23	222.6	222.6	222.6	222.6
74	16.2	16.0	16.0	16.1	78.2	78.4	78.5	78.4
58	19.8	20.6	20.8	19.9	75.6	76.0	77.2	76.0
59	1.96	1.71	1.74	1.96	57.3	56.3	55.5	56.4
64	1.7	1.6	1.8	1.9	52.1	55.6	54.5	55.7

* mg KOH g^{-1}

Method 1 Used bands 1850-2080 nm plus 1430-1560 nm. PLS 8th dimension

Method 2 Used bands 1850-2060 nm plus 1430-1540 nm. PLS 8th dimension

Method 3 Used bands 1850-2080 nm plus 1430-1540 nm. PLS 8th dimension

As may be seen, all three methods give reasonable results for the hydroxyl number with methods 1 and 3 being slightly better than method 2, whereas methods 2 and 3 give slightly better results for acid value. Therefore, method 3 was adopted as the preferred method. In order to explore the effect of the reduced hydrogen bonding at 100°C, the spectra were re-examined using the PLS Quant method 3 technique. The correlation was as good as that at 60°C, but not appreciably better. However, there was no correlation between the spectra of unknowns taken at 60°C and the spectra of standards taken at 100°C.

When the method for the determination of hydroxyl number was developed it had been found that the absorbance differences between the pure adipate polyesters and the mixed adipate/phthalate polyesters detracted from the accuracy of the method, if the calibration was based on both types. However, on re-examination of the data using the non-linear PLS software a good correlation was obtained giving good results for both the acid value and the hydroxyl number as shown in the Table 10.6.

Table 10.6 Acid value and hydroxyl number of polyhexane adipates.

Polyester	Acid value, mg KOH g^{-1}		Hydroxyl number, mg KOH g^{-1}	
	Titration	NIR Determined	Titration	NIR Determined
atpe43	0.1	0.07	114	117
atpe43/1	0.1	0.3	114	117
atpe48	10	9.5	140	137

The method of disrupting the hydroxyl-carboxyl hydrogen bonding by the addition of chloroform reported in Chapter 2 was used on the polyesters to see if it also improved the accuracy of the results. Small amounts of chloroform were added to polyesters to see if

any obvious differences could be seen. No observable difference in the spectra on addition of 0.5-5.0%$^{v}/_{v}$ of $CHCl_3$ to polyhexane adipate polyesters was seen. However, it is only when looking at the correlation between absorbance and substrate concentration, that subtle differences in the sensitivity of the method can be seen. The calibration of the absorbance of the polybutane adipate polyesters against concentration was then repeated after the addition of approximately 1% of chloroform. The correlation improved from 0.997 to 0.999. This increase was expected to be small because these were commercial polyesters and the acid numbers were all below 1%, so there was only a small hydroxyl concentration to be freed from association with the carbonyl groups of the acid ends.

The correlation between acid number and the absorbance at the hydroxyl overtone region was then studied after the addition of $CHCl_3$. An excellent inverse correlation between the acid number and absorbance at 2028-2050 nm was noted. This confirmed the above point that the method is able to detect the additional hydroxyl groups that have been freed from association with carbonyl groups. However, this is not a satisfactory method for the routine measurement of the actual acid number of the polyester, as it depends on the relative amount of hydroxyl in the polyester and requires the measurement of the absorbance both before and after the addition of chloroform.

A similar increase in the correlation between the absorbance at 2028-2050 nm and hydroxyl number, from 0.997 to 0.999, was observed with a series of polyhexane adipate polyesters using the same technique. The net absorbance, at the carbonyl overtone at 1937 nm to a base-point at 1886 nm, gave a poor correlation of 0.80 to the acid number. However, as these were all commercial polyesters with very low acid numbers the correlation was not expected to be very good, as the titrimetric method does not have the accuracy to give a better correlation.

The NIR method was then used to determine the acid value and hydroxyl value of polyhexane adipate polyesters produced by the enzymatic process. The calibration graph shown in Figure 10.1 for the polyhexane adipates was used, however the values obtained for the hydroxyl number and acid value of polyesters prepared by the enzymatic process gave a very poor correlation with the actual values determined titrimetrically. Therefore the PLS method 3 for determining the hydroxyl and acid values of the hexane adipate polyesters was used on the esters prepared by enzymatic synthesis. However, no satisfactory correlation was found using this method. It was considered that the poor correlation was almost certainly due to the fact that the calibration curve had been developed using conventional Lewis acid catalysed polyesters as standards. An alternative calibration, using seven enzymatic esters as standards gave a very satisfactory correlation with unknowns, as shown in Table 10.7.

Table 10.7 Acid and hydroxyl values of enzymatic polyesters.

Polyester	Acid value, mg KOH g^{-1}		Hydroxyl value, mg KOH g^{-1}	
	Actual	Predicted	Actual	Predicted
Polybutane adipate	2.0	2.0	31.0	39.0
"	3.75	2.5	36.0	34.0
Polyhexane adipate	0.89	1.0	21.0	19.0
"	1.54	1.0	14.0	16.0

Near Infrared spectroscopy is extremely sensitive to differences between standards and the samples being analysed. It does not, however, shine any light on what the differences between the samples may be. In the case of the enzymatic polyesters the difference could be due to the unique character of the enzymatic esters, or to the fact that they were of much higher molecular weight and thus much lower hydroxyl number than the standards

used to prepare the calibration curve. The lower hydroxyl numbers being outside of the lower end of the linear calibration for method 3.

Polyesters prepared by the enzymatic process had been examined using Maldi-Tof spectrometry.[17] It was considered that one of the reasons for the different properties of the enzymatic polyesters was the near absence of carboxyl groups on the ends of the higher molecular weight polyesters. It was decided to look at the enzymatic polyesters using ^{13}C NMR spectroscopy and to compare the spectra with similar polyesters prepared by the conventional process in an effort to confirm this hypothesis.

A preliminary examination of the ^{13}C NMR spectra of polyhexane adipate polyesters prepared by the conventional process and enzymatic process showed little difference. Therefore, it was decided to obtain an extended Fourier Transform by using 90,000 scans with a relaxation time of 1.0 second for each polyester over a 2 day period. The ^{13}C spectra obtained are shown in Figures 10.6 and 10.7.

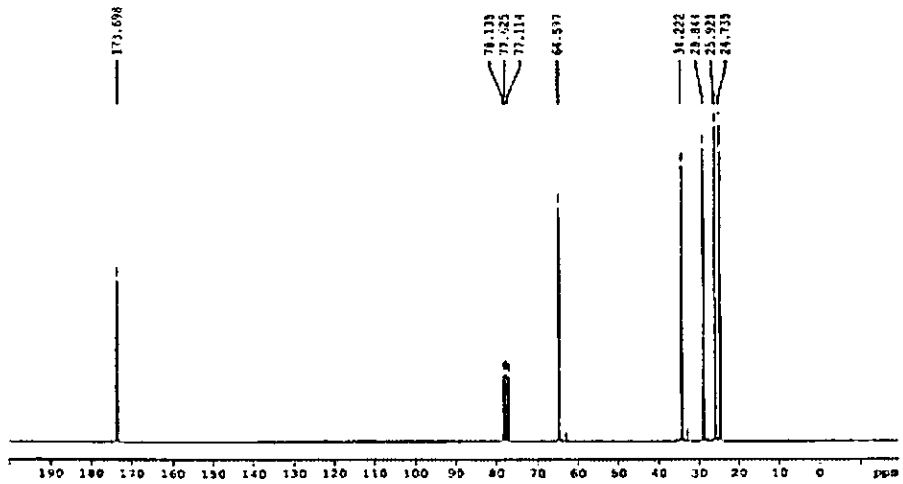

Figure 10.6 ^{13}C NMR spectrum of conventional polyhexane adipate.

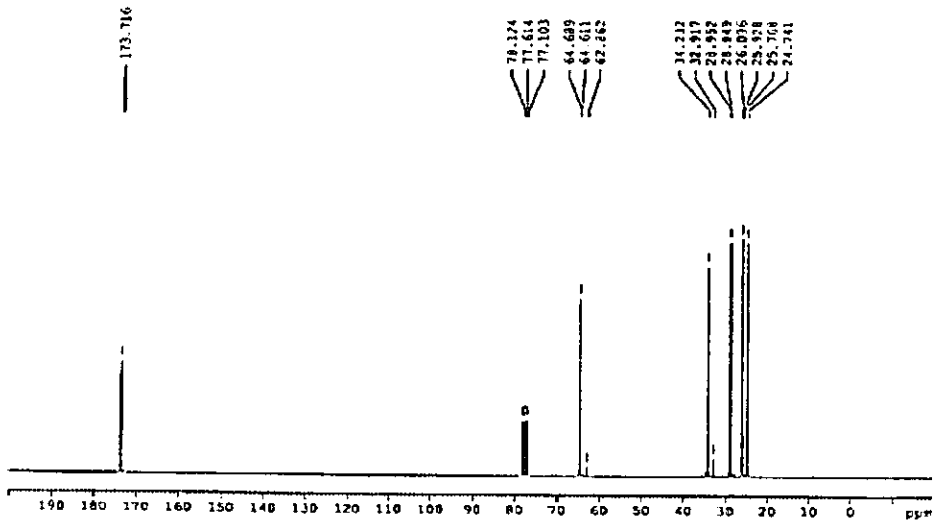

Figure 10.7 ^{13}C NMR spectrum of enzymatic polyhexane adipate

A superficial examination of these spectra shows no difference, however a close examination of the region near the peak at δ 173 ppm reveals a small peak just down field of the main peak in the spectrum of the conventional polyester, which is absent in the spectrum of the enzymatic polyester. This region of the two spectra is expanded in Figures 10.8 and 10.9.

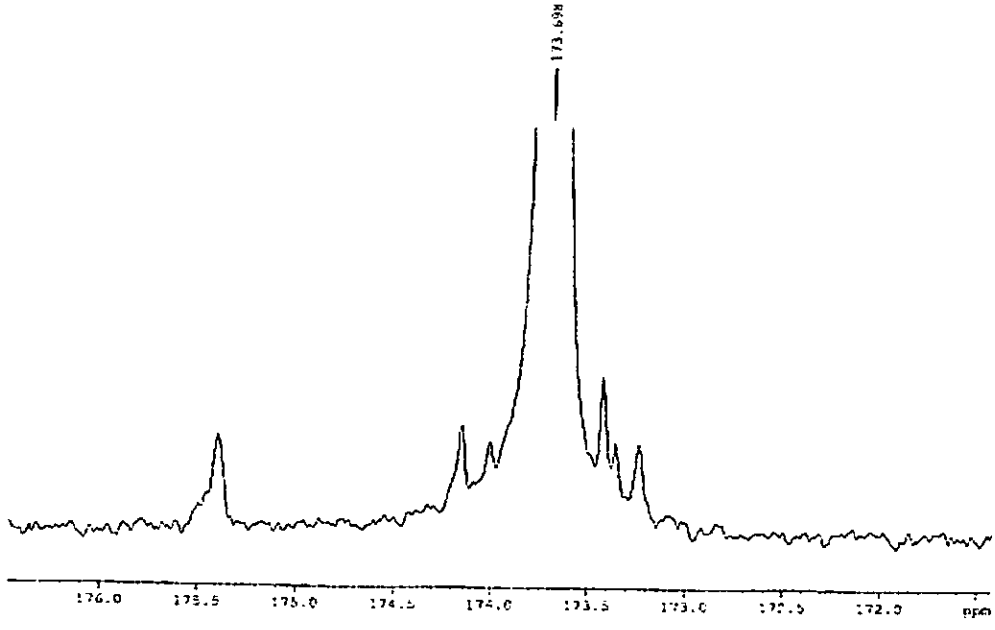

Figure 10.8 Expansion of the ^{13}C NMR spectrum of conventional polyhexane adipate.

The large cropped peak is the main carbonyl shift at δ 173.7 ppm immediately downfield is the much smaller, but nevertheless distinct peak with a shift at δ 175.4 ppm. This peak is due to the shift of the carbonyl carbon in a terminal carboxyl group. When the spectrum of the enzymatic polyester was examined in detail the small peak at δ 175.4 ppm could not be seen, therefore the accumulation was extended to 178,000 scans. However, even after this length of time the shift due to the carbonyl group of the terminal carboxyl could not be seen (see Figure 10.9).

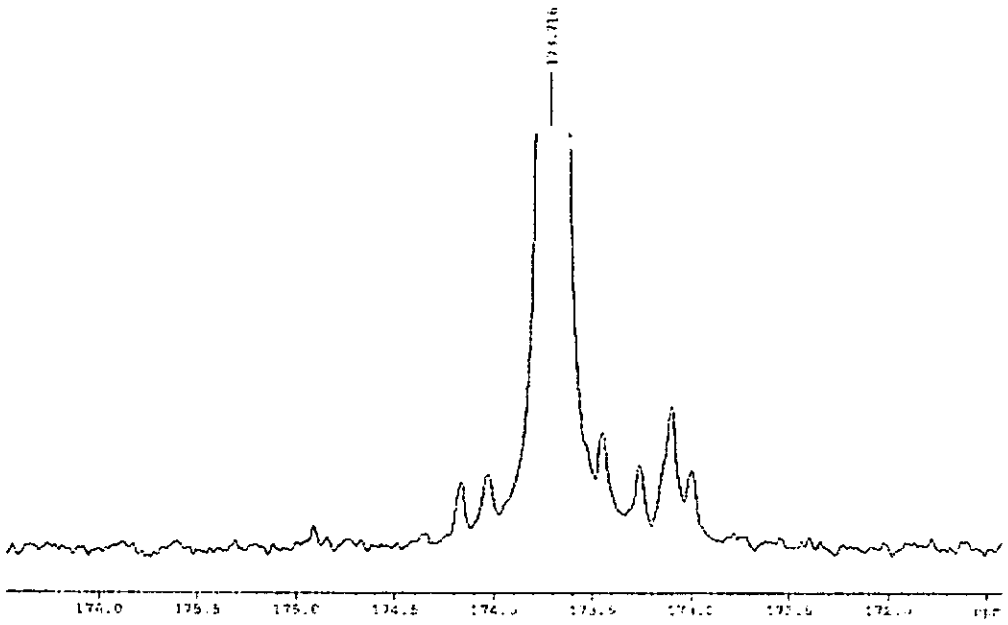

Figure 10.9 Expansion of the ^{13}C NMR spectrum of enzymatic polyhexane adipate.

Examination of the expanded spectrum shows the absence of the shift due to the carbonyl in a terminal carboxyl group. Therefore the conclusion is that the essential difference between the polyesters made by the conventional and enzymatic processes is the virtual absence of terminal acid groups in the enzymatic esters. It is proposed that the effect is due to the lack of transesterification in the high molecular weight enzymatic polyesters.

The differences between enzymatic and conventional polyesters of the same chemical composition have been exploited commercially. However, the reasons for the difference

in physical properties between enzymatic and conventional polyesters has been studied, but not explained.[181] In an effort to understand the differences and to relate these to composition, the crystallisation of two polyhexane adipate and two polyhexane dodecandioate polyesters were studied using a hot stage microscope. The results are shown in Table 10.8.

Table 10.8 Hot stage microscopy of enzymatic and conventional polyesters.

Polyester	OH Value mg KOH g^{-1}	Cooling rate °C	Melting point °C	Crystallisation Temperature °C
PHA Enz.	12.0	0.1	63.0	54.0
PHA Conv.	12.0	0.1	62.0	55.0
PHA Enz.	12.0	0.5	59.0	48.0
PHA Conv.	12.0	0.5	59.0	48.0
PHA Enz.	30.0	2.0	56.5	46.7
PHA Conv.	30.0	2.0	57.7	47.0
PHDD Enz.	30.0	2.0	74.5	64.5
PHDD Conv.	30.0	2.0	72.7	63.7

As may be seen from these results, the actual differences in melting point and crystallisation temperature between the enzymatic and conventional polyesters are negligible. However, the video recordings of the crystallisation process show significant differences in the crystallisation process for each polyester. A summary of the results is given in Table 10.9.

Table 10.9 Crystallisation of enzymatic and conventional polyhexane adipate (PHA) and polyhexane dodecandioate (PHDD) polyesters.

Polyester	OH value*	Cooling rate	Observation
PHA Enz	12.0	0.1	Small sausage shaped crystals form, quickly and regularly.
PHA Conv	12.0	0.1	Large irregular sausage shapes form over a longer period.
PHA Enz	12.0	0.5	Very even small crystals formed evenly.
PHA Conv	12.0	0.5	Much slower forming bead like crystals.
PHA Enz	30.0	2.0	Small sausage shape crystals form very evenly over the stage with time.
PHA Conv	30.0	2.0	Large sausage shapes form erratically and merge to form star like clusters.
PHDD Enz	30.0	2.0	Very even distribution and growth of masses of small sphaerulites.
PHDD Conv	30.0	2.0	Long needle like crystals form and grow quickly to form star like clusters.

* mg $KOH\ g^{-1}$

In an effort to identify the cause of the observed differences in crystallisation behaviour, the concentration of nucleating sites was estimated over a 10 x 10cm square marked on the TV screen. It is difficult to be precise, but there is a clear indication that there are more nucleating sites in the enzymatic polyesters. This would explain the consistent observation that the crystallisation of the enzymatic polyesters is more regular and starts with many more small crystals than the conventional polyester.

Why the enzymatic ester should have more nucleating sites is difficult to explain. The narrower molecular weight distribution of the enzymatic polyesters may be the explanation. The ^{13}C NMR spectrum has shown that the polyester has virtually no acid

terminated chains, yet the material has an acid value. This leads to the conclusion that the residual acid is present as monomer or low molecular weight oligomers. These materials may be insoluble in the high molecular weight polyester and thus act as nucleating agents. A more mundane explanation may be that conventional polyesters are made using dibutyl tin dilaurate as catalyst and this is soluble in the polyester. However the *Candida antarctica* lipase B protein is not soluble in the polyester and this may be acting as a nucleating agent.

11 Conclusions

Both Near Infrared spectroscopy and Thermogravimetric analysis have been shown to have utility in following the lipase catalysed synthesis of polyesters. From the results of the determination of the reaction kinetics with different acyl substrates it appears that there is a direct relationship between the C logP of the acyl substrate and the reaction rate, however this appears to be more an effect of chain length than polarity of the substrate. The optimum chain length of the dicarboxylic acid used in the synthesis of the polyesters includes both C5 and C6, i.e. the glutaric and adipic acids. The longer and shorter chain fatty acids being much slower to react. As stated by other authors,[58] the acyl binding site is not that selective as to the form of the acylating substrate, however, it has been found that substitution in the 2-position appears to interfere with the hydrogen bonding that stabilises the tetrahedral intermediate: the 1-carboxyl group of 2-oxoadipic acid being quite un-reactive in the acylation of the enzyme.

The polarity, as measured by C logP, of the reaction medium, i.e. the diol in all solvent free syntheses, has a significant effect on the reaction rate. The more polar diols such as polytetramethylene ether glycol and polyethyleneglycol giving significant increases in reaction rate compared to the more hydrophobic diols. It is hypothesised that this is due to the more effective desolvation of the water product of the acylation step and the more rapid mass transport of the water from the active site by the more hydrophilic medium.

It has been shown both by kinetic and calorimetric techniques that, in accordance with theory, the carbonyl of an ester is more susceptible to the nucleophilic attack of the serine of the catalytic triad. This is the reason why the polyester is susceptible to transesterification with both monomeric diol and with itself. It has been shown by studies using both Gel Permeation Chromatography and ^{2}H Nuclear Magnetic Resonance

spectroscopy that the only media in which the developing polyester is not transesterified are those in which it is not very soluble, in particular the diols used in the syntheses. The observation that it is only the ester groups near to the ends of the polyester chain that are susceptible to transesterification when dispersed in the diol medium, leads to the conclusion that the visceral ester carbonyls are not available to the enzyme. This is probably due to the polyester molecule having a coiled conformation in the diol whereas in solution it is not coiled and any ester group is available for transesterification.

The secondary structure of *Candida antarctica* lipase B in aqueous buffer at pH 5.0-7.0 is very close to the natural structure determined by X-ray crystallography. However, at the extremes of pH 4.0 and 9.2 there are significant differences in the α-helix content. The observed reduction in activity at the extremes of pH is undoubtedly due to the inhibition of the ionisation of the key residues of the catalytic triad; histidine, with a pK_a of 6.0 and aspartic acid with a pK_a of 3.5. The extremes of pH will also affect the formation of the hydrogen bonds stabilising the tetrahedral intermediates. The loss of activity therefore would be expected to disappear once the enzyme returned to its optimum pH of 7.0. However, some loss of activity is permanent, this can be seen when one recycles the bound enzyme; it is never as active after the initial reaction with adipic acid. This permanent loss of activity is almost certainly due to the loss of helix seen at the extremes of pH. The short helix α5 forms part of the oxyanion hole, if any part of this unfolds, or changes in any way, the Glu 106 and Thr 40 residues will not be in the correct position to form the hydrogen bonds with the tetrahedral intermediate. The Ser 105 of the active site has been shown by the induced circular dichroism effects to be very close to the helix, α4. If the serine is close enough to the helix to give induced circular dichroism on binding, then it is highly likely that its position or orientation will be disturbed if that helix unfolds.

In solvents, there are some very interesting effects. In hexane there appears to be little difference in the secondary structure of either α-chymotrypsin or *Candida antarctica* lipase B to that obtained in aqueous buffer. This confirms the work of Yennawar who also found that α-chymotrypsin did not change structure when dissolved in hexane.[167] The low result for α-helix in toluene is an enigma and is most likely to be due to the problems of obtaining a CD spectrum in such a strong absorber of UV light. All the experiments were very noisy because of the very low levels of light passing through the sample, however, when the spectra from the first ten scans were averaged and compared to the average of the last ten scans, no significant difference was seen. Therefore, it is highly unlikely that the sample has deteriorated over time due either to radiation or temperature effects. The most likely explanation being that under these conditions, the usual UV absorbance of the α-helix is shifted towards the far ultra violet, thus giving an artificially low result for the amount of helix in the protein.

The low α-helix results in 1,4-butanediol are more surprising. Diols such as pentanediol are used in protein folding experiments, where they are added to the aqueous medium to enhance the formation of the correct protein structure. It seems strange that when used as the total medium they cause the unfolding of α-helix. When one examines the secondary structure of *Candida antarctica* lipase B it may be seen that there are several large helices away from the active site. Longer helices tend to be meta-stable and therefore are more susceptible to unfolding. If the remote helices partly unfold without disturbing the secondary structure essential to the activity of the enzyme then there would be no observable difference in the behaviour of the enzyme in the differing media.

Molecular modelling has shown that the active site of *Candida Antarctica* lipase B is not that specific to the shape of the substrate. Large substrates such as macrolactones are

easily accommodated into the active site. Modelling has confirmed the theory that the higher molecular weight polyesters remain in association with the protein molecule for a substantial time outside the active site; there being a significant number of hydrogen bonding possibilities between the ester carbonyl groups and polar residues on the surface of the enzyme. This may well explain the observation made in the ^{2}H NMR studies of the transesterification reaction that it is the terminal and near terminal ester bonds that are most likely to be transesterified.

A difference between enzymatic polyesters and the homologous esters synthesised using conventional catalysis has been confirmed by both Near Infrared spectroscopy and hot stage microscopy. Examination of the polyesters using ^{13}C NMR spectroscopy with a large number of scans to give good signal to noise ratios, has proven that the enzymatic polyesters lack any significant carboxyl termination compared to those synthesised using conventional catalysis. This is probably due to the fact that we will always have an acyl enzyme present which will react with an alcohol or water, with very little water present the alcohol will be the predominant nucleophile. The alcohol will either be residual diol or the hydroxyl end of a polyester, whichever, the polyester chain will always be hydroxyl terminated.

12 Experimental

All reagents were used as supplied without further purification. The proteases, subtilisin Carlsberg, chymotrypsin, papain and protease N were purchased from Aldrich. *Candida antarctica* lipase B was a gift from Novo A/S. Chirazyme L-2 lyo was a gift from Roche Diagnostics GmbH. Novozyme 435 (ex Novo A/S) was supplied by Baxenden Chemicals Ltd.

The 6-carboxy-11-hydroxy-7-oxaundecanoic acid (AB) and the di-(4'-hydroxybutyl) 1,6-hexanedioate (BAB) were synthesised by Paul Harffey at the University of Liverpool.

All NMR spectra were obtained on a Bruker DPX250 spectrometer and coupling constants are in Hz. The FTIR spectra were recorded using the Mattson Infinity 1 FTIR spectrometer. Gel permeation chromatography was done using a Waters HPLC with a 510 pump and a Waters 410 refractive index detector together with a Waters 717 autosampler. The column used was a Polymer Labs, 1000A polystyrene copolymer packing. Melting points were obtained on a Gallenkamp melting point apparatus and are uncorrected.

11.1 Thermogravimetric analysis (TGA).

TGA measurements were made on the Shimadzu TA 50, which has a sensitivity of ±1μg and is capable of controlling the reaction pan at ±1°C in the temperature range relevant to the enzyme studies. The water of reaction is removed by a constant flow of 50ml min^{-1} of dry nitrogen over the sample. The surface area to volume ration was kept constant by ensuring that the sample in the pan was between 20-25μl.

It was found that the raw materials contained varying amounts of water; therefore, they were dried and stored under anhydrous conditions. The adipic acid was stored in a desiccator over phosphorus pentoxide; the diols 1,4-butanediol and 1,6-hexanediol were heated to 100°C for 24 hours and then stored in a sealed container over molecular sieves at 45°C. It was found subsequently that certain materials such as acid solutions in 1,4-butanediol, AB and BAB were quite hygroscopic; therefore, a further drying cycle was carried out in the instrument under a flow of dry nitrogen. A solution of the acid in diol was prepared at an accurately known concentration and approximately 25µl was placed in the sample pan and weighed accurately.

After the sample had been weighed into the TGA pan the instrument was closed and the sample heated to 110°C for 15min under a flow of 50ml min^{-1} dry nitrogen. The sample was then cooled under nitrogen and when the temperature was below 40°C, the enzyme was added. In all cases except the variable temperature studies, the reactions were carried out at 60°C. The standard heating rate for all experiments was 20°C min^{-1} to 50°C, 7°C min^{-1} to 58°C and finally 1°C min^{-1} to 60°C

This procedure was followed for all experiments except for the studies on levulinic and acetylvaleric acids as these were found to be too volatile and too much substrate was lost. These acids were therefore dried over phosphorous pentoxide only.

In all experiments the points shown are the results of single observations, that is n=1.

12.2 Enzyme preparation.

The enzyme needs to be at constant water content in order to maintain a steady state of hydration of the enzyme throughout all the experiments, with a minimum of excess water. In order to condition the enzyme it was stored over a saturated solution of lithium

chloride in a desiccator for 48 hours. A saturated solution of lithium chloride has a thermodynamic water activity w_a of 0.113, which gives a relative humidity in the head space of 11.3 %. Unlike other lipases, *Candida antarctica* lipase B is not supposed to be that sensitive to variations in the water content of the substrates, however for the TGA experiments we required a constant water content. After storage over the saturated solution of lithium chloride, the enzyme was kept in a sealed container at 4°C.

12.3 Near Infra Red Analysis.

Spectra were recorded on the Mattson Infinity 1 dual NIR/FTIR instrument. The instrument was fitted with a Peltier cell to heat the sample rapidly and to maintain the 6mm cuvette at a temperature of ±0.5°C.

Most polyesters of the type studied were liquid at room temperature or melted between 40°-55°C; therefore, we chose to carry out all the measurements at 60°C. The NIR spectrum of any material is extremely temperature dependent; therefore, the temperatures of the samples in the cuvettes were maintained at 60°±0.5°C. As many of the samples were very viscous at 60°C, it was quite difficult to get the samples into the cuvette without incorporating air into the specimen. The best method for liquid polymers was to heat the polymer and cuvette to 100°C, fill the cuvette and maintain at this temperature for 15min to allow the sample to degas. Solid polymers were put into the cuvette as solids and then stored at 100°C for 15 minutes to allow the air to come out of the sample. In both cases, the cuvettes were cooled to approximately 60°C before putting into the Peltier cell and then left for 5min to stabilise at 60°C before taking the spectrum.

12.4 Circular dichroism spectroscopy

All conventional circular dichroism spectra were obtained on the Jasco J715 spectropolarimeter at Warwick University using a protein concentration of 3mg ml^{-1}. In the case of the Chirazyme, where the exact protein concentration was not known, an estimate was made using the UV absorbance at 280nm against a pre-prepared calibration graph of protein content against UV absorbance at 280nm.

12.5 Reactions for the synthesis of novel polyesters.

12.5.1 Synthesis of di(hydroxyethyl)hexamethylene *bis*-carbamate.

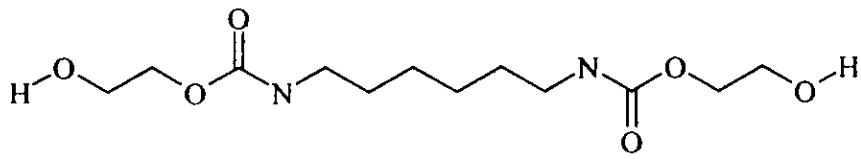

Ethylene carbonate (0.32moles, 28.23g) was added to a flask and heated to 50°C. Hexamethylene diamine (0.069moles, 8.0g) was added with stirring. An exotherm to 85°C followed and after 40 minutes the mixture solidified. Toluene (25g) was added as an adjuvant and the temperature increased to 60°C. The remainder of the hexamethylene diamine (0.09 moles, 10.42g) was added, producing an exotherm to 85°C. The mixture again solidified and hot toluene (15g) was added to triturate. The crystalline product was filtered off on cooling. The product was recrystallised twice from ethanol and dried to give the *bis*-carbamate as white crystals. (28g, 60%), m.p. 94°C. δ_{1H} ($CDCl_3$, 250MHz), ppm 1.19 (4H, bm, -(NH-CH_2-CH_2-$C\underline{H_2}$)$_2$), 1.60 (4H, bm, -(NH-CH_2-$C\underline{H_2}$-CH_2)$_2$), 3.26 (4H, bm, -(NH-$C\underline{H_2}$-CH_2-CH_2)$_2$), 3.74 (4H, bm, -O-CH_2-$C\underline{H_2}$-OH), 4.18 (4H, bm, -O-

$C\underline{H}_2$-CH_2-OH), 5.24 (2H, bm, -(N$\underline{H}$-CH_2-CH_2-CH_2)$_2$). $\delta^{13}C$ ($CDCl_3$, 63MHz), ppm 26.10 (t, NH-CH_2-CH_2-$\underline{C}H_2$)$_2$), 29.12 (t, -(NH-CH_2-$\underline{C}H_2$-CH_2)$_2$), 40.70 (t, -(NH-$\underline{C}H_2$-CH_2-CH_2)$_2$), 61.76 (t, -O-CH_2-$\underline{C}H_2$-OH), 66.64 (t, -O-$\underline{C}H_2$-CH_2-OH), 157.30 (s, -O-$\underline{C}$O-N-).

12.52 Synthesis of a polyester containing di(hydroxyethyl)hexamethylene *bis*-carbamate.

The *bis*-carbamate synthesised in the above reaction was used to make a polyester containing urethane groups.

Dihydroxyethyl hexamethylene *bis*-carbamate (0.0248 moles, 7.25g) and 1,4-butanediol (0.252 moles, 22.72g) were placed in a flask and heated to 90°C under an atmosphere of nitrogen. Adipic acid (0.055moles, 8g) was added and stirred until dissolved. The reactants were cooled to 60°C and Novozyme 435 (0.7g) was added. The pressure was reduced to 400mmHg after 2 hours further adipic acid (0.17 moles, 25g) were added and left for 16 hours. The remaining adipic acid (0.049 moles, 7.17g) was added and the pressure was reduced to 100mmHg and left for 24 hours. A further amount of Novozyme 435 (0.5g) was added. The reaction temperature was raised to 70°C and the pressure reduced to 50mmHg for a further 24 hours. The reaction was stopped and the polyester product sampled. The molecular weight determined by GPC, M_w was 9350, M_n 5345 and the dispersity 1.75.

12.5.3 Synthesis of di(hydroxyethyl)ethane *bis*-carbamate.

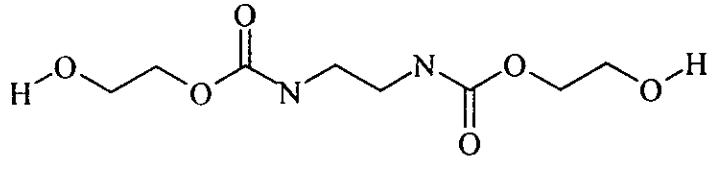

Ethylene carbonate (1.216moles, 107g) was added to a flask and heated to 50°C. Ethylene diamine (0.604moles, 36.26g) was added via a dropping funnel such that the exotherm maintained the temperature at approximately 60°C. After the initial exotherm was observed toluene (40g) was added to reduce the viscosity. When all the ethylene diamine had been added the reaction was maintained at 65°C for 4 hours. The white crystalline *bis*-carbamate product was recrystallised from ethanol, washed and dried (86.5g, 61%), m.p. 93°C.

$\delta_{^1H}$ ($CDCl_3$, 250MHz), ppm 3.22 (4H, q if the molecule is symmetrical then this should be a d not q!!, ^3J 6.5Hz, (-NH-C$\underline{H_2}$-)$_2$), 3.82 (4H, bm, (-O-CH_2-C$\underline{H_2}$-OH)$_2$), 4.17 (4H, t, ^3J 8.75Hz, (-O-C$\underline{H_2}$-CH_2-OH)$_2$), 5.28 (2H, bm, (-O-CH_2-CH_2-O$\underline{H}$)$_2$), 7.35 (2H, bm, (-CO-N$\underline{H}$)$_2$). $\delta_{^{13}C}$ ($CDCl_3$, 63MHz), ppm 40.70 (t, $\underline{CH_2}$-NCO), 61.66 (t, -O-CH_2-$\underline{C}H_2$-OH), 66.68 (t, -O-$\underline{C}H_2$-CH_2-OH), 157.21 (s, -C-N-$\underline{C}$O-).

12.5.4 Synthesis of a polyester containing di(hydroxyethyl)ethane *bis*-carbamate.

Di(hydroxyethyl)ethane *bis*-carbamate (0.064 moles, 15.0g) was dissolved in 1,4-butanediol (0.25 moles, 22.5g) at 70°C and adipic acid (0.034 moles, 5g) was added and stirred until dissolved. Further adipic acid (0.034 moles, 5g) was added followed by Novozyme 435 (0.78g). The reaction was held for 22 hours at 60°C and a pressure of 200mmHg, further portions of adipic acid (0.068 moles, 10g) and (0.11 moles, 16.5g) being added after 2 and 4 hours respectively. A further portion of Novozyme 435 (0.71g) was added, the pressure reduced to 50mmHg for 24 hours and then to 10mmHg for the final 8 hours. The product was an extremely water soluble polyester of molecular weight M_w 4500 and a dispersity of 2.4.

12.5.5 Synthesis of di(hydroxypropyl)isophorone *bis*-carbamate.

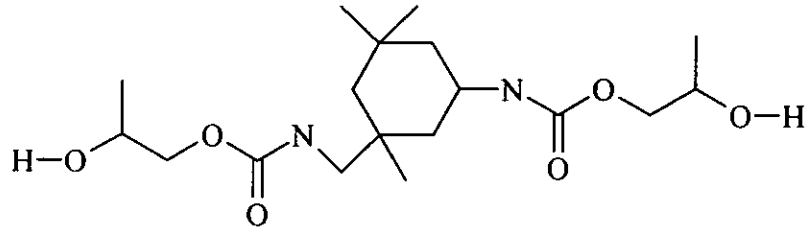

Propylene carbonate (0.5 moles, 51g) was heated to 50°C and isophorone diamine (0.059 moles, 10.0g) added under nitrogen, no exotherm being observed. The remainder of the isophorone diamine (0.191 moles, 32.5g) was added gradually. The reactants were heated to 80°C, when a slight exotherm was observed. The reaction was left overnight at 80°C. Analysis by NMR spectroscopy and GPC indicated that the reaction had gone to completion. The *bis*-carbamate was a straw coloured liquid (93.5g, 100%). The ^{1}H NMR spectrum of isophorone diamine is quite complex because of the 4 chiral centres, 4 ABX systems and 3 AB systems in the molecule. However, the hydrogen of the primary amine in the starting material gives a very clear peak at a shift of δ 2.09 ppm and an AB system at δ 2.25 and 2.50 ppm and these peaks had completely disappeared from the ^{1}H NMR spectrum of the *bis*-carbamate product.

12.5.6 Synthesis of a polyester containing di(hydroxypropyl)isophorone *bis*-carbamate.

Dihydroxypropylisophorone *bis*-carbamate (0.061moles, 22.85g) was dissolved in 1,4-butanediol (0.454 moles, 40g) at a temperature of 70°C. Adipic acid (0.21 moles, 30.15g) was added and after dissolution the reactants were cooled to 60°C and Novozyme 435 (2.5g) added. The mixture was heated at 60°C at 400mmHg for 4 hours, when the remaining adipic acid (0.296 moles, 43.66g) was added. The temperature was maintained

at 60°C and the pressure at 200mmHg for 24 hours. The pressure was then reduced to 10mmHg for a further 24 hours. The product (117g, 85.5%), a pale straw coloured resin, was filtered and analysed by GPC. The molecular weight M_w was found to be 6000 Daltons with a dispersity of 2.14.

12.5.7 Synthesis of *bis*-[hydroxyethyl(3-carbamatopropyl)]polytetrahydrofuran

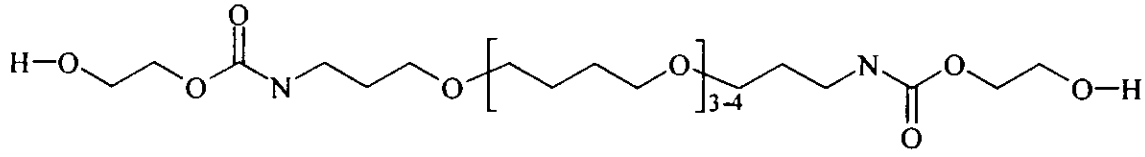

Ethylene carbonate (0.686 moles, 60.37g) was heated to 60°C and *bis*-(3-aminopropyl)polytetrahydrofuran (0.343 moles, 120.1g) added, an immediate exotherm to 90°C was observed. The reaction mixture was cooled to 60°C and maintained at this temperature for 16 hours. The product was a reddish brown viscous liquid (180g, 99.5%). Analysis by ^{1}H NMR spectroscopy showed that all the ethylene carbonate had been consumed with only a trace of starting amine remaining.

$\delta_{^1H}$ ($CDCl_3$, 250MHz), ppm, of *bis*-(3-aminopropyl)PTHF 1.61 (4H, bm, -O-CH_2-C$\underline{H_2}$-CH_2-NH_2), 1.64 (~16H, t, ^{3}J 8Hz -O-[CH_2-C$\underline{H_2}$-C$\underline{H_2}$-CH_2-O]$_n$), 2.75 (4H, bm,-O-CH_2-CH_2-C$\underline{H_2}$-NH_2), 3.42 (~16H, t, ^{3}J 8Hz, -O-[C$\underline{H_2}$-CH_2-CH_2-C$\underline{H_2}$-O]$_n$), 3.47 (4H, bm, -O-CH_2-CH_2-CH_2-N$\underline{H_2}$).

$\delta_{^1H}$ ($CDCl_3$, 250MHz), ppm, of the *bis*-carbamate 1.42 (4H, bm, -O-CH_2-C$\underline{H_2}$-CH_2-NH-CO), 1.51 (~16H, bm, -O-[CH_2-C$\underline{H_2}$-C$\underline{H_2}$-CH_2-O]$_n$), 1.61 (4H, bm, -O-C$\underline{H}$2-CH2-CH2-NH), 3.45 (~16H, t, ^{3}J 8Hz, -O-[C$\underline{H_2}$-CH_2-CH_2-C$\underline{H_2}$-O]$_n$), 3.32 (4H, q, ^{3}J 6.7Hz, (-C$\underline{H_2}$-

NH-CO-O)$_2$), 3.79 (4H, bm, (-O-CH$_2$-C<u>H</u>$_2$-OH)$_2$), 4.19 (4H, bm, (-O-C<u>H</u>$_2$-CH$_2$-OH)$_2$), 5.28 (2H, s, -CH2-CH2-O<u>H</u>), 5.52 (2H, bm, (-CH$_2$-N<u>H</u>-CO-O)$_2$).

12.5.8 Synthesis of a polyester containing *bis*-[hydroxyethyl(3-carbamatopropyl)]-polytetrahydrofuran units.

bis-[Hydroxyethyl(3-carbamatopropyl)]polytetrahydrofuran (0.153 moles, 70.32g) was heated to 60°C and Novozyme 435 (0.83g) added. Adipic acid (0.153 moles, 22.36g) was added in 4 equal amounts over a period of 4 hours. The temperature was maintained at 60°C and the pressure at 50mmHg for 12 hours and then reduced to 10mmHg for 12 hours. The pressure was then reduced to 2mmHg for the final 12 hours. The polyester formed (how can you get 87.12g, 94%) had a molecular weight by GPC of Mw 6500 Daltons and a dispersity of 2. The acid number of the polyester was 5.0mg KOH g^{-1}.

12.5.9 Synthesis of di(hydroxyethyl)polyoxypropylene *bis*-carbamate.

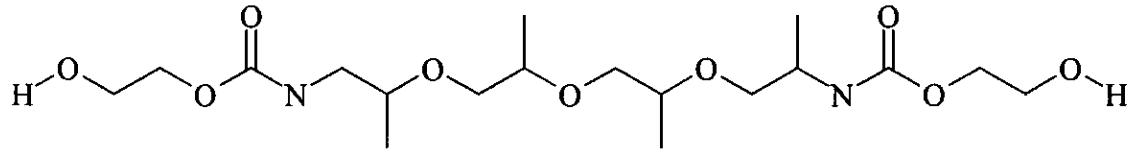

Ethylene carbonate (0.466moles, 41g) was heated to 60°C and polyoxypropyleneamine D230 (0.233 moles, 53.6g) added in three portions over 3 hours; a slight exotherm being observed after each addition. The reaction was left at 80°C under nitrogen for 16 hours. TLC showed only a single product (94g, 99.4%). The ^{1}H NMR spectrum was complex and gave no useful information at 250MHz, however, the primary amine shift at 2.55ppm was barely visible, this indicated only a trace of residual free amine.

12.5.10 Synthesis of a polyester containing di(hydroxyethyl)polyoxypropylene *bis*-carbamate units.

Dihydroxyethyl polyoxypropylene *bis*-carbamate (0.075 moles, 30g) and 1,4-butanediol (0.074 moles, 6.7g) were heated to 60°C. Novozyme 435 (0.83g) was added and adipic acid (0.149 moles, 21.6g) was added in three equal amounts over three hours whilst a pressure of 100mmHg was applied. The pressure was maintained at 100mmHg for a further 48 hours to give the product as a viscous brown resin (52g, 98%) of molecular weight M_w 6750 Daltons.

12.5.11 One pot process for the synthesis of polyesters containing urethane groups.

Ethylene carbonate (0.50 moles, 44.32g) and 1,4-butanediol (0.44 moles, 40g) were added to a reactor and heated to 60°C. 1,6-Hexamethylenediamine (0.25 moles, 29g) was added over 1 hour making sure the exotherm did not exceed 88°C. The reaction was maintained at 60°C for 16 hours. The product was a clear liquid at 60°C, but crystallises rapidly on cooling to a white waxy solid. GPC showed that the reaction had gone to completion with only the peaks of the diol and the *bis*-carbamate remaining; the composition being 64.7% $^{w}/_{w}$ *bis*-carbamate and 35.3% $^{w}/_{w}$ 1,4-butanediol. A portion of this mixture (25g) was heated at 100°C with adipic acid (0.071 moles, 10.42g) until the acid had dissolved. The reactants were cooled to 60°C and Novozyme 435 (1.04g) added and the pressure maintained at 200mmHg. The remaining adipic acid (0.102 moles, 14.86g) was added in three equal amounts over 5 hours, the temperature being maintained at 60°C and the pressure 200mmHg for a further 11 hours. The pressure was then reduced to 80mmHg for 8 hours and finally to 2mmHg for 24 hours. The resulting

polyester (43g, 97.5%) had a molecular weight M_w of 9350 Daltons and a dispersity of 1.75.

12.5.12 Synthesis of di-[2-(2-isopropyl-1,3-oxazolidin-3-yl)ethyl] hexane-1,6-dioate.

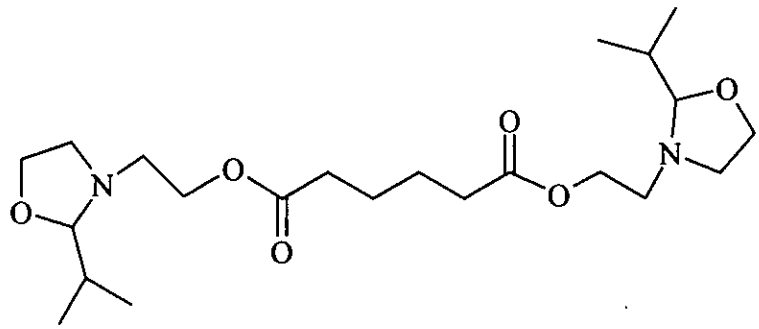

2-(2-*iso*-Propyl-1,3-oxazolidin-3-yl)ethanol (0.38 moles, 60g) and dimethyl adipate (0.19 moles, 33.03g) were heated to 60°C and Novozyme 435 (2.02g) added. The reaction was maintained at a temperature of 60°C and a pressure of 400mmHg for 8 hours. The pressure was then reduced to 185mmHg for 16 hours then further reduced to 100mmHg for 24 hours and finally reduced to 10mmHg for 24 hours. Evolved methanol (11g) was collected in a liquid nitrogen trap. Analysis by GCMS showed less than 0.1% of un-reacted dimethyl adipate remained. GPC showed a single peak for the white crystalline product (86.2g, 99%). $C_{22}H_{40}N_2O_6$ requires C 61.66%, H 9.41%, N 6.54%, found C 60.83%, H 9.71%, N 6.54% for the crude product without recrystallisation. δ^1_H ($CDCl_3$, 250MHz), ppm, 0.93 (12H, bm, (-CH($C\underline{H}_3$)$_2$)$_2$), 1.66 (4H, bm, -CO-CH_2-$C\underline{H}_2$-$C\underline{H}_2$-CH_2-CO-), 2.65 (4H, bm, -CO-$C\underline{H}_2$-CH_2-CH_2-$C\underline{H}_2$-CO-), 3.20 (2H, bm, (-C-$C\underline{H}$(CH_3)$_2$)$_2$), 3.81 (4H, bm, (-CH_2-$C\underline{H}_2$-O)$_2$), 3.83 (4H, bm, (-N-$C\underline{H}_2$-CH_2)$_2$), 3.91 (4H, bm, (-N-$C\underline{H}_2$-CH_2-O)$_2$), 4.15 (4H, bm, (-CH_2-$C\underline{H}_2$-O-CO)$_2$), 4.99 (2H, s, (-O-CH-N)$_2$.

References

1 "Encyclopaedia of Chemical Technology", 3rd Ed., G.R. Davis and E.S. Hill, Kirk-Othmer, **18,** 534-535 (1982).

2 "Encyclopaedia of Chemical Technology", 3rd Ed, G.R. Davis and E.S. Hill, Kirk-Othmer, **18**, 549-563 (1982).

3 "Polymer synthesis", S.R. Sandler and W. Karo, *Organic Synthesis*, **29**, 196-200 (1974).

4 "Encyclopaedia of Chemical Technology", 3rd Ed, G.R. Davis and E.S. Hill, Kirk-Othmer, **23**, 576-598 (1983).

5 "High Performance Polymers", R.B. Seymour and G.S. Kirshenbaum, Elsevier, 409-410 (1986).

6 "Encyclopaedia of Chemical Technology", 3rd Ed, G.R. Davis and E.S. Hill, Kirk-Othmer, **18**, 535-536 (1982).

7 "Polyesterification reactions of Adipic acid based Polyesters", W.L. Chang and T. Karalis, *J. Poly. Sci., Pt A,* **31**, 493-504 (1993).

8 "Synthesis of high molecular weight resins", W.H. Carothers, G.L. Dorough and J.A. Arvin, *J. Am. Chem. Soc.*, **52**, 3292-3297 (1930).

9 "Novel polyesters", J.R. Winfield and J.T. Dickson, *Brit. Pat.*, 578,079 (1940).

[10] "A new approach to preparative enzyme synthesis", A.M. Klibanov, G.P. Samokhin and I.V. Berezin, *Biotech. Bioeng.*, **19**, 1351-1361 (1977).

[11] "Comparison of different strategies for lipase catalysed resolution of racemic acids and alcohols", B. Cambou and A.M. Klibanov, *Biotech. Bioeng.*, **26**, 1449-1454 (1984).

[12] "Biocatalytic synthesis of polymers, preparation of AA-BB polyesters by lipase catalysed transesterification in low polarity organic solvents", J.S. Wallace and C.J. Morrow, *J. Poly. Sci., Pt. A*, **27**, 3271-3284 (1989).

[13] "Enzymic polymerisation of an unactivated diol/diacid system", F. Binns, S.M. Roberts, A. Taylor and C.F. Williams, *J. Chem. Soc. Perkin Trans. I*, 899-904 (1993).

[14] "Enzymatic synthesis", A. Taylor and F. Binns, *UK Patent* 2,286,401 (1993).

[15] "Moisture curing hot melt adhesives", A. Taylor and J. Waugh, *UK Patent WO 97/40083* (1997).

[16] "Studies of lipase-catalysed polyesterification of an unactivated diacid/diol system", F. Binns, P. Harffey, S.M. Roberts and A. Taylor, *J. Polym. Sci., Pt. A*, **36**, 2069-2080 (1998).

[17] "Studies leading to the large scale synthesis of polyesters using enzymes", F. Binns, P. Harffey, S.M. Roberts and A. Taylor, *J. Chem. Soc. Perkin Trans. I*, 2671-2676 (1999).

[18] "How do enzymes work?", L. Pauling, *Chem. Eng. News,* **24**, 1375-1381 (1946).

[19] "Role of a buried acid group in the mechanism of action of Chymotrypsin", D.M. Blow, J.J. Britkoft and B.S. Hartley, *Nature*, **221**, 337-341 (1969).

[20] "A serine protease triad forms the catalytic centre of a triacylglycerol lipase", L. Brady, A.M. Brzozowski, Z.S. Derewanda, E. Dodson, G. Dodson, J.P. Turkenburg, B.L. Christiansen, B. Huge-Jensen, L. Norskov and U. Menge, *Nature*, **343**, 767-770 (1990).

[21] "Comparison of experimental binding data and theoretical models in proteins containing sub-units", D.E. Koshland, G. Nemethy and D. Filmer, *Biochem.*, **5**, 365-368 (1965).

[22] "Calculations of enzymatic reactions: calculations of pK_a, proton transfer reactions and general acid catalysis in enzymes", A.W. Warshel, *Biochem.*, **20**, 3167-3177 (1981).

[23] "Reaction energetics of a mutant triose phosphate isomerase in which active site glutamate has been changed to aspartate", R.T. Raines, E.L. Sutton, D.R. Strauss and J.R. Knowles, *Biochem.*, **25**, 7142-7154 (1986).

[24] "Mechanisms of thiamine catalysed reactions", J. Crosby, R. Stone and G.E. Reinhard, *J. Am. Chem. Soc.*, **92**, 2891-2900 (1970).

[25] "Alternative view of enzyme reactions", M.J.S. Dewar and D.M. Storch, *Proc. Nat. Acad. Sci.*, **82**, 2225-2229 (1985).

[26] "Enzymes work by solvation substitution rather than by desolvation", A.W. Warshel, J. Aqvist and S. Creighton, *Proc. Nat. Acad. Sci.*, **86**, 5820-5824 (1989).

[27] "Entropic contributions to rate accelerations in enzymic and intramolecular reactions", M.I. Page and W.P. Jencks, *Proc. Nat. Acad. Sci.*, **68**, 1678-1683 (1971).

[28] "Importance of orientation factors in enzymatic reactions", D.R. Storm and D.E. Koshland, *J. Am. Chem. Soc.*, **94**, 5805-5811 (1972).

[29] "Pertinent aspects of mechanism as determined with small molecules", T.C. Bruice, *Ann. Rev. Biochem.*, **45**, 331-373 (1976).

[30] "Cooperativity in protein folding kinetics", K.A. Dill, K.M. Fiebig and H.S. Chan, *Proc. Nat. Acad. Sci.*, **90**, 1942-1946 (1993).

[31] "Structure as basis for understanding interfacial properties of lipases", M. Cygler and J.D. Schrag, *Meth. in Enzymol.*, **284**, 3-27 (1997).

[32] "Inhibition of the pancreatic lipase by diethyl *p*-nitrophenyl phosphate", P. Desnuelle, L. Sarda and G. Ailhard, *Biochim. Biophys. Acta*, **37**, 570-577 (1960).

[33] "Influence of surface hydrophilic/hydrophobic balance on enzyme properties", M.A. Longo and D. Combes, *J. Biotech.*, **58**, 21-32 (1997).

[34] "Some factors in the interpretation of protein denaturation", W. Kauzmann, *Adv. Protein Chem.*, **14**, 1-63 (1959).

[35] "Relevance of dielectric constant and solvent hydrophobicity to the organic solvent effect in enzymology", P. Maurel, *J. Biol. Chem.*, **253**, 1677-1683 (1978).

[36] "Binding energy, specificity and enzymic catalysis the Circe effect", W.P. Jencks, *Adv. Enzymol.*, **43**, 219-410 (1975).

[37] "Dissection of the structure and activity of tyrosyl RNA synthetase by site directed mutagenesis", A. Fersht, *Biochem.*, **26**, 8031-8037 (1987).

[38] "Orbital steering, entropy and rate acceleration", W.P. Jencks, *Biochem. Biophys. Res. Comm.*, **57**, 887-892 (1974).

[39] "Enzymes give strong binding to the transition state", R.A. Lerner, S.T. Berkovic and B.G. Schultz, *Science*, **263**, 659-666 (1991).

[40] "Demonstration of the catalytic role of binding interactions in the enzymatic reaction", G.J. Narlikar and D. Herschlag, *Biochem.*, **37**, 9902-9911 (1998).

[41] "Introduction to Macromolecular Science", P. Munk, 448-450, J. Wiley, (1989).

[42] "High resolution NMR study of the His-Asp hydrogen bond in chymotrypsin", G. Robillard, *J. Mol. Biol.*, **71**, 507-510 (1992).

[43] "A new concept for the mechanism of action of chymotrypsin, the role of the low barrier hydrogen bond", C.S. Cassidy J. Lin and P.A. Frey, *Biochem.*, **36**, 4576-4584 (1997).

[44] "Protonation state dependence of hydrogen bond strengths and exchange rates in a serine protease catalytic triad", J.L. Markley and W.M. Westler, *Biochem.*, **35**, 11092-11097 (1996).

[45] "A low-barrier hydrogen bond in Subtilisin: ^{1}H and ^{15}N NMR studies", C.J. Halkides, Y.Q. Wu and C.J. Murray, *Biochem.*, **35**, 15941-15948 (1996).

[46] "The low barrier hydrogen bond in enzymatic catalysis", W.W. Cleland, P.A. Freyt, and J.A. Gerlt, *J. Biol. Chem.*, **273**, 25529-25532 (1998).

[47] "The nature of general base–acid catalysis in serine proteases", L. Polgar and M.L. Bender, *Proc. Nat. Acad. Sci.*, **64**, 1335-1342 (1969).

[48] "C13 NMR studies of the histidine residue in alpha-lytic protease. Implications for the catalytic mechanism of serine proteases", M.W. Hunkerpillar, S.H. Smallcombe, D.R. Whitaker and J.R. Richards, *Biochem.*, **12**, 4732-4743 (1973).

[49] "Direct determination of protonation state of aspartate 102 and histidine 57 in the tetrahedral intermediate of the serine proteases", A.A. Kossiakoff and R. Spencer, *Biochem.*, **20**, 6462-6474 (1981).

[50] "Electrostatic basis of enzyme catalysis", G. Naray-Szabo, M. Fuxreiter and A. Warshel, *Computational Approaches to Biochemical Activity*, 237-293 (1997).

[51] "The catalytic role of the aspartic acid in serine proteases", C.S. Craik, S. Roczniak, C. Longman and W.J. Rutter, *Science*, **237**, 909-913 (1987).

[52] "Dissecting the catalytic triad of a serine protease", P. Carter and J.A. Wells, *Nature*, **332**, 564-568 (1988).

[53] "Unusual ^{1}H NMR chemical shifts support (His) $C^{\varepsilon 1}H$-OC H-bond: Proposal for reaction driven ring flip mechanism in serine protease catalysis," E.L. Ash, J.L.

Sudmeier, R.M. Day, M. Vincent, E.V. Torchilin, K.C. Haddad, E.M. Bradshaw, D.G. Sanford and W.W. Bachovkin, *P.N.A.S.*, **97**(19), 10371-10376 (2000).

[54] "(His)C epsilon H –OC < hydrogen bond in the active sites of serine hydrolases", Z.S. Derewanda, U. Derewanda and P.M. Kobos, *J. Mol. Biol.*, **241**, 83-93 (1994).

[55] ExPASy Database, Swiss Institute for Bioinformatics, Geneva; (www.expasy.ch./).

[56] "Grease pit chemistry", E.D. Rubin, *Nat. Struct. Biol.*, **1**, 568-572 (1994).

[57] "A model for interfacial activation in lipases from the structure of a lipase-inhibitor complex", A.M. Brzozowski, U. Derewanda, Z.S. Derewanda, G.G. Dodson, D.M. Lawson and S.A. Paktar, *Nature*, **221**, 491-497 (1991).

[58] "Anatomy of lipase binding sites: the scissile fatty acid binding site", J. Pleiss, M. Fischer and R.D. Schmid, *Chemistry and Physics of Lipids*, **93**, 67-80 (1998).

[59] "A structural basis for the chiral preferences of lipases", M. Cygler, P. Grochulski, J.D. Schrag, F. Bouthillier and A.K. Gupta, *J. Am. Chem. Soc.*, **116**, 3180-3186 (1994).

[60] "Enzymatic catalysis and dynamics in low water environments", R. Affleck, Z.F. Xu, V. Suzawa, D.S. Clark and J.S. Dordick, *Proc. Natl. Acad. Sci.*, **89**, 1100-1104 (1992).

[61] "Flexibility of enzymes suspended in organic solvents probed by time resolved fluorescence anisotropy. Evidence that activity and enantioselectivity are directly

related to enzyme flexibility", J. Broos, A.J.W. Visser, W. Verboom, A. van Hoek and D.N. Reinhoudt, *J. Am. Chem. Soc.*, **117**, 12657-12663 (1995).

62 "Measuring enzyme hydration in non-polar organic solvents using NMR", M.C. Parker, B.D. Moore and A.J. Blacker, *Biotech. and Bioeng.*, **46**, 452-458 (1995).

63 "Multinuclear NMR study of enzyme hydration in an organic solvent", C.S. Lee, M.T. Ru, M. Haake, J. Dordick and D.S. Clark, *Biotech. and Bioeng.*, **57**, 686-693 (1998).

64 "Encyclopaedia of Chemical Technology", 3rd Ed, R.J. Welglos, Kirk-Othmer, **18**, 420-421 (1982).

65 "Enzymatic catalysis in non-aqueous solvents", A. Zaks and A.M. Klibanov, *J. Biol. Chem.*, **263**, 3194-3201 (1993).

66 "Enzyme crystal structure in neat organic solvent", P.A. Fitzpatrick, A.C. Steinmetz, D. Ringe and A.M. Klibanov, *Proc. Nat. Acad. Sci.*, **90**, 8653-8657 (1993).

67 "Correlation between catalytic activity and secondary structure of Subtilisin dissolved in organic solvents", K. Xu, K. Griebenow and A.M. Klibanov, *Biotech. and Bioeng.*, **56**, 485-491 (1997).

68 "Mechanistic dissection of the plunge in enzymatic activity upon transition from water to anhydrous solvent", J.L. Schmittke, C.R. Westcott and A.M. Klibanov, *J. Am. Chem. Soc.*, **118**, 3360-3365 (1996).

[69] "Thermodynamic predictions for biocatalysis in non-conventional media", P.J. Halling, *Enz. Microb. Tech.*, **16**, 178-206 (1994).

[70] "Enhancement of *C. antarctica* lipase B selectivity and activity in organic solvents", M.C. Parker, S.A. Brown, L. Robertson and N.J. Turner, *Chem. Comm.*, **20**, 2247-2248 (1998).

[71] "Steady state kinetics", W.W. Cleland, *The Enzymes*, **2**, 1-64 (1970).

[72] "The progress of the Bi-Bi reaction", W.W. Cleland, *Biochim. Biophys. Acta*, **67**, 104-137 (1963).

[73] "Concepts in Physical Chemistry", O.U.P., P.W. Atkins, (1995).

[74] "Fluorescence methods for measuring reaction equilibria and kinetics", W.B. Dandlikar, J. Dandlikar, S.A. Levison and R.J. Kelly, *Meth. in Enzymol.*, **48**, 380-415 (1978).

[75] "The reaction of *p*-nitrophenyl esters with chymotrypsin", B.S. Hartley and B.A. Kilby, *Biochem. J.*, **56**, 288-291 (1954).

[76] "Analysis of alcohols by NIR", L.G. Weyer, *Applied Spect. Rev.*, **21**, 1-7 (1985).

[77] "Determination of hydroxyl number in polymers by infrared spectroscopy: comparison of near-IR and mid-IR", K.A. Bunding Lee, R.W. Chylla, and T.E. Janota, *Applied Spect.*, **47**(1), 94-97 (1993).

[78] "Determination of hydroxyl concentration in pre-polymers from the NIR absorption band of hydroxyl groups", S.F. Lau and A. Kawasaki, *Anal. Chem.*, **54**, 232-238 (1982).

[79] "Shifting of OH absorption bands on NIR spectra of esters", W.G. Hansen, *Applied Spect.*, **47**(10), 1623-1625 (1993).

[80] "Application of NIRA techniques for the determination of polymer end and functional groups", R.B. Roy and C.J. Kradjel, *Polymer Sci., Pt. A*, **26**, 1733-1742 (1988).

[81] "The determination of OH number in polyols using NIR spectroscopy", S. Cooke and J. Oelichmann, *J. fur Praktische Chemie Zeit.*, **339**, 746-749 (1997).

[82] "Handbook of NIR Analysis", Marcel Dekker Inc., D.A. Burns and E.W. Ciurzak, (1992).

[83] "1H-NMR and thermodynamic study of self association and complex formation equilibria by hydrogen bonding", M. Tkadlekcova, V. Donal and M. Costas, *Physical Chemistry. Chem. Phys.*, **1**, 1479-1486 (1999).

[84] "A new method to determine the a_w range in which immobilised lipases display optimum activity in organic media", M Arroyo, J.M. Sanchez-Montero and J.V. Sinisterra, *Biotech. Techniques*, **10**, 263-266 (1996).

[85] "The *Candida antarctica* lipase catalysed kinetic resolution of seudenol in non-aqueous media of controlled water activity", C. Orrenius, T Norin, K. Hult and G. Carrea, *Tetrahedron: Asymmetry*, **6**, 3023-3030 (1995).

[86] "Purification of two lipases from *Candida antarctica* and their inhibition by various inhibitors", S.A. Paktar, F. Bjorkling, M. Zyndel, M. Schulein, A. Svendsen and E. Gormsen, *Indian J. Chem.*, **32B**, 76-80 (1993).

[87] Handbook of Chemistry and Physics, 76th Edn., CRC Press, (1998).

[88] "Lipase catalysed esterification of lactic acid", M. From, P. Adlercreutz and B. Mattiasson, *Biotech. Letts.*, **19**(4), 315-317 (1997).

[89] "Lipases and esterases: a review of their sequences and structure", H.W. Anthonsen, F. Drablos, P. Martel, S.B. Petersen and L. Vaz, *Biotech. Ann. Rev.*, 315-371 (1995).

[90] "How do lipases and esterases work: the electrostatic contribution", M.T.N. Petersen, P. Fojan and S.B. Petersen, *J. Biotech.*, **85**, 115-147 (2001).

[91] "Water activity and substrate concentration effects on lipase activity", E. Wehtje and P. Adlercreutz, *Biotech. and Bioeng.*, **55**, 798-806 (1997).

[92] "The pH dependence of the tryptic hydrolysis of benzoyl-L-arginine ethyl ester in cooled mixed solvents", P. Maurel, G. Huibonhoa and P. Douzou, *J. Biol. Chem.*, **250**, 1376-1382 (1975).

[93] "Solvent temperature perturbations of ionisable groups as a tool for the investigation of the active site of enzymes", P. Maurel and P. Douzou, *J. Biol. Chem.*, **250**, 2678-2680 (1975).

[94] "How do additives affect enzyme activity and stability in non-aqueous media", A.O. Triantafyllou, E. Wehtje and P. Adlercreutz, *Biotech. and Bioeng.*, **54**(1), 67-76 (1997).

[95] "The solvent dependence of enzyme specificity", C.R. Westcott and A.M. Klibanov, *Biochim. Biophys. Acta*, **1206**, 1-9 (1994).

[96] "Structure as a basis for understanding interfacial properties of lipases", M. Cygler and J.D. Schrag, *Methods in Enzymol.*, **284**, 3-27 (1997).

[97] "The sequence and crystal structure determination of two forms of lipase B from *Candida antarctica*", J. Uppenberg, M.T. Hansen, S. Paktar and T.A. Jones, *Structure*, **2**(4), 293-308 (1994).

[98] Handbook of Chemistry and Physics, 47th Edition, CRC Press, (1966).

[99] "Kinetics of triglyceride lipases", M. Martinelle and K. Hult, in: Lipases their structure, biochemistry and application, Eds. P. Woolley and S.B. Petersen, C.U.P., 159-180 (1994).

[100] "Ester synthesis via acyl transfer", P. Andersch, M. Berger, J. Hermann, K. Laumann, and M. Lobell, *Meth. in Enzymol.*, **286**, 406-442 (1997).

[101] "Substituent Constants for Correlation Analysis in Chemistry and Biology", C. Hansch and A. Leo, Wiley, (1986).

[102] "Substrate specificity and kinetics of *Candida rugosa* lipase in organic media", A.E.M. Janssen, A.M. Vaidya and P.J. Halling, *Enz. Microb. Tech.* **18,** 340-346 (1996).

[103] "Alcohol inhibition and specificity studies of lipase B from *Candida antarctica* in organic solvents", L.F. Garcia-Alles and V. Gotor, *Biotech and Bioeng.*, **59**, 163-170 (1998).

[104] "Fundamentals of Enzyme Kinetics", A. Cornish-Bowden, Portland Press, 32-34 (1999).

[105] "Non inverted versus inverted plots in enzyme kinetics", B.H.J. Hofstee, *Nature*, **184**, 1296-1298 (1959).

[106] "Structure and Mechanism in Protein Science", A. Fersht, 340-341, Freeman, (1999).

[107] "Solvent effects on Biocatalysis in Organic Systems: Equilibrium Position and Rates of Lipase Catalysed Esterification", R.H. Valivety, G.A. Johnston, C.J. Suckling and P.J. Halling, *Biotech. and Bioeng.* **38**, 1137-1143 (1991)

[108] "Intrinsic effects of solvent polarity on enzymatic activation energies", J. Kim, D.S. Clark and J.S. Dordick, *Biotech and Bioeng.*, **67**, 112-116 (2000).

[109] "Crystallographic and molecular modelling studies of lipase B from *Candida antarctica* reveal a stereospecificity pocket for secondary alcohols", J. Uppenberg, M.T. Hansen, S. Paktar and T.A. Jones, *Biochemistry*, **34**, 16838-16851 (1995).

[110] "Structure as a basis for the chiral preferences of lipases", M. Cygler, P. Grochulski, R.J. Kazlauskas, J.D. Schrag, B. Rubin, A.N. Serreqi and A.K. Gupta, *J. Am. Chem. Soc.*, **116**, 3180-3186 (1994).

[111] "Organic Chemistry", R.D. Raber and V.T. Raber, West Publishing, 849-851 (1988).

[112] "Reaction mechanisms in Organic Chemistry", F. Badea and R. Badea, Abacus Press, 514-515 (1977).

[113] "One step biocatalytic synthesis of linear polyesters with pendant hydroxyl groups", B.J. Kline, E.J. Beckman and A.J. Russell, *J. Am. Chem. Soc.*, **120**, 9475-9479 (1998).

[114] "*Candida antarctica* lipase B catalysed transesterification: New synthetic routes to copolyesters", A. Kumar and R.A. Gross, *J. Am. Chem. Soc.*, **122**, 11767-11770 (2000).

[115] "Lipase B from *Candida antarctica*: Application to industrial polyester synthesis", P. Harffey, Ph.D. Thesis, University of Liverpool (1998).

[116] "Isolation, synthesis and reactivity of a key macrobislactone; 1,4,7-trioxacyclo-tridecane-8,13-dione", F. Binns and A. Taylor, *Tetrahedron*, **51**(47), 12929-12938 (1995).

[117] Private Communication Baxenden Chemicals Ltd. (1998).

[118] "Characterisation of binding interactions by isothermal titration calorimetry", M.L. Doyle, *Curr. Opinion. Biotech.*, **8**, 31-35 (1997).

[119] "Calorimetric methods for interpreting protein-ligand interactions", H.F. Fisher and N. Singh, *Methods in Enzymol.*, **259**, 194-221 (1995).

[120] "The association of carboxylic acids", G. Allen and E.F. Coldin, *Quart. Reviews (London)*, **7**, 255-278 (1953).

[121] "The infra red spectra of complex molecules", L.J. Bellamy, Chapman and Hall, (1980).

[122] "The crystal structure of adipic acid", J.D. Morrison and J.M. Robertson, *J. Chem. Soc.*, 987-992 (1949).

[123] "Infrared spectra and crystallinity of α,ω–dicarboxylic acids", P.J. Corish and W.H.T. Davison, *J. Chem. Soc.*, 2431-2436 (1955).

[124] "Consistent Force Field studies of internal forces in Hydrogen bonded crystals. The CO···H-OH bond of carboxylic acids", A.T. Hagler, *J. Am. Chem. Soc.*, **101**, 5131-5141 (1979).

[125] "$CHCl_3$ interaction with pyridine and triethylamine", D. Allerhand and G.J.. Schlegel, *J. Am. Chem. Soc.*, **85**, 1715-1718 (1963).

[126] "The acetone-chloroform association", M.L. McGlashan and K. Rastogi, *Trans. Farad. Soc.*, **54**, 496-501 (1958).

[127] "Strong hydrogen bonds in aqueous and aqueous-acetone solutions of dicarboxylic acids: Activation energies for exchange and deuterium fractionation factors", Jing Lin and P.A. Frey, *J. Am. Chem. Soc.*, **122**, 11258-11259 (2000).

[128] "$CDCl_3$ in ethers and esters", J. Lord, *J. Am. Chem. Soc.*, **77**, 1365-1368 (1955).

[129] "The C-D stretch and heat of solution of $CDCl_3$ in solvents", D. Huggins, *J. Chem. Phys.*, **23**, 896-898 (1955).

[130] "NMR studies of chloroform-acetone and chloroform-triethylamine complexes show hydrogen bonding", D. Huggins, *J. Chem. Phys.*, **23**, 1244-1247 (1955).

[131] "Enthalpy of formation of 1:1 chloroform -acetone complex", T. Moelwyn-Hughes and Z. Sherman, *J. Chem. Soc.*, **10**, 101-111 (1936).

[132] "Thermo-mechanical properties of chloroform-acetone mixtures", L.A. Staveley, *Trans. Farad. Soc.*, **51**, 323-343 (1955).

[133] "The heat of solution and Infra-red spectra of esters and lactones in $CHCl_3$ and $CDCl_3$", S. Searles, M. Tamres and G.M. Barrow, *J. Am. Chem. Soc.*, **75**, 71-73 (1953).

[134] "The Hydrogen Bond", G.C. Pimental and A. McClellan, Freeman, (1960).

[135] "Hydrogen Bonding", P. Vinogradov and M. Linnell, Van Nostrand, (1971).

[136] "Infrared study of the interactions of the C-H bond", D.N. Boobyer, *Spectrochim. Acta*, **23A**, 325-329 (1967).

[137] "Molecular parameters and bond structure", D.N. Boobyer and M. Jones *Spectrochim. Acta*, **22**, 147-152 (1966).

[138] "Hydrogen bonding thermodynamics measured by temperature dependant NMR and modelled with MOPAC", K.E. Johnson and E.L. Green, www.chem.pacificu.edu:80/johnson/course/hbond.html.

[139] "Cross correlation in the longitudinal relaxation of heteronuclear spin systems", L. Maler and J. Kowalewski, *Chem. Phys. Letters*, **190**, 241-246 (1992).

[140] "*Ab initio* and localised molecular orbital studies of the integrated intensities of infrared absorption bands of polyatomic molecules and chloroform. Complexes between $CHCl_3$ and three aliphatic nitriles. The influence of hydrogen bonding on the C-H and C-N infrared characteristics", H.P. Figeys, P. Geerling and D. Berckmans, *J. Chem. Soc., Farad. Trans. II*, 77, 721-740 (1981).

[141] Private communication, D. Chama, Centre D'Etude Fondamentales, University of Perpignan, (2000).

[142] "Lipases: Interfacial enzymes with attractive applications". R. Schmid and R. Verger, *Ang. Chem., Int. Edn.*, **37**, 1609-1633 (1998).

[143] "Identification of conserved residues in a family of esterase and lipase sequences", F. Drablos and S.B. Peterson, *Methods in Enzymol.*, **284**, 28-61 (1997).

[144] "The α–β hydrolase fold", D.L. Ollis, E. Cheah, M. Cygler, B. Dijkstra, S.M. Franken, S.J. Remington and J.D. Schrag, *Protein Eng.*, **5**, 197-211 (1992).

[145] "Relationships among serine hydrolases; evidence for a common structural motif in triacylglycerol lipases and esterases", Z.S.Derewenda and U.Derewenda, *Biochem. Cell Biol.*, **69**, 842-847 (1991).

[146] "Structure of human pancreatic lipase", F.K. Winkler, A.D. D'Arcy and W. Hunzikar, *Nature*, **351**, 570-571 (1991).

[147] (a) "Effect of pH on rate of interfacial inactivation of serine proteases in aqueous-organic systems", A.C. Ross, G. Bell and P.J. Halling, *Biotechnol. Bioeng.*, **67**, 498-503 (1999).

(b) "Differences between lipases and proteases at interfaces", P. Halling *Private Communication* (2000).

[148] "On the interfacial activation of *Candida antarctica* lipase A and B compared to *Humicola lanuginosa*", M. Martinelle, M. Holmquist and K. Hult, *Biochim. et Biophys. Acta*, **1258**, 272-276 (1995).

[149] "Molecular modelling of enantioselectivity in lipase catalysed transesterification", F. Haeffner, T. Norin and K. Hult, *Biophysical J.*, **74**, 1251-1262 (1998).

[150] "A model for interfacial activation in lipases from the structure of a fungal lipase-inhibitor complex", A.M Brzozowski, U. Derewanda, Z.S. Derewanda, G.G. Dodson, D.M. Lawson, J.P. Turkenburg, F. Bjorkling, S. Paktar and L. Thim,, *Nature*, **351**, 491-493 (1991).

[151] "Lipase protein engineering", A. Svendsen, *Biochim. et Biophys. Acta*, **1543**, 223-238, (2000).

[152] "Fatty acid specificity in lipase catalysed synthesis of glucoside esters", O. Kirk, F. Bjoerkling and T.O. Larsen, *Biocatalysis*, **6**(2), 127-134 (1992).

[153] "Multi-competitive enzyme reactions in organic media", M.S. Rangheard, C. Triantphylides and J. Baratti, *Biochim. et Biophys. Acta*, **1004**, 20-28 (1989).

[154] "Chiral recognition of secondary alcohol enantiomers in acyl transfer reactions catalysed by *Candida antarctica* lipase B", C. Orrenius, F. Haeffner, D. Rotticci, N. Ohner, T. Norin and K. Hult *Biocatal. and Biotransform.*, **16**, 1-15 (1998).

[155] "On the role of transition state substrate desolvation", S. Luque, Tao Ke and A.M. Klibanov, *Biocatal. and Biotransform.*, **16**, 233-248 (1998).

[156] "Circular and Linear Dichroism", A. Rodger and B. Norden, O.U.P. 15-32 (1996).

[157] "Mechanism of extraction of chymotrypsin into isooctane at very low concentrations of Aerosol OT in the absence of reversed micelles", V.M. Paradkar and J.S. Dordick, *Biotech Bioeng.*, **43**, 529-540 (1994).

[158] "Information content in the circular dichroism of proteins", J.P. Hennessey and W. Curtis Johnson, *Biochemistry*, **20**, 1085-1094 (1981).

[159] "SELCON secondary structure prediction", N. Sreerama and R.W. Woody, *Biochemistry*, **33**, 10022-10025 (1994).

[160] "Knowledge based secondary structure assignment", D. Frishman and P. Argos, *Proteins. Structure Function and Genetics*, **23**, 566-579 (1995).

[161] "Effects of pH and KCl on the conformations of creatine kinase from rabbit muscle", C. Raimbault, F. Couthon and R. Buchet, *Eur. J. Biochem.*, **234**, 570-578 (1995).

[162] "Aqueous like activity of α-chymotrypsin dissolved in nearly anhydrous organic solvent", J.S. Dordick and V.M. Paradkar, *J. Am. Chem. Soc.*, **116**, 5009-5010 (1994).

[163] "Assessing the structural integrity of a lyophilised protein in organic solvents", U.R. Desai and A.M. Klibanov, *J. Am. Chem. Soc.*, **117**, 3940-3945 (1995).

[164] "Circular dichroism induced by helical host molecule", M. Kodaka, *J. Chem. Soc., Faraday Trans.*, **93**(11), 2057-2059 (1997).

[165] "DNA-ligand binding", A. Rodger and B. Norden, in: Circular and Linear Dichroism, Eds. OUP, 30-31 (1997).

[166] "Private communication, S.A. Paktar, Novo A/S

[167] "X-ray crystal structure of γ-chymotrypsin in hexane", N.H. Yennawar, H.P. Yennawar and G.K. Farber, *Biochemistry*, **33**, 7326-7336 (1994).

[168] *Sequence Finder*. http://www.expasy.org/sprot/

[169] "Structure and molecular model refinement of *Rhizomucor miehei* triacylglyceride lipase", A.M. Brzozowski, Z.S. Derewanda, E.J. Dodson, G.G. Dodson, J.P. Turkenburg,*Acta Crystallogr. B*, **48**, 307-311 (1992).

[170] "Insights into interfacial activation from an open structure of *Candida rugosa* lipase", P. Grochulski, Y. Li, J.D.Schrag, F. Bouthillier, P. Smith, D. Harrison and M. Cygler „*J. Biol. Chem.*, **268**, 12843-12848 (1993).

[171] "1.8Å refined structure of the lipase from *Geotrichum candidum*", J.D. Schrag and M. Cygler, *J. Mol. Biol.*, **230**, 575-591 (1993).

[172] "Enzyme catalysed synthesis of sugar containing monomers and linear polymers", O.J. Park, D.Y. Kim and J.S. Dordick, *Biotech. and Bioeng.*, **70**, 208-216 (2000).

[173] "Enzyme catalysed synthesis of macromolecules in organic solvents", J.A. Akkara and F.F. Bruno, US Patent 5,981,240 (1999).

[174] "Synthese de quelque diiodures de *bis*-(carbamoylcholine) doues d'activite curarisante", R. Delaby, P. Chabrier and H. Najer, *Memoires Presentes a la Societe Chimique*, 1616-1622 (1956).

[175] "Synthese de biscarbamat des amines", R. Delaby, A. Sekera, P. Chabrier et P. Pignaniol, *Bull. Soc. Chem.*, **20**, 278-285 (1953).

[176] "*bis*-Oxazolidines and mixtures thereof and their use as hardeners for plastic precursors containing isocyanate groups", H. Blum, J. Pedain, and K.H. Hentschel, US Patent 5,189,176 (1993).

[177] "Chemistry and Technology of Isocyanates", H. Ulrich, J. Wiley & Sons, (1996).

[178] "Polymer Synthesis", P. Remp and E.W. Merrill, Huther and Wepf, 29-34 (1991).

[179] Determination of acid value, hydroxyl value and water content in reactions between diacids and diols using NIR", R.I. Heikka, K.T. Immonen, Y.O. Erkki and T.O. Salmi, *Anal. Chim. Acta*, **349**, 287-294 (1997).

[180] "The near infra red analysis of polyols", P. Brush, *NIR News*, **5**(5), 14-15 (1994).

[181] "Structural studies of aliphatic polyester polyols suitable for use in polyurethane synthesis", C. Salou, M.Sc. Thesis, University of Manchester Institute of Science and Technology, (year).

Appendices

Appendix 1 Determination of acid number of polyesters (Baxenden Method).

Duplicate samples of 200mg polyester were weighed out into two 100ml conical flasks. 20ml of Analar pyridine added from a measuring cylinder and 5ml of water added using a pipette. Stirred with a magnetic stirrer for 30 minutes and titrated against 0.02M NaOH with phenolphthalein (1% in isopropanol) as indicator.

Repeat using a blank.

$$\text{Calculation of Acid number} = \frac{(Vs-Vb) \times M \times 56.1}{W}$$

Where Vs is the sample titre, Vb is the blank titre, M is the molarity of the NaOH and W is the weight of the sample.

Therefore the Acid number = 5.5 x (Vs-Vb) where M = 0.02 and W = 1

Calculated accuracy of the test is 98.7%

Appendix 2 Determination of Hydroxyl Number of polyesters by acetylation (Baxenden Method).

Reagents used are: Pyridine in acetic anhydride. (Transfer 48ml of Analar pyridine into a 100ml screw top bottle add 2ml of Analar acetic anhydride, shake and leave to stand for 2 hours). Duplicate, 1g samples of polyester are weighed into two 50ml conical flasks. 5ml of the pyridine/acetic anhydride acetylating reagent are added by pipette.

Fit condenser and reflux for 1 hour. Cool contents in ice for 15 minutes, wash condenser down with further 10ml of pyridine and leave for further 10 minutes in ice. Add 2ml of water.

Measure a blank by mixing 5ml of the acetic anhydride pyridine reagent into conical flask and add 20ml pyridine plus 2ml water. Titrate against 0.5M NaOH with phenolphthalein (1% in isopropanol) as indicator.

Repeat titration with the samples.

Calculation Hydroxyl value $= \frac{(Vb-Vs) \times 0.5 \times 56.1}{W}$

Where Vs is the average of the two sample titres, Vb is the blank titre, M is the molarity of the NaOH and W is the weight of the sample.